

# **CONTROLLED POLYMERISATION AND INDUSTRIAL APPLICATION OF POLY(2-CHLORO-1,3-BUTADIENE)**

**by**

**Nicola Pullan**

**Doctor of Philosophy**

**Aston University**

**Chemical Engineering and Applied Chemistry**

**June 2014**

©Nicola Pullan, 2014

Nicola Pullan asserts her moral right to be identified as the author of this thesis.

This copy of the thesis has been supplied on condition that anyone who consults it is understood to recognise that its copyright rests with its author and that no quotation from the thesis and no information derived from it may be published without appropriate permission or acknowledgement.

Aston University

Controlled Polymerisation and Industrial Application of  
Poly(2-Chloro-1,3-Butadiene)

Nicola Pullan

Doctor of Philosophy

2014

Poly(2-chloro-1,3-butadiene) (PCB, polychloroprene) has wide-ranging applications as neoprene rubber. Favourable chemical and physical properties in the material are attributed to a three-dimensional network of polymer chains, which is realised through cross-linking. Ethylene thiourea (ETU) and zinc oxide (ZnO) are the standard reagents which facilitate this in industrial processes. However, ETU is a suspected carcinogen and its usage is due to become severely restricted, so much so that the future production of neoprene rubber is at risk. Hence, an alternative, non-toxic cross-linking agent is required which can cross-link PCB in the same fashion. The way in which the ETU/ZnO system functions must first be understood before a replacement can be proposed. Thus, mechanistic studies were initially undertaken with PCB oligomers in order to elucidate the reaction.

To this end, a synthetic protocol was established for 2-chloro-1,3-butadiene (CB) and the monomer was subsequently adopted in numerous polymerisation reactions. Investigations into the reversible addition-fragmentation chain transfer (RAFT) polymerisation of CB proceeded to predefine low molecular weight PCB. A successful procedure was realised, employing 2-cyano-2-propylbenzodithioate (CPD) CTA and conditions which were able to furnish <1000 g/mol to 50,000 g/mol, low dispersity PCB in a controlled manner. This invention was novel in that PCB has historically been synthesised *via* conventional (uncontrolled) free radical techniques.

PCB oligomers were adopted in cross-linking reactions with ETU and various model compounds, alone, and with ZnO, to aid the interpretation of the ETU/ZnO mechanism. Spectroscopic analyses and the observation of by-products revealed that three disparate reactions occur; ETU and ZnO were found to act both synergistically and independently of each other. A newly-proposed mechanism describes activation of the polymer chain by ZnO and subsequent reaction through sulfur. As a result of this discovery, alternative compounds have been tested and found capable of cross-linking PCB.

In a second industrial study, the eradication of allergy-causing cross-linking additives for PCB latex (gloves) was investigated. PCB latex films were generated under various conditions and the materials physically tested. A novel amine-dithiocarbamate complex, combined with a xanthogen polysulfide, afforded comparable properties in PCB latex and as such is a potential replacement system.

**Keywords:** Polychloroprene; Ethylene thiourea; Cross-linking; RAFT; Latex

## List of Publications

N. Pullan, M. Liu and P. D. Topham, Reversible Addition-Fragmentation Chain Transfer Polymerization of 2-Chloro-1,3-Butadiene, *Polymer Chemistry*, 2013, **4**, 2272-2277.

D. T. W. Toolan, N. Pullan, M. J. Harvey, P. D. Topham and J. R. Howse, In Situ Studies of Phase Separation and Crystallization Directed by Marangoni Instabilities During Spin-Coating, *Advanced Materials*, 2013, **25**, 7033-7037.

K. I. Berry, M. Liu, K. Chakraborty, N. Pullan, A. West, C. Sammon and P. D. Topham, A New Mechanism for Cross-linking Polychloroprene with Ethylene Thiourea and Zinc Oxide, *Rubber Chemistry and Technology*, Accepted.

## **Acknowledgements**

My sincere thanks go to Dr. Paul Topham, who provided a great deal of guidance and support throughout my time at Aston.

The EPSRC are acknowledged for funding this project through a CASE studentship with Robinson Brothers Ltd. (RBL), West Bromwich. I am grateful for the help of my co-workers at RBL, in particular Dr. Max Liu. The various FP7-funded SafeRubber consortium members, especially PERA Technology, are also recognised for their input.

Dr. Keith Berry has been invaluable to this project, notably for the cross-linking studies, and was a superb companion during the numerous (often extensive) meetings. Members of the Topham group, past and present, have provided endless amusement and I am thankful for their support and friendship.

It has been a genuine pleasure to be a part of the CEAC department of Aston University, where the students and staff alike create a friendly, fun atmosphere in which to work. All of my friends, and the numerous times we have enjoyed together, will be remembered with fondness. Rarely did a day go by where I didn't smile or laugh because of you.

Special thanks go to Prof. Brian Tighe and BRU for use of their FTIR instrument. Dr. Jon Howse and Daniel Toolan, of The University of Sheffield, are also acknowledged for spin-coating collaboration.

Without a doubt, those most deserving of my appreciation are my family. Always there for me and wanting to help in any way possible, through everything and anything, they have been an ever-present rock. Mum and Dad, words cannot describe how proud I am to be yours. I love you all dearly.

## Abbreviations

AIBN	$\alpha,\alpha'$ -azoisobutyronitrile
ATRP	atom transfer radical polymerisation
nBA	<i>n</i> -butyl acrylate
BIIR	bromobutyl rubber
Bz	benzyl
CB	2-chloro-1,3-butadiene
CDCl <sub>3</sub>	deuterated chloroform
CMPCD	cyanomethyl methyl(phenyl)carbamodithioate
CPD	2-cyano-2-propylbenzodithioate
CTA	chain transfer agent
$\bar{D}$	(molecular weight) dispersity
DAB	1,4-diaminobutane
DBTU	dibutyl thiourea
DDMAT	S-1-dodecyl-S'-( $\alpha,\alpha'$ -dimethyl- $\alpha''$ -acetic acid)trithiocarbonate
DIBPO	diisobutyryl peroxide
DIXP	diisopropyl xanthogen polysulfide
DPG	diphenyl guanidine
DPTU	diphenyl thiourea
ETU	ethylene thiourea
EU	ethylene urea
FTIR	fourier transform infrared
GPC	gel permeation chromatography
HCl	hydrochloric acid

LAM	less-activated monomer
MAM	more-activated monomer
MFA	multi-functional additive
MMA	methyl methacrylate
$M_n$	number-average molecular weight
$M_w$	weight-average molecular weight
NMP	nitroxide-mediated radical polymerisation
NMR	nuclear magnetic resonance spectroscopy
NR	natural rubber
ODT	1,8-octanedithiol
PCB	poly(2-chloro-1,3-butadiene)
phr	parts per hundred rubber
PIP	piperazine
PNA	proposed new accelerator
ppm	parts per million
PRE	persistent radical effect
PSt	polystyrene
PTC	phase-transfer catalyst
RAFT	reversible addition-fragmentation chain transfer
SMO	sodium salt of sulfated methyl oleate
St	styrene
TBTA	S-(thiobenzoyl)thioglycolic acid
TbuT	tetrabutylthiuram disulfide
TBzTD	tetrabenzylthiuram disulfide
TETD	tetraethylthiuram disulfide

THF	tetrahydrofuran
TMS	trimethylsilane
TMTD	tetramethylthiuram disulphide
TMTM	tetramethylthiuram monosulphide
TSC	total solids content
UTS	ultimate tensile strength
VC	vinyl chloride
WAQ	sodium alkyl sulfate
ZnCl <sub>2</sub>	zinc chloride
ZnO	zinc oxide

## Contents

<b>Thesis Summary</b>	2
<b>List of Publications</b>	3
<b>Acknowledgements</b>	4
<b>Abbreviations</b>	5
<b>Contents</b>	8
<b>List of Tables</b>	13
<b>List of Figures</b>	15
<b>List of Schemes</b>	20
<b>List of Equations</b>	22
<b>Chapter 1 Introduction</b>	24
1.1 Definitions for polymers and polymerisation methods	24
1.1.1. Conventional (uncontrolled) free radical chain polymerisation	26
1.1.1.1. Free radical chain polymerisation mechanism	26
1.1.1.2. Other factors influencing polymerisation	29
1.1.1.2.1. Temperature	29
1.1.1.2.2. Form of polymerisation	29
1.1.1.2.3. Inhibitors/retarders	30
1.1.1.3. General features of conventional free radical chain polymerisation	30
1.1.2. Controlled-radical polymerisation methods	31
1.1.2.1. General features of nitroxide-mediated radical polymerisation (NMP)	34
1.1.2.2. General features of atom transfer radical polymerisation (ATRP)	35
1.1.2.3. Reversible addition-fragmentation chain transfer polymerisation (RAFT)	36
1.1.2.3.1. The reversible addition-fragmentation chain transfer (RAFT) mechanism	37
1.1.2.3.2. Application of the RAFT CTA	38
1.1.2.3.3. Other reaction considerations	42
1.1.2.3.4. General features of RAFT polymerisation	44
1.2 Cross-linking	44
1.2.1. Cross-linking methods and additives in the rubber industry	45



1.2.1.1. The role of sulfur (and nitrogen) -containing compounds as accelerators	46
1.2.1.2. The role of zinc oxide (ZnO) in cross-linking	47
1.2.1.3. The role of multi-functional additives (MFAs) in cross-linking	48
1.2.2. Cross-linking poly(2-chloro-1,3-butadiene)	48
1.2.2.1. Typical PCB cross-linking additives	49
1.2.2.2. PCB cross-linking theories – ZnO alone	51
1.2.2.3. PCB cross-linking theories – ETU alone	53
1.2.2.4. PCB cross-linking theories – ETU and ZnO	54
1.3 Latex technology	55
1.3.1. Emulsion polymerisation	55
1.3.1.1. Emulsion polymerisation components	55
1.3.1.2. Emulsion polymerisation mechanism	56
1.3.1.2.1. The Harkins theory	57
1.3.1.2.2. The Smith and Ewart theory	58
1.3.2. Latex formulation	59
1.3.2.1. Formulations	59
1.3.2.2. Latex compounding	61
1.3.2.2.1. Latex dipping	62
1.3.2.2.2. Latex characterisation	63
1.3.2.3. Applications of latexes	64
1.3.3. Poly(2-chloro-1,3-butadiene) latex	65
1.3.3.1. PCB latex composition	66
1.3.3.2. PCB latex applications	67
1.4 Aims	70
1.5 References	71
<b>Chapter 2 Materials and experimental methods</b>	<b>77</b>
2.1 Materials	77
2.2 Experimental methods	79
2.2.1. Synthesis of 2-chloro-1,3-butadiene	79
2.2.2. Synthesis of poly(2-chloro-1,3-butadiene) <i>via</i> uncontrolled polymerisation	79
2.2.3. Synthesis of poly(2-chloro-1,3-butadiene) <i>via</i> RAFT polymerisation	80
2.2.3.1. Chain extension experiment	81
2.2.4. Compounding and cross-linking of poly(2-chloro-1,3-butadiene) oligomers	81

2.2.5. Poly(2-chloro-1,3-butadiene) latex compounding	82
2.2.5.1. Preparation of PNA-5 dispersion	84
2.2.6. Preparation of poly(2-chloro-1,3-butadiene) latex films	85
2.3 Characterisation methods	86
2.3.1. Nuclear Magnetic Resonance Spectroscopy	86
2.3.1.1. Monitoring monomer conversion	87
2.3.2. Gel Permeation Chromatography	88
2.3.3. Fourier Transform Infrared Spectroscopy	89
2.3.4. Viscosity measurements	89
2.3.5. Tensometer	89
2.4 References	90
<b>Chapter 3 RAFT Polymerisation of 2-chloro-1,3-butadiene</b>	<b>92</b>
3.1 Synthesis of 2-chloro-1,3-butadiene	92
3.1.1. Varying sodium hydroxide concentration	93
3.1.2. Water as a by-product	94
3.1.3. Variable yields in the synthesis of 2-chloro-1,3-butadiene	95
3.1.4. NMR Characterisation of 2-chloro-1,3-butadiene	96
3.1.5. Stability of 2-chloro-1,3-butadiene	97
3.2 Synthesis of poly(2-chloro-1,3-butadiene) <i>via</i> uncontrolled polymerisation	100
3.2.1. The effect of monomer purity	101
3.2.2. Polymerisation	102
3.2.3. Spectroscopic characterisation of poly(2-chloro-1,3-butadiene)	103
3.3 Synthesis of poly(2-chloro-1,3-butadiene) <i>via</i> RAFT polymerisation	108
3.3.1. Selection of chain transfer agents (CTAs)	109
3.3.1.1. S-(Thiobenzoyl)thioglycolic acid (TBTA)	110
3.3.1.2. Cyanomethyl methyl(phenyl)carbamdithioate (CMPCD)	115
3.3.1.3. S-1-Dodecyl-S'-( $\alpha,\alpha'$ -dimethyl- $\alpha''$ -acetic acid)trithiocarbonate (DDMAT)	119
3.3.1.4. 2-Cyano-2-propylbenzodithioate (CPD)	123
3.3.2. DDMAT and CPD RAFT polymerisation reactions in bulk	127
3.3.3. Optimum system	131
3.4 Conclusion and future work	136
3.5 References	137
<b>Chapter 4 Spectroscopic analysis of the cross-linking of poly(2-chloro-1,3-butadiene)</b>	<b>140</b>

4.1	Cross-linking poly(2-chloro-1,3-butadiene)	140
4.1.1.	Cross-linking PCB with ETU	143
4.1.2.	Cross-linking PCB with ZnO	144
4.1.3.	Cross-linking PCB with ETU and ZnO	147
4.1.4.	Cross-linking PCB with model compounds and other standard accelerators	153
4.1.4.1.	Cross-linking PCB with model compounds	153
4.1.4.2.	Cross-linking PCB with model compounds combined with ZnO	156
4.1.4.3.	Cross-linking PCB with tetrabutylthiuram disulfide (TbuT)	159
4.1.4.4.	Cross-linking PCB with tetrabutylthiuram disulfide (TbuT) combined with ZnO	160
4.1.5.	Conclusions for the current cross-linking mechanism of poly(2-chloro-1,3-butadiene)	161
4.1.5.1.	Cross-linking of PCB by ETU compared with other compounds	161
4.1.5.2.	The ETU/ZnO mechanism of cross-linking PCB	162
4.1.6.	Towards a safer accelerator system for cross-linking poly(2-chloro-1,3-butadiene)	165
4.2	References	169
<b>Chapter 5</b>	<b>Poly(2-chloro-1,3-butadiene) latex development</b>	172
5.1	Introduction	172
5.2	PCB latex films from the standard DPTU/DPG accelerator system	174
5.3	Alternative accelerator system for PCB latex comprising PNA-5	176
5.3.1.	Development and stability of the PNA-5 dispersion reagent	177
5.3.2.	PCB latex formulated with PNA-5 alone	179
5.3.3.	PCB latex formulated with PNA-5 and 1,4-MFA	181
5.3.4.	PCB latex formulated with PNA-5 and DIXP	184
5.3.5.	PCB latex formulated with PNA-5 and TBzTD	187
5.4	Alternative accelerator system comprising DIXP and PNA-8	190
5.5	Comparisons for the development of poly(2-chloro-1,3-butadiene) latex films	193
5.5.1.	Effect of reducing ZnO in PCB latex formulations	194
5.5.2.	Summary of accelerator systems for PCB latex	199
5.5.3.	Further PCB latex development work	202
5.6	References	204
<b>Chapter 6</b>	<b>Conclusions and future work</b>	206
6.1	Outline of the project	206

6.2	Conclusions	207
6.2.1.	Synthesis of 2-chloro-1,3-butadiene	207
6.2.2.	Synthesis of poly(2-chloro-1,3-butadiene)	208
6.2.2.1.	Uncontrolled polymerisation of 2-chloro-1,3-butadiene	208
6.2.2.2.	RAFT polymerisation of 2-chloro-1,3-butadiene	209
6.2.3.	Industrial applications of poly(2-chloro-1,3-butadiene)	212
6.2.3.1.	Cross-linking poly(2-chloro-1,3-butadiene)	212
6.2.3.1.1.	A safer accelerator system for cross-linking PCB rubber	214
6.2.3.2.	Poly(2-chloro-1,3-butadiene) latex development	215
6.2.3.2.1.	The effect of ZnO in PCB latex films	215
6.2.3.2.2.	New accelerators for the production of PCB latex films	216
6.3	Future work	217
6.3.1.	Further development of the 2-chloro-1,3-butadiene synthetic protocol	217
6.3.2.	Future studies for the RAFT polymerisation of 2-chloro-1,3-butadiene	218
6.3.3.	Optimisation of oligomer cross-linking experiments	218
6.3.4.	Further development of poly(2-chloro-1,3-butadiene) latex	219
6.4	References	220

## List of Tables

<b>Table 1.1.</b>	Additives commonly used in the industrial cross-linking of rubbers.	46
<b>Table 1.2.</b>	Common organic accelerators adopted in rubber cross-linking.	47
<b>Table 1.3.</b>	Reagents typically employed in latex formulation.	60
<b>Table 1.4.</b>	Summary of latex applications.	65
<b>Table 1.5.</b>	Reagents typically employed in PCB latex formulations, as taken predominantly from Blackley.	66
<b>Table 1.6.</b>	Accelerators which are latex glove allergens.	68
<b>Table 2.1.</b>	List of reagents adopted in the syntheses of 2-chloro-1,3-butadiene (CB) and polymers thereof (PCB).	77
<b>Table 2.2.</b>	List of reagents adopted in the poly(2-chloro-1,3-butadiene) cross-linking trials.	78
<b>Table 2.3.</b>	List of aqueous dispersions adopted for the poly(2-chloro-1,3-butadiene) latex films.	78
<b>Table 2.4.</b>	Reaction mixtures adopted in PCB oligomer cross-linking studies, where levels are given in phr.	82
<b>Table 2.5.</b>	Formulation details for the compounding of PCB latex films (depicted as A – I), where quantities are given in parts per hundred (phr).	83
<b>Table 2.6.</b>	Formulation details for the compounding of PCB latex films with the DIXP/PNA-8 accelerator system (I); adjustment to 40 % TSC is outlined.	84
<b>Table 2.7.</b>	Formulation details for (35 % w/w) PNA-5 dispersion.	85
<b>Table 2.8.</b>	Approximate percentage monomer conversion during the CPD/THF RAFT polymerisation, by comparison of <sup>1</sup> H NMR integrals relating to the vinyl and alkene protons of CB and PCB.	88
<b>Table 3.1.</b>	Table showing how varying sodium hydroxide concentrations in CB syntheses affected percentage yields.	93
<b>Table 3.2.</b>	Experimental data highlighting the variable yields obtained during the synthesis of CB.	95
<b>Table 3.3.</b>	Approximate percentage degradation of uninhibited CB (a) by comparison of <sup>1</sup> H NMR integrals relating to vinyl and alkene protons in CB and PCB.	100
<b>Table 3.4.</b>	Experimental data for the (uncontrolled) polymerisation of CB.	102
<b>Table 3.5.</b>	FTIR peaks assigned in PCB, as aided by the literature.	105

<b>Table 3.6.</b>	Comparison of initial apparent rate constants, $k_{app}$ , in the RAFT polymerisations of CB employing DDMAT and CPD CTAs (obtained under solution and bulk conditions).	131
<b>Table 3.7.</b>	Comparison of theoretical ( $M_n^{th}$ ) and experimental ( $M_n^{GPC}$ ) molecular weights, and dispersities ( $\mathcal{D}$ ), obtained for the optimum CB RAFT system targeting different degrees of polymerisation ( $D_p$ ).	133
<b>Table 4.1.</b>	FTIR peaks assigned in PCB, as aided by the literature.	142
<b>Table 4.2.</b>	List of additives used in the cross-linking studies.	142
<b>Table 4.3.</b>	Model compounds and accelerators adopted in PCB cross-linking studies.	153
<b>Table 4.4.</b>	List of original potential new accelerators (PNAs) for cross-linking PCB, designated by the SafeRubber consortium.	166
<b>Table 5.1.</b>	Individual components in the PCB latex formulations.	173
<b>Table 5.2.</b>	Accelerators adopted in the PCB latex formulations.	174
<b>Table 5.3.</b>	Formulation details for the compounding of PCB/DPTU/DPG latex films (A).	175
<b>Table 5.4.</b>	Tensile results for the PCB/DPTU/DPG latex films (A).	176
<b>Table 5.5.</b>	Formulation details for the compounding of PCB/PNA-5 latex films (B).	180
<b>Table 5.6.</b>	Tensile results for the PCB/PNA-5 latex films (B).	181
<b>Table 5.7.</b>	Formulation details for the compounding of PCB/PNA-5/1,4-MFA latex films (C and D).	182
<b>Table 5.8.</b>	Tensile results for the PCB/PNA-5/1,4-MFA latex films (C and D).	182
<b>Table 5.9.</b>	Formulation details for the compounding of PCB/PNA-5/DIXP latex films (E and F).	185
<b>Table 5.10.</b>	Tensile results for the PCB/PNA-5/DIXP latex films (E and F).	185
<b>Table 5.11.</b>	Formulation details for the compounding of PCB/PNA-5/TBzTD latex films (G and H).	188
<b>Table 5.12.</b>	Tensile results for the PCB/PNA-5/TBzTD latex films (G and H).	189
<b>Table 5.13.</b>	Formulation details for the compounding of PCB/DIXP/PNA-8 latex films (I).	191
<b>Table 5.14.</b>	Tensile results for the PCB/DIXP/PNA-8 latex films (I).	192
<b>Table 5.15.</b>	Overall tensile results table for the PCB latex films furnished using various accelerator systems, where mean values are quoted plus/minus the standard deviations.	200

## List of Figures

<b>Figure 1.1.</b>	Graph illustrating the change in degrees of polymerisation ( $D_p$ ) with monomer conversion for the different types of polymerisation reactions.	26
<b>Figure 1.2.</b>	1-Methoxy-1-trimethylsiloxy-2-methyl-1-propene initiator adopted in group transfer polymerisation (GTP).	32
<b>Figure 1.3.</b>	Generic structure of the RAFT CTA.	36
<b>Figure 1.4.</b>	Generic structures for the types of CTAs employed in RAFT.	39
<b>Figure 1.5.</b>	General guidelines for designing the RAFT CTA, as adapted from the literature.	40
<b>Figure 1.6.</b>	Summary of the types of monomers polymerised in RAFT.	42
<b>Figure 1.7.</b>	Generic structure for a chemically cross-linked polymer network.	45
<b>Figure 1.8.</b>	Inorganic accelerator systems comprising the zinc dication: zinc dibutyldithiocarbamate (ZDBC) and zinc isopropylxanthate (ZIX).	48
<b>Figure 1.9.</b>	General representation of a multi-functional additive (MFA).	48
<b>Figure 1.10.</b>	The four isomers of poly(2-chloro-1,3-butadiene) (PCB).	49
<b>Figure 1.11.</b>	Comparison of the structures of 1,4- <i>cis</i> -polyisoprene and 1,4- <i>trans</i> -PCB	50
<b>Figure 1.12.</b>	Structure of PCB cross-linked <i>via</i> bis-alkylation with ethylene thiourea (ETU), as suggested by Kovacic.	53
<b>Figure 1.13.</b>	Structures of ETU and piperazine.	53
<b>Figure 1.14.</b>	Generic structures for a surfactant molecule and a micelle.	56
<b>Figure 1.15.</b>	General representation of an emulsion polymerisation system, as adapted from the literature.	57
<b>Figure 1.16.</b>	Illustration of the latex compounding/dipping procedure.	63
<b>Figure 1.17.</b>	Simplified diagram of a typical tensometer.	64
<b>Figure 1.18.</b>	Structure of diisopropyl xanthogen polysulfide (DIXP), where $n = 3, 4$ or $5$ .	69
<b>Figure 2.1.</b>	The dipping procedure adopted for the preparation of PCB latex films.	86
<b>Figure 2.2.</b>	Comparative $^1\text{H}$ NMR spectra (in $\text{CDCl}_3$ ) illustrating the progress of CB polymerisation (RAFT, in CPD/THF conditions) through the appearance of PCB vinyl protons at 5 – 6 ppm (z) and the disappearance of the monomer vinyl proton (y).	87
<b>Figure 2.3.</b>	Simplified diagram of a typical tensometer.	90
<b>Figure 3.1.</b>	$^1\text{H}$ NMR spectrum of CB before (b) and after (a) drying over $\text{MgSO}_4$ .	94
<b>Figure 3.2.</b>	Pure CB $^1\text{H}$ NMR spectrum (a) and PENDANT $^{13}\text{C}$ NMR spectrum (b).	97

<b>Figure 3.3.</b>	Comparative $^1\text{H}$ NMR spectra (in $\text{CDCl}_3$ ) showing the self-polymerisation of CB (a) neat and (b) with 0.1% (w/w) phenothiazine (3.1), under ambient conditions.	99
<b>Figure 3.4.</b>	Comparative GPC data (normalised RI response) for poly(2-chloro-1,3-butadiene) (PCB) originating from pure (—) and crude (---) monomer.	101
<b>Figure 3.5.</b>	The various isomers possible in PCB.	104
<b>Figure 3.6.</b>	FTIR spectrum of PCB.	104
<b>Figure 3.7.</b>	PENDANT $^{13}\text{C}$ NMR spectrum of PCB.	105
<b>Figure 3.8.</b>	$^1\text{H}$ NMR spectra of (a) PCB, indicating the major 1,4- <i>trans</i> isomer, and (b) 1-dodecanethiol.	106
<b>Figure 3.9.</b>	$^1\text{H}$ NMR spectra of PCB, highlighting the minor signals specific to the 1,2- isomer (a), and the major polymer backbone signals ( $\text{CH}_2$ , b).	107
<b>Figure 3.10.</b>	HSQC NMR spectrum for PCB.	108
<b>Figure 3.11.</b>	Structures of the CTAs trialled in the RAFT polymerisation of CB.	110
<b>Figure 3.12.</b>	Styrene, St (3.2), methyl methacrylate, MMA (3.3), and <i>n</i> -butyl acrylate, nBA (3.4): the monomers studied using ethyl <i>S</i> -(thiobenzoyl)thioacetate (3.5), ethyl <i>S</i> -thiobenzoyl-2-thiopropionate (3.6) and <i>S</i> -(thiobenzoyl)thioglycolic acid, TBTA (3.7), RAFT CTAs in work by Farmer and Patten. TBTA was studied herein for CB.	112
<b>Figure 3.13.</b>	Kinetic plots for the polymerisation of CB, in THF and xylene (50 % w/w each), under the following conditions: $[\text{AIBN}]_0/[\text{TBTA}]_0/[\text{CB}]_0 = 0.2/1/45$ at 60 °C. Where $\bullet = M_n$ , $\square = D$ , --- = $M_n^{\text{th}}$ .	113
<b>Figure 3.14.</b>	GPC traces (normalised RI response) showing polymer formation over time for the TBTA polymerisation systems in xylene (a) and THF (b).	114
<b>Figure 3.15.</b>	Structures of vinyl chloride, VC, diisobutyl peroxide, DIBPO and $\alpha,\alpha'$ -azoisobutyronitrile, AIBN.	116
<b>Figure 3.16.</b>	Kinetic plots for the polymerisation of CB, in THF and xylene (50 % w/w each), under the following conditions: $[\text{AIBN}]_0/[\text{CMPCD}]_0/[\text{CB}]_0 = 0.2/1/45$ at 60 °C. Where $\bullet = M_n$ , $\square = D$ , --- = $M_n^{\text{th}}$ .	117
<b>Figure 3.17.</b>	GPC traces (normalised RI response) showing polymer formation over time for the CMPCD polymerisation systems in xylene (a) and THF (b).	118
<b>Figure 3.18.</b>	Kinetic plots for the polymerisation of CB, in THF and xylene (50 % w/w each), under the following conditions: $[\text{AIBN}]_0/[\text{DDMAT}]_0/[\text{CB}]_0 = 0.2/1/45$ at 60 °C. Where $\bullet = M_n$ , $\square = D$ , --- = $M_n^{\text{th}}$ .	121
<b>Figure 3.19.</b>	GPC traces (normalised RI response) showing polymer formation over time for the DDMAT polymerisation systems in xylene (a) and THF (b).	122



<b>Figure 3.20.</b>	Kinetic plots for the polymerisation of CB, in THF and xylene (50 % w/w each), under the following conditions: $[AIBN]_0/[CPD]_0/[CB]_0 = 0.2/1/45$ at 60 °C. Where $\bullet = M_n$ , $\square = \mathcal{D}$ , $--- = M_n^{th}$ .	125
<b>Figure 3.21.</b>	GPC traces (normalised RI response) showing polymer formation over time for the CPD polymerisation systems in xylene (a) and THF (b).	126
<b>Figure 3.22.</b>	Kinetic plots for the polymerisation of CB in bulk at 60 °C for DDMAT and CPD under the following conditions: $[AIBN]_0/[DDMAT]_0/[CB]_0 = 0.2/1/45$ and $[AIBN]_0/[CPD]_0/[CB]_0 = 0.2/1/113$ . Where $\bullet = M_n$ , $\square = \mathcal{D}$ , $--- = M_n^{th}$ .	129
<b>Figure 3.23.</b>	GPC traces (normalised RI response) showing polymer formation over time for the polymerisation systems comprising DDMAT (a) and CPD (b).	130
<b>Figure 3.24.</b>	Kinetic plots for the RAFT polymerisation of CB under the following conditions: $[AIBN]_0/[CPD]_0/[CB]_0 = 0.2/1/45$ at 60 °C in THF (50 % w/w).	132
<b>Figure 3.25.</b>	GPC traces (normalised RI response) of PCB with varying molecular weights, synthesised by RAFT using CPD at 60 °C in THF (50 % w/w).	133
<b>Figure 3.26.</b>	GPC traces (normalised RI response) of the PCB macroCTA and the corresponding PCB- <i>b</i> -PCB following chain extension using CPD CTA.	134
<b>Figure 4.1.</b>	The four isomers of poly(2-chloro-1,3-butadiene) (PCB).	141
<b>Figure 4.2.</b>	FTIR spectrum of PCB.	141
<b>Figure 4.3.</b>	Representative FTIR spectrum collected during the PCB/ETU reaction, highlighting a new peak at 1548 $cm^{-1}$ .	144
<b>Figure 4.4.</b>	Representative FTIR spectrum collected during the PCB/ZnO reaction.	145
<b>Figure 4.5.</b>	Representative FTIR spectrum collected during the PCB/ZnO reaction (A) <i>versus</i> FTIR spectra of ZnCl <sub>2</sub> (B) and ZnO (C).	147
<b>Figure 4.6.</b>	FTIR spectra collected at the start (A) and during (B) the PCB/ETU/ZnO reaction, with emphasis on the new peak formed at 1545 $cm^{-1}$ .	148
<b>Figure 4.7.</b>	FTIR spectrum of the solid by-product from the PCB/ETU/ZnO reaction, whereby the polymer background (neat PCB) has been subtracted.	149
<b>Figure 4.8.</b>	FTIR spectra of the solid products from (A) the ETU/ZnO/HCl test reaction and (B) the ETU/ZnCl <sub>2</sub> test reaction.	150
<b>Figure 4.9.</b>	FTIR spectra of (A) ethylene urea (EU) and (B) solid extracts from the PCB rubber ETU/ZnO reaction performed by Berry, each displaying carbonyl peaks in the 1670 – 1640 $cm^{-1}$ region.	151
<b>Figure 4.10.</b>	FTIR spectra collected during the PCB/PIP reaction (A) and that of the water washed, dried final material (B), where the peaks at 1565 $cm^{-1}$ and 1535 $cm^{-1}$ were eradicated.	155

<b>Figure 4.11.</b>	FTIR spectra, displayed in the 1750 – 525 cm <sup>-1</sup> region, of PIP (A) and acidified PIP (B); the highlighted 1542 cm <sup>-1</sup> peak confirms salt formation.	156
<b>Figure 4.12.</b>	FTIR spectra collected during the PCB/DAB/ZnO reaction, at five minutes (A) and 60 minutes (B), where distinct changes occur in the 1600 – 1500 cm <sup>-1</sup> region.	157
<b>Figure 4.13.</b>	FTIR spectra collected at the start of the PCB/ODT/ZnO reaction (A), and after 10 minutes (B), where the 1569 cm <sup>-1</sup> peak disappears.	158
<b>Figure 4.14.</b>	FTIR spectra collected during the PCB/TbuT reaction, where the 1486 cm <sup>-1</sup> peak at the start (A) disappears within 30 minutes (B).	159
<b>Figure 4.15.</b>	FTIR spectrum collected at the end of the PCB/TbuT/ZnO reaction, highlighting a new peak at 1560 cm <sup>-1</sup> .	160
<b>Figure 4.16.</b>	Comparison of Zn <sup>2+</sup> -complexed TbuT and PNA-5 structures, where Bu denotes a linear butyl group.	167
<b>Figure 4.17.</b>	FTIR spectrum of PNA-5 (A) and representative spectrum collected during a PCB/PNA-5 cross-linking reaction (B).	168
<b>Figure 4.18.</b>	Representative FTIR spectrum collected during the PCB/PNA-5/ZnO cross-linking reaction, with newly formed peaks highlighted.	168
<b>Figure 4.19.</b>	Structure of 1,4-MFA.	169
<b>Figure 5.1.</b>	Image of the final PCB/DPTU/DPG latex film (A), which has been cut into dumbbells prior to tensile testing.	176
<b>Figure 5.2.</b>	The change in viscosity over time for the PNA-5 dispersion, stored at 40 °C (1, denoted by ●) and at room temperature (2, denoted by □).	178
<b>Figure 5.3.</b>	Image of the final PCB/PNA-5 latex film (B).	181
<b>Figure 5.4.</b>	Structure of 1,4-MFA.	181
<b>Figure 5.5.</b>	Images of the final PCB/PNA-5/1,4-MFA latex films, whereby the formulations comprised contrasting levels of ZnO (film C: 5 phr ZnO; film D: 1 phr ZnO).	183
<b>Figure 5.6.</b>	Structure of diisopropyl xanthogen polysulfide (DIXP), where n = 3, 4 or 5.	184
<b>Figure 5.7.</b>	Images of the final PCB/PNA-5/DIXP latex films, whereby the formulations comprised contrasting levels of ZnO (film E: 5 phr ZnO; film F: 1 phr ZnO).	186
<b>Figure 5.8.</b>	Images of the final PCB/PNA-5/TBzTD latex films, whereby the formulations comprised different levels of ZnO (film G: 5 phr ZnO; film H: 1 phr ZnO) and film H comprised 1,4-MFA (0.5 phr).	190
<b>Figure 5.9.</b>	Structure of 2,2'-dithio di(ethylammonium)-bis(dibenzylthiocarbamate) (PNA-8).	191
<b>Figure 5.10.</b>	Image of the final PCB/DIXP/PNA-8 latex films (I).	192

- Figure 5.11.** Comparison of UTS for PCB latex films made using PNA-5 combined with 1,4-MFA (red, C and D), DIXP (green, E and F) and TBzTD (blue, G and H), where the latter datum represents a lower level of ZnO in each case (1 phr *versus* 5 phr). Error bars indicate one standard deviation from ten data points. The dashed line represents the industrial standard UTS value (*i.e.* film A, 23.7 MPa). 195
- Figure 5.12.** Comparison of 300 % modulus for PCB latex films made using PNA-5 combined with 1,4-MFA (red, C and D), DIXP (green, E and F) and TBzTD (blue, G and H), where the latter datum represents a lower level of ZnO in each case (1 phr *versus* 5 phr). Error bars indicate one standard deviation from ten data points. The dashed line represents the industrial standard 300 % modulus value (*i.e.* film A, 2.40 MPa). 196
- Figure 5.13.** Comparison of elongation at break for PCB latex films made using PNA-5 combined with 1,4-MFA (red, C and D), DIXP (green, E and F) and TBzTD (blue, G and H), where the latter datum represents a lower level of ZnO in each case (1 phr *versus* 5 phr). Error bars indicate one standard deviation from ten data points. The dashed line represents the industrial standard elongation at break value (*i.e.* film A, 861 %). 197
- Figure 5.14.** Comparison of tensile test data for PCB latex films made using DPTU/DPG (purple, A) and DIXP/PNA-8 (orange, I). Error bars indicate one standard deviation from ten data points. 201
- Figure 6.1.** Structures of the CTAs trialled in the RAFT polymerisation of CB. 209
- Figure 6.2.** Kinetic plots for the optimum RAFT polymerisation of CB under the following conditions:  $[AIBN]_0/[CPD]_0/[CB]_0 = 0.2/1/45$  at 60 °C in THF (50 % w/w). 210
- Figure 6.3.** Structure of piperazine-1-carbodithioic acid 1,3-diaminopropane complex (PNA-5). 214

## List of Schemes

<b>Scheme 1.1.</b>	The mechanism of conventional free radical chain polymerisation.	27
<b>Scheme 1.2.</b>	The decomposition of $\alpha,\alpha'$ -azoisobutyronitrile (AIBN).	27
<b>Scheme 1.3.</b>	Examples of termination by combination of styrene, St, (a) and disproportionation of methyl methacrylate, MMA, (b).	28
<b>Scheme 1.4.</b>	General scheme for the persistent radical effect (PRE).	33
<b>Scheme 1.5.</b>	The method of reversible termination (deactivation) of NMP, as mediated by the TEMPO radical.	34
<b>Scheme 1.6.</b>	The reversible redox process of the ATRP mechanism, catalysed by a transition metal complex. Mt represents the metal atom and L is the ligand; Y can be a counterion or another ligand.	35
<b>Scheme 1.7.</b>	The mechanism of RAFT polymerisation.	37
<b>Scheme 1.8.</b>	The zwitterionic canonical form of an O-alkylxanthate (also applicable to dithiocarbamates, where the oxygen atom is replaced by nitrogen)	40
<b>Scheme 1.9.</b>	Allylic rearrangement of the chlorine atom in 1,2-PCB.	50
<b>Scheme 1.10.</b>	The tautomeric forms of ethylene thiourea (ETU, 1.5).	50
<b>Scheme 1.11.</b>	The cationic mechanism for cross-linking PCB, as facilitated by ZnO, proposed by Desai <i>et al.</i>	52
<b>Scheme 1.12.</b>	The mechanism of cross-linking PCB with ETU and ZnO, as originally proposed by Pariser and modified from the literature.	54
<b>Scheme 2.1.</b>	The synthesis of 2-chloro-1,3-butadiene (CB) by the dehydrochlorination of 3,4-dichloro-1-butene, where PTC denotes a phase-transfer catalyst.	79
<b>Scheme 2.2.</b>	The uncontrolled polymerisation of 2-chloro-1,3-butadiene (CB) using 1-dodecanethiol CTA (the main 1,4- <i>trans</i> polymer isomer configuration is shown).	79
<b>Scheme 2.3.</b>	The RAFT polymerisation of 2-chloro-1,3-butadiene (CB,) using 2-cyano-2-propylbenzodithioate, CPD, CTA (the main 1,4- <i>trans</i> polymer isomer configuration is shown).	80
<b>Scheme 3.1.</b>	The synthesis of 2-chloro-1,3-butadiene (CB) by the dehydrochlorination of 3,4-dichloro-1-butene, where PTC denotes a phase-transfer catalyst.	92
<b>Scheme 3.2.</b>	The dehydrochlorination of 3,4-dichloro-1-butene by base, the <i>E1</i> reaction.	94

<b>Scheme 3.3.</b>	The uncontrolled polymerisation of 2-chloro-1,3-butadiene (CB) using 1-dodecanethiol CTA (the main 1,4- <i>trans</i> polymer isomer configuration is shown).	100
<b>Scheme 3.4.</b>	The RAFT polymerisation of 2-chloro-1,3-butadiene (CB) using <i>S</i> -(thiobenzoyl)thioglycolic acid, TBTA, CTA (the main 1,4- <i>trans</i> polymer isomer configuration is shown).	112
<b>Scheme 3.5.</b>	The RAFT polymerisation of 2-chloro-1,3-butadiene (CB) using cyanomethyl methyl(phenyl)carbamodithioate, CMPCD, CTA (the main 1,4- <i>trans</i> polymer isomer configuration is shown).	116
<b>Scheme 3.6.</b>	The RAFT polymerisation of 2-chloro-1,3-butadiene (CB) using <i>S</i> -1-dodecyl- <i>S'</i> -( $\alpha,\alpha'$ -dimethyl- $\alpha''$ -acetic acid)trithiocarbonate, DDMAT, CTA (the main 1,4- <i>trans</i> polymer isomer configuration is shown).	120
<b>Scheme 3.7.</b>	The RAFT polymerisation of 2-chloro-1,3-butadiene (CB) using 2-cyano-2-propylbenzodithioate, CPD, CTA (the main 1,4- <i>trans</i> polymer isomer configuration is shown).	124
<b>Scheme 4.1.</b>	The PCB/ETU cross-linking mechanism according to Kovacic.	143
<b>Scheme 4.2.</b>	The ether linkage theory of cross-linking PCB with ZnO, as adapted from the review by Aprem <i>et al.</i>	145
<b>Scheme 4.3.</b>	The Desai (2a) and Vukov (2b) mechanisms of cross-linking PCB, where both are preceded by allylic rearrangement of 1,2-PCB (step 1).	146
<b>Scheme 4.4.</b>	The mechanism of cross-linking PCB with ETU and ZnO, as originally proposed by Pariser and adapted from the literature.	152
<b>Scheme 4.5.</b>	The tautomeric forms of ethylene thiourea (ETU, 4.1), where mercaptoimidazoline (4.2) is present at 58 %.	154
<b>Scheme 4.6.</b>	Allylic rearrangement of the 1,2-PCB isomer.	161
<b>Scheme 4.7.</b>	The Kovacic mechanism of cross-linking PCB with ETU and ZnO in unison.	163
<b>Scheme 4.8.</b>	The new mechanism of cross-linking PCB by ETU and ZnO in unison, which is similar to that of Pariser.	164
<b>Scheme 5.1.</b>	Zn <sup>2+</sup> -complexed TBzTD, where Bz denotes a benzyl group.	188
<b>Scheme 6.1.</b>	The synthesis of 2-chloro-1,3-butadiene (CB) by the dehydrochlorination of 3,4-dichloro-1-butene, where PTC denotes a phase-transfer catalyst.	207
<b>Scheme 6.2.</b>	The uncontrolled polymerisation of 2-chloro-1,3-butadiene (CB) using 1-dodecanethiol CTA (the main 1,4- <i>trans</i> polymer isomer configuration is shown).	208

## List of Equations

<b>Equation 1.1.</b>	Number-average molecular weight ( $M_n$ ).	24
<b>Equation 1.2.</b>	Weight-average molecular weight ( $M_w$ ).	24
<b>Equation 1.3.</b>	Molecular weight dispersity ( $\mathcal{D}$ ).	25
<b>Equation 1.4.</b>	The Mayo Equation.	28
<b>Equation 1.5.</b>	Estimating transfer coefficient (of RAFT CTA).	38
<b>Equation 1.6.</b>	Rate of (emulsion) polymerisation ( $R_p$ ).	58
<b>Equation 2.1.</b>	Conversion of CB into PCB through $^1\text{H}$ NMR spectroscopy.	88

# **CHAPTER 1**

## **INTRODUCTION**

## 1. Introduction

This thesis comprises six distinct chapters, including a general survey of the relevant literature to introduce the project (Chapter 1), a description of the experimental procedures undertaken (Chapter 2) and three disparate sections devoted to the discussion of results. The final chapter provides an overall conclusion and explores the future research which is to be undertaken. A concise introduction precedes each of the results chapters, which in turn discuss the controlled polymerisation of 2-chloro-1,3-butadiene (CB, Chapter 3) and two industrially-driven ventures, concerning the cross-linking of poly(2-chloro-1,3-butadiene) (PCB) oligomers and the development of a novel latex formulation for this polymer (chapters 4 and 5, respectively).

### 1.1. Definitions for polymers and polymerisation methods

A polymer is defined by its size or molecular weight, which can in turn determine the application which it is suitable for. High molecular weight can contribute considerable mechanical strength,<sup>1</sup> but this can be detrimental to other properties, such as solubility. Polymeric material is comprised of molecules of different sizes, so there can only ever exist an average molecular weight.<sup>2</sup> Commonly stated is the number-average molecular weight, denoted by  $M_n$ , which describes the average of the molecular weights within the sample,<sup>2</sup> *i.e.* the total mass of all the polymer chains divided by the total number of chains (Equation 1.1).  $M_n$  can be found experimentally through techniques such as gel permeation chromatography (GPC) and end group analysis (*e.g.* using nuclear magnetic resonance, NMR, spectroscopy). The weight-average molecular weight, expressed as  $M_w$  (see Equation 1.2), can also be calculated through GPC, but additionally by light scattering which is a method more influenced by the size of the polymer molecules,<sup>3</sup> where larger chains are more significant as they take up more of the sample. From  $M_n$  and  $M_w$ , one can calculate the dispersity ( $\mathcal{D}$ ), which expresses the distribution of molecular weight in a polymer sample (Equation 1.3). This can be conveniently obtained from GPC analysis, which separates polymer molecules according to their size.<sup>2</sup> The closer the dispersity value is to 1, the more monodisperse the sample (*i.e.* the molecular weight distribution is narrow); as the value of  $\mathcal{D}$  increases, the more disperse the molecular weight of the polymer (*i.e.* the bigger the range of molecular weights).

$$\text{Number-average molecular weight, } M_n = w / \sum N_x = \sum N_x M_x / \sum N_x \quad (\text{Eq}^n \text{ 1.1})$$

$$\text{Weight-average molecular weight, } M_w = \sum w_x M_x = \sum W_x M_x / \sum W_x \quad (\text{Eq}^n \text{ 1.2})$$



$$\text{Molecular weight dispersity, } \bar{D} = M_w / M_n \quad (\text{Eq}^n \text{ 1.3})$$

Where  $W_x$  defines the weight,  $w_x$  is the weight-fraction of molecules with a molecular weight  $M_x$  and the number of moles is given by  $N_x$ .

Two classes of polymer synthesis methods exist: step-growth and chain polymerisation. The former class comprises polymers which are synthesised by intermolecular reactions between monomers with different functionalities. Step-growth polymerisation was pioneered by Carothers, who originally termed this as “condensation” because the reaction between two different types of monomer molecules typically eliminated water.<sup>4</sup> This is now known to not be the case as water is not exclusively the by-product of these reactions and, as for polyurethanes, the step-growth reaction may proceed without any elimination occurring at all.<sup>3</sup> Polyesters, polyamides, polyanhydrides and polysiloxanes are also step-growth polymers and have important applications as a variety of materials, such as in fibres, adhesives and elastomers.<sup>3</sup>

Chain polymerisation comprises addition reactions whereby no elimination of by-products occurs, as in step-growth polymerisation. Figure 1.1 adequately summarises the difference between the two systems,<sup>1, 2</sup> and how the degree of polymerisation (or molecular weight) evolves over time for each. It is demonstrated that chain polymerisation forms high molecular weight polymer in the early stages of the reaction, whereas the molecular weight increases slowly in a step-growth reaction, as small polymers (e.g. dimers, trimers) and monomers are prevalent until high conversion is reached.<sup>2</sup> Notably, chain polymerisation also furnishes higher molecular weight polymer than in step-growth, due to the random, rapid nature of active centres reacting together. Also shown in Figure 1.1 is the trend line for controlled polymerisation systems for comparison, where the molecular weight increases linearly with monomer conversion. Controlled polymerisation is discussed in Section 1.1.2, with a heavy emphasis on controlled-radical techniques.

Chain polymerisation is discussed in more detail in Section 1.1.1, in terms of the type of free radical mechanism, as it is more relevant to the reactions of 2-chloro-1,3-butadiene (CB) undertaken during this project. Whilst such conventional methods are favoured generally in industry,<sup>5</sup> the subsequent discovery of controlled reaction systems<sup>6-9</sup> has enabled polymer chemists to accurately predefine polymers, achieving targeted molecular weights, narrow molecular weight distributions and designing complex architectures.<sup>2</sup>

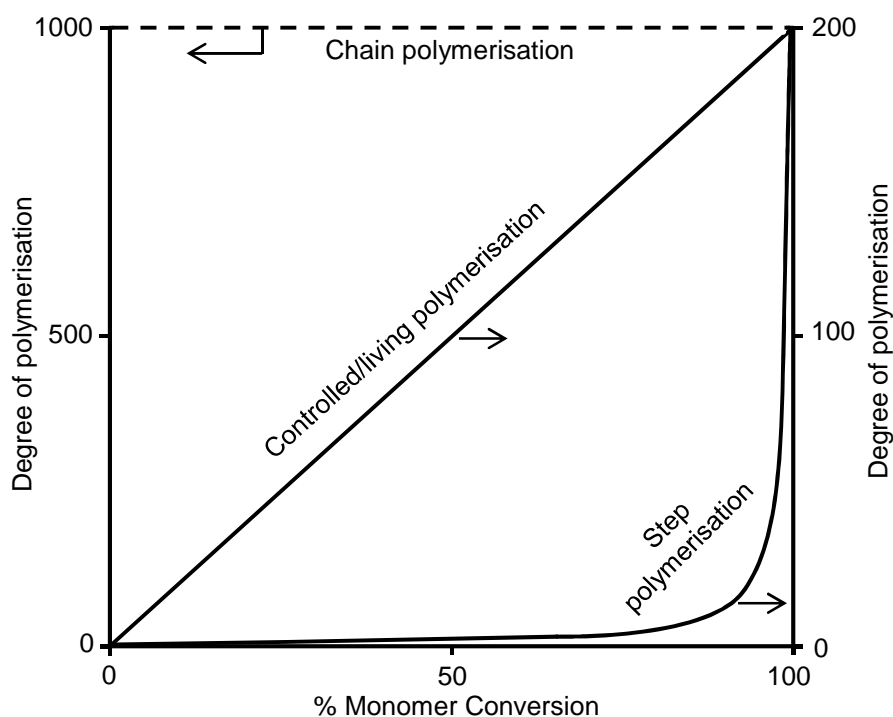


**Figure 1.1. Graph illustrating the change in degrees of polymerisation ( $D_p$ ) with monomer conversion for the different types of polymerisation reactions.<sup>1,2</sup>**

### **1.1.1. Conventional (uncontrolled) free radical chain polymerisation**

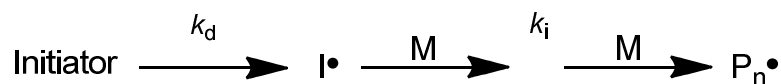
Free radical chain polymerisation is widely used to synthesise high molecular weight polymers readily; due to its versatility, such a reaction can incorporate a wide range of monomer types and can be carried out under a wide range of reaction conditions.<sup>10, 11</sup> Regarded as a 'conventional' system (*i.e.* within industry) throughout this thesis, the process essentially comprises a chain reaction which is facilitated by the breakdown of an initiator reagent and subsequently carried through by a carbon-centred radical.<sup>2</sup>

#### 1.1.1.1. Free radical chain polymerisation mechanism

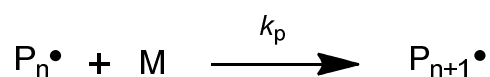
Monomers which are polymerised by chain reactions generally possess the necessary  $\pi$ -bonds which can be activated by an initiator, causing electrons to move and the generation of propagating radicals. The free radical mechanism comprises three stages, instigated by the breakdown of initiator and creation of an active centre (which the monomer reacts with) during *initiation*. Sequential addition of monomer units to this radical in the *propagation* step then causes the macromolecular chain to grow. This growth is eventually *terminated* when

the active centres combine, disproportionate or are transferred elsewhere.<sup>3</sup> Scheme 1.1 illustrates these processes, as adapted from the version of Mandal.<sup>2</sup>

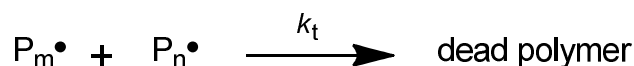
### 1. Initiation



### 2. Propagation

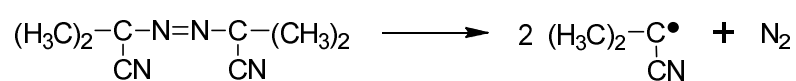


### 3. Termination



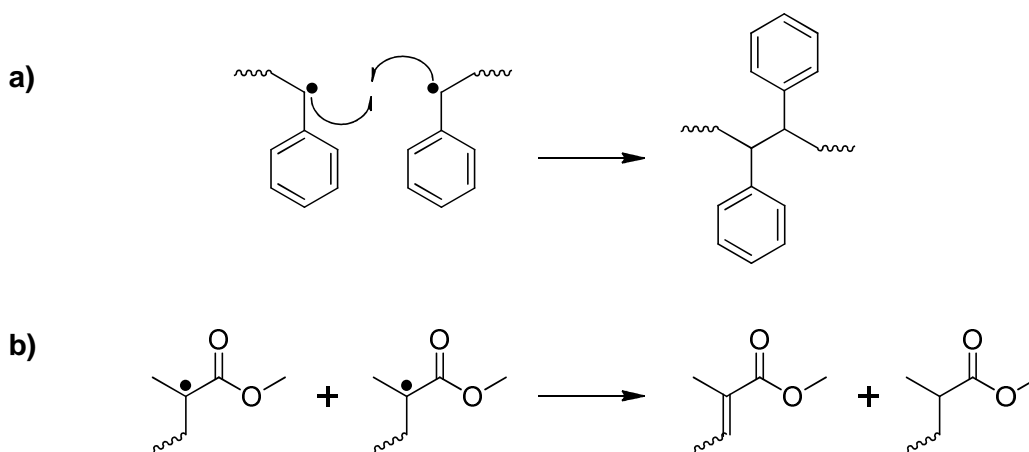
**Scheme 1.1. The mechanism of conventional free radical chain polymerisation.<sup>2</sup>**

Initiator compounds undergo homolytic fission, which produces the free radicals necessary to react with monomer, in turn generating the active centre. This is achieved either thermally, chemically or by the use of radiation.<sup>3</sup> Common types of initiator are azo compounds (e.g.  $\alpha,\alpha'$ -azoisobutyronitrile, AIBN), peroxides (e.g. lauroyl peroxide) and persulfates (e.g. potassium persulfate). Notably, when initiators decompose, two radicals are formed, as shown in Scheme 1.2 for AIBN, which has a half-life ( $t_{1/2}$ ) of 1.3 hours at 80 °C,<sup>12</sup> or 21 hours at 60 °C,<sup>13</sup> and was the principal initiator used during this research.



**Scheme 1.2. The decomposition of  $\alpha,\alpha'$ -azoisobutyronitrile (AIBN).<sup>3</sup>**

Propagation simply involves the addition of monomer molecules to the chain carrier, which orchestrates chain growth. This is halted most commonly when two radicals either combine (combination) or when one radical abstracts a hydrogen atom from the end of another activated chain (disproportionation). In combination, a single long chain is produced, whereas disproportionation yields two 'dead' polymer chains of which one becomes unsaturated.<sup>3</sup> Each of these instances is demonstrated in Scheme 1.3; styrene (St) terminates most commonly by combination to give a head-to-head product,<sup>14</sup> whereas methyl methacrylate (MMA) terminates mainly by disproportionation.<sup>3</sup>



**Scheme 1.3. Examples of termination by combination of styrene, St, (a)<sup>14</sup> and disproportionation of methyl methacrylate, MMA, (b).<sup>3</sup>**

Whereas termination sees the active radical become paired up and ultimately destroyed, the free radical is never destroyed during propagation, merely transferred. Chain transfer of this unpaired electron to another molecule can also occur and is effectively another means to terminate polymer growth.<sup>15</sup> The initiator (such as a peroxide), a solvent, a polymer chain, or another reagent, such as an alkyl mercaptan (*i.e.* a modifier), can be the objects of transfer reactions. As the average polymer chain length is defined by the rate of polymerisation ( $R_p$ ) divided by the sum of all termination reactions,<sup>15</sup> it can be appreciated that chain transfer generally causes a decrease in the observed polymer molecular weight (as termination is more widespread).

Chain transfer to initiator, solvent or modifier reduces the degree of polymerisation ( $D_p$ ), whereas branching results when polymer chains are the subjects of these (inter- or intramolecular) reactions.<sup>3, 15</sup> Modifiers are often employed to regulate the molecular weight, as these purposefully bring about chain transfer; the weak sulfur-hydrogen bond of thiols, for example, can facilitate this as such molecules possess high chain transfer constants ( $C_s$ ).<sup>3</sup> The value of  $C_s$  can be derived using the Mayo equation,<sup>16</sup> as given in Equation 1.4, which is itself defined as the ratio of the rate of transfer to the rate of propagation ( $k_{tr} / k_p$ ).<sup>17</sup> In the expression,  $D_p$  is the number-average degree of polymerisation at any given time in the polymerisation, whereas the term  $(D_p)_0$  is that in the absence of chain transfer. When chain transfer can occur to a variety of species in the reaction (initiator, monomer, polymer and solvent, for instance), additional terms within this equation are necessary; herein, [T] denotes the concentration of the generic chain transfer agent and [M] is the concentration of monomer.<sup>17</sup> Where chain transfer takes place in a free radical chain polymerisation, the value of  $D_p$  is reduced.<sup>17</sup>

$$1 / D_p = 1 / (D_p)_0 + C_s([T] / [M]) \quad (\text{Eq}^n 1.4)$$

### 1.1.1.2. Other factors influencing polymerisation

Polymerisations are complex systems and reaction conditions are tailored to suit the monomer/s involved. Whilst the monomer-initiator combination is directly related to the free radical mechanism, other factors, such as temperature, can influence how the reaction proceeds and thus affect the molecular weight and dispersity of the final polymer.

#### 1.1.1.2.1. Temperature

Selecting the appropriate temperature for a given polymerisation is a compromise between various factors, including the properties of the initiator (*i.e.* the half-life value,  $t_{1/2}$ ), and the boiling points of the monomer and solvent. The temperature influences the decomposition rate of the initiator and the rates of propagation, termination and chain transfer. In particular, the decomposition temperature of the initiator should match that adopted for the reaction so that an appropriate source of radicals is made available (as defined by  $t_{1/2}$ ). Generally, an increase in temperature will enhance the overall polymerisation rate,<sup>2</sup> but, in these conventional systems, the lengths of the polymer chains will be detrimentally affected due to more termination being effected (as a result of the higher concentration of free radicals present). This can also cause broadening of the molecular weight distribution (as indicated by higher values of  $\mathcal{D}$ ).<sup>3</sup>

#### 1.1.1.2.2. Form of polymerisation

Polymerisation reactions can be carried out in homogenous conditions, whereby all of the reagents dissolve in the reaction medium (*i.e.* solutions), or the reactions can be heterogeneous (*i.e.* suspensions, dispersions or emulsions).

Bulk polymerisation reactions are those carried out without any solvent, where the monomer itself acts as the reaction medium. Free radical polymerisations are exothermic in nature; in the absence of solvent, the reaction medium becomes highly viscous very readily, leading to laboured mixing and thus poor distribution of evolved heat.<sup>18</sup> Solution conditions, in contrast, are those where solvent is employed, which helps to reduce the viscosity of the reaction medium and encourage heat transfer. However, the presence of solvent can be an added complication, especially considering the varying solubilities of reagents, and, as already ascertained in Section 1.1.1.1, chain transfer to solvent can occur.<sup>3</sup> Removal of the solvent (post-polymerisation) is also a necessity, which can be costly for industrial processes; environmental concerns may also arise due to an associated toxicity with the solvent.

Although the rate of polymerisation can be lowered by dilution of the monomer in a solvent,<sup>19-</sup>  
<sup>21</sup> the practical difficulties of a bulk system are avoided.

Heterogeneous systems comprise one or more components which are insoluble in the reaction medium. These can be the polymer itself, for example in precipitation, or “popcorn”, polymerisation,<sup>22</sup> where each constituent is soluble, except the polymer. In this instance the polymer precipitates out of solution once a certain molecular weight is surpassed.<sup>23</sup> Conversely, dispersion polymerisation sees the polymer remain dispersed in an aqueous medium, owing to the presence of a stabiliser reagent. Suspension polymerisation can also comprise water; in this case, however, organic solvents can also be adopted provided that the monomer, initiator and polymer are insoluble. Polymerisation then proceeds within monomer droplets, which are suspended in the solvent and the resultant polymer particles are prevented from aggregating by a polymeric stabiliser.<sup>2</sup>

Emulsion polymerisation is another heterophase system comprising aqueous media and is especially beneficial because the system again counteracts the exothermic free radical reaction.<sup>18</sup> On the whole, however, this system is particularly complex and was not necessary to adopt during this project. A number of publications comprehensively review this subject and should be regarded for reference;<sup>24-26</sup> an overview is provided in Section 1.3.1.

#### *1.1.1.2.3. Inhibitors/retarders*

Chemical reagents can also be employed to reduce the rate or degree of polymerisation (known as retarders), or evade it altogether (inhibitors).<sup>2</sup> The former are especially useful for the safe storage of monomers and are commonly used for particularly reactive derivatives, such as butadiene compounds. In these cases, an organic compound (inhibitor) is incorporated at a low concentration to scavenge any free radicals and prevent self-polymerisation from taking place. Such compounds include phenothiazine,<sup>27</sup> which has proven vital in stabilising 2-chloro-1,3-butadiene (CB) monomer during this research<sup>28</sup> (see Section 3.1.5) and 4-hydroxy-TEMPO which has been shown to stabilise methacrylic macromonomers.<sup>29</sup> Chain transfer agents effectively act as retarders.<sup>3</sup> Free radical (chain) polymerisations are generally carried out under an inert atmosphere, where oxygen is eradicated from the system entirely. Oxygen is a radical scavenger and a notorious inhibitor.<sup>30</sup>

#### *1.1.1.3. General features of conventional free radical chain polymerisation*

In summary, relatively long polymer chain lengths are furnished in the early stages of a conventional free radical (chain) polymerisation and shorter chains form once the monomer

becomes exhausted, as the reaction progresses.<sup>11</sup> The reaction time can be increased, but this will only potentially improve the yield, and not necessarily enhance the molecular weight. Similarly, a more rapid reaction rate can be achieved by increasing the temperature of the system, but the degree of polymerisation ( $D_p$ ) will be sacrificed, due to more radicals being present and the propensity of them to terminate.<sup>3</sup> Broad molecular weight distributions are another fundamental trait, often yielding high  $\bar{D}$  values (typically  $>2$ ).<sup>11</sup> As each free radical only has a finite lifetime, and reactions can proceed for a considerable duration, each polymer chain has a short lifetime, and controlling the polymer architecture is thus not possible.<sup>31</sup> The following section (1.1.2) discusses how this conventional system can be modified in such a way that polymer syntheses can be precisely controlled.

### **1.1.2. Controlled-radical polymerisation methods**

Ahead of discussing the various controlled-radical polymerisation techniques, certain alternative polymerisation methods not involving radicals are summarised herein, for comparative purposes. Of particular significance is anionic polymerisation, which was discovered by Szwarc in the 1950s.<sup>32</sup> This chain technique adopts anions as the active centres (rather than radicals), which are generated by electron transfer from an alkali metal, for example. The anionic mechanism proceeds in such a way that termination and chain transfer can be completely avoided by employing the correct solvent-initiator combination.<sup>2</sup> Unlike radical chain polymerisation, anionic termination does not involve two growing species; termination is achieved most often through chain transfer of the negative charge to solvent or monomer. If no reactive solvent is therefore present, termination will not occur until the monomer becomes completely exhausted (*i.e.* full conversion is reached). Hence, the polymers furnished in this way retain active sites which can react further upon addition of extra monomer.<sup>33</sup> The potential absence of termination is the key feature of the anionic process and the polymers manufactured in this way. However, such a procedure is somewhat restricted by stringent reaction conditions; special efforts to completely exclude moisture, and the use of high purity reagents, mean that controlled-radical techniques are often preferred, especially in industry.<sup>10</sup>

Group transfer polymerisation (GTP) is another (non-radical) controlled polymerisation method, which is especially suited to polar monomers.<sup>3</sup> This technique was originally developed because a controlled polymerisation process was required for application in industry; the typically low temperature (sub-zero) anionic polymerisations of (meth)acrylates are not industrially cost-effective.<sup>2</sup> Webster and co-workers conceived GTP at DuPont, USA, in the mid-1980s, working with MMA and other acrylate monomers,<sup>34, 35</sup> the process has since become integral to the company, particularly in manufacturing pigmented inks for ink

jet printers.<sup>36</sup> The basis of the GTP reaction is a successive Michael addition of an organosilicon compound to an  $\alpha,\beta$ -unsaturated ester, ketone, nitrile or carboxamide derivative.<sup>34</sup> This is initiated by a silyl ketene acetal, such as 1-methoxy-1-trimethylsiloxy-2-methyl-1-propene (Figure 1.2). A small amount of a nucleophilic co-catalyst, in the form of Lewis acids (e.g. zinc halides or dialkylaluminium chlorides or oxides) or anions (e.g. cyanides, fluorides, bifluorides or azides),<sup>37</sup> reversibly activates the initiator.<sup>2</sup> Propagation then proceeds through the transfer of the silyl group to the monomer, so that polymer chains grow intermittently through activation-deactivation cycles.<sup>2</sup> The distinction between GTP and anionic polymerisation is the form of the (dormant) polymer end group, which, in the former, comprises silyl functionality.<sup>2</sup> Upon introducing additional monomer, this end group is capable of reacting further, which can facilitate the efficient production of well-defined copolymers and other complex architectures.<sup>38-40</sup> Although a diverse range of monomers can be polymerised by GTP, such as (meth)acrylates,<sup>41-44</sup> acrylonitrile<sup>45</sup> and *N,N*-dialkyl(meth)acrylamides,<sup>34, 37, 46</sup> this method also requires comparably stringent reaction conditions to those necessary for regular anionic polymerisation.<sup>3</sup>

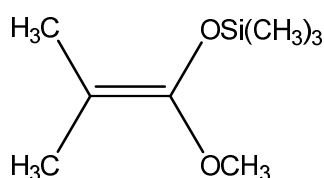


**Figure 1.2. 1-Methoxy-1-trimethylsiloxy-2-methyl-1-propene initiator adopted in group transfer polymerisation (GTP).**

Further discussions on other (non-radical) controlled methods, such as cationic and ring-opening polymerisation, are not provided herein; the reader is directed to the appropriate reviews for details on these processes.<sup>47-49</sup> This project primarily concerned controlled-radical polymerisation methods, which are considered in the following sections.

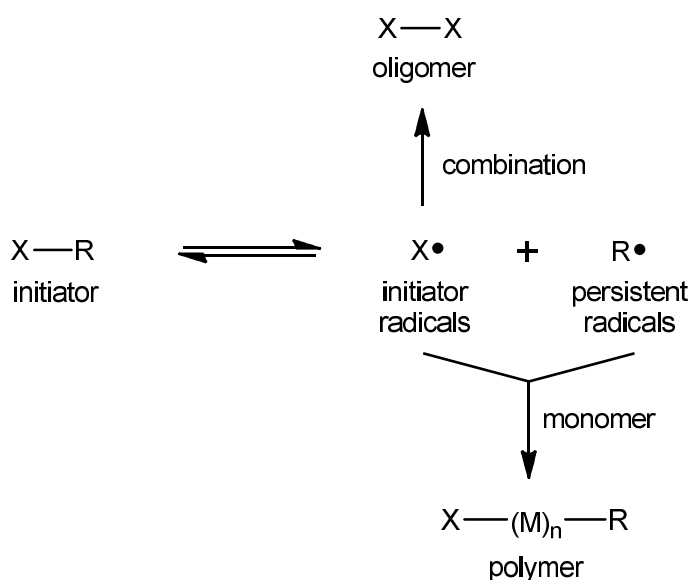
Controlled polymerisations (compared to conventional processes, discussed in Section 1.1.1) involve minimal termination during the reaction (*N.B.* it cannot be eradicated completely due to the propensity of radicals to combine or neutralise through disproportionation). Controlled-radical polymerisations achieve this through either reversible termination or reversible (degenerative) chain transfer, which is facilitated by specialised reagents and reaction conditions. Both of these types of mechanisms involve an equilibrium existing between active and dormant/stable species. Controlled systems allow for the prediction of molecular weight and enable the synthesis of near-monodisperse ( $\mathcal{D}$  usually  $<1.1$ ),<sup>50</sup> dormant polymer with defined, reactive chain ends.<sup>2</sup>

In contrast to the conventional method, when a radical polymerisation is controlled, all polymer chains grow at similar rates and survive for the duration of the polymerisation.



Initiation is fast with respect to propagation and termination is suppressed, which ultimately ensures narrow dispersity. Specialised reagents enable the reversible deactivation of propagating radicals, rendering most polymer chains dormant, whilst only a low concentration of active species are present at any time. Thus, rapid equilibration between active and dormant species provides all chains an equal chance of growing, albeit intermittently. These conditions allow the molecular weight to increase linearly with monomer conversion, whereas conventional, uncontrolled systems afford high molecular weight polymer in the initial stages.<sup>11</sup> This is adequately demonstrated previously in Figure 1.1, alongside the trends for step-growth and uncontrolled chain polymerisations.

Those techniques which impart controlled character to a radical system include atom transfer radical polymerisation (ATRP), nitroxide-mediated radical polymerisation (NMP) and RAFT polymerisation. NMP and ATRP achieve control by reversible termination (or deactivation),<sup>51</sup> where the growing polymer chain interacts with the metal halide of a complex (ATRP),<sup>52</sup> or an alkoxyamine initiator is employed (NMP).<sup>11</sup> This is known as the persistent radical effect (PRE). As depicted in Scheme 1.4, mediating or persistent radicals are expelled through the breakdown of initiator and do not self-terminate because they are highly stable. Thus, R• radicals are present at a higher concentration than initiator radicals (X•); as the concentration of R• increases, the formation of dormant polymer with defined chain ends becomes more efficient. This relationship between termination and mediation ultimately defines PRE and is what ultimately causes the polymerisation process to be controlled.<sup>10</sup>



**Scheme 1.4. General scheme for the persistent radical effect (PRE).<sup>10</sup>**

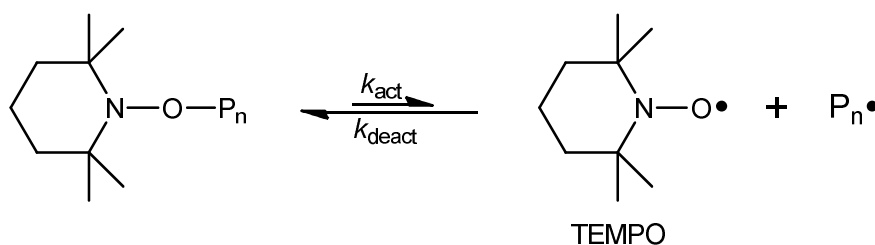
The primary controlled-radical technique adopted over the course of this project was RAFT polymerisation, whereby the mechanism involves reversible (degenerative) chain transfer.<sup>53</sup> This concerns interchange of the active centre<sup>54</sup> and furnishes new dormant and active

species of the same relative reactivity to the originals.<sup>55</sup> RAFT is discussed after briefly defining NMP and ATRP, respectively.

#### 1.1.2.1. General features of nitroxide-mediated radical polymerisation (NMP)

As is typical for a controlled polymerisation, the polymer molecular weight increases linearly with monomer conversion in NMP. This means that all polymer chains are initiated at the start of the reaction and subsequently grow at the same rate, where control is imparted by the reversible termination of propagating radicals. It is also possible to deduce the theoretical molecular weight by specifying the monomer:initiator ratio. Narrow molecular weight distribution (low  $\bar{D}$ ) polymer can be afforded, but this is only achievable if the initiation step is more rapid than propagation, as is the case for controlled-radical methods in general.

The key reagents in NMP are nitroxides, or their alkylated derivatives, alkoxyamines, which take the form of  $R\bullet$  and act as initiators and mediators. They function by reversibly capping growing polymer chains, therefore minimising the occurrence of termination. 2,2',6,6'-Tetramethyl-1-piperidinyloxy (TEMPO) nitroxide has been integral to a number of NMP studies;<sup>56-60</sup> Scheme 1.5 illustrates the crucial reversible termination (deactivation) step in the NMP reaction with TEMPO, where nitroxides reversibly “trap” the propagating radicals ( $P_n\bullet$ ).<sup>61</sup>



**Scheme 1.5. The method of reversible termination (deactivation) of NMP, as mediated by the TEMPO radical.**<sup>62, 63</sup>

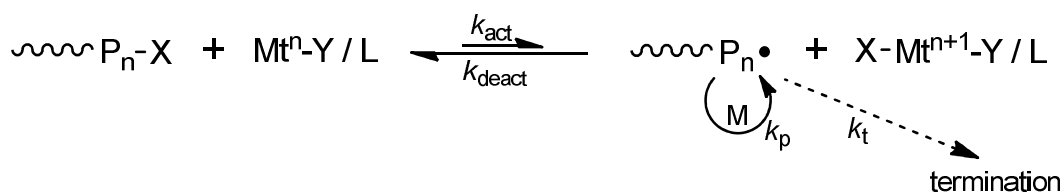
NMP can be conducted in a wide range of conditions, but certain disadvantages exist for this technique, including the high temperatures generally required and the complex initiator systems.<sup>64</sup> For instance, reactions involving TEMPO (and derivatives thereof) require temperatures higher than the boiling point of water, which has thus necessitated the use of high pressure apparatus.<sup>10</sup> The rate of polymerisation can also be slow because of the low concentration of propagating radicals<sup>65</sup> and an induction period can often be observed when nitroxides are generated *in situ*.<sup>61</sup> Overall, NMP can be a complicated process to master and other techniques, such as ATRP and RAFT, are more versatile and can be simpler to

conduct (especially in case of the latter). These are considered, in turn, in the succeeding sections.

#### 1.1.2.2. General features of atom transfer radical polymerisation (ATRP)

As for NMP, the polymer molecular weight increases linearly over time in ATRP reactions. Again, this is the key feature and advantage of this polymerisation technique, along with the narrow molecular weight distributions (low  $\bar{D}$  values) which are attainable.

The distinguishing feature of ATRP is that it is a catalytic process; a transition metal catalyst is present at typically 1000 ppm relative to the monomer.<sup>66</sup> Copper (I) is the most versatile metal for the complex, which directly influences the shift of the reaction equilibrium and the exchange between active and dormant entities.<sup>50</sup> Alkyl halides act as initiators, whereby the halogen atom (commonly bromine or chlorine) is transferred to the catalyst, which subsequently causes oxidation of the metal and free radicals to be formed. Termination can take place, again through the regular routes of combination and disproportionation, but a successful ATRP reaction only sees this occur with a minimal portion of polymer chains ( $\leq 5\%$ ),<sup>50</sup> largely due to the persistent radical effect (PRE),<sup>67</sup> as highlighted in Section 1.1.2. ATRP imparts control by allowing all polymer chains to grow in a uniform manner, which is in turn brought about by fast initiation and the crucial reversible termination (deactivation) step, as illustrated in Scheme 1.6.<sup>50</sup>



**Scheme 1.6. The reversible redox process of the ATRP mechanism, catalysed by a transition metal complex.**<sup>50</sup> Mt represents the metal atom and L is the ligand; Y can be a counterion or another ligand.<sup>50</sup>

ATRP can be conducted under various conditions and is without doubt an effective controlled-radical technique, but certain disadvantages still exist. For instance, the catalyst reagent, although crucial to the reaction, is restrictive. If a high concentration is adopted, the furnished polymer requires extensive purification in order to remove the metal, which renders the process particularly undesirable for large scale industrial procedures.<sup>68</sup> Variations of ATRP have been realised which enable far reduced levels to be adopted, where the activator is generated *in situ*. These techniques include reverse ATRP,<sup>69, 70</sup> activator generated by electron transfer (AGET),<sup>71, 72</sup> activator regenerated by electron transfer (ARGET)<sup>66, 73-75</sup> and

initiators for continuous activator generation (ICAR).<sup>76-78</sup> Such processes employ the metal in a higher oxidation state (at as low a level as <50 ppm), which thus becomes reduced.<sup>50</sup> This in turn simplifies the ATRP reaction and enhances its capabilities; conventional ATRP systems require highly stringent conditions, where exclusion of moisture and air are necessary in order to avoid premature oxidation of the metal.

ATRP is more versatile than NMP,<sup>11</sup> as its various forms are able to furnish high molecular weight polymers without compromising control over the polymerisation (*i.e.* obtaining low  $\bar{D}$  values).<sup>73</sup> However, ATRP has itself been arguably overshadowed by the subsequent discovery of reversible addition-fragmentation chain transfer polymerisation (RAFT).<sup>9</sup> This can be an even simpler method to synthesise predefined, monodisperse polymers and is especially favourable because it does not require a metal catalyst.

### 1.1.2.3. Reversible addition-fragmentation chain transfer polymerisation (RAFT)

RAFT is a relatively straightforward method for synthesising a wide range of predefined polymers, whereby such processes can be scaled-up for industrial application.<sup>79, 80</sup> The RAFT technique is now often preferred to NMP and ATRP because it is generally accepted as the most convenient and versatile.<sup>19, 53, 81</sup> RAFT was invented by CSIRO in the late 1990s<sup>9</sup> and the technique has grown in popularity ever since. The key component to this free radical polymerisation is the specialised thiocarbonylthio chain transfer agent (CTA), represented as  $Z(C=S)SR$  in Figure 1.3.<sup>82</sup> A CTA, which is also known as a RAFT agent, is reactive towards radical addition at the  $C=S$  bond<sup>11</sup> and transfers reactivity between dormant and growing polymer chains in the RAFT mechanism, to regulate the growth of molecular weight.<sup>79</sup> The diverse and numerous CTA derivatives and their applications have been extensively reviewed over the years, particularly by the RAFT inventors, Moad *et al.*<sup>11, 53, 81, 83-85</sup>

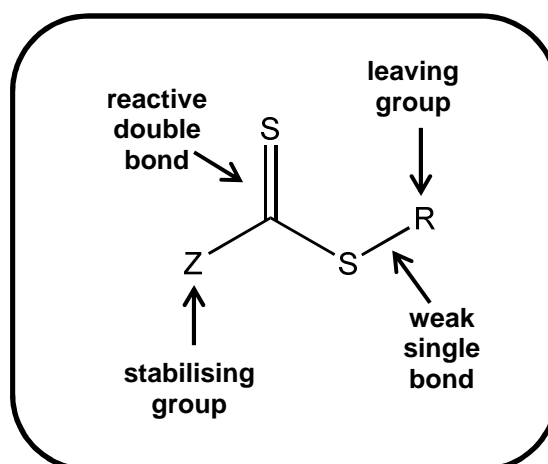
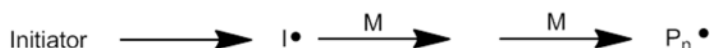


Figure 1.3. Generic structure of the RAFT CTA.

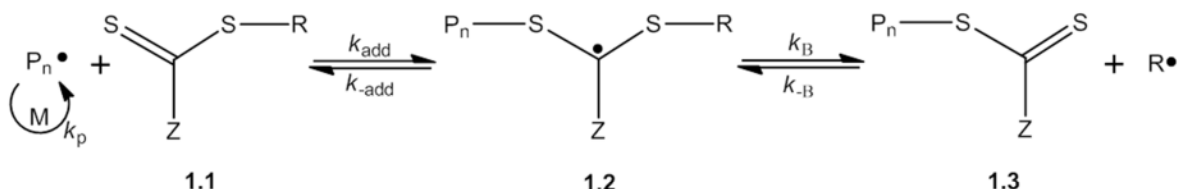
### 1.1.2.3.1. The reversible addition-fragmentation chain transfer (RAFT) mechanism

As shown in Scheme 1.7,<sup>81, 83, 86</sup> initiation (via the decomposition of an appropriate initiator) generates free radicals which react with monomer, generating propagating radicals ( $P_n^\bullet$ ). This stage compares to that of the conventional free radical mechanism, even in the possible initiators. However, in RAFT, the propagating radical can add to the CTA itself (1.1), rather than the monomer, because of the highly reactive C=S (thiocarbonyl) bond, thus forming an intermediate radical (1.2). This readily fragments to give rise to a dormant polymeric CTA compound (1.3) and  $R^\bullet$ . New propagating radicals ( $P_m^\bullet$ ) then form after further reaction of  $R^\bullet$  with monomer and the whole process is repeated. Equilibration between active propagating radicals ( $P_n^\bullet$  and  $P_m^\bullet$ ) and the dormant dithio species (1.3) allows all polymer chains an equal chance to grow whilst minimising termination, owing to the reduced active radical concentration. This ultimately gives rise to low dispersity ( $\mathcal{D}$ ) polymers and makes RAFT unique. Termination proceeds as in conventional free radical polymerisation, by combination or disproportionation, yielding a small amount of 'dead' polymer, without CTA functionality.

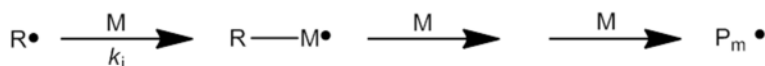
#### 1. Initiation



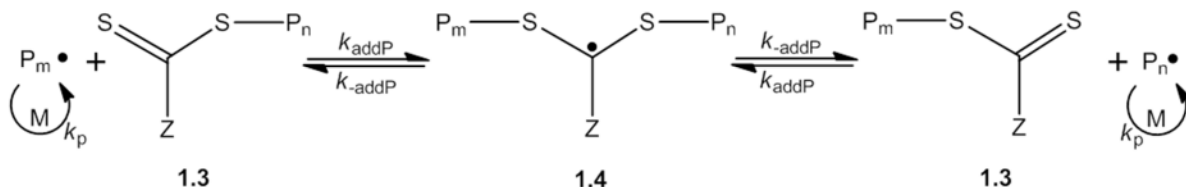
#### 2. Reversible chain transfer/propagation



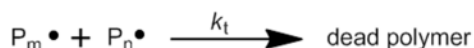
#### 3. Reinitiation



#### 4. Chain equilibration/propagation



#### 5. Termination



**Scheme 1.7. The mechanism of RAFT polymerisation.**<sup>81, 83</sup>

Crucially, macroCTA (the dormant species, **1.3** in Scheme 1.7) is the major isolated product and is capable of reacting further because of the CTA end group present on the polymer chains.<sup>83</sup> Hence the reason why RAFT polymerisation is a vital tool in the production of block copolymers.<sup>84</sup> If fragmentation is slow, it is possible for intermediate adducts **1.2** and **1.4** to be consumed in side reactions and, if reinitiation is inefficient, retardation or inhibition can occur. Optimal control over the reaction to avoid these instances relies heavily on the choice of CTA, whereby the specific structure and functionality are vital.<sup>85</sup>

The effectiveness of the RAFT CTA can be qualitatively understood by the narrowness of the polymer molecular weight distribution (low  $\mathcal{D}$  value) and how closely the experimental molecular weight (often expressed as  $M_n^{\text{exp}}$ ) correlates with the theoretical value ( $M_n^{\text{th}}$ , as calculated through the monomer:CTA molar ratio). A more quantitative measure is to determine the transfer coefficient of the reagent. The conventional Mayo equation,<sup>16</sup> provided in Section 1.1.1.1, is not applicable for such highly active mediators and so alternative, more complex mathematics are required. One way to estimate the transfer coefficient is to calculate the rates of consumption of the CTA and monomer. In terms of the RAFT mechanism, the rate of consumption of the CTA depends on two transfer coefficients,  $C_{\text{tr}}$  ( $= k_{\text{tr}} / k_{\text{p}}$ ) and  $C_{\text{-tr}}$  ( $= k_{\text{-tr}} / k_{\text{i}}$ ), which respectively describe the reactivities of  $\text{P}_n\bullet$  and  $\text{R}\bullet$ . These terms are incorporated within the following equation:<sup>87, 88</sup>

$$d[\mathbf{1.1}] / d[\text{M}] \approx C_{\text{tr}} \times [\mathbf{1.1}] / ([\text{M}] + C_{\text{tr}}[\mathbf{1.1}] + C_{\text{-tr}}[\mathbf{1.3}]) \quad (\text{Eq}^n \text{ 1.5})$$

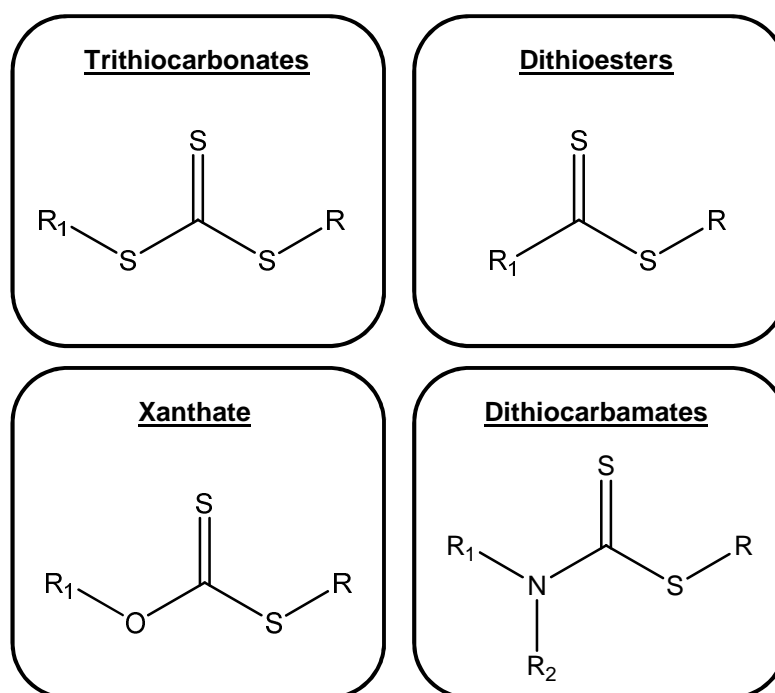
The numbers assigned in Equation 1.5 refer to the species in Scheme 1.7;  $k_{\text{tr}} = k_{\text{add}} \times [k_{\beta} / (k_{\text{-add}} + k_{\beta})]$  and  $k_{\text{-tr}} = k_{\beta} \times [k_{\text{-add}} / (k_{\text{-add}} + k_{\beta})]$ .<sup>53</sup> Such calculations can be applied to estimate the transfer coefficient of the CTA and ultimately helps to define its behaviour in a RAFT polymerisation reaction. These equations are based, however, on the assumption that the adduct radical (**1.2**) is involved in no reaction other than fragmentation.<sup>53</sup>

#### 1.1.2.3.2. Application of the RAFT CTA

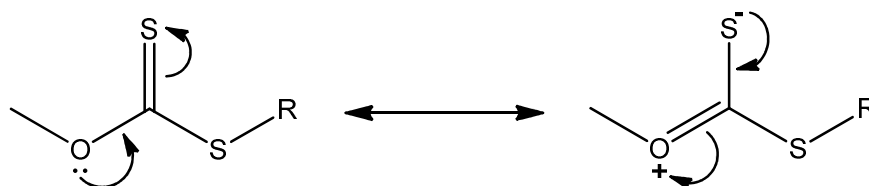
With a generic structure denoted by  $\text{Z}(\text{C}=\text{S})\text{SR}$  (see Figure 1.3), the Z group of the CTA provides stability to the intermediate radicals and can be modified to alter the reactivity of the molecule towards propagating radicals. The R group is required to be a good homolytic leaving group, and  $\text{R}\bullet$  must be capable of reinitiating polymerisation.<sup>11</sup> Adapting the functionality of either of these groups can affect the efficiency and outcome of the polymerisation, depending on the monomer type. The roles of each group have been reviewed by Chong *et al.* (R)<sup>87</sup> and Chiefari *et al.* (Z),<sup>88</sup> whereby an extensive account of the general features of RAFT CTAs is provided by Keddie *et al.*<sup>85</sup>

Figure 1.4 shows generic structures for the different types of CTAs known to be effective in RAFT polymerisations. These include trithiocarbonates ( $Z = SR_1$ ), dithioesters ( $Z = R_1$ ), dithiocarbamates ( $Z = NR_1R_2$ ) and xanthates ( $Z = OR_1$ ), of which aromatic or alkyl derivatives can exist.<sup>85</sup> Dithioesters and trithiocarbonates, where a carbon or sulfur atom is adjacent to the thiocarbonyl group, are the most active;<sup>85, 88</sup> CTAs with a lone pair of electrons on a nitrogen or oxygen atom in this position, such as xanthates and dithiocarbamates, are less reactive towards addition.<sup>85</sup> The latter have lower rate coefficients owing to their zwitterionic canonical forms, as illustrated in Scheme 1.8. Here, the interaction between the lone pair and  $C=S$  reduces the double bond character of the thiocarbonyl group, thus stabilising the CTA relative to its adduct radical.<sup>85</sup>

In electing the CTA for any given polymerisation, the reaction conditions, including the nature of the monomer/s involved, will influence how effective the CTA will be. Temperature has a role, for instance, in that CTAs can degrade at elevated temperatures.<sup>89-92</sup> Hence, the stabilities of certain CTAs have been investigated and the mechanisms and by-products of their breakdown (under certain conditions) have been elucidated.<sup>89</sup> Decomposition is undesirable as this can cause retardation of the polymerisation rate, brought about by radical quenching.<sup>89</sup> Dithioesters, in particular dithiobenzoates, are most notorious for causing retardation, in both homogeneous and emulsion media,<sup>80</sup> despite them being the most common type of CTA.<sup>93</sup> Dithiobenzoates are less stable than trithiocarbonates, xanthates and dithiocarbamates<sup>89</sup> and are known to retard polymerisation when present at high concentrations.<sup>11, 85</sup> Retardation has been deemed less likely to occur with trithiocarbonates due to their enhanced stability.<sup>94</sup>



**Figure 1.4. Generic structures for the types of CTAs employed in RAFT.**



**Scheme 1.8. The zwitterionic canonical form of an O-alkylxanthate (also applicable to dithiocarbamates, where the oxygen atom is replaced by nitrogen).<sup>85</sup>**

The CTA can be designed and synthesised according to the monomer application. General guidelines exist for selecting the appropriate Z and R groups, as summarised in Figure 1.5.<sup>11, 53, 81, 83</sup> Generally, for Z, a nitrogen or oxygen atom adjacent to the thiocarbonyl group (as in O-alkylxanthates, *N,N*-dialkyldithiocarbamates and *N*-alkyl-*N*-aryldithiocarbamates) are less reactive to addition as these afford lower rate coefficients. Electron-withdrawing Z groups create higher transfer coefficients, but this can lead to side reactions occurring, which can hinder polymerisation.<sup>85</sup> The stability of the R group determines the rate of fragmentation in the RAFT mechanism; generally, more stable, more electrophilic, bulkier R radicals are superior leaving groups.<sup>87</sup> In turn, the leaving group ability of R and the propagating radical determines the transfer coefficient of the CTA,<sup>87</sup> which has been found to increase from primary through to tertiary radicals.<sup>85</sup>

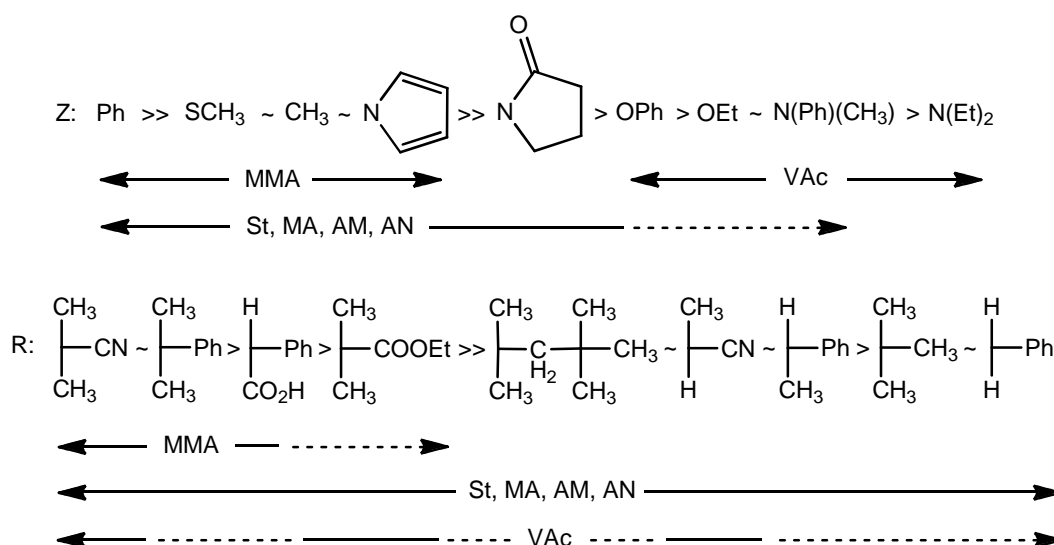


**Figure 1.5. General guidelines for designing the RAFT CTA, as adapted from the literature.<sup>11, 53, 81, 83</sup> For the Z group, addition rates decrease and fragmentation rates increase from left to right. For the R group, fragmentation rates decrease from left to right. Dashed lines represent partial control over polymerisation; solid lines infer full control.**



The suitability of the CTA can depend on whether the monomer is “more-activated” (a MAM) or “less-activated” (a LAM); these types are summarised in Figure 1.6.<sup>11</sup> This “activity” relates to the efficiency of the homolytic leaving group (R) of the growing polymer propagating radical. For instance, poly(MAM)s have effective homolytic leaving groups, whereas those of poly(LAM)s are poor, and, as a consequence, the stability and side reactions of their intermediates (formed by addition to the CTA) can lead to retardation or inhibition.<sup>85</sup>

MAMs and LAMs are defined according to the relative positions of their unsaturated carbon-carbon double bonds. For instance, MAMs generally contain a carbon-carbon double bond which is conjugated to an aromatic ring, carbonyl or cyano group; the carbon-carbon double bond in a LAM is adjacent to a hetero-aromatic ring, a saturated carbon, oxygen atom or a nitrogen lone pair.<sup>85</sup> Controlled RAFT polymerisations of the latter are notoriously more difficult as they generally proceed slower; monomers in this genre include vinyl esters (such as vinyl acetate, VAc) and vinyl amides (such as *N*-vinylcarbazole and *N*-vinylpyrrolidone). Xanthate and dithiocarbamate CTAs are generally adopted in these cases. Conversely, the “more-activated” monomer class list (MAM) is more extensive, comprising vinyl aromatics (St, and vinylpyridine), methacrylics (MMA, methacrylic acid and methacrylamide) and acrylics (MA, acrylic acid, AA, acrylamide, AM, and acrylonitrile, AN). For these, a broader range of CTAs are effective, including aromatic dithioesters (where Z = aryl), trithiocarbonates (Z = S-alkyl), aromatic dithiocarbamates (Z = pyrrole) and dithioesters (Z = alkyl or aryl).<sup>11</sup>

Much research has been undertaken on designing CTAs appropriately to suit the vast array of monomers which exist for RAFT polymerisations, and this has often involved computational studies to predict the probability of success. In particular, molecular orbital calculations have been used to predict the chain transfer constants of CTAs.<sup>88</sup> The nature of each constituent or group within the CTA structure is important. For example, in the work of Benaglia *et al.*,<sup>95</sup> various types of dithioesters were compared in the RAFT polymerisation of MMA. The Z and R groups were altered and the derivatives compared against a parent molecule, 2-cyano-2-propylbenzodithioate (CPD), where Z = phenyl and R = C(Me<sub>2</sub>)CN. It was deduced that electron-withdrawing substituents (such as the cyano functionality) on the Z phenyl ring ultimately afforded monodisperse polymers, as these encouraged more effective addition to the thiocarbonyl (C=S) group. For the R group, bulkier constituents provided more stability and also resulted in superior control.<sup>95</sup>

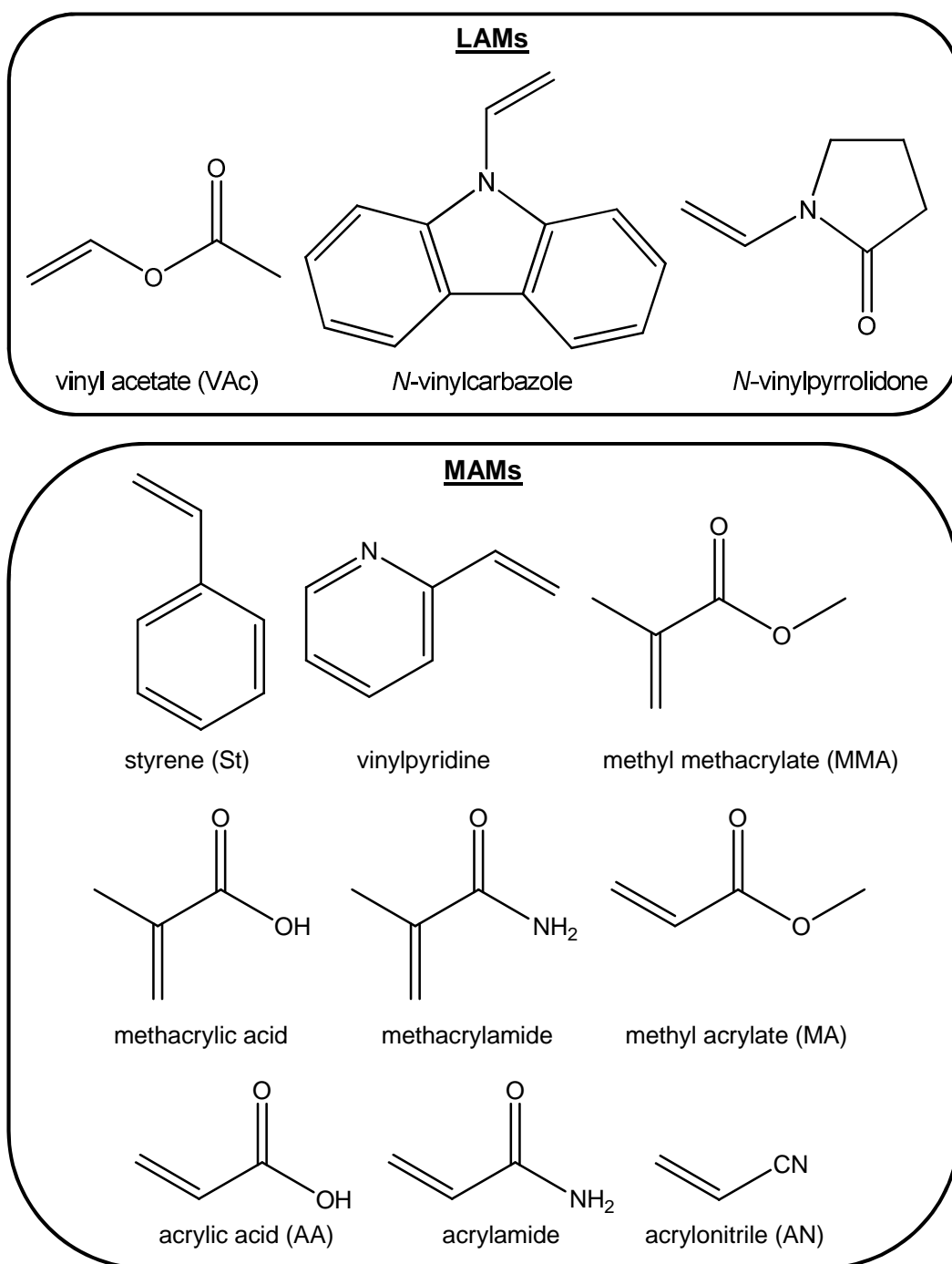


**Figure 1.6. Summary of the types of monomers polymerised in RAFT.<sup>11</sup>**

#### 1.1.2.3.3. Other reaction considerations

A RAFT polymerisation can proceed in bulk conditions,<sup>96</sup> or in organic<sup>97</sup> or aqueous<sup>98, 99</sup> media, although it is generally accepted that bulk reactions proceed faster due to a higher concentration of free radicals and monomer present.<sup>19-21</sup> There have been few comprehensive studies focussing on the effect of different organic solvents in RAFT,<sup>19, 20, 95, 100</sup> and there has been difficulty rationalising the exact influence that solvent has. The degree

of solubility of the medium has most often been the reason behind any change in polymerisation profile. The ability of a solvent to dissolve the CTA<sup>95</sup> or initiator<sup>100</sup> has, for instance, enabled higher conversions to be reached.<sup>95</sup> Certain other characteristics of the medium, such as the viscosity,<sup>100</sup> aromaticity or polarity,<sup>20</sup> have been deemed insignificant.

Interestingly, supercritical dioxide (scCO<sub>2</sub>) is also a viable solvent in RAFT (and ATRP) reactions, as predominantly investigated by Howdle and co-workers.<sup>101-103</sup> For instance, RAFT-controlled dispersion polymerisation utilising scCO<sub>2</sub> has enabled high purity block copolymers of MMA and benzyl methacrylate (BzMA) or St to be furnished in a more efficient manner than in an emulsion system.<sup>101</sup> Here, 'efficiency' relates to the ratio of block copolymer formed to residual homopolymer impurities (*i.e.* 'dead' chains without CTA functionality, resulting from termination). More efficient copolymerisations yield higher purity copolymer. scCO<sub>2</sub> was so effective because it plasticised the PMMA, expanding the particles and encouraging better diffusion (than a water medium would enable). By simply releasing the pressure, it was also easier to separate the polymer and continuous phases, compared to the more elaborate process of high-temperature drying.<sup>101</sup> Similar conclusions have been met for a wide range of other monomer/polymer combinations in RAFT.<sup>102</sup> Additional benefits of scCO<sub>2</sub> include that it is readily available, chemically inert and inexpensive, and it can be an environmentally friendly alternative to otherwise harmful solvents, hence it can be applied in the diverse area of materials processing.<sup>104</sup> The effects of solvent in RAFT are also discussed within Chapter 3.

The temperature of a RAFT polymerisation is generally understood to be influential in much the same way as for a conventional free radical reaction. Specific investigations into the effects of temperature in RAFT polymerisation have concluded that, generally, faster rates of polymerisation result from higher temperatures and often afford higher monomer conversions.<sup>95, 105-108</sup> Raising the temperature reduces the half-life ( $t_{1/2}$ ) of the initiator and results in the more rapid production of free radicals, as expected.<sup>3</sup> Higher temperatures, however, can compromise the degree of control and cause broader molecular weight distributions.<sup>90, 108, 109</sup> Optimising the temperature is challenging and conditions are chosen depending on the properties of the reagents employed. The CTA can be particularly temperature-sensitive and can decompose at elevated temperatures (depending on its nature), thus hindering the polymerisation mechanism.<sup>89-92</sup> Given such difficulties, it is not surprising that efforts are being made to achieve controlled polymerisation at lower temperatures, which would certainly be economically advantageous in industrial applications.<sup>110, 111</sup>

Less attention has been paid to the effect of pressure on RAFT polymerisations, but this is nevertheless another experimental factor.<sup>112</sup> Rzayev *et al.* have introduced polymer chemists

to high-pressure RAFT systems,<sup>113, 114</sup> where the group was able to control the polymerisation of methyl methacrylate and other sterically-hindered  $\alpha$ -substituted acrylates by at five kbar pressure.<sup>114</sup> Similarly, linear polymers of MMA were synthesised under comparable conditions using 2-cyano-2-propylbenzodithioate (CPD) CTA, achieving molecular weights of up to 1.25 million g/mol and retaining low dispersity ( $\bar{D} < 1.2$ ).<sup>113</sup> The justification for adopting such high pressure conditions is usually to enhance the rates of otherwise slow reactions and to obtain higher degrees of polymerisation, which would not necessarily be achieved by simply raising the temperature. Crucially, such processes would be more applicable in appropriately equipped industrial laboratories. The aforementioned application of  $scCO_2$  in RAFT is an additional example of high pressure polymerisation systems.<sup>101-103</sup>

#### 1.1.2.3.4. General features of RAFT polymerisation

In summary, RAFT can be a very efficient method for producing low dispersity, predefined polymer, once the technique has been mastered. After tackling the various factors, and the appropriate CTAs have been designed, it is possible to predetermine the molecular weights in the synthesis of a diverse range of polymers.

The CTA is vital to the RAFT reaction, where [in the  $Z(C=S)SR$  structure] the Z group determines radical stability and  $R\bullet$  reinitiates polymerisation. In the mechanism, equilibration between active and dormant chains suppresses termination and provides all polymer chains an equal chance to grow. An efficient process results in narrow molecular weight distributions (low  $\bar{D}$  values). The resulting isolated macroCTA polymer is able to react further, which allows for the synthesis of copolymers.

Overall, RAFT can be conducted in a variety of reaction media, including water. As industrial processes can still adopt organic solvents, the possibility of more environmentally friendly aqueous systems render this a viable alternative. The absence of complex reagents (or metals) renders RAFT a potentially more straightforward polymerisation method (*versus* NMP and ATRP). RAFT was the principal controlled-radical polymerisation of choice throughout this research in the novel syntheses of predefined poly(2-chloro-1,3-butadiene) (PCB).

## 1.2. Cross-linking

A cross-linked polymer is defined as one where the polymer chains are linked together forming a network system, as illustrated in Figure 1.7.<sup>1</sup> In industry, terms such as

“vulcanisation” or “curing” are commonly used to describe the cross-linking process, which is employed to introduce certain favourable properties into a polymeric material, such as elasticity,<sup>115</sup> as is necessary for rubbers (elastomers).

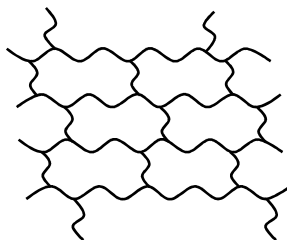


**Figure 1.7. Generic structure for a chemically cross-linked polymer network.**

Chemical cross-links can be introduced through a variety of different methods, including UV,<sup>116</sup> chemical<sup>117</sup> or thermal<sup>118</sup> reactions. The exact nature and extent of this process dictates the characteristics of the final material. In terms of cross-link density, tighter networks (which are denser) offer more rigidity, whereas loosely cross-linked chains result in softer, more elastic products because the chains are more mobile.<sup>119</sup> As a result of the physical and chemical changes that transpire through cross-linking, the polymer becomes less soluble and more viscous until it is rendered a completely insoluble solid.<sup>119</sup> Specific physical properties which are enhanced by introducing an increasing number of cross-links include stiffness and hardness; elongation is negatively affected by a higher cross-link density, as the material becomes more rigid and less elastic.

Cross-linking can take place after polymerisation has occurred, so that polymer chains become interconnected through an independent chemical reaction,<sup>120</sup> or this can be achieved effectively during polymerisation, in one combined reaction.<sup>121</sup> The latter case is important for generating firm materials for industry, such as plastics, because a higher cross-link density is achieved. The two-stage cross-linking process, however, is adopted in rubber technology,<sup>119</sup> for instance, which was more relevant to this project.

### **1.2.1. Cross-linking methods and additives in the rubber industry**

Cross-linking was first realised in the nineteenth century when Charles Goodyear was researching natural rubber [poly(2-methyl-1,3-butadiene), commonly known as polyisoprene, where the 1,4-*cis* isomer is prevalent] and discovered that it reacted with elemental sulfur to form a network of polymer chains.<sup>122</sup> Technology has improved somewhat since then in that various cross-linking additives and methods have been optimised according to the different types of polymer systems. The cross-linking of poly(2-chloro,1-3-butadiene) (commonly known as polychloroprene, but denoted herein as PCB), for instance, is considered in the

subsequent section (1.2.2), as the cross-linking of this polymer was of particular interest during this project.

A diverse range of chemical additives exist to bring about cross-linking. These can be directly involved in forming the cross-links themselves, used to speed-up (accelerate) the reaction, or to enhance the physical properties of the final material. Sulfur (and nitrogen) -containing molecules are prevalent as accelerators, but metal oxides can also be effective. Table 1.1 summarises the main types of additives adopted within the rubber industry.

Cross-links can also be introduced chemically using peroxides,<sup>123</sup> silanes<sup>124</sup> or irradiation techniques.<sup>125</sup> A variety of miscellaneous compounds can also be involved in industrial reactions but do not actually facilitate cross-linking. These include antioxidants,<sup>126</sup> fillers<sup>127</sup> and other processing aids.<sup>128</sup> Such concepts are not directly linked to the focus of this project and are beyond the scope of this thesis.

**Table 1.1. Additives commonly used in the industrial cross-linking of rubbers.**

Type of compound	Example/acronym	Primary function/s
Metal oxide	ZnO	accelerator
Multi-functional additive	MFA	accelerator, processing aid
Sulfur (or nitrogen) -containing organic compound	*	accelerator

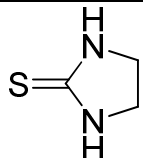
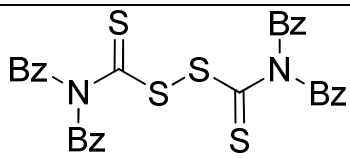
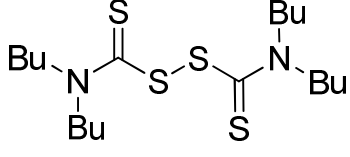
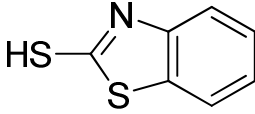
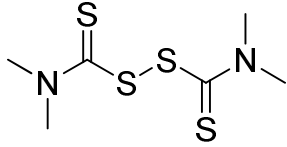
Refer to Table 1.2 in the subsequent section for a list of applicable molecules.

#### 1.2.1.1. The role of sulfur (and nitrogen) -containing compounds as accelerators

Accelerators do not only facilitate the cross-linking reaction by providing the necessary structures or atoms for the chemical bridges, but they can also speed up the process. Various compounds now exist which supersede elemental sulfur as the standard cross-linking agent (or cross-linker). Cross-linking can occur much more quickly with these chemicals, than with sulfur alone, and they can be used at reduced concentrations because of their superior activity.

Table 1.2 indicates that a variety of molecules exist which do not only contain a sulfur atom, such as thioureas, thiuram disulfides and thiazole derivatives. Indeed, the exact nature of the final cross-links within a reacted polymer is not always known, which is highlighted in the discussion surrounding PCB (in Section 1.2.2). These different types of accelerator compound can be used in conjunction with one another, or with other additives, to furnish the desired final product. A metal oxide, for example ZnO, can also help to activate the system towards the cross-linking reaction, as is discussed subsequently in Section 1.2.1.2.

**Table 1.2. Common organic accelerators adopted in rubber cross-linking.**

Full name	Abbreviation	Structure
Ethylene thiourea	ETU	
Tetrabenzylthiuram disulfide	TBzTD	
Tetrabutylthiuram disulfide	TbuT	
Mercaptobenzylthiazole	MBT	
Tetramethylthiuram disulfide	TMTD	

#### 1.2.1.2. The role of zinc oxide (ZnO) in cross-linking

Zinc oxide (ZnO) has evolved as an additive in rubber technology. Once adopted as a filler to reinforce the rubber,<sup>115</sup> the modern-day role of ZnO is in activating cross-linking reactions and improving the physical characteristics of a material.<sup>129</sup> Overall, ZnO has a varied role, also acting as a scavenger for by-products, such as acids.<sup>130</sup>

The zinc dication,  $Zn^{2+}$ , is the actual key component in a cross-linking reaction involving ZnO. This form facilitates complexation with sulfur-containing reagents which results in the reaction being accelerated.<sup>129</sup> Figure 1.8 shows two classes of accelerator – a

dithiocarbamate and a xanthate – which exemplify accelerator complex systems activated by the zinc dication.

Despite the importance of ZnO, this is classified as an environmental hazard. Thus, it has been necessary for industry to reduce its overall usage of ZnO and, in so doing, this has resulted in the development of multi-functional additives (MFAs).<sup>131</sup>

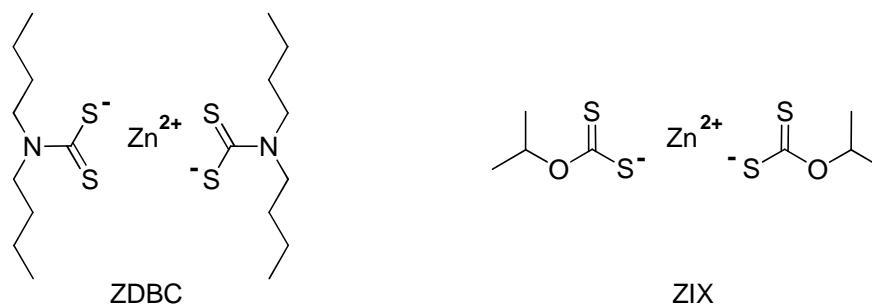


**Figure 1.8. Inorganic accelerator systems comprising the zinc dication: zinc dibutyldithiocarbamate (ZDBC)<sup>132</sup> and zinc isopropylxanthate (ZIX).<sup>133</sup>**

#### 1.2.1.3. The role of multi-functional additives (MFAs) in cross-linking

A multi-functional additive (MFA) is a diamine-fatty acid complex, as illustrated in Figure 1.9. The MFA is designed to simultaneously act as a processing aid and an accelerator,<sup>131</sup> whereby the fatty acid has the former function and the diamine is the cross-linker. In a thermal cross-linking reaction, the fatty acid and diamine fragments separate, so that they can act independently.<sup>131</sup> Crucially, MFAs have a non-toxic (hazard) classification, which is vital for commercial applications.

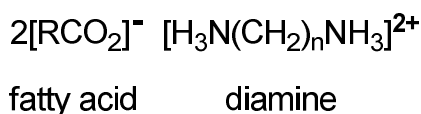


**Figure 1.9. General representation of a multi-functional additive (MFA).**

#### 1.2.2. Cross-linking poly(2-chloro-1,3-butadiene)

Poly(2-chloro-1,3-butadiene) (PCB) is one of the first synthetic elastomers to have been successfully industrialised and is commonly referred to as neoprene.<sup>134</sup> PCB has vast commercial applications in construction, for automotive parts and in adhesives.<sup>134</sup>



The wide-ranging uses of PCB are the result of excellent chemical and physical properties of this material. In particular, the rubber is very durable where it can be exposed to deterioration by a range of environmental factors;<sup>134</sup> PCB has good chemical, oxidation, temperature and ozone resistance.<sup>115</sup> Overall, these attributes make this a functional material which can operate under variable conditions. PCB is also relatively inexpensive, making it even more attractive for the industries.

The cross-linking of PCB was studied as part of the industrial component of this project and is introduced herein. Subsequently, the experimental results and discussion for this particular element of work are provided in Chapter 4.

PCB consists of four possible isomers, as shown in Figure 1.10. The commercial rubber comprises mainly the 1,4-*trans* configuration (78 – 96 %), as assigned through FTIR studies.<sup>135</sup> Thereafter, the other isomers present are fairly minor; the 1,4-*cis* isomer exists within 4 – 18 %, followed by the 3,4- (0.2 – 2 %) and the 1,2- (0.3 – 2 %).<sup>135</sup> The presence of these four isomers can make the accurate analysis of this polymer and related reactions difficult (as discussed further in Section 3.2.3). For the remainder of this review section, the PCB rubber discussed pertains to the overall composition of the material, with each isomer defined only where appropriate.

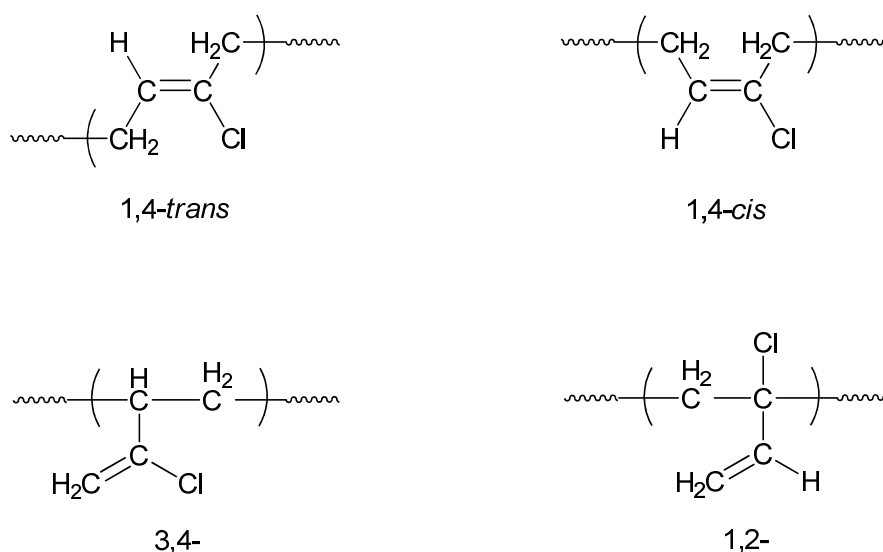


**Figure 1.10. The four isomers of poly(2-chloro-1,3-butadiene) (PCB).**

#### 1.2.2.1. Typical PCB cross-linking additives

The PCB cross-linking reaction has always been topical because this polymer behaves differently to others,<sup>136</sup> such as 1,4-*cis*-polyisoprene (the main constituent of natural rubber).<sup>134</sup> As Figure 1.11 shows, the primary difference between 1,4-*cis*-polyisoprene and



project (“SafeRubber”)<sup>143</sup> whose objective was to replace ETU as the cross-linker for PCB, due to the associated health hazards. ETU is under scrutiny mainly because of its potential carcinogenicity.<sup>144-147</sup> Considerable animal testing has been performed with ETU, which has correlated possible thyroid problems<sup>148-150</sup> and the potential danger to unborn foetuses<sup>151</sup> with humans who came in contact with the substance.

Hence, it was vital to know exactly how ETU functioned during the cross-linking of PCB, so that a safer, non-toxic replacement could be sought. This alternative should react in the same way as ETU so as to yield properties in the rubber which are comparable to, or an improvement on, the predecessor system. The cross-linking of PCB was thus researched and complemented the work of K. Berry at Robinson Brothers Ltd. (RBL), West Bromwich.<sup>152</sup>

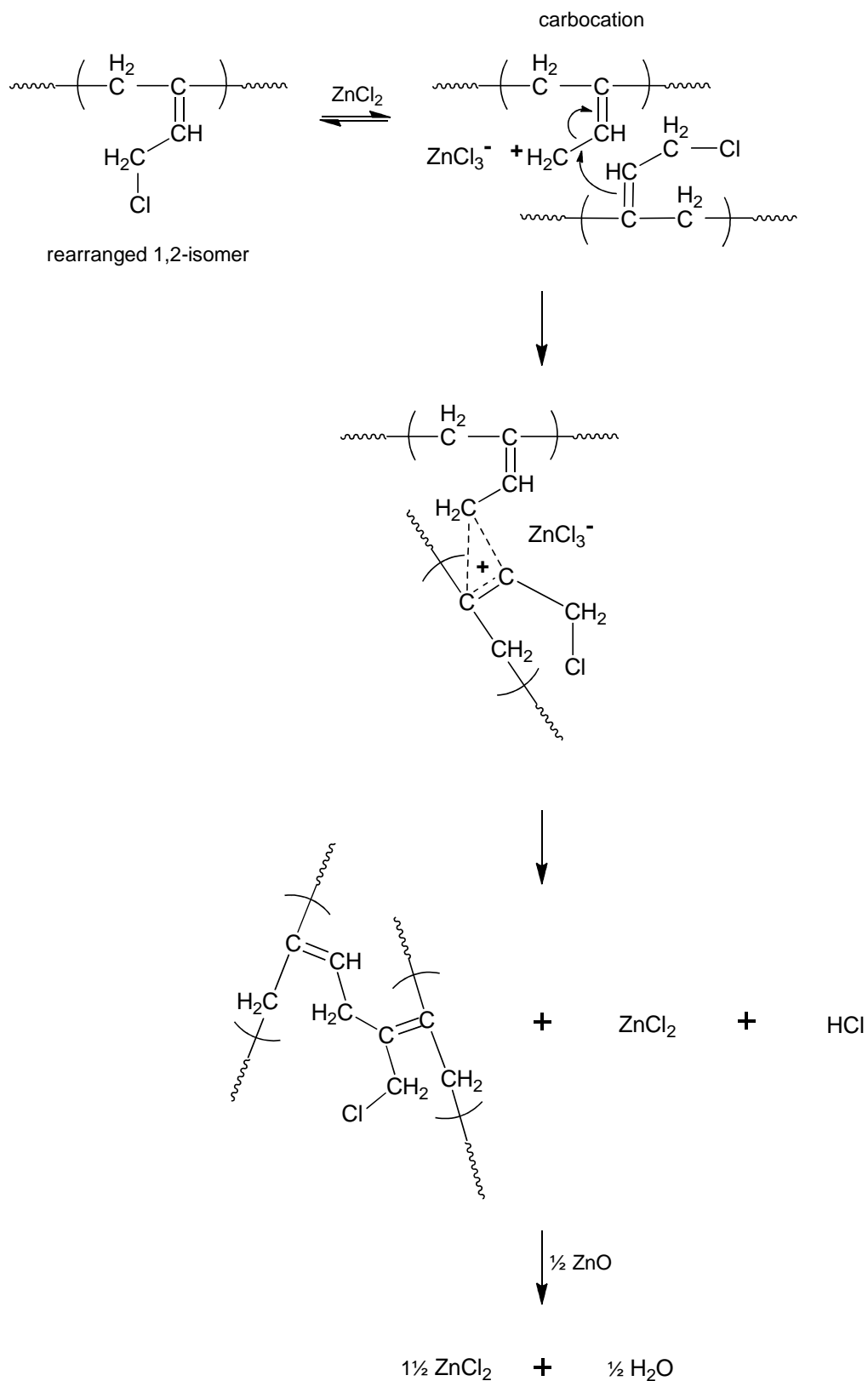
Investigations have been undertaken elsewhere, attempting to elucidate the PCB cross-linking mechanism, with ETU alone or in combination with metal oxides. These studies are discussed in the following sub-sections, as appropriate.

#### 1.2.2.2. PCB cross-linking theories – ZnO alone

As mentioned in Section 1.2.1.2, one of the vital roles of a metal oxide is to activate cross-linking *via* the Zn<sup>2+</sup> dication. ZnO, and magnesium oxide (MgO), are also able to absorb acids which are evolved during a reaction (such as hydrochloric acid, HCl, a consequence of the chlorine atom of PCB). Metal chlorides can thus eventually form and these in turn help to facilitate activation. It has been found that MgO does not act in this way as efficiently as ZnO and adopting MgO can negatively affect the degree of cross-linking in the final material.<sup>153, 154</sup> This is due to the MgO-sulfur intermediate complexes being less able to progress to cross-linking because MgO has a higher affinity for sulfur (than ZnO); sulfur-containing compounds are less capable of forming cross-links when MgO is present in the reaction.<sup>153, 154</sup> Hence, ZnO generally features more prominently in reports and is more relevant here, to PCB.

ZnO is capable of cross-linking PCB without any additional reagents present, which is an unusual characteristic for a metal oxide, whose main responsibility is to accelerate the reaction. The generally accepted initial step of the ZnO mechanism is allylic rearrangement of the tertiary chlorine atom of 1,2-PCB.<sup>137-141</sup> Hereafter, a number of different views are taken. The most prominent theories for the cross-linking of PCB by ZnO alone propose cationic mechanisms. For instance, Vukov<sup>155</sup> used model compounds to propose the concept of diene formation, which would act as a catalyst. Similarly, Desai<sup>137</sup> proposed a three-stage mechanism, which comprised the generation of a carbocation. This mechanism is shown in Scheme 1.11, with the initial isomerisation step omitted as this was shown previously (Scheme 1.9). Crucially, this theory involved zinc chloride (ZnCl<sub>2</sub>) in place of ZnO. To note,

Desai postulates that  $\text{ZnCl}_3^-$  forms during this reaction (as illustrated in the scheme), but the author does not believe that it is possible for this species to chemically exist.



**Scheme 1.11. The cationic mechanism for cross-linking PCB, as facilitated by ZnO, proposed by Desai *et al.*<sup>137</sup>**

Other studies support a cationic mechanism, for instance Baldwin *et al.*<sup>156</sup> who employed a related chlorinated polymer as a model compound and concluded that ZnCl<sub>2</sub> could form *in situ*. Further publications by Hendrikse *et al.*,<sup>157-159</sup> also helped to substantiate the claims of a cationic system originally provided by Vukov<sup>155</sup> and Desai.<sup>137</sup>

A number of additional theories for the cross-linking of PCB by metal oxides have been suggested and subsequently disproved. These include the possibility of an ether linkage forming between polymer chains, or direct insertion of the zinc atom, as detailed in a review by Aprem.<sup>160</sup> Overall, the most comprehensive evidence for cross-linking by ZnO alone is presented by Vukov<sup>155</sup> and Desai.<sup>137</sup>

### 1.2.2.3. PCB cross-linking theories – ETU alone

The key theory in the cross-linking of PCB with ETU is the bis-alkylation mechanism of Kovacic.<sup>161</sup> This work concentrated on the use of bifunctional amines in the cross-linking of PCB, which is suitable given the structure of ETU. In this reaction, the diamine ‘slots in’ between the polymer chains, as shown with ETU in Figure 1.12. Originally, Kovacic evaluated his theory using piperazine, a six-membered, saturated heterocycle, instead of ETU. Figure 1.13 illustrates the structures of ETU and piperazine, for comparison. To note, Kovacic also confirms that the metal oxide (MgO) quenches the HCl evolved.

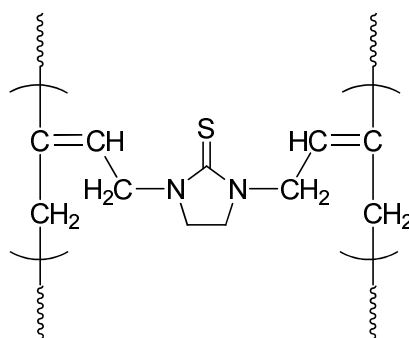


**Figure 1.12. Structure of PCB cross-linked *via* bis-alkylation with ethylene thiourea (ETU), as suggested by Kovacic.<sup>161</sup>**

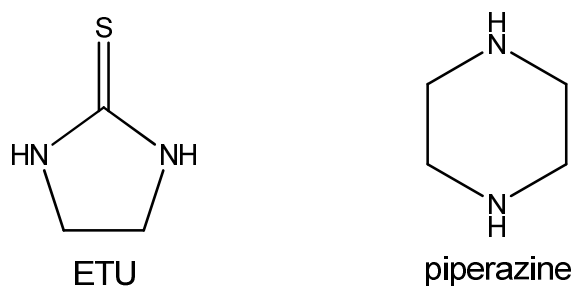
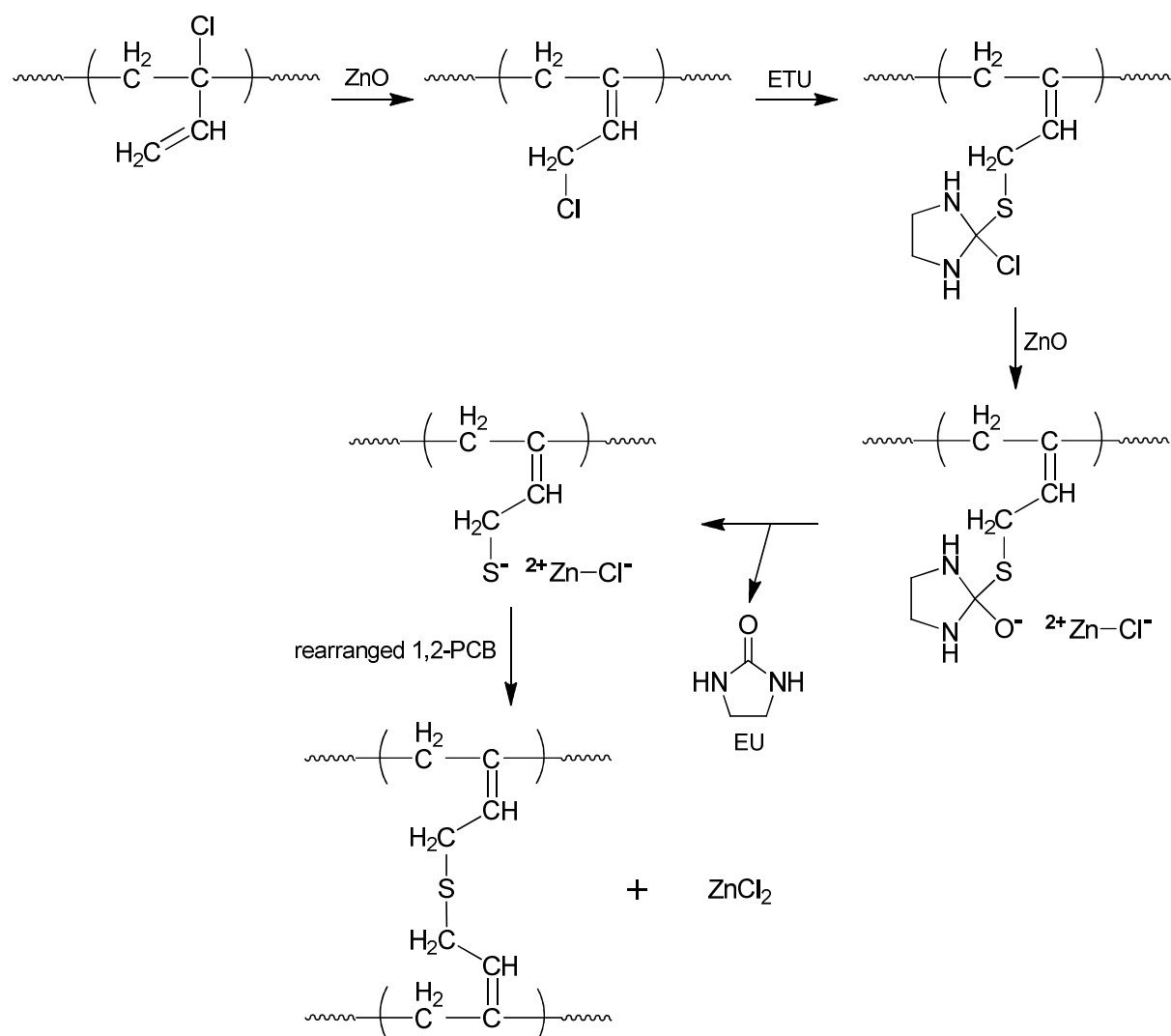


**Figure 1.13. Structures of ETU and piperazine.**

The bis-alkylation theory<sup>161</sup> is the foremost proposal for the ETU cross-linking mechanism and has prompted further research into the use of amines as cross-linking reagents.<sup>162</sup>

#### 1.2.2.4. PCB cross-linking theories – ETU and ZnO

Just as Kovacic is the main player in the ETU cross-linking mechanism, one theory stands alone for ETU/ZnO and is accredited to Pariser.<sup>163</sup> In fact, this is the only work published which combines the two reagents. Scheme 1.12 shows how it is apparently possible for ETU and ZnO to work concurrently in the reaction, ultimately forming a sulfide bridge. As a result, ethylene urea (EU) is formed because the sulfur atom of the original ETU carbon-sulfur double bond is replaced by oxygen (from ZnO). Crucially, this mechanism also generates ZnCl<sub>2</sub>, which was deemed significant in the ZnO reaction (as discussed previously in Section 1.2.2.2).



**Scheme 1.12.** The mechanism of cross-linking PCB with ETU and ZnO, as originally proposed by Pariser and modified from the literature.<sup>163</sup>

### 1.3. Latex technology

Latexes are often referred to as polymer dispersions or polymer colloids, where emulsion polymers are dispersed in water.<sup>164, 165</sup> In stark contrast to the solid rubber attained through cross-linking (previously described in Section 1.2), latexes are predominantly synthesised whilst in the liquid (usually aqueous) form. Monomer emulsions are the precursors for latexes, where monomer droplets are dispersed in water. Subsequent polymerisation of the monomer forms the basis for emulsion polymerisation;<sup>164</sup> an understanding of this is key to latex technology and is described in general in the following section.

#### 1.3.1. Emulsion polymerisation

Emulsion polymerisation is crucial to the large-scale, industrial production of numerous polymers, including polyacrylics, poly(vinyl chloride) (PVC) and various copolymers.<sup>3, 166</sup> Adopting an aqueous reaction medium is particularly beneficial as water is environmentally friendly and inexpensive.<sup>2, 166</sup> Water also enables simple, fluid agitation within a reaction, due to the low viscosity, which allows facile heat transfer and low reaction temperatures (*i.e.* <100 °C).<sup>2, 166</sup> Overall, emulsion polymerisation, which is facilitated by radicals, can be used to synthesise high molecular weight polymers very readily, whereby the low viscosity of the medium is maintained even at high polymer concentrations.<sup>2, 18, 166</sup> On the other hand, there does exist the potential problem regarding water removal at the end of the reaction; evaporation of such solvent can be timely and expensive when performed on a large scale.<sup>166</sup> This, however, can be avoided by applying the polymer in the latex (aqueous) form.

##### 1.3.1.1. Emulsion polymerisation components

In general, an emulsion polymerisation reaction comprises monomer, a water-soluble initiator and a surfactant, which are all dispersed in an aqueous medium.<sup>2, 3, 166</sup> The surfactant is a crucial reagent in emulsions and over the years has accrued various nomenclature including terms such as “emulsifier”, “dispersing agent” or “soap”. Surfactant molecules are amphiphiles, as they contain hydrophilic and hydrophobic segments. Their structures comprise a hydrophobic tail and a hydrophilic head, as displayed in Figure 1.14.<sup>3</sup> Examples of this type of surfactant include salts of various fatty acids<sup>167</sup> and, most commonly, sodium dodecyl sulfate.<sup>168</sup> In water, these molecules aggregate to form micelles, which are spherical structures where the hydrophobic tails are directed inwards and the hydrophilic heads form an exterior shell which is in contact with water, protecting the hydrophobic interior from

interacting with the water molecules.<sup>2</sup> Surfactants provide the necessary stability for an emulsion between monomer and water,<sup>166</sup> as explained in Section 1.3.1.2.

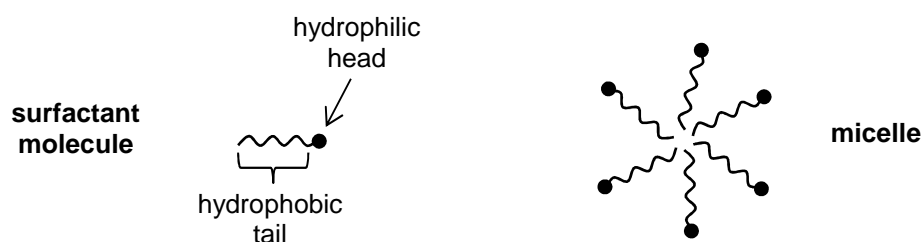


**Figure 1.14. Generic structures for a surfactant molecule and a micelle.**

Redox initiators are typically employed to provide the radicals for an emulsion polymerisation, such as organic or inorganic peroxides,<sup>166</sup> or persulfates.<sup>2, 3</sup> Chain transfer agents (CTAs) can also be present to influence the polymer molecular weight and/or dispersity<sup>166</sup> (their role in polymerisation has already been discussed in Section 1.1.1.1).

### 1.3.1.2. Emulsion polymerisation mechanism

Emulsion polymerisation is complex and is comprehensively explained by two separate theories: Harkins<sup>26</sup> and Smith and Ewart.<sup>169</sup> These are each considered in turn after providing an overall outline of the emulsion process.

As aforementioned (in Section 1.3.1.1), surfactant molecules associate in water to form micelles, which only occurs at, and above, the critical micelle concentration (cmc). The point of the cmc lies just above the maximum concentration of surfactant molecules which is possible to exist in the water phase; the cmc is directly related to factors such as the temperature and ionic strength of the reaction medium, and the hydrophilic/hydrophobic balance of the surfactant.<sup>164, 166</sup>

Partially water-soluble monomer forms droplets when added to the reaction medium; radicals generated from the redox initiator penetrate these droplets and the micelles.<sup>3</sup> Monomer then diffuses through the water into micelles and these become the primary location for polymerisation, as they are present in abundance.<sup>3</sup> As micelles become swollen with polymer, polymer particles are generated and this continues until all of the monomer is consumed.

The surfactant acts as a colloidal stabiliser, essentially forming a barrier between the water and monomer/polymer phases by adsorbing to the droplet-particle interface. This causes droplets (and particles) to repel each other, thus avoiding coalescence (and coagulation).<sup>164</sup> Figure 1.15 depicts a typical emulsion polymerisation system.<sup>2, 164</sup>



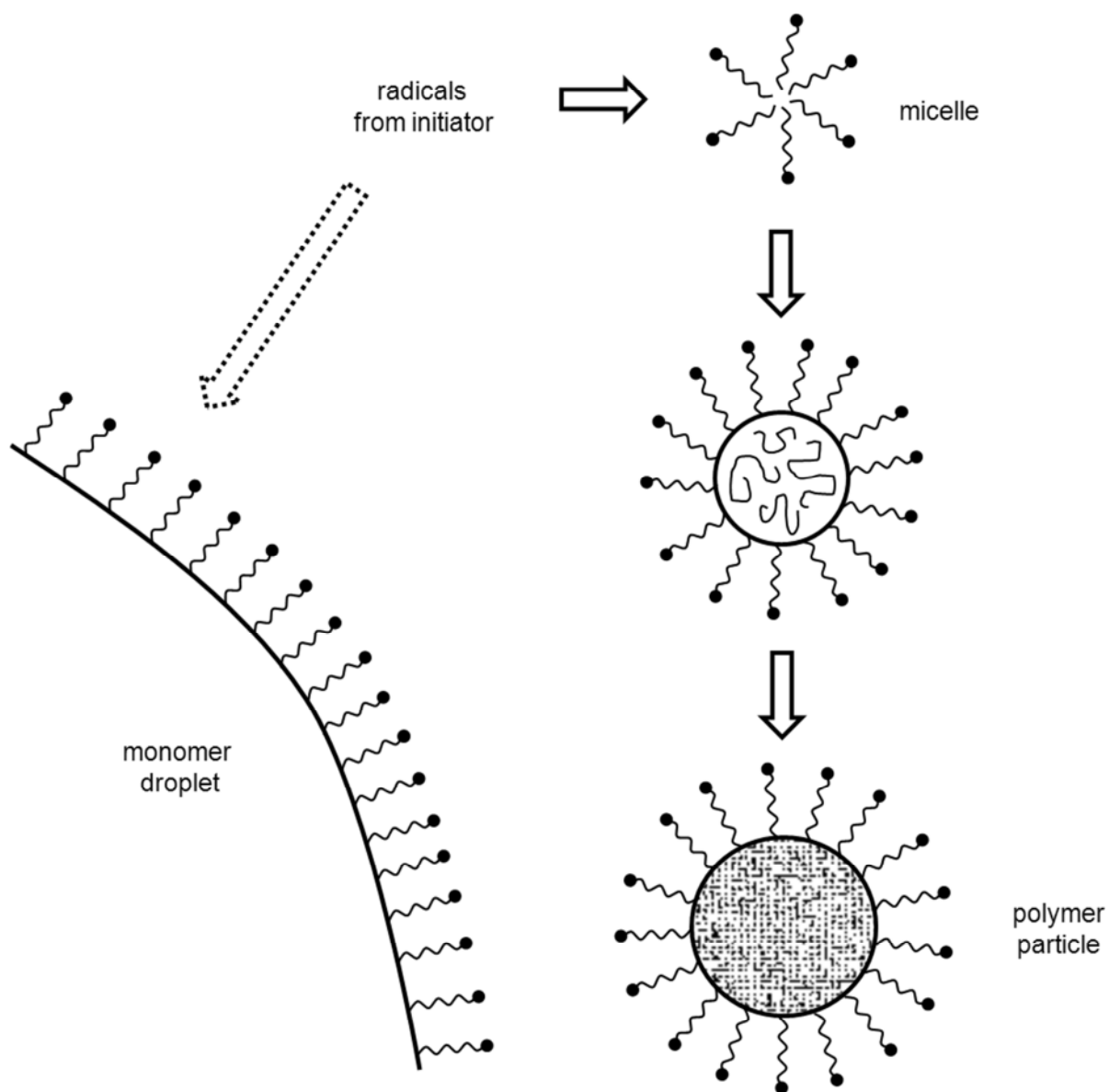


**Figure 1.15. General representation of an emulsion polymerisation system, as adapted from the literature.<sup>164</sup>**

#### 1.3.1.2.1. The Harkins theory

The Harkins theory of emulsion polymerisation<sup>26</sup> is a qualitative view of the process and is based on three defined intervals occurring during the reaction. As summarised in the previous account (Section 1.3.1.2), radicals are firstly generated in the aqueous phase and diffuse mostly into monomer-swollen micelles, which offer an overall larger surface area than monomer droplets. Within the micelle, a polymer chain is initiated and growth continues as monomer is continually stripped from droplets. As this reaction progresses, the micelle transforms into a polymer particle, which is the primary location for polymerisation. This

defines the first interval of Harkins,<sup>26</sup> which transpires over a very short period of time (up to just 5 % monomer conversion), as the polymerisation rate is rapid.

The rate of the second interval of polymerisation is approximately constant. Here, polymer particles remain saturated with monomer, which is continually diffusing from droplets. The concentrations of the monomer in the aqueous phase and in the polymer particles are at a thermodynamic equilibrium.

Interval three occurs after ~60 – 65 % conversion has been reached,<sup>2, 166</sup> where monomer is depleted and the droplets have disappeared. Thus, the concentration of monomer in the polymer particle decreases because of this deficiency, which yields a reduced rate of polymerisation. The reaction ceases when almost all of the monomer (~99 % conversion) is consumed and the polymer particles are fully grown.

#### 1.3.1.2.2. *The Smith and Ewart theory*

The Smith and Ewart theory is a quantitative explanation of the emulsion polymerisation process and includes the derivation of kinetics equations.<sup>169</sup> This was developed around the same time (*i.e.* the late 1940s) and complements the discovery of Harkins.<sup>26</sup>

This theory also assumes that the monomer-containing micelle is penetrated by a radical diffusing through water, whereby chain propagation is initiated. At this point, the radical is active and growth will continue until another radical enters the micelle, where they are then terminated by each other. Propagation is thus postponed until a third radical arrives to re-initiate growth. This forms the basis of the Smith and Ewart theory, where only one radical can be tolerated in a micelle at any one time. It can thus be imagined that it is a somewhat 'start/stop' process and the rate of the 'on/off' switching is determined by the number of micelles present and the rate of radical generation. Furthermore, it can be seen that the probability of a polymer chain growing in a micelle is 50:50, which gives rise to the primary kinetics equation (Equation 1.6) for the rate of emulsion polymerisation:<sup>3</sup>

$$R_p = k_p[M^*][N^* / 2] \quad (\text{Eq}^n \text{ 1.6})$$

Where  $k_p$  = the propagation rate constant;  $M^*$  = the concentration of monomer present in the micelle;  $N^* / 2$  = the number of active micelles.

From this, it can be understood that the polymerisation rate is dependent on the concentration of micelles, if the concentration of the initiator remains fixed. A larger number of micelles present in the system will clearly enable more polymer particles to form. Thus, given that micelles are aggregates of surfactant molecules, the concentration of the

surfactant should be increased in order to enhance the rate (without varying the initiator concentration). Furthermore, the degree of polymerisation ( $D_p$ ) is directly related to the number of monomer molecules polymerised in a particle,<sup>2</sup> which is also directly related to the number of micelles and the surfactant initially employed. Therefore, the surfactant concentration not only dictates the rate of polymerisation, but also the final polymer molecular weight achieved. This undoubtedly reaffirms how crucial the role of the surfactant is in emulsion polymerisation.

Variations of the rate equation provided (Equation 1.6) are present amongst the literature and  $N$  can also be defined as the number of polymer particles per volume of water.<sup>2, 164</sup> Given that polymer particles are generated within micelles, the concentrations of the two are directly related. Hence, it is not surprising that all versions draw the same conclusion: the surfactant concentration is fundamental in influencing the rate and molecular weight.<sup>169</sup>

Considering the theoretical aspects of emulsion polymerisation provided up to this point, the practical aspects of latex formulation are now discussed, including the typical reaction reagents and how latex films are practically obtained.

### **1.3.2. Latex formulation**

A general discussion is provided herein concerning the various latex reagents which can comprise a typical formulation. Thereafter, a standard technique adopted in obtaining rubber latex films is explained followed by an introduction to tensile testing.

#### **1.3.2.1. Formulations**

Table 1.3 illustrates the various reagents which are employed in latex formulations; this is edited from a report by Anderson<sup>164</sup> and accompanied by specific references where appropriate. This list represents a composition which includes the additives necessary for polymerisation, such as monomer, initiator, *etc*, but it is also possible to formulate latexes using pre-prepared polymer (*i.e.* where polymerisation is performed separately, beforehand). In this latter case, only the relevant accelerators, antioxidants and various modifiers would be required; this approach was specifically adopted in the experiments detailed in Chapter 5, which is of a similar format to the studies by Rattanasom *et al.*<sup>170</sup>

Compounds acting as biocides or fungicides can also be incorporated into a latex (usually post-polymerisation). These are especially important when the product is intended for use in environments where microbes thrive, such as for exterior latex paints. Also, pigments or dyes

can be added for decorative purposes. Not included in Table 1.3 is the reaction medium (water), which is crucial in ensuring low viscosity and facilitating efficient heat transfer. The initiator, surfactant and buffer reside in the aqueous phase.<sup>164</sup>

**Table 1.3. Reagents typically employed in latex formulation.**<sup>164</sup>

Reagent type	Examples <sup>‡</sup>	Properties/functions
Monomers <sup>*</sup>	vinyl acetate (VAc), vinyl chloride (VC), acrylonitrile (AN), styrenic, (meth)acrylic and butadiene derivatives	Typically sparingly water-soluble; systems can comprise comonomers.
Cross-linking agents (accelerators) <sup>*</sup>	sulfur, metal oxides, <sup>166, 170-172</sup> thiuram disulfides, <sup>166, 172, 173</sup> thiourea and guanidine derivatives, <sup>171</sup> sulfenamides <sup>170</sup>	Link polymer chains to create three-dimensional insoluble networks.
CTAs <sup>*</sup>	alkyl thiols, such as dodecanethiol <sup>174</sup>	Regulate molecular weight.
Initiators <sup>*</sup>	persulfates, <sup>174</sup> peroxides, <sup>175</sup> azo derivatives <sup>176</sup>	Provide radical flux and promote polymer chain growth.
Surfactants <sup>*</sup>	anionic, <sup>177</sup> cationic, <sup>178</sup> non-ionic <sup>177</sup>	Provide colloidal stability by preventing coagulation; form micelles at polymerisation loci; stabilise monomer droplet 'reservoirs'.
Buffers <sup>*</sup>	sodium bicarbonate <sup>177</sup>	Moderate fluctuations in pH, e.g. when initiators decompose.
Modifiers <sup>†</sup>	celluloses <sup>179</sup>	Enhance viscosity of latex product.
Antioxidants <sup>†</sup>	phenols, amines <sup>173</sup>	Protect against thermal, UV and oxidative degradation.
Fillers <sup>†</sup>	carbon black, <sup>170</sup> clays <sup>180</sup>	Aid processing and abrasion resistance of the rubber; provide bulk to the latex, e.g. for natural rubber (NR).

<sup>\*</sup>Invariably added before polymerisation. <sup>†</sup>Added after polymerisation. <sup>‡</sup>Where specific references are not provided, the review of Anderson<sup>164</sup> should be consulted.

In compounding a latex formulation, the total solids content (TSC) is an important factor. This is defined as the fraction of the total composition which is non-aqueous under atmospheric

conditions and is often expressed as a weight percentage (% w/w).<sup>171</sup> Practically, this simply represents the quantity of solid additives which are dispersed in the water phase. The TSC is typically at least 40 %, <sup>165</sup> but varies according to the (co)polymer being adopted and the final latex application.<sup>115</sup>

Most of the technology for a latex formulation is similar to that in standard rubber compounding; the main difference is simply that the reaction proceeds in water, so that the final product is not a mass of solid rubber, but a soft, elastic material. The reagents employed for cross-linking (as discussed in the section devoted to this topic, 1.2) are typically the same and are determined by the base polymer.<sup>171</sup> An identical cross-linking reaction occurs, which is often activated by metal oxides, and more than one accelerator type can be present.<sup>170</sup>

Other noteworthy latex ingredients include antioxidants, which provide stability to the final product. This is especially crucial given the thinness of latex films, in general, which expose a larger surface area and are therefore more susceptible to degradation by the atmosphere (UV, heat, *etc.*).<sup>171</sup> Fillers seem rather unusual, but are basic reagents employed primarily to bulk out the latex formulation and to aid processing (therefore reducing large-scale production costs). Kaolin clay is a common filler due to its fine particle size and was adopted in these studies (see Chapter 5).<sup>171</sup>

#### 1.3.2.2. Latex compounding

Formulating a latex, which is referred to as ‘compounding’ throughout the rubber industry (irrespective of the state of the rubber), involves the mixing of the reagents (also termed ingredients or additives) in the form of water dispersions.<sup>115</sup> These are mostly water-insoluble solids and so they are initially ground down (or milled) so that fine particles exist to be more readily dispersed;<sup>165</sup> fine particles are especially important when thin latex films are intended.<sup>171</sup> Additionally, a dispersing agent, such as sodium naphthalene formaldehyde sulfonate, can be added to aid the incorporation of additives into the latex.<sup>165</sup>

After a polymer is synthesised *via* emulsion polymerisation, it remains within an aqueous medium and additional ingredients intended for the final latex product are added to this within a single (chemically unreactive) vessel. The reagent dispersions are shaken thoroughly before being added dropwise to the main solution, which is set to stir slowly. It is important that the latex formulation does not become stationary for a length of time, otherwise the solid constituents are likely to settle, which will render the final films inhomogeneous.<sup>165</sup>

Overall, the compounding of latexes is a slow process which requires due care; any debris or imperfections in the vessel can affect the outcome of the final film, such as in compromising

the smoothness of the material. Hence, it is important to use clean, unblemished glassware and minimise the potential for any contamination.<sup>165</sup> Latexes are also known to become unstable when subjected to considerable shear conditions, as shear-induced desorption of the stabilisers can occur.<sup>181</sup> Therefore, the transport and industrial processing of latexes also requires precaution.<sup>165</sup>

#### *1.3.2.2.1. Latex dipping*

A dipping technique is commonly adopted for furnishing latex films, whereby a mould is submerged within a bath containing the compounded mixture and the surface of the mould becomes coated. The mould can be made of porcelain or glass, (*i.e.* unreactive material with a smooth surface), and is more commonly known as a 'former'.<sup>164, 171</sup> The size and shape of the former is dictated by the application intended for the latex product; for example, hand-shaped formers are adopted to yield latex gloves. A coagulant solution can be used to pre-treat the former surface, which enables facile removal of a smooth film product.<sup>164</sup>

During the dipping procedure, the former is generally affixed to a frame and the bath containing the latex formulation can either be raised on a bench to meet it, or the former can be lowered into the solution, all by the means of a cacophony of pulleys and hydraulics.<sup>171</sup> Once immersed in the solution, the former dwells for up to five minutes, where the latex uniformly coats the surface. Leaching typically completes the process (removing excess compounds or dust fragments), then drying and thermal curing (cross-linking). The films themselves are manually stripped from the former either before or after the last stage.<sup>171</sup> To vary the thickness of the material, the immersion (dwell) period can be extended, the dipping/drying steps can be repeated, or the formulation composition can be adjusted.<sup>164</sup>

The overall process employed in manufacturing PCB films for the latex development component of this project comprised the following basic procedure:

- A)** dwelling of former in coagulant solution, followed by brief drying,
- B)** dwelling of former in compounded latex (dipping),
- C)** leaching of coated former in warm water bath,
- D)** drying to remove water,
- E)** manual stripping of latex films from former surface, and
- F)** cross-linking in a pre-set oven.

Figure 1.16 illustrates the key steps of the procedure: compounding, dipping and leaching (**B** and **C** in the previous outline).

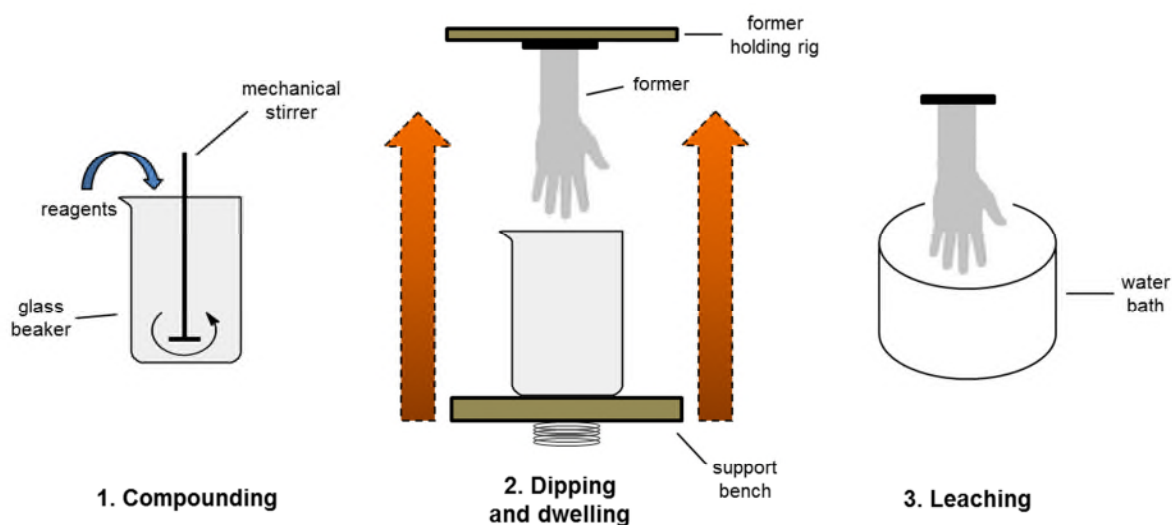


**Figure 1.16. Illustration of the latex compounding/dipping procedure.**

#### 1.3.2.2.2. Latex characterisation

As an industrial product, a latex material is subjected to a range of specifications and standards, namely those of the International Standards Organisation (ISO) and the British Standard (BS). This means that the large-scale production is controlled according to defined, standardised qualities.<sup>171, 173</sup> The adoption of such standards is particularly relevant regarding the physical testing of materials, especially by means of analytical equipment such as the tensometer, which is depicted in Figure 1.17. A tensometer can be adopted for a variety of polymeric materials, including rubbers and plastics, and is a common industrial tool. The basic function is to stretch a sample until it breaks, measuring the tensile strength, modulus and elongation (at break). Latex films are cut into dumbbell shapes (as represented by **D** in the figure) to a predetermined size and gripped into position. The top beam (**A**) then moves upwards to pull the dumbbell; the lower bench remains fixed.

The tensile results are effectively a measure of the quality of the sample, which is in turn determined by the intended application and associated standard/s. Latex gloves, for instance, are known for their stretchiness (*i.e.* affording a large elongation at break test result) and softness (*i.e.* high modulus); healthcare professionals trust these materials to remain intact during use to avoid coming into contact with potentially harmful substances. The set-up of the tensometer is determined by specific ISO and BS standards relevant to the application; the test results need to meet specific requirements in order for the material to be fit for public use. During this project the appropriate “BS903: Part 2A: Type 2 Dumbbells

(small)” standard was adopted in the tensile testing of the PCB latex films, which is typical for rubber grade materials.

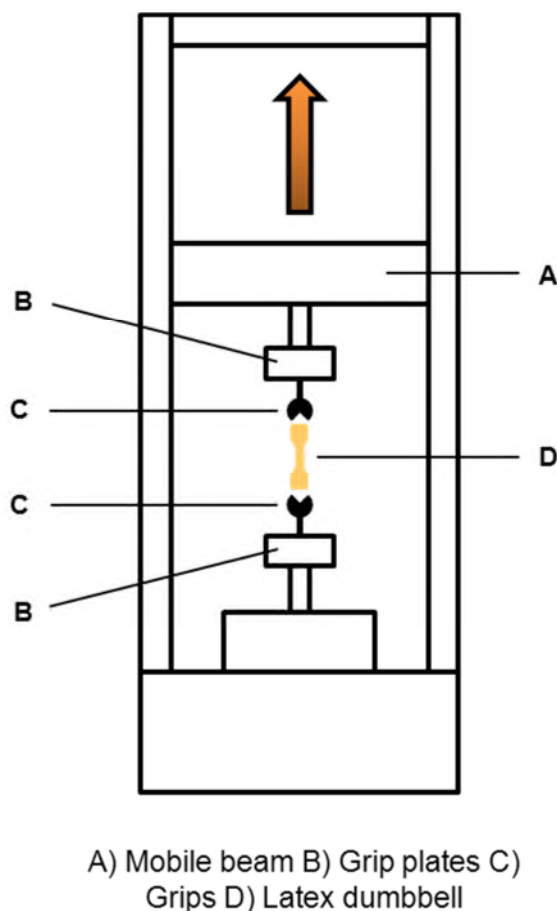


**Figure 1.17. Simplified diagram of a typical tensometer.**

### 1.3.2.3. Applications of latexes

Latexes themselves are not always the final, applied polymer product, rather they can be adopted to enhance the properties, or complement the function of, another material for a given application.<sup>164</sup> Table 1.4 summarises a selection of latex applications and the associated polymers.<sup>134, 164</sup>

Latex polymers are most commonly used in adhesives and as coatings or linings. The latter application is a good example of how latexes function; latex particles are able to form a film on a substrate, which, on drying, can act as a protective layer.<sup>164</sup> This is how textiles and coatings are closely related; the latex can act as a binder, locking threads of a fabric together, creating a layer which can be water repellent or fire retardant.<sup>164</sup> The carpet industry is one of the largest users of latexes, especially for carpet backing or underlay, whereby the polymer ensures that the fabric is adequately anchored to the base cloth<sup>182</sup> and



minimises fraying at the edges.<sup>171</sup> Similarly, the latexes in certain types of (emulsion) paints enable binding of a pigment to the surface which is being coated (*i.e.* for decoration); the latex enables the paint to stick to the surface whilst also allowing it to spread smoothly.<sup>183</sup> Latex adhesives are applicable to materials such as paper, leather, metals, ceramics and in bonding rubbers to textiles.<sup>171</sup>

**Table 1.4. Summary of latex applications.**<sup>134, 164</sup>

<b>Application</b>	<b>Polymer types typically adopted*</b>
Coatings and linings	polyacrylics, PVC, poly(vinylidene chloride), PCB, PVAc, polyacrylamide, poly(vinyl ethers), polyurethanes
Textiles	polyacrylics
Adhesives	polyacrylics, polyurethanes, poly(vinyl pyridine), PCB, polyacrylamide, poly(vinyl ethers), PVA
Gloves	polyacrylonitrile, natural rubber (NR), <sup>†</sup> poly(2-methyl-1-,3-butadiene) (polyisoprene), PCB
Automotive <sup>‡</sup>	NR, PCB
Paints	polyacrylics, polybutadienes, PVAc, poly(vinyl ethers)

\*The final latex composition is often based on copolymers, rather than homopolymers; single polymers are listed here to represent the primary constituent for each material in the given application. <sup>†</sup>The principal polymer of NR is 1,4-*cis*-polyisoprene. <sup>‡</sup>Automotive parts include the tyres and seals.

Latex gloves were the focal application of this project, in particular concerning PCB (the results and discussion of which forms the basis of Chapter 5). This is an instance when the rubber latex is the definitive final product and is used directly, rather than being incorporated into another material. Polyisoprene and PCB are alternative materials to NR for latex gloves.<sup>164</sup> PCB latex gloves in particular are considered safer overall, as they are less likely to afford contact dermatitis or cause skin sensitivity; NR latexes are known to contain leachable proteins, which can cause hypersensitivity (skin) reactions.<sup>184</sup> Such gloves are commonly adopted by the public services and throughout scientific professions, effectively acting as a secondary skin safety barrier.<sup>164</sup> The glove material itself is generally not the safety concern, rather the chemicals employed in latex production are potentially harmful.<sup>185</sup>

### **1.3.3. Poly(2-chloro-1,3-butadiene) latex**

The large-scale industrial syntheses of poly(2-chloro-1,3-butadiene) (PCB) are typically undertaken in emulsion conditions.<sup>173, 174</sup> As a polymer application, PCB is a crucial material when cross-linked (or cured/vulcanised) and is known commercially as neoprene rubber.

This section details the current standard additives for PCB rubber latex and outlines the relevance to this project.

### 1.3.3.1. PCB latex composition

The composition of a PCB latex formulation closely resembles that generally described in Section 1.3.2.1. Table 1.5 lists the specific reagents which are currently employed in producing PCB latex films (namely gloves).<sup>171</sup> This illustration is based on adopting pre-prepared polymer in emulsion form; compounding would involve adding these supplementary reagents directly to the PCB latex (as aqueous dispersions).

**Table 1.5. Reagents typically employed in PCB latex formulations, as taken predominantly from Blackley.<sup>171</sup>**

Reagent type	Example/s	Approximate dispersion level (w/w)
Cross-linking agents (accelerators)	ZnO in combination with diphenyl thiourea (DPTU) and 1,3-diphenylguanidine (DPG) <sup>171</sup>	ZnO: 50 % <sup>171</sup> Organic accelerators: various %
Surfactants/stabilisers	sodium salt of sulfated methyl oleate (SMO) and sodium alkyl sulfate (WAQ)	25 – 35 %
Antioxidant	phenyl-β-naphthylamine or hindered phenols	25 %
Filler	kaolin clay	67 %

Typically, the TSC for a PCB latex is 35 – 60 %, <sup>166</sup> whereby the level adopted at RBL (the industrial sponsor of this project) was 40 %. The TSC is adjusted at the end of the formulation through the addition of (distilled or deionised) water. Variations of PCB latexes exist with different degrees of TSC; a higher solids content affords a firmer material, such as in thicker gloves.<sup>171</sup> PCB gloves are usually prepared by the dipping method (as previously described in Section 1.3.2.2.1) and in this case it is common for a coagulant to be utilised so that the films do not adhere too strongly to the former.<sup>171</sup>

Kaolin clay is a filler for PCB latex and is comprised of hydrated aluminium silicates; this aids the even deposition of the film. SMO and WAQ have stabilising effects and act as surfactants, whilst SMO also contributes to the softness and glossiness of the final film.<sup>171</sup>

The peculiar abbreviations ascribed to these additives were adopted by the supplier, Vanderbilt Chemicals, USA, and are denoted DARVAN<sup>®</sup> SMO and DARVAN<sup>®</sup> WAQ in full.

The nature of the accelerators is discussed in the subsequent section (1.3.3.2), with a focus on their associated hazards. DPTU and DPG are generally recognised as the standard industrial accelerators for PCB latexes<sup>171</sup> and these have been adopted at RBL. Other accelerator types which have been studied include thiuram derivatives, dithiocarbamates and thiazoles, as listed in Table 1.6 in Section 1.3.3.2.

#### 1.3.3.2. PCB latex applications

PCB latexes are used in a wide variety of applications, such as in coatings, adhesives, automotive parts and gloves.<sup>134, 164</sup> The latter application is pertinent to this project and is discussed in more detail herein.

PCB is a successful alternative to NR in latex gloves, as it does not cause harm to, or skin sensitivity in, the end-user (due to the absence of proteins in the material).<sup>184</sup> Attention has thus shifted largely towards further verifying the safety of PCB latex gloves. A review by Rose *et al.* summarises the various hazards associated with latex gloves in general and identifies the offending chemicals to mostly be the accelerators used for cross-linking.<sup>186</sup> Geier *et al.* has also summarised the results of patch tests performed on human subjects with various types of accelerator and deduced that thiurams were the most harmful.<sup>187</sup> The particular compounds highlighted as potential allergens are shown in Table 1.6.

In some cases, it is not the parent molecule which poses the risk; thiazoles and sulfenamides can liberate amines during cross-linking, which can subsequently leach out from the rubber and thus potentially cause harm to the user.<sup>185</sup> Similarly, thiuram disulfides can also liberate amines, such as the particularly undesirable *N*-nitrosamine, which initiated the investigations of Debnath and Basu.<sup>188</sup> Notably, the majority of development concerning accelerator systems has not been undertaken on the latexes themselves, but whilst adopting the solid rubber equivalent, as this material is generally easier to handle and process.<sup>188</sup>

The work undertaken on PCB for this section of the project was performed on the latex directly at RBL. These studies aimed to develop a safer accelerator system for the material, with hopes to eradicate the health issues previously raised with latex gloves, in general. RBL identified the standard PCB system to comprise the accelerators DPTU and DPG, *i.e.* known allergens, as listed in Table 1.6. The aim here was to replace DPTU and DPG in the PCB latex with safer alternatives, which is a similar enterprise to that of the oligomeric PCB cross-

linking studies, where ethylene thiourea (ETU) was the issue, (this is introduced in Section 1.2.2 and is discussed in Chapter 4).

**Table 1.6. Accelerators which are latex glove allergens.**<sup>187</sup>

Accelerator	Abbreviation	Structure
Tetraethylthiuram disulfide <sup>*</sup>	TETD	
Tetramethylthiuram monosulfide <sup>*</sup>	TMTM	
Tetramethylthiuram disulfide <sup>*</sup>	TMTD	
Dipentamethylenethiuram disulfide <sup>*</sup>	DPTD	
Zinc diethyldithiocarbamate <sup>†</sup>	ZDEC	
Zinc dibutyldithiocarbamate <sup>†</sup>	ZDBC	
Diphenyl guanidine <sup>‡</sup>	DPG	
Mercaptobenzothiazole <sup>¶</sup>	MBT	
<i>N</i> -Cyclohexyl-2-benzothiazolesulfenamide <sup>¶</sup>	CBS	
Dibenzothiazole disulfide <sup>¶</sup>	MBTS	
Dibutyl thiourea <sup>§</sup>	DBTU	
Diphenyl thiourea <sup>§</sup>	DPTU	

<sup>\*</sup>Thiuram disulfide. <sup>†</sup>Dithiocarbamate. <sup>‡</sup>Guanidine. <sup>¶</sup>Benzothiazole. <sup>§</sup>Thiourea.

There are few studies in the literature concerning the development of PCB latex; it is strongly expected that industrial research teams have not necessarily publicised their work openly as they wish to retain the Intellectual Property (IP) of their findings. One particular report, however, does concern PCB latex but this focusses on using silica as a filler and optimises the dispersion thereof by ultrasonication; this research was not concerned with altering the standard DPTU/DPG accelerator system.<sup>170</sup>

It is common for systems to comprise two active organic accelerator compounds, *i.e.* they act in a binary fashion. As described by Mathew *et al.*,<sup>189</sup> and Debnath and Basu,<sup>188</sup> accelerators can complement, and be activated by, one another. For instance, thiazole-based derivatives, such as CBS, MBT and MBTS, or thioureas, can work efficiently with thiuram disulfides.<sup>188, 189</sup> Both of these particular studies, however, were concerned with NR and used selected allergens (listed previously in Table 1.6).

One report of particular interest is that of Ohbi *et al.*, who developed a novel accelerator system comprising a xanthogen polysulfide.<sup>185</sup> This work aimed to replace the standard sulfenamide- and thiazole-based accelerators in bromobutyl rubber (BIIR, which incorporates isobutylene and brominated isoprene units); the same health issue was being addressed, to avoid residues leaching out from the rubber material. Diisopropyl xanthogen polysulfide (DIXP), illustrated in Figure 1.18, was found to be a successful alternative, as it did not liberate any residual by-products during the cross-linking reaction. The rubber produced using this accelerator afforded comparable physical properties to that formed *via* the original composition.<sup>185</sup> Given that the copolymer of BIIR comprises polyisoprene units, this new type of accelerator was a worthy contender for these studies with PCB, as both of these polymer backbones are butadiene-based.

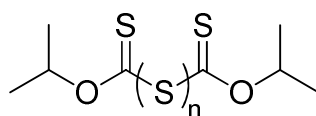


**Figure 1.18. Structure of diisopropyl xanthogen polysulfide (DIXP), where  $n = 3, 4$  or  $5$ .**

#### 1.4. Aims

Poly(2-chloro-1,3-butadiene) (PCB) exists as one of the most widely used elastomers, boasting exceptional chemical and physical properties. Cross-linking introduces a three-dimensional network into the polymer which ultimately affords the favourable properties of this material; this is typically achieved through the use of ethylene thiourea (ETU). Concerns have arisen regarding the carcinogenic nature of this compound and so an alternative reagent was sought which should perform in the same way. The manner in which ETU cross-links PCB has not been resolved; one of the objectives of the Europe-wide “SafeRubber” campaign was to elucidate the reaction mechanism. Both low molecular weight polymer (*i.e.* oligomers) and the PCB rubber was investigated separately by the author and K. Berry, respectively. This collaborative effort characterised the cross-linking reactions physically, through tensile testing, and using spectroscopic techniques; the use of oligomers was anticipated to offer a greater insight into the chemistry taking place. In elucidating the mechanism, the SafeRubber consortium looked to replace ETU in the cross-linking of PCB with a non-toxic alternative.

PCB is synthesised industrially *via* conventional free radical polymerisation in emulsion conditions, which cannot accurately and reproducibly predefine the molecular weight. The initial objective of this PhD project was to design a controlled polymerisation system which enabled the predetermination of low molecular weight PCB, which was subsequently intended for cross-linking investigations. It was conceivable that reversible addition-fragmentation chain transfer (RAFT) polymerisation would facilitate this, as it is arguably the most versatile, straightforward controlled-radical technique. RAFT was a novel enterprise for PCB, as this method had not been successfully adopted for this polymer to-date.

The second industrial contribution to this PhD project was in developing an alternative accelerator system for PCB latex. Diphenyl thiourea (DPTU) and diphenyl guanidine (DPG) are the standard compounds employed in the industrial production of PCB latex gloves, but these chemicals are known allergens. Thus, this binary accelerator system should be replaced by non-hazardous compounds which are able to yield PCB latex of a similar grade. Investigations proceeded by furnishing various PCB latexes with alternative reagents and assessing their relative performances in tensile tests.

## 1.5. References

1. G. Odian, *Principles of Polymerization*, Wiley Interscience, New York, 1991.
2. B. M. Mandal, *Fundamentals of Polymerization*, World Scientific, Singapore, 2013.
3. J. M. G. Cowie, *Polymers: Chemistry & Physics of Modern Materials*, Chapham & Hall, Bath, 1991.
4. W. H. Carothers, *Chem. Rev.*, 1931, **8**, 353-426.
5. J. I. Cunneen, E. H. Farmer and H. P. Koch, *J. Chem. Soc.*, 1943, 472-476.
6. *US Pat.*, 4581429, 1986.
7. M. Kato, M. Kamigaito, M. Sawamoto and T. Higashimura, *Macromolecules*, 1995, **28**, 1721-1723.
8. J.-S. Wang and K. Matyjaszewski, *J. Am. Chem. Soc.*, 1995, **117**, 5614-5615.
9. T. P. T. Le, G. Moad, E. Rizzardo and S. H. Thang, *Chem. Abst.*, 1998, **128**, 115390.
10. C. J. Hawker, A. W. Bosman and E. Harth, *Chem. Rev.*, 2001, **101**, 3661-3688.
11. G. Moad, E. Rizzardo and S. H. Thang, *Acc. Chem. Res.*, 2008, **41**, 1133-1142.
12. M. P. Stevens, *Polymer Chemistry: An Introduction*, Oxford University Press, New York, 1990.
13. J. P. Van Hook and A. V. Tobolsky, *J. Am. Chem. Soc.*, 1958, **80**, 779-782.
14. D. R. Hensley, S. D. Goodrich, A. Y. Huckstep, H. J. Harwood and P. L. Rinaldi, *Macromolecules*, 1995, **28**, 1586-1591.
15. J. Carraher, C. E., *Introduction to Polymer Chemistry*, Taylor and Francis Group, Boca Raton, 2010.
16. F. R. Mayo, *J. Am. Chem. Soc.*, 1943, **65**, 2324-2329.
17. G. Moad and D. H. Solomon, *The Chemistry of Free Radical Polymerization*, Elsevier Science, Oxford, 1995.
18. R. J. Young and P. A. Lovell, *Introduction to Polymers*, Chapman and Hall, London, 1991.
19. R. P. Babu and R. Dhamodharan, *Polym. Int.*, 2008, **57**, 365-371.
20. M. R. Wood, D. J. Duncalf, P. Findlay, S. P. Rannard and S. Perrier, *Aust. J. Chem.*, 2007, **60**, 772-778.
21. S. Perrier and P. Takolpuckdee, *J. Polym. Sci. Part A: Polym. Chem.*, 2005, **43**, 5347-5393.
22. M. Tatsumi and S. Yamamoto, *Polym. Bull.*, 1983, **10**, 452-457.
23. S. Slomkowski, J. V. Aleman, R. G. Gilbert, M. Hess, K. Horie, R. G. Jones, P. Kubisa, I. Meisel, W. Mormann, S. Penczek and R. F. T. Stepto, *Pure Appl. Chem.*, 2011, **83**, 2229-2259.
24. D. C. Blackley, *Emulsion Polymerisation - Theory and Practice*, Applied Science Publishers, London, 1975.
25. J. W. Vanderhoff, *J. Polym. Sci. Polym. Sym.*, 1985, **72**, 161-198.
26. W. D. Harkins, *J. Am. Chem. Soc.*, 1947, **69**, 1428-1444.
27. S. Schulze and H. Vogel, *Chem. Eng. Technol.*, 1998, **21**, 829-837.
28. N. Pullan, M. Liu and P. D. Topham, *Polym. Chem.*, 2013, **4**, 2272-2277.
29. P. D. Topham, N. Sandon, E. S. Read, J. Madsen, A. J. Ryan and S. P. Armes, *Macromolecules*, 2008, **41**, 9542-9547.
30. C. E. Barnes, *J. Am. Chem. Soc.*, 1945, **67**, 217-220.
31. M. Save, Y. Guillaneuf and R. G. Gilbert, *Aust. J. Chem.*, 2006, **59**, 693-711.
32. M. Szwarc, M. Levy and R. Milkovich, *J. Am. Chem. Soc.*, 1956, **78**, 2656-2657.
33. M. Szwarc, *Die Makromolekulare Chemie*, 1960, **35**, 132-158.
34. O. W. Webster, W. R. Hertler, D. Y. Sogah, W. B. Farnham and T. V. RajanBabu, *J. Am. Chem. Soc.*, 1983, **105**, 5706-5708.
35. W. R. Hertler, D. Y. Sogah, O. W. Webster and B. M. Trost, *Macromolecules*, 1984, **17**, 1415-1417.
36. O. W. Webster, *J. Polym. Sci. Part A: Polym. Chem.*, 2000, **38**, 2855-2860.
37. D. Y. Sogah, W. R. Hertler, O. W. Webster and G. M. Cohen, *Macromolecules*, 1987, **20**, 1473-1488.
38. D. M. Haddleton and M. C. Crossman, *Macromol. Chem. Phys.*, 1997, **198**, 871-881.
39. A. D. Jenkins, E. Tsartolia, D. R. M. Walton, J. Horská-Jenkins, P. Kratochvíl and J. Stejskal, *Die Makromolekulare Chemie*, 1990, **191**, 2511-2520.
40. C. S. Patrickios, W. R. Hertler, N. L. Abbott and T. A. Hatton, *Macromolecules*, 1994, **27**, 930-937.
41. T. C. Krasia and C. S. Patrickios, *Polymer*, 2002, **43**, 2917-2920.
42. R. Zhuang and A. H. E. Mueller, *Macromolecules*, 1995, **28**, 8043-8050.
43. P. F. W. Simon and A. H. E. Müller, *Macromolecules*, 2001, **34**, 6206-6213.
44. C. N. Costa and C. S. Patrickios, *J. Polym. Sci. Part A: Polym. Chem.*, 1999, **37**, 1597-1607.
45. J. Zhang, M. Wang, J. Wang, Y. Shi, J. Tao and D. Wang, *Polym. Bull.*, 2005, **54**, 157-161.

46. M. Eggert and R. Freitag, *J. Polym. Sci. Part A: Polym. Chem.*, 1994, **32**, 803-813.
47. C. W. Bielawski and R. H. Grubbs, *Prog. Polym. Sci.*, 2007, **32**, 1-29.
48. S. Aoshima and S. Kanaoka, *Chem. Rev.*, 2009, **109**, 5245-5287.
49. N. E. Kamber, W. Jeong, R. M. Waymouth, R. C. Pratt, B. G. G. Lohmeijer and J. L. Hedrick, *Chem. Rev.*, 2007, **107**, 5813-5840.
50. K. Matyjaszewski and J. Xia, *Chem. Rev.*, 2001, **101**, 2921-2990.
51. S. C. Farmer and T. E. Patten, *J. Polym. Sci., Part A: Polym. Chem.*, 2002, **40**, 555-563.
52. T. B. Zheltonozhskaya, S. V. Fedorchuk and V. G. Syromyatnikov, *Russ. Chem. Rev.*, 2007, **76**, 731-765.
53. G. Moad, E. Rizzardo and S. H. Thang, *Aust. J. Chem.*, 2005, **58**, 379-410.
54. P. B. Zetterlund, Y. Kagawa and M. Okubo, *Chem. Rev.*, 2008, **108**, 3747-3794.
55. S. Penczek and G. Moad, *Pure Appl. Chem.*, 2008, **80**, 2163-2193.
56. P. J. MacLeod, R. Barber, P. G. Odell, B. Keoshkerian and M. K. Georges, *Macromol. Symp.*, 2000, **155**, 31-38.
57. L. I. Gabaston, R. A. Jackson and S. P. Armes, *Macromolecules*, 1998, **31**, 2883-2888.
58. P. Lacroix-Desmazes, P. Andre, J. M. Desimone, A.-V. Ruzette and B. Boutevin, *J. Polym. Sci. Part A: Polym. Chem.*, 2004, **42**, 3537-3552.
59. E. Bultz and T. P. Bender, *Macromolecules*, 2011, **44**, 3666-3669.
60. Y. Guo, M. E. Tysoe and P. B. Zetterlund, *Polym. Chem.*, 2013, **4**, 3256-3264.
61. C. Detrembleur, C. Jerome, J. De Winter, P. Gerbaux, J.-L. Clement, Y. Guillaeneuf and D. Gigmes, *Polym. Chem.*, 2014, **5**, 335-340.
62. C. Marestin, C. Noël, A. Guyot and J. Claverie, *Macromolecules*, 1998, **31**, 4041-4044.
63. D. Greszta and K. Matyjaszewski, *J. Polym. Sci. Part A: Polym. Chem.*, 1997, **35**, 1857-1861.
64. D. S. Germack and K. L. Wooley, *J. Polym. Sci., Part A: Polym. Chem.*, 2007, **45**, 4100-4108.
65. J. He, J. Chen, L. Li, J. Pan, C. Li, J. Cao, Y. Tao, F. Hua, Y. Yang, G. E. McKee and S. Brinkmann, *Polymer*, 2000, **41**, 4573-4577.
66. K. Min, H. Gao and K. Matyjaszewski, *Macromolecules*, 2007, **40**, 1789-1791.
67. H. Fischer, *J. Polym. Sci. Part A: Polym. Chem.*, 1999, **37**, 1885-1901.
68. W. Jakubowski, K. Min and K. Matyjaszewski, *Macromolecules*, 2005, **39**, 39-45.
69. J. Xia and K. Matyjaszewski, *Macromolecules*, 1997, **30**, 7692-7696.
70. G. Moineau, P. Dubois, R. Jérôme, T. Senninger and P. Teyssié, *Macromolecules*, 1998, **31**, 545-547.
71. W. Jakubowski and K. Matyjaszewski, *Macromolecules*, 2005, **38**, 4139-4146.
72. H. Tang, M. Radosz and Y. Shen, *Macromol. Rapid Commun.*, 2006, **27**, 1127-1131.
73. H. Dong, W. Tang and K. Matyjaszewski, *Macromolecules*, 2007, **40**, 2974-2977.
74. W. Jakubowski, B. Kirci-Denizli, R. R. Gil and K. Matyjaszewski, *Macromol. Chem. Phys.*, 2008, **209**, 32-39.
75. A. Simakova, S. E. Averick, D. Konkolewicz and K. Matyjaszewski, *Macromolecules*, 2012, **45**, 6371-6379.
76. K. Mukumoto, Y. Wang and K. Matyjaszewski, *ACS Macro Lett.*, 2012, **1**, 599-602.
77. X.-h. Liu, J. Wang, F.-j. Zhang, S.-l. An, Y.-l. Ren, Y.-h. Yu, P. Chen and S. Xie, *J. Polym. Sci. Part A: Polym. Chem.*, 2012, **50**, 4358-4364.
78. G. Zhu, L. Zhang, Z. Zhang, J. Zhu, Y. Tu, Z. Cheng and X. Zhu, *Macromolecules*, 2011, **44**, 3233-3239.
79. S. Perrier, P. Takolpuckdee, J. Westwood and D. M. Lewis, *Macromolecules*, 2004, **37**, 2709-2717.
80. J. B. McLeary and B. Klumperman, *Soft Matter*, 2006, **2**, 45-53.
81. G. Moad, E. Rizzardo and S. H. Thang, *Aust. J. Chem.*, 2009, **62**, 1402-1472.
82. J. Chiefari, Y. K. Chong, F. Ercole, J. Krstina, J. Jeffery, T. P. T. Le, R. T. A. Mayadunne, G. F. Mejis, C. L. Moad, G. Moad, E. Rizzardo and S. H. Thang, *Macromolecules*, 1998, **31**, 5559-5562.
83. G. Moad, E. Rizzardo and S. H. Thang, *Aust. J. Chem.*, 2006, **59**, 669-692.
84. G. Moad, E. Rizzardo and S. H. Thang, *Polymer*, 2008, **49**, 1079-1131.
85. D. J. Keddie, G. Moad, E. Rizzardo and S. H. Thang, *Macromolecules*, 2012, **45**, 5321-5342.
86. E. Rizzardo, J. Chiefari, Y. K. Chong, F. Ercole, J. Krstina, J. Jeffery, T. P. T. Le, R. T. A. Mayadunne, G. F. Mejis, C. L. Moad, G. Moad and S. H. Thang, *Macromol. Symp.*, 1999, **143**, 291-307.
87. Y. K. Chong, J. Krstina, T. P. T. Le, G. Moad, A. Postma, E. Rizzardo and S. H. Thang, *Macromolecules*, 2003, **36**, 2256-2272.
88. J. Chiefari, R. T. A. Mayadunne, C. L. Moad, G. Moad, E. Rizzardo, A. Postma, M. A. Skidmore and S. H. Thang, *Macromolecules*, 2003, **36**, 2273-2283.
89. Y. Zhou, J. He, C. Li, L. Hong and Y. Yang, *Macromolecules*, 2011, **44**, 8446-8457.



90. V. Jitchum and S. Perrier, *Macromolecules*, 2007, **40**, 1408-1412.
91. B. Chong, G. Moad, E. Rizzardo, M. A. Skidmore and S. H. Thang, *Aust. J. Chem.*, 2006, **59**, 755-762.
92. J. Xu, J. He, D. Fan, W. Tang and Y. Yang, *Macromolecules*, 2006, **39**, 3753-3759.
93. C. Li and B. C. Benicewicz, *J. Polym. Sci., Part A: Polym. Chem.*, 2005, **43**, 1535-1543.
94. O. I. Strube, L. Nothdurft, M. Drache and G. Schmidt-Naake, *Macromol. Chem. Phys.*, 2011, **212**, 574-582.
95. M. Benaglia, E. Rizzardo, A. Alberti and M. Guerra, *Macromolecules*, 2005, **38**, 3129-3140.
96. A. Goto, K. Sato, Y. Tsujii, T. Fukuda, G. Moad, E. Rizzardo and S. H. Thang, *Macromolecules*, 2001, **34**, 402-408.
97. M. H. Allen, S. T. Hemp, A. E. Smith and T. E. Long, *Macromolecules*, 2012, **45**, 3669-3676.
98. C. J. Ferguson, R. J. Hughes, B. T. T. Pham, B. S. Hawke, R. G. Gilbert, A. K. Serelis and C. H. Such, *Macromolecules*, 2002, **35**, 9243-9245.
99. S. W. Prescott, M. J. Ballard, E. Rizzardo and R. G. Gilbert, *Macromolecules*, 2002, **35**, 5417-5425.
100. C. J. Dürr, S. G. J. Emmerling, A. Kaiser, S. Brandau, A. K. T. Habicht, M. Klimpel and C. Barner-Kowollik, *J. Polym. Sci. Part A: Polym. Chem.*, 2012, **50**, 174-180.
101. J. Jennings, M. Beija, J. T. Kennon, H. Willcock, R. K. O'Reilly, S. Rimmer and S. M. Howdle, *Macromolecules*, 2013, **46**, 6843-6851.
102. J. Jennings, M. Beija, A. P. Richez, S. D. Cooper, P. E. Mignot, K. J. Thurecht, K. S. Jack and S. M. Howdle, *J. Am. Chem. Soc.*, 2012, **134**, 4772-4781.
103. J. Zhou, S. Villarroya, W. Wang, M. F. Wyatt, C. J. Duxbury, K. J. Thurecht and S. M. Howdle, *Macromolecules*, 2006, **39**, 5352-5358.
104. H. M. Woods, M. M. C. G. Silva, C. Nouvel, K. M. Shakesheff and S. M. Howdle, *J. Mater. Chem.*, 2004, **14**, 1663-1678.
105. S. Kanagasabapathy, A. Sudalai and B. C. Benicewicz, *Macromol. Rapid Commun.*, 2001, **22**, 1076-1080.
106. J. B. McLeary, F. M. Calitz, J. M. McKenzie, M. P. Tonge, R. D. Sanderson and B. Klumperman, *Macromolecules*, 2004, **37**, 2383-2394.
107. S. E. Shim, H. Lee and S. Choe, *Macromolecules*, 2004, **37**, 5565-5571.
108. T. Arita, M. Buback and P. Vana, *Macromolecules*, 2005, **38**, 7935-7943.
109. J. D. Flores, J. Shin, C. E. Hoyle and C. L. McCormick, *Polym. Chem.*, 2010, **1**, 213-220.
110. A. J. Convertine, N. Ayres, C. W. Scales, A. B. Lowe and C. L. McCormick, *Biomacromolecules*, 2004, **5**, 1177-1180.
111. J. F. Quinn, E. Rizzardo and T. P. Davis, *Chem. Commun.*, 2001, 1044-1045.
112. A. Favier and M.-T. Charreyre, *Macromol. Rapid Commun.*, 2006, **27**, 653-692.
113. J. Rzayev and J. Penelle, *Angew. Chem.*, 2004, **116**, 1723-1726.
114. J. Rzayev and J. Penelle, *Macromolecules*, 2002, **35**, 1489-1490.
115. C. M. Blow and C. Hepburn, eds., *Rubber Technology and Manufacture*, Butterworths, London, 1982.
116. C. D. Vo, D. Kuckling, H. J. P. Adler and M. Schönhoff, *Colloid Polym Sci*, 2002, **280**, 400-409.
117. H. A. Khonakdar, J. Morshedjan, U. Wagenknecht and S. H. Jafari, *Polymer*, 2003, **44**, 4301-4309.
118. X.-R. Zeng and T.-M. Ko, *J. Appl. Polym. Sci.*, 1998, **67**, 2131-2140.
119. J.-M. Charrier, *Polymeric Materials and Processing: Plastics, Elastomers and Composites*, Hanser, New York, 1990.
120. M. Krumova, D. López, R. Benavente, C. Mijangos and J. M. Pereña, *Polymer*, 2000, **41**, 9265-9272.
121. W. Huang, G. L. Baker and M. L. Bruening, *Angew. Chem.*, 2001, **113**, 1558-1560.
122. H. L. Fisher, *Ind. Eng. Chem. Res.*, 1939, **31**, 1381-1389.
123. L. D. Loan, *J. Polym. Sci., Part A: Gen. Pap.*, 1964, **2**, 3053-3066.
124. C. Jiao, Z. Wang, Z. Gui and Y. Hu, *Eur. Polym. J.*, 2005, **41**, 1204-1211.
125. A. Oshima, S. Ikeda, E. Katoh and Y. Tabata, *Radiat. Phys. Chem.*, 2001, **62**, 39-45.
126. M. N. Ismail, M. S. Ibrahim and M. A. Abd El-Ghaffar, *Polym. Degrad. Stabil.*, 1998, **62**, 337-341.
127. N. Rattanasom, T. Saowapark and C. Deeprasertkul, *Polym. Test.*, 2007, **26**, 369-377.
128. S. Dasgupta, S. L. Agrawal, S. Bandyopadhyay, S. Chakraborty, R. Mukhopadhyay, R. K. Malkani and S. C. Ameta, *Polym. Test.*, 2008, **27**, 277-283.
129. G. Heideman, R. N. Datta, J. W. M. Noordermeer and B. v. Baarle, *J. Appl. Polym. Sci.*, 2005, **95**, 1388-1404.

130. G. Heideman, R. N. Datta and J. W. M. Noordermeer, *Rubber Chem. Technol.*, 2004, **77**, 512-541.
131. G. Heideman, J. W. M. Noordermeer and R. N. Datta, *Rubber Chem. Technol.*, 2006, **79**, 561-588.
132. J. K. Kurian, N. R. Peethambaran, K. C. Mary and B. Kuriakose, *J. Appl. Polym. Sci.*, 2000, **78**, 304-310.
133. S. Palaty and R. Joseph, *J. Appl. Polym. Sci.*, 2000, **78**, 1769-1775.
134. H. Ulrich, *Introduction to Industrial Polymers*, Hanser, Munich, 1993.
135. R. C. Ferguson, *J. Polym. Sci., Part A: Gen. Pap.*, 1964, **2**, 4735-4741.
136. P. R. Johnson, *Rubber Chem. Technol.*, 1976, **49**, 650-702.
137. H. Desai, K. G. Hendrikse and C. D. Woolard, *J. Appl. Polym. Sci.*, 2007, **105**, 865-876.
138. P. E. Mallon, W. J. McGill and D. P. Shillington, *J. Appl. Polym. Sci.*, 1995, **55**, 705-721.
139. Y. Miyata and M. Atsumi, *Rubber Chem. Technol.*, 1989, **62**, 1-12.
140. I. Kuntz, R. L. Zapp and R. J. Pancirov, *Rubber Chem. Technol.*, 1984, **57**, 813-825.
141. Y. Miyata and M. Atsumi, *J. Polym. Sci. Part A: Polym. Chem.*, 1988, **26**, 2561-2572.
142. L. Krause and M. A. Whitehead, *Mol. Phys.*, 1973, **25**, 99-111.
143. SafeRubber, <http://www.saferubber.eu/>, Accessed 11/03/2014.
144. D. M. Smith, *Occup. Med.*, 1976, **26**, 92-94.
145. D. M. Smith, *Br. J. Ind. Med.*, 1984, **41**, 362-366.
146. R. S. Chhabra, S. Eustis, J. K. Haseman, P. J. Kurtz and B. D. Carlton, *Fundam. Appl. Toxicol.*, 1992, **18**, 405-417.
147. J. Ashby, *Mutagenesis*, 1986, **1**, 3-16.
148. S. L. Graham, W. H. Hansen, K. J. Davis and C. H. Perry, *J. Agric. Food Chem.*, 1973, **21**, 324-329.
149. S. L. Graham and W. H. Hansen, *Bull. Environ. Contam. Toxicol.*, 1972, **7**, 19-25.
150. S. L. Graham, K. J. Davis, W. H. Hansen and C. H. Graham, *Food Cos. Toxicol.*, 1975, **13**, 493-499.
151. T. Iwase, M. Yamamoto, M. Shirai, F. Akahori, T. Masaoka, T. Takizawa, K. Arishima and Y. Eguchi, *J. Vet. Med. Sci.*, 1997, **59**, 59-61.
152. K. I. Berry, The Quest for a Safer Accelerator for Polychloroprene Rubber, PhD Thesis, Aston University, Birmingham, 2013.
153. M. Guzmán, B. Vega, N. Agulló, U. Giese and S. Borrós, *Rubber Chem. Technol.*, 2012, **85**, 38-55.
154. M. Guzmán, B. Vega, N. Agulló and S. Borrós, *Rubber Chem. Technol.*, 2012, **85**, 56-67.
155. R. Vukov, *Rubber Chem. Technol.*, 1984, **57**, 284-290.
156. F. P. Baldwin, D. J. Buckley, I. Kuntz and S. B. Robinson, *Rubber Plast. Age*, 1961, **42**, 500-510.
157. K. G. Hendrikse, W. J. McGill, J. Reedijk and P. J. Nieuwenhuizen, *J. Appl. Polym. Sci.*, 2000, **78**, 2290-2301.
158. K. G. Hendrikse and W. J. McGill, *J. Appl. Polym. Sci.*, 2000, **78**, 2302-2310.
159. K. G. Hendrikse and W. J. McGill, *J. Appl. Polym. Sci.*, 2001, **79**, 1309-1316.
160. A. S. Aprem, K. Joseph and S. Thomas, *Rubber Chem. Technol.*, 2005, **78**, 458-488.
161. P. Kovacic, *Ind. Eng. Chem. Res.*, 1955, **47**, 1090-1094.
162. Y. Xue, Z. Chen and H. L. Frisch, *J. Appl. Polym. Sci.*, 1994, **51**, 1353-1355.
163. R. Pariser, *Kunststoffe*, 1960, **50**, 623-627.
164. C. D. Anderson and E. S. Daniels, *RAPRA Review Reports*, 2003, **14**, Report 160.
165. K. O. Calvert, in *Polymer Latices and their Applications*, ed. K. O. Calvert, Applied Science Publishers, London, 1982, pp. 1-10.
166. A. A. J. Feast, in *Polymer Latices and their Applications*, ed. K. O. Calvert, Applied Science Publishers, London, 1982, pp. 21-46.
167. H. Hopff and I. Fakla, *Br. Polym. J.*, 1970, **2**, 40-44.
168. B. Emlie, C. Pichot and J. Guillot, *Die Makromolekulare Chemie*, 1991, **192**, 1629-1647.
169. W. V. Smith and R. H. Ewart, *J. Chem. Phys.*, 1948, **16**, 592-599.
170. N. Rattanasom, P. Kueseng and C. Deeprasertkul, *J. Appl. Polym. Sci.*, 2012, **124**, 2657-2668.
171. D. C. Blackley, *High Polymer Latices - Their Science and Technology. Volume 2: Testing and Applications*, Maclaren & Sons Ltd., London, 1966.
172. K. O. Calvert, in *Polymer Latices and their Applications*, ed. K. O. Calvert, Applied Science Publishers, London, 1982, pp. 11-20.
173. K. O. Calvert, in *Polymer Latices and their Applications*, ed. K. O. Calvert, Applied Science Publishers, London, 1982, pp. 47-69.
174. K. Itoyama, N. Hirashima, J. Hirano and T. Kadowaki, *Polym. J.*, 1991, **23**, 859-864.

175. J. E. L. Joensson, H. Hassander, L. H. Jansson and B. Toernell, *Macromolecules*, 1991, **24**, 126-131.
176. J. L. Luna-Xavier, A. Guyot and E. Bourgeat-Lami, *J. Colloid. Interface Sci.*, 2002, **250**, 82-92.
177. G. Pan, L. Wu, Z. Zhang and D. Li, *J. Appl. Polym. Sci.*, 2002, **83**, 1736-1743.
178. H.-H. Chu and H.-Y. Hwang, *Polym. Bull.*, 1997, **38**, 295-302.
179. K. Dimic-Misic, P. A. C. Gane and J. Paltakari, *Ind. Eng. Chem. Res.*, 2013, **52**, 16066-16083.
180. S. Varghese and J. Karger-Kocsis, *Polymer*, 2003, **44**, 4921-4927.
181. S. H. Chang and I. J. Chung, *Macromolecules*, 1991, **24**, 567-571.
182. D. Porter, in *Polymer Latices and their Applications*, ed. K. O. Calvert, Applied Science Publishers, London, 1982, pp. 71-91.
183. K. Sellars and G. R. Brown, in *Polymer Latices and their Applications*, ed. K. O. Calvert, Applied Science Publishers, London, 1982, pp. 145-171.
184. S. H. Wakelin and I. R. White, *Clin. Exp. Dermatol.*, 1999, **24**, 245-248.
185. D. S. Ohbi, T. S. Purewal, T. Shah and E. Siores, *J. Appl. Polym. Sci.*, 2007, **106**, 526-533.
186. R. F. Rose, P. Lyons, H. Horne and S. M. Wilkinson, *Contact Dermatitis*, 2009, **61**, 129-137.
187. J. Geier, H. Lessmann, W. Uter and A. Schnuch, *Contact Dermatitis*, 2003, **48**, 39-44.
188. S. C. Debnath and D. K. Basu, *J. Appl. Polym. Sci.*, 1996, **60**, 845-855.
189. C. Mathew, V. T. E. Mini, A. P. Kuriakose and D. J. Francis, *J. Appl. Polym. Sci.*, 1994, **54**, 1033-1041.

## **CHAPTER 2**

# **MATERIALS AND EXPERIMENTAL METHODS**

## 2. Materials and experimental methods

This chapter provides an overview of the materials and experimental methods employed during the project.

### 2.1. Materials

The following tables list the various reagents adopted throughout the project; lists are segregated according to their applications in the different types of experiment, such as the syntheses of 2-chloro-1,3-butadiene and polymers thereof (2.1), the cross-linking reactions (2.2), and the latex development work (2.3).

**Table 2.1. List of reagents adopted in the syntheses of 2-chloro-1,3-butadiene (CB) and polymers thereof (PCB).**

Name	Denotation	Supplier	Grade/purity (%)
$\alpha,\alpha'$ -azoisobutyronitrile	AIBN	Molekula	
2-chloro-1,3-butadiene	CB	synthesised	
2-chloro-1,3-butadiene	CB	ABCR	50 (v/v in xylene)
cyanomethyl methyl(phenyl)carbamdithioate	CMPCD	Sigma-Aldrich	98
2-cyano-2-propylbenzodithioate	CPD	Sigma-Aldrich	>97
3,4-dichloro-1-butene	SM	TCI	>99
1-dodecanethiol		Sigma-Aldrich	$\geq 98$
S-1-dodecyl-S'-( $\alpha,\alpha'$ -dimethyl- $\alpha''$ -acetic acid)trithiocarbonate	DDMAT	Sigma-Aldrich	98
magnesium sulfat	MgSO <sub>4</sub>	VWR	100.4 (anhy)
methanol	MeOH	Fisher	99.5
phenothiazine		Fisher	99
sodium hydroxide	NaOH	Fisher	97
tetrabutyl ammonium bromide	PTC	Acros	99
tetrahydrofuran	THF	Fisher	99.5
S-(thiobenzoyl)thioglycolic acid	TBTA	Sigma-Aldrich	99
toluene		Fisher	99.5
xylene		Fisher	99.5

**Table 2.2. List of reagents adopted in the poly(2-chloro-1,3-butadiene) cross-linking trials.**

Name	Denotation	Supplier	Grade/purity (%)
1,4-diaminobutane	DAB	Sigma-Aldrich	99
dibutyl thiourea	DBTU	Sigma-Aldrich	97
ethylene thiourea	ETU	Linkwell	98
1,8-octanedithiol	ODT	Sigma-Aldrich	97
piperazine	PIP	Sigma-Aldrich	99
piperazine-1-carbodithioic acid 1,3-diaminopropane complex	PNA-5	RBL	
tetrabutylthiuram disulfide	TbuT	RBL	
zinc oxide	ZnO	Lanxess	93 ("active")

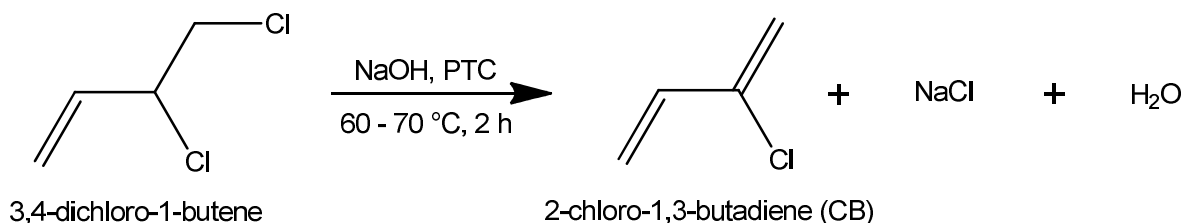
**Table 2.3. List of aqueous dispersions adopted for the poly(2-chloro-1,3-butadiene) latex films.**

Name	Denotation	Supplier	Dispersion (%)
Aquanox 2246		Aquaspersions	45
Darvan <sup>®</sup> SMO		Vanderbilt	30
Darvan <sup>®</sup> WAQ		RBL	25
diisopropyl xanthogen polysulfide	DIXP	RBL	40
diphenyl guanidine	DPG	Flexsys	40
diphenyl thiourea	DPTU	Sigma-Aldrich	50
DISPERBYK 191 <sup>®</sup>		BYK-Chemie	
2,2'-dithio di(ethylammonium)- bis(dibenzylthiocarbamate)	PNA-8	RBL	35
kaolin clay		RBL	40
multi-functional additive	1,4-MFA	RBL	25
Neoprene 750	PCB	DuPont	50
piperazine-1-carbodithioic acid 1,3-diaminopropane complex	PNA-5	RBL	35
tetrabenzylthiuram disulfide	TBzTD	RBL	50
zinc oxide	ZnO	Aquaspersions	50

## 2.2. Experimental methods

Herein provides the details of the various experimental procedures undertaken throughout the project.

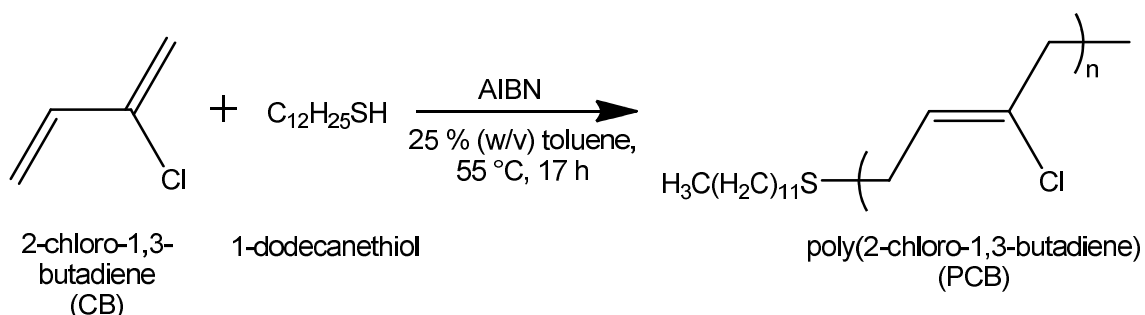
### 2.2.1. Synthesis of 2-chloro-1,3-butadiene



**Scheme 2.1. The synthesis of 2-chloro-1,3-butadiene (CB) by the dehydrochlorination of 3,4-dichloro-1-butene, where PTC denotes a phase-transfer catalyst.**

NaOH solution (6.2 M, 210 ml) and PTC (14 g, 43.4 mmol) were charged to a 500 ml three-necked round bottomed flask. A condenser was fitted and the mixture was stirred and heated. At 55 °C, 3,4-dichloro-1-butene (80.5 g, 0.644 mol) was added dropwise over five minutes. Heating continued and at 62 °C the product distilled as a hazy liquid; 60 – 70 °C was maintained for two hours. Drying over MgSO<sub>4</sub> yielded a clear, colourless liquid (yields varied mostly within the range 50 – 70 %). <sup>1</sup>H NMR (300 MHz, CDCl<sub>3</sub>, δ ppm from tetramethylsilane, TMS): reference CDCl<sub>3</sub> = 7.28 ppm, δ = 6.45 (m, 1H), 5.69 (d, 2H), 5.38 (dd, 2H). Details of the full spectroscopic characterisation of CB are provided in Section 3.1.4.

### 2.2.2. Synthesis of poly(2-chloro-1,3-butadiene) via uncontrolled polymerisation

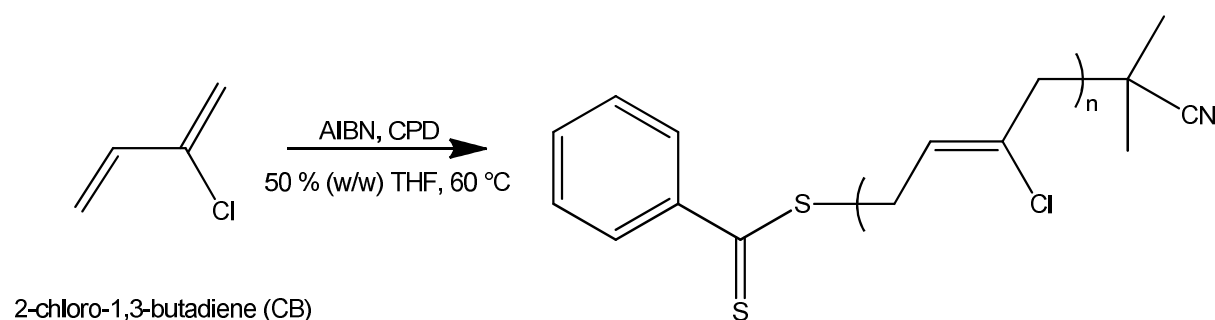


**Scheme 2.2. The uncontrolled polymerisation of 2-chloro-1,3-butadiene (CB) using 1-dodecanethiol CTA (the main 1,4-*trans* polymer isomer configuration is shown).**

A 50 ml round bottomed flask, equipped with a magnetic follower, was charged with a mixture of toluene (1 ml), CB (3.681 g, 41.6 mmol) and 1-dodecanethiol (0.252 g, 1.3 mmol).

The solution was stirred and purged with nitrogen for 30 minutes. Following which, the solution was left under nitrogen atmosphere, the flask sealed and placed in an oil bath at 55 °C. At this point, AIBN (0.078 g, 0.5 mmol) was weighed directly into the solution. The reaction progressed for 17 hours and then termination proceeded by addition of a 0.02 % (w/v) toluene solution of 4-*tert*-butylcatechol (0.101 g). THF (2 ml) was mixed with the polymer solution and this was subsequently added dropwise to methanol (50 ml). After decanting, the remaining solvent was removed in *vacuo*. Yields varied but were generally in the region 40 – 70 %. GPC (RI, calculated *versus* PSt standards):  $M_n = 3300$  g/mol,  $D = 2.10$ . The following analytical data correspond to the main 1,4-*trans* isomer in the PCB product, unless otherwise stated.  $^1\text{H}$  NMR: (300 MHz,  $\text{CDCl}_3$ ,  $\delta$  ppm from TMS): reference  $\text{CDCl}_3 = 7.28$  ppm,  $\delta = 5.90\text{--}5.03$  (br,  $-\text{CH}_2\text{C}(\text{Cl})\text{C}(\text{H})\text{CH}_2-$ ), 2.56 (br,  $-\text{CH}_2\text{C}(\text{Cl})\text{C}(\text{H})\text{CH}_2-$ ), 2.55–2.35 (br,  $-\text{CH}_2\text{C}(\text{Cl})\text{C}(\text{H})\text{CH}_2-$ ), 1.15 (m, dodecanethiol chain end  $\text{CH}_2$ ), 0.90 (m, dodecanethiol chain end  $\text{CH}_3$ ).  $^{13}\text{C}$  NMR (75 MHz,  $\text{CDCl}_3$ ,  $\delta$  ppm): reference  $\text{CDCl}_3 = 77.17$  ppm,  $\delta = 134.86$  ( $-\text{CH}_2\text{C}(\text{Cl})\text{C}(\text{H})\text{CH}_2-$ ), 124.08 ( $-\text{CH}_2\text{C}(\text{Cl})\text{C}(\text{H})\text{CH}_2-$ ), 39.00–24.00 ( $-\text{CH}_2\text{C}(\text{Cl})\text{C}(\text{H})\text{CH}_2-$ ,  $-\text{CH}_2\text{C}(\text{Cl})\text{C}(\text{H})\text{CH}_2-$  and dodecanethiol chain end  $\text{CH}_2$ ), 14.00 (dodecanethiol chain end  $\text{CH}_3$ ). FTIR *assigned peaks* ( $\text{cm}^{-1}$ ): 2921, 2848 ( $\text{CH}_2$  asymmetric stretching), 1659 (*trans*-1,4-PCB C=C stretching), 1630 (*cis*-1,4-PCB C=C stretching), 1445, 1426 ( $\text{CH}_2$  deformation), 1302 ( $\text{CH}_2$  wagging), 1115, 1081 (C—C stretching), 925 (1,2-PCB  $\text{CH}=\text{CH}_2$  stretching), 889 (3,4-PCB  $\text{C}=\text{CH}_2$  stretching), 823 ( $\text{CH}_2$  rocking), 665 (C—Cl stretching). Details of the full spectroscopic characterisation of PCB are provided in Section 3.2.3.

### 2.2.3. Synthesis of poly(2-chloro-1,3-butadiene) via RAFT polymerisation



**Scheme 2.3.** The RAFT polymerisation of 2-chloro-1,3-butadiene (CB,) using 2-cyano-2-propylbenzodithioate, CPD, CTA (the main 1,4-*trans* polymer isomer configuration is shown).

The following example describes the polymerisation of CB in THF at 60 °C with  $[\text{AIBN}]_0/[\text{CPD}]_0/[\text{CB}]_0 = 0.2/1/45$  (*i.e.* a target degree of polymerisation,  $D_p$ , of 45); this is



representative of all polymerisations undertaken during this work. A 50 ml round bottomed flask, equipped with a magnetic follower, was charged with a mixture of CPD (276 mg, 1.247 mmol), AIBN (39 mg, 0.238 mmol), CB (5.027 g, 56.8 mmol) and THF (5 g). The solution was stirred and purged with nitrogen for 30 minutes. Following which, the solution was left under nitrogen atmosphere, the flask sealed and placed in an oil bath at 60 °C. Aliquots of the solution were taken periodically and the polymerisation was monitored up to high conversion. Termination proceeded by rapidly cooling the reaction mixture in ice. THF was added (6 ml) and the resulting polymer solution was added dropwise to methanol (70 ml). After decanting, the remaining solvent was removed in *vacuo*, yielding a viscous dark red liquid. The following analytical data correspond to the main 1,4-*trans* isomer in the PCB product, unless otherwise stated. <sup>1</sup>H NMR (300 MHz, CDCl<sub>3</sub>, δ ppm from TMS): reference CDCl<sub>3</sub> = 7.28 ppm, δ = 5.90–5.03 (br, –CH<sub>2</sub>C(Cl)C(H)CH<sub>2</sub>–), 2.55 (br, –CH<sub>2</sub>C(Cl)C(H)CH<sub>2</sub>–), 2.52–2.25 (br, –CH<sub>2</sub>C(Cl)C(H)CH<sub>2</sub>–). <sup>13</sup>C NMR (75 MHz, CDCl<sub>3</sub>, δ ppm): reference CDCl<sub>3</sub> = 77.17 ppm, δ = 134.92 (–CH<sub>2</sub>C(Cl)C(H)CH<sub>2</sub>–), 124.11 (–CH<sub>2</sub>C(Cl)C(H)CH<sub>2</sub>–), 38.30–26.70 (–CH<sub>2</sub>C(Cl)C(H)CH<sub>2</sub>– and –CH<sub>2</sub>C(Cl)C(H)CH<sub>2</sub>–). FTIR assigned peaks (cm<sup>-1</sup>): 2918, 2857 (CH<sub>2</sub> asymmetric stretching), 1660 (*trans*-1,4-PCB C=C stretching), 1602 (*cis*-1,4-PCB C=C stretching), 1444, 1430 (CH<sub>2</sub> deformation), 1303 (CH<sub>2</sub> wagging), 1115, 1045 (C–C stretching), 827 (CH<sub>2</sub> rocking), 667 (C–Cl stretching).

#### 2.2.3.1. Chain extension experiment

The experiment was performed in a similar way to the polymerisation previously described, but using PCB macroCTA (35 % conv) (976 mg,  $M_n^{\text{GPC}} = 1500$  g/mol, approx. 0.126 mmol), AIBN (3.9 mg, 0.024 mmol), THF (1.9 g) and previously distilled (synthesised) CB (1.9 g, 22.1 mmol). The reaction proceeded at 60 °C for 10 hours to yield the final extended, PCB-*b*-PCB, material (63 % conv).

#### 2.2.4. Compounding and cross-linking of poly(2-chloro-1,3-butadiene) oligomers

Poly(2-chloro-1,3-butadiene) (PCB) oligomers (~3000 g/mol) synthesised *via* the uncontrolled polymerisation method outlined in Section 2.2.2 were predominantly used in cross-linking studies. The various reaction mixtures are outlined in Table 2.4, where levels are given in parts per hundred rubber (phr), as is typical within the rubber industry.

For each reaction, the various additives were first weighed accurately into an appropriately-sized glass vial, followed by addition of the oligomer. Given the high viscosity of the oligomer, the mixtures were not easily rendered homogeneous, so sonication was often adopted for up to two hours (or overnight where larger particle sizes existed, whilst ensuring that the

temperature of the mixtures did not exceed ambient through the use of a thermostat controller) to facilitate easier mixing.

Reaction vessels were equipped with magnetic followers and lowered into an oil bath held at 160 °C to initiate the reaction, which proceeded for one hour.

**Table 2.4. Reaction mixtures adopted in PCB oligomer cross-linking studies, where levels are given in phr.**

	PCB	ETU	ZnO	PIP	DAB	DBTU	ODT	TbuT	PNA-5
1	100	2							
2	100	2	1						
3	100			2					
4	100		1	2					
5	100				2				
6	100		1		2				
7	100					2			
8	100		1			2			
9	100						2		
10	100		1				2		
11	100							2	
12	100		1					2	
13	100								2
14	100		1						2

Ethylene thiourea (ETU); zinc oxide “active” grade (ZnO); piperazine (PIP); 1,4-diaminobutane (DAB); dibutyl thiourea (DBTU); 1,8-octanedithiol (ODT); tetrabutylthiuram disulfide (TbuT); piperazine-1-carbodithioic acid 1,3-diaminopropane complex (PNA-5).

### **2.2.5. Poly(2-chloro-1,3-butadiene) latex compounding**

An appropriate volume of commercially available PCB (neoprene) latex dispersion (50 % w/w) was filtered through two layers of muslin into a clean, dry 2 l beaker and slowly stirred. For each formulation, the various reagents were shaken vigorously before being added dropwise to the stirring PCB solution, over approximately 90 minutes, in the orders

depicted in Table 2.5 (*i.e.* from left to right). The total percentage solids present (TSC) was approximately 40 % in all cases; correction to this level was achieved through addition of deionised water. Slow stirring of the final formulation proceeded overnight; the following day, the solution was filtered through two layers of muslin into another clean, dry 2 l beaker, before dipping commenced (as described in Section 2.2.6).

**Table 2.5. Formulation details for the compounding of PCB latex films (depicted as A – I), where quantities are given in parts per hundred (phr).**

Reagent	A	B	C	D	E	F	G	H	I
<b>50 % PCB latex</b>	100	100	100	100	100	100	100	100	100
<b>25 % Darvan<sup>®</sup> WAQ</b>	0.3	0.3	0.3	0.3	0.3	0.3	0.3	0.3	0.3
<b>50 % ZnO</b>	5	5	5	1	5	1	5	1	5
<b>45 % Aquanox 2246</b>	1.5	1.5	1.5	1.5	1.5	1.5	1.5	1.5	1.5
<b>40 % Kaolin clay</b>	10	10	10	10	10	10	10	10	10
<b>30 % Darvan<sup>®</sup> SMO</b>	1	1	1	1	1	1	1	1	1
<b>50 % DPTU</b>	2								
<b>40 % DPG</b>	2								
<b>40 % DIXP</b>					1.5	1.5			1.5
<b>35 % PNA-8</b>									1.5
<b>35 % PNA-5</b>		2.5	2.5	2.5	1.5	1.5	2.5	2	
<b>25 % 1,4-MFA</b>			1	1				0.5	
<b>50 % TBzTD</b>							0.5	0.5	

Diphenyl thiourea (DPTU); diphenyl guanidine (DPG); diisopropyl xanthogen polysulfide (DIXP); 2,2'-dithio di(ethylammonium)-bis(dibenzylthiocarbamate) (PNA-8); piperazine-1-carbodithioic acid 1,3-diaminopropane complex (PNA-5); 1,4-multi-functional additive based on a 1:2 stoichiometric ratio of 1,4-diaminobutane (DAB) and stearic acid (1,4-MFA); tetrabenzylthiuram disulfide (TBzTD).

Table 2.6 is an example of how a latex formulation was comprised, including the adjustment of the overall total solids content (TSC) to 40 % (w/w). Provided herein are the full details of the PCB/DIXP/PNA-8 latex formulation (denoted as I in the previous Table 2.5), including the actual quantities adopted for each reagent. Following this is an explanation of how the initial formulation was adjusted with an additional measure of water to afford an optimum TSC of 40 % (w/w).

**Table 2.6. Formulation details for the compounding of PCB latex films with the DIXP/PNA-8 accelerator system (I); adjustment to 40 % TSC is outlined.**

Reagent	Dispersion level (% w/w)	Dry wt (g) <sup>‡</sup>	Wet wt (g) <sup>†</sup>	Actual wt (g) <sup>‡</sup>
PCB latex	50	100.00	200.00	800.00
Darvan <sup>®</sup> WAQ	25	0.30	1.20	4.80
ZnO	50	5.00	10.00	40.00
Aquanox 2246	45	1.50	3.33	13.33
Kaolin clay	40	10.00	25.00	100.00
Darvan <sup>®</sup> SMO	30	1.00	3.33	13.33
DIXP	40	1.50	3.75	15.00
PNA-8	35	1.50	4.29	17.14
<b>Total wt (g)</b>		<b>120.80 = x</b>	<b>250.90 = y</b>	<b>1003.60</b>
<b>Adjustment by H<sub>2</sub>O (g)<sup>¶</sup></b>				<b>204.40</b>

<sup>‡</sup>Equivalent to phr. <sup>†</sup>Dry wt x (100 / dispersion level). <sup>‡</sup>Wet wt x 4; a minimum of 1000 g (or 1 l) of total solution was required in the 2 l beaker, so as to adequately cover the surfaces of the former during dipping. <sup>¶</sup>As calculated to afford 40 % TSC, *i.e.* addition of water.

Given the values of x and y in Table 2.6, the initial TSC is given by:  $(x / y) \times 100 = 48.15 \%$ . Hence, additional water was required to lower this value so that it became 40 %, as advised by RBL and stated in literature.<sup>1</sup> Considering that the dry weight of the formulation cannot be altered (as the phr values are fixed) and if  $120.80 / y = 40 \%$ , y should therefore equate to 302 g. Hence, 302 minus 250.9 (*i.e.* the current value of y) equals 51.10 g, which reflects the additional water required to adjust the formulation to 40 % TSC. However, this is further multiplied by 4 (as undertaken for all of the 'actual weights') to achieve the most suitable overall quantity within a 2 l beaker; 204.40 g of water was the final amount required.

#### 2.2.5.1. Preparation of PNA-5 dispersion

An aqueous dispersion of piperazine-1-carbodithioic acid 1,3-diaminopropane complex (PNA-5) was formulated using the reagents listed in Table 2.7. It was necessary to furnish this dispersion for encompassing in the relevant PCB latex films (compounding is detailed in Section 2.2.5). PNA-5 was a novel accelerator and the dispersion was based on that for 2,2'-dithio di(ethylammonium)-bis(dibenzylthiocarbamate) (PNA-8), which was already an

established reagent at RBL. Deionised water was adopted here and throughout the latex studies; DISPERBYK® 191 acted as a surfactant and wetting agent.

**Table 2.7. Formulation details for (35 % w/w) PNA-5 dispersion.**

<b>Reagent</b>	<b>Quantity (g)</b>	<b>Total concentration (% w/w)</b>
PNA-5	100	35.09
DISPERBYK® 191	8	2.81
Water	177	62.11
<b>Total quantity (g)</b>	<b>285</b>	

All of the reagents were weighed directly into an appropriate, clean and dry ceramic vessel, which also comprised numerous zirconia milling balls. The vessel was tightly sealed and affixed into a vibromill machine; the solution was subjected to high frequency vibrations for up to one hour, whereby the solid reagent (PNA-5) was milled and dispersed into the aqueous medium. Thereafter, the solution was decanted into clean, dry glass jars; the solution was homogeneous and green/yellow-coloured.

#### **2.2.6. Preparation of poly(2-chloro-1,3-butadiene) latex films**

The following procedure describes the typical 'dipping' technique employed in the preparation of PCB latex films. This was developed as a standard method at RBL before the commencement of this PhD project.

Two clean glass formers, each comprising three separate glass faces which measured 10 cm x 25 cm (width x length), were warmed in an oven at 50 °C for at least 30 minutes. Approximately 1.5 l of pre-prepared coagulant solution\* was thoroughly shaken and poured into a clean, dry 2 l beaker. One former was removed from the oven, inverted and submerged into the coagulant solution for 10 seconds. The former was removed and carefully upturned so as to minimise drips settling on the glass faces. Applying a hairdryer on a low temperature setting for 4 minutes, the solution was dried onto the former as evenly as possible. In a dipping cabinet, comprising a pre-set variable-height holding bench, the former was inverted and attached to ceiling brackets. The beaker containing the formulation solution was positioned on the bench directly underneath the former and was then quickly raised so that the former became submerged so that at least one third of the surface faces were covered. This position was maintained for 60 seconds to thoroughly dwell the former. The

bench was slowly lowered to uncover the former, which was then transferred to a water bath (35 °C) for 30 minutes. Thereafter, drying proceeded using a hair dryer (high temperature setting, ~50 °C) for 7 minutes. Further, extensive drying was then undertaken in an oven at 70 °C for one hour. The former was removed from the oven and left to cool to ambient. Latex films were gently stripped from the surface of the former by hand, using talc to ensure that the material did not become stuck to itself. The films were then suspended in an oven at 120 °C for one hour to facilitate cross-linking (curing).

This procedure was repeated in full for the second former, so that a total of six films resulted for each formulation (2 x 3 films). Figure 2.1 illustrates the main steps for the process.

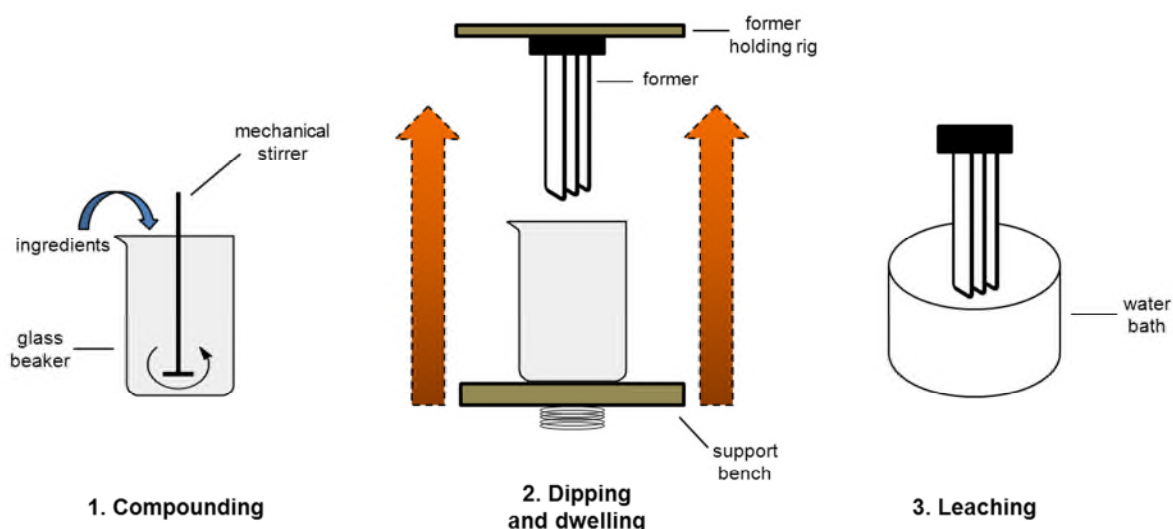


**Figure 2.1. The dipping procedure adopted for the preparation of PCB latex films.**

\*Coagulant solution comprised 40 % (w/v) calcium nitrate tetrahydrate in IMS, containing 0.1 % (w/v) IGEPAL® CO-630 wetting agent and 1.5 % (w/v) talc.

### 2.3. Characterisation methods

Herein describes the methods used to characterise the synthesised materials.

#### 2.3.1. Nuclear Magnetic Resonance Spectroscopy

Nuclear magnetic resonance spectroscopy (NMR) was used to confirm the structures of synthesised compounds and was the primary tool in monitoring monomer conversion during polymerisations. Appropriate deuterated solvents were used (typically  $\text{CDCl}_3$ ) to dissolve analytes to approximately 10 % (w/v). Spectra were recorded on a Bruker Avance

spectrophotometer at 300 MHz and 75 MHz for  $^1\text{H}$  and  $^{13}\text{C}$  analyses, respectively. For  $^{13}\text{C}$ , PENDANT spectra were collected. Chemical shifts (ppm) were relative to TMS.

### 2.3.1.1. Monitoring monomer conversion

The conversion of CB (to PCB) during the RAFT polymerisation reactions was assessed by  $^1\text{H}$  NMR spectroscopy under the conditions described in Section 2.3.3. Figure 2.2 illustrates the spectra collected over time during the optimum CPD/THF reaction, highlighting the 5.0 – 6.6 ppm region in particular. Appropriate protons pertaining to the monomer and polymer are illustrated in this area, notably the sole vinyl proton of CB (given by integral **y** at 6.5 ppm), the four alkene protons of CB and the vinyl proton of 1,4-*trans*-PCB (all five appear within 5 – 6 ppm and are represented by integral **z**). Only this major PCB isomer was considered, given the complications arising from the potential presence of four isomers (1,4-*trans*, 1,4-*cis*, 1,2- and 3,4-, as explained in Section 3.2.3) and the resulting complex spectra. Hence, the monomer conversions provided are approximate values as only one entity was considered.

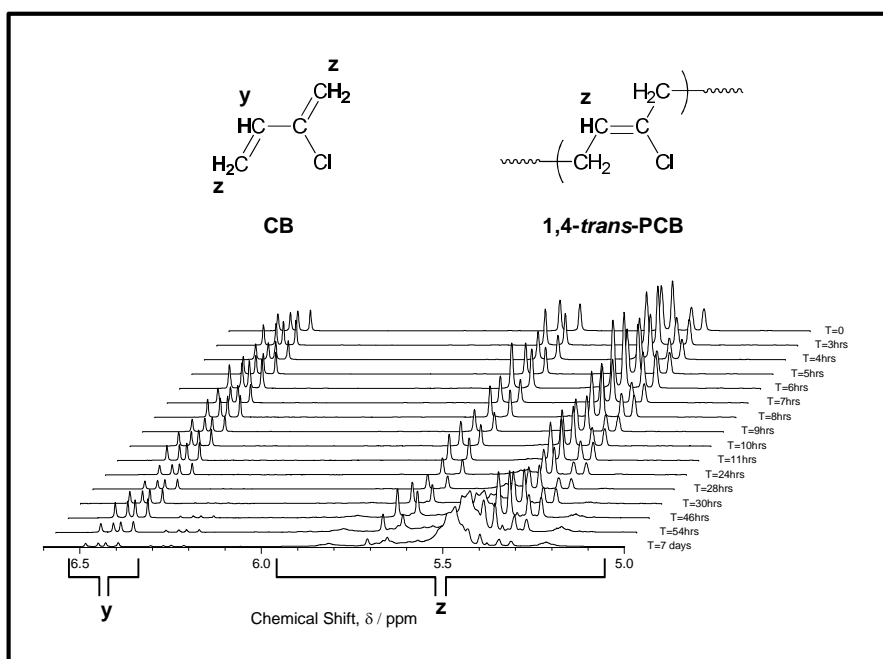


**Figure 2.2. Comparative  $^1\text{H}$  NMR spectra (in  $\text{CDCl}_3$ ) illustrating the progress of CB polymerisation (RAFT, in CPD/THF conditions) through the appearance of PCB vinyl protons at 5 – 6 ppm (z) and the disappearance of the monomer vinyl proton (y).**

The values of the **y** and **z** integrals in Figure 2.2 are shown in Table 2.8 and were applied in Equation 2.1 in order to determine monomer conversion (**x**). The final step of this calculation was to multiply **x** by 100 in order to give the percentage conversion. For reference, the NMR spectra of CB and PCB are elucidated fully in Chapter 3.

$$y / z = (1 - x) / (4 - 3x) \quad (\text{Eq}^n 2.1)$$

**Table 2.8. Approximate percentage CB conversion\* during CPD/THF RAFT polymerisation by comparison of <sup>1</sup>H NMR integrals relating to the vinyl and alkene protons of CB and PCB.**

Time	Integral y <sup>†</sup>	Integral z <sup>‡</sup>	% Conversion
3hrs	1	4.257	20
4hrs	1	4.284	22
5hrs	1	4.319	24
6hrs	1	4.390	28
7hrs	1	4.411	29
8hrs	1	4.492	33
9hrs	1	4.564	36
10hrs	1	4.586	37
11hrs	1	4.645	39
24hrs	1	5.568	66
28hrs	1	6.639	72
30hrs	1	7.257	76
46hrs	1	9.725	85
54hrs	1	17.809	93
7 days	1	38.657	97

\*Applying Equation 2.1. For simplicity, only the protons of the major 1,4-*trans*-PCB isomer were considered. <sup>†</sup>Represents the sole vinyl proton of CB. <sup>‡</sup>Represents the vinyl proton of PCB plus the four alkene protons of CB.

### 2.3.2. Gel Permeation Chromatography

Gel permeation chromatography (GPC) was used to measure polymer molecular weight ( $M_n$ ) and dispersity ( $M_w/M_n$ , denoted by  $\mathcal{D}$ ). Three PL gel 5  $\mu\text{m}$  300 x 7.5 mm mixed-C columns, preceded by a guard column, constructed the GPC system. Laboratory grade THF, stabilised with 0.05 % (w/v) BHT and mixed with 2 % (v/v) TEA before degassing, was used as the eluent (mobile phase), at a flow rate of 1 ml/min and the temperature of the columns was 40 °C. Laboratory grade toluene acted as the flow rate marker. Regular calibration was carried out using polystyrene ( $M_p$  range = 162 to 6,035,000 g/mol) near-monodisperse standards. Samples were formulated directly from eluent THF to a concentration of approximately 4 mg/ml. Data were analysed using Cirrus GPC software (version 3.2) provided by Agilent Technologies (formerly Polymer Laboratories).



### **2.3.3. Fourier Transform Infrared Spectroscopy**

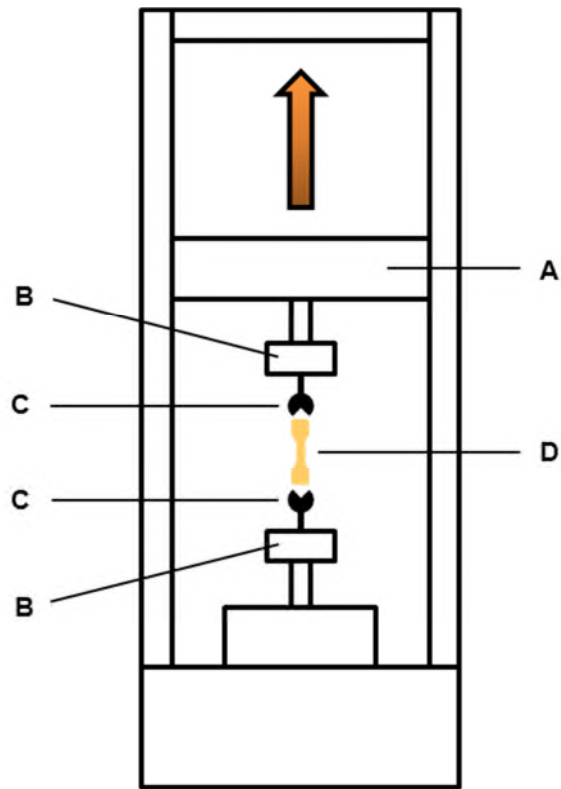
Fourier transform infrared (FTIR) spectroscopy was performed primarily on a Thermo Scientific Nicolet 380 instrument. Samples were assessed in the solid state, being placed directly onto a diamond plate and collecting 32 scans of attenuated total reflectance (ATR). The background was assessed through the analysis of a blank sample. A resolution of  $4\text{ cm}^{-1}$  was adopted over the range  $525 - 4000\text{ cm}^{-1}$ .

### **2.3.4. Viscosity measurements**

Viscosity measurements of the PNA-5 dispersion reagent used in the latex formulations were taken using a Brookfield LVDV-E digital viscometer. Solutions were mechanically stirred using an appropriately-sized stainless steel spindle (typically of grade 3, 4, 5 or 6). Results were given in centipoise (cP) and were noted once the readings stabilised. A rotation speed of 60 rpm (revolutions per minute) was adopted throughout; samples were tested at ambient temperature. The torque required to rotate the spindle dictated the size/grade required, whereby 40 – 50 % torque was optimum. Spindles with smaller discs (as denoted by larger numbers) were required for more accurate readings (*i.e.* within this torque range) at high viscosity; larger discs (of grade 3 or 4, for instance) could be adopted at low viscosity.

### **2.3.5. Tensometer**

Tensile testing of the PCB latex films was undertaken at RBL on an Instron 4302 machine (portrayed in Figure 2.3). Test pieces were cut into the appropriate dumbbell shapes using a metal cutting die and were subsequently pulled at 500 mm/min according to the standard BS903: Part 2A: Type 1 Dumbbells (Small). A Mitutoyo Digimatic multiplexer MUX-10 micrometer evaluated the thickness of the dumbbells prior to testing, as required for calculating the tensile results. Blue Hill software generated the test results, such as the 300 % modulus, ultimate tensile strength (UTS) and elongation at break.



A) Mobile beam B) Grip plates C) Grips D) Latex dumbbell

**Figure 2.3. Simplified diagram of a typical tensometer.**

## 2.4. References

1. A. A. J. Feast, in *Polymer Latices and their Applications*, ed. K. O. Calvert, Applied Science Publishers, London, 1982, pp. 21-46.

## **CHAPTER 3**

# **RAFT POLYMERISATION OF 2-CHLORO-1,3-BUTADIENE**

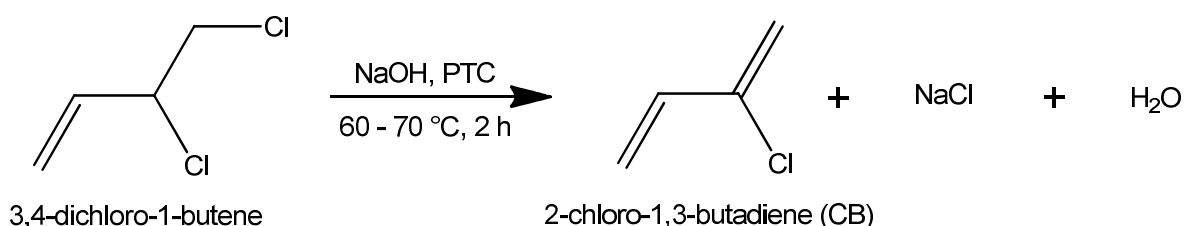
### 3. RAFT Polymerisation of 2-chloro-1,3-butadiene

2-Chloro-1,3-butadiene (CB), more commonly known as chloroprene, was the principal monomer of interest during this study. In the polymerised form, poly(2-chloro-1,3-butadiene) (PCB), has important applications as neoprene rubber and is used extensively in everyday life, for example forming the material for types of latex gloves and vehicle tyres.<sup>1</sup> The polymer is only practical as such, though, once the polymer chains have been cross-linked; the presence of polymer networks enhances the physical properties of the material, rendering it viable for industrial applications.<sup>2</sup>

Ethylene thiourea (ETU) is the most effective cross-linker for PCB in forming the solid synthetic rubber, but the use of this additive is in jeopardy because of the associated toxicity.<sup>2, 3</sup> The EU (REACH) is thus striving to completely withdraw the use of ETU in industry and so an alternative cross-linker is sought, which should react with PCB to form rubber with similar or improved physical properties. Initial CB polymerisation reactions described herein aimed to readily synthesise low molecular weight polymers which could then be adopted for cross-linking mechanistic studies. As opposed to the ~250 kg/mol molecular weight industrial PCB rubber, oligomers would be more straightforward to analyse, owing to their ability to dissolve following the 'cross-linking' process (the oligomers become heavily branched rather than fully cross-linked). Prior to polymerisation studies, it was necessary to develop a synthetic protocol for CB monomer, as the neat material was not commercially available.

#### 3.1. Synthesis of 2-chloro-1,3-butadiene

The most common synthetic procedure for CB amongst the literature is the chlorination of butadiene and subsequent dehydrochlorination (removal of HCl) of 3,4-dichloro-1-butene using base (Scheme 3.1).<sup>4-7</sup> Fortunately, the second-stage product was available commercially and inexpensive, so it was possible to use this as the starting material and immediately omit the first reaction step. In this instance, dehydrochlorination of 3,4-dichloro-1-butene was carried out using sodium hydroxide.



**Scheme 3.1. The synthesis of 2-chloro-1,3-butadiene (CB) by the dehydrochlorination of 3,4-dichloro-1-butene, where PTC denotes a phase-transfer catalyst.**

Most reported syntheses suggest simply heating the starting material directly with a solid base, but these processes involve high temperatures (up to 90 °C).<sup>5</sup> This was a concern, given that premature polymerisation of CB could occur with prolonged overheating,<sup>8, 9</sup> whereby product purity and yield could suffer. A modification was therefore made and a phase-transfer catalyst (PTC) in the form of tetrabutylammonium bromide was included. This reagent allowed the reaction to proceed at a lower, more practical temperature (not exceeding 70 °C) and reduced the overall reaction time.

For this new protocol, the base and PTC were charged to the reactor, which was fitted to a condenser, and the 3,4-dichloro-1-butene was added dropwise over a few minutes once the temperature reached 55 °C. The reaction proceeded at atmospheric pressure and the product invariably distilled over as a hazy liquid once 62 °C was reached, 60 – 90 minutes after addition of 3,4-dichloro-1-butene. The presence of water was found to be the cause of this haziness, as described in Section 3.1.2. After drying over MgSO<sub>4</sub>, CB underwent further purification by vacuum distillation.

### **3.1.1. Varying sodium hydroxide concentration**

Owing to the fact that this was a new, modified synthetic protocol for CB, it was necessary to design optimal reaction conditions which would attain maximum yields of the highest purity material, as simply as possible. The literature suggested that the optimum conditions for the dehydrochlorination of 3,4-dichloro-1-butene required a minimum base concentration of 25 % (w/v).<sup>8</sup> This was indeed verified through a handful of small-scale CB syntheses, where the sodium hydroxide concentration was varied and the final yields compared, as illustrated in Table 3.1.

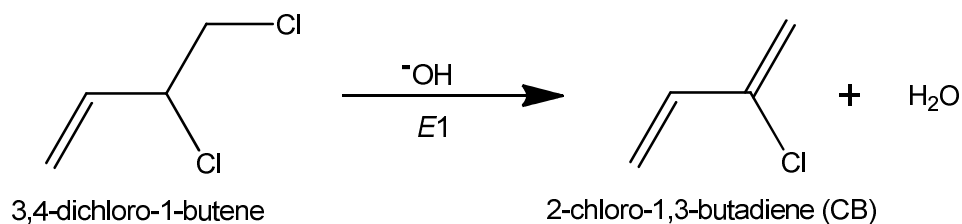
**Table 3.1. Table showing how varying sodium hydroxide concentrations in CB syntheses affected percentage yields.**

<b>NaOH<sub>(aq)</sub> concentration % (w/v)</b>	7	15	25
<b>% Yield</b>	---	64	88

The reaction utilising 25 % (w/v) sodium hydroxide afforded the highest yield, whereas reducing this resulted in a significant depreciation; levels as low as 7 % (w/v) failed to initiate any CB production whatsoever. Lower concentration levels reducing the yield is thought to be a consequence of fewer hydroxide ions being present to facilitate dehydrochlorination. Concentrations in excess of 25 % (w/v) were not investigated as 88 % yield was sufficient.

### 3.1.2. Water as a by-product

The dehydrochlorination reaction forms water as a by-product (Scheme 3.2), so it is not surprising that this was identified in the initial crude CB product. Water seemingly distils over with the CB and this would be the reason for the hazy liquid initially collected. Given that water boils at a much higher temperature than CB (*i.e.* 100 °C *versus* 62 °C), an azeotrope must form between the two components, whereby the two liquids mix together and subsequently become inseparable by distillation.<sup>10</sup>



**Scheme 3.2.** The dehydrochlorination of 3,4-dichloro-1-butene by base, the  $E1$  reaction.

The presence of water was confirmed by  $^1\text{H}$  NMR spectroscopy ( $\text{CDCl}_3$ ), whereby a singlet peak at 1.55 ppm in the crude product was vastly reduced or eradicated upon drying the material over magnesium sulfate ( $\text{MgSO}_4$ ) (see Figure 3.1 for comparative spectra). Removal of the water was also physically observed as the hazy liquid quickly became clear and colourless when mixed with the drying agent.

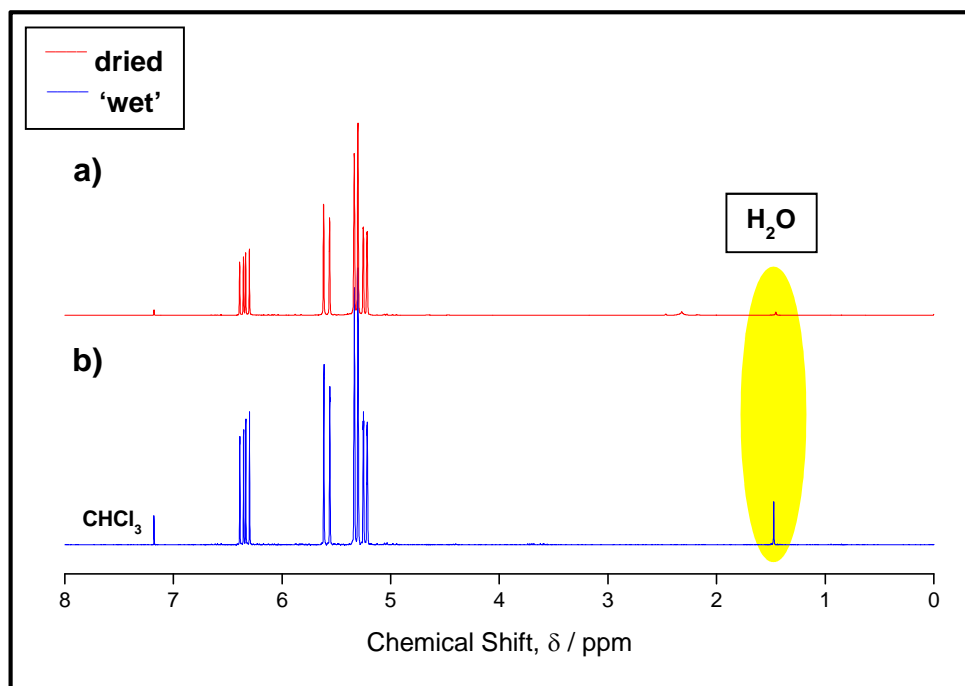


**Figure 3.1.**  $^1\text{H}$  NMR spectra of CB before (b) and after (a) drying over  $\text{MgSO}_4$ .

### 3.1.3. Variable yields in the synthesis of 2-chloro-1,3-butadiene

The dehydrochlorination of 3,4-dichloro-1-butene was a fairly capricious reaction, in that the yields obtained were not at all consistent. Despite the reaction appearing so simple, involving only three reagents, a single step and basic apparatus; two reactions undertaken side-by-side, under seemingly identical conditions, never produced the same yield. Table 3.2 shows data from a representative set of syntheses, highlighting how varied the end result was each time.

**Table 3.2. Experimental data highlighting the variable yields obtained during the synthesis of CB.**

Experiment	Starting material (SM) mass (g)	Addition period (min)	Temperature rise* (°C)	Yield (%)
1	80.5	2	62 – 85 (2 h)	88
2	103.5	3	63 – 80 (1.5 h)	22
3	103.5	2	65 – 85 (3 h)	92
4	103.5	2	65 – 85 (3 h)	57
5	80.5	3	62 – 80 (2 h)	87
6	80.5	3	62 – 80 (2 h)	68

\*The reaction medium temperature at the point of starting material (SM) addition was 55 °C for each synthesis; noted is the temperature range over which CB distilled and the duration of this.

The data presented in Table 3.2 represent six reactions which were carried out as described in the Experimental Chapter (Section 2.2.1). For each one, a fresh batch of 3,4-dichloro-1-butene, was used and addition was carried out at comparable temperatures, proceeding over only a few minutes. The rise in temperature once CB began distilling over was controlled at similar rates and reactant molar equivalents were comparable. However, with this in mind,

the final CB yields (crude, before the drying stage) fluctuated incredibly, varying from 22 % to 92 %.

On two separate occasions, a pair of reactions was carried out side-by-side employing identical conditions and apparatus (*i.e.* experiments **3** and **4**, **5** and **6**). The only difference between these sets was the scale of the reactions, where the former (**3** and **4**) involved a smaller amount of SM. Despite replicated conditions, the product yields varied for each set. For instance, the CB yields for experiments **3** and **4** were 92 % and 57 %; for experiments **5** and **6**, the CB yields were 87 % and 68 %, respectively. Given that the concentrations of reagents and the apparatus were identical, and the addition rate and temperature changes were the same, it is difficult to rationalise these varying yields. It was postulated that this could be attributed to the rate of stirring, but it seems highly improbable that this alone could have such dramatic effects on the extent of the reaction. It is possible that the system is extremely sensitive to minor impurities in the starting material (which were undetected by NMR analysis, as such).

CB syntheses persevered through this route, despite the unreliable yields, as it was important to begin generating monomer which could be fed into subsequent polymerisation reactions. Were the focus of this project more dependent on this stage, there would have been more deliberation over improving the efficiency of the process and could be the basis of future work.

#### **3.1.4. NMR Characterisation of 2-chloro-1,3-butadiene**

NMR spectroscopy was the primary technique employed for characterising CB and confirming its purity. The annotated proton ( $^1\text{H}$ ) and carbon ( $^{13}\text{C}$ ) spectra of (pure) CB, synthesised by the route described previously, are shown in Figure 3.2 (plots **a** and **b**, respectively).

CB has three different proton environments, which are represented by three respective sets of signals in the  $^1\text{H}$  NMR spectrum; a sole vinyl =CH proton exists in the molecule, along with two types of terminal  $\text{CH}_2$  alkene proton. The signal for the vinyl CH (**1**) is situated furthest downfield, at 6.4 – 6.5 ppm and two singlets arise at 5.7 ppm for the terminal  $\text{CH}_2$  closest to the chlorine-bonded carbon (**2**). Lastly, the signals at 5.3 – 5.4 ppm are attributed to the terminal  $\text{CH}_2$  protons situated furthest away from the chlorine atom (**3**). Interpretation of the  $^1\text{H}$  NMR spectra of CB was supported by data presented in the literature.<sup>11</sup>  $^{13}\text{C}$  NMR spectroscopy was used for more qualitative analysis and to complement the  $^1\text{H}$  NMR spectrum in confirming CB purity. Figure 3.2 (b) shows the PENDANT  $^{13}\text{C}$  spectrum of pure



CB, with the four signals assigned. The NMR characterisation of CB synthesised in this work indicates high purity, overall; this was essential for future polymerisation studies.

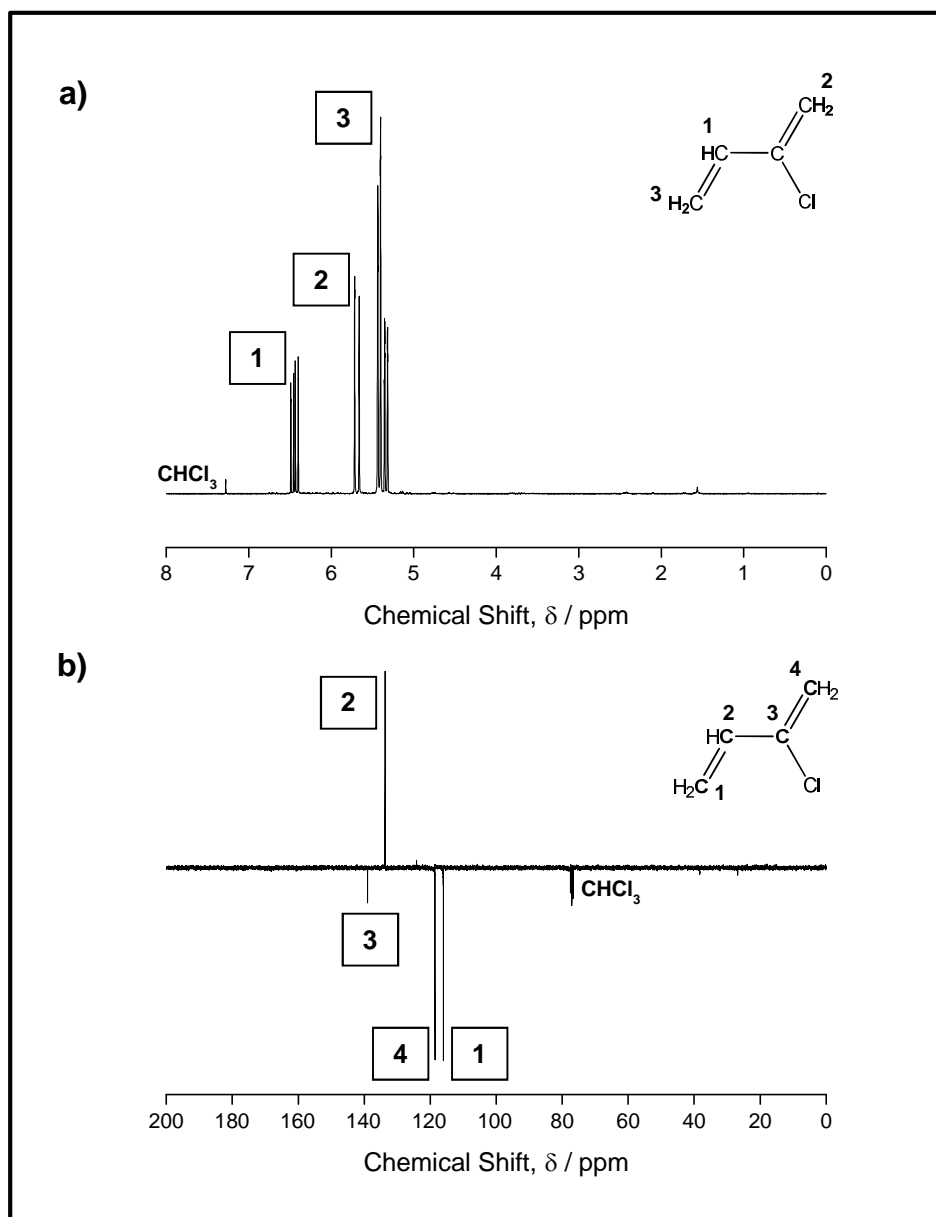


Figure 3.2. Pure CB  $^1\text{H}$  NMR spectrum (a) and PENDANT  $^{13}\text{C}$  NMR spectrum (b).

### 3.1.5. Stability of 2-chloro-1,3-butadiene

CB is known to be highly unstable<sup>12</sup> and was indeed found to readily self-polymerise under ambient conditions. Thus, the degradation of CB had to be prevented so that subsequent polymerisation reactions were not hindered or impaired in any way.

The self-polymerisation of CB was monitored through periodic  $^1\text{H}$  NMR ( $\text{CDCl}_3$ ) analyses of a sample of freshly synthesised, dried monomer which was held at room temperature.

Degradation was observed after only two hours in these conditions, as polymeric peaks began to appear in the spectrum at 2.4 – 2.6 ppm (see Figure 3.3, **a**). These signals prove that CB was self-polymerising rapidly on standing, as these signals relate to  $\text{CH}_2$  protons from the polymer backbone.<sup>13</sup> Furthermore, a broad peak pertaining to the vinyl proton of PCB is eventually apparent at 5.5 ppm, which is additional evidence of polymerisation. This occurs more slowly than for the backbone region, as there are fewer vinyl protons in the polymer structure, given the isomer ratio (see Section 3.2.3). Nonetheless, both regions become more prolific over time as the PCB forms, with the final sample showing a great deal of polymer to be present, relative to monomer, after two weeks. The approximate percentage degradation of sample **a**, as listed in Table 3.3, was calculated by comparing the integrals of the sole CB vinyl proton peak (**y**, at 6.5 ppm) with the signals at 5 – 6 ppm (integral **z**), which represent the four alkene protons of CB plus the vinyl proton of PCB. PCB  $^1\text{H}$  NMR spectra are complex due to the potential presence of four isomers (see Section 3.2.3) which renders the backbone region (2.4 – 2.6 ppm) especially complicated. Hence, for an estimation of the rate of CB self-polymerisation, the vinyl region was scrutinised and peaks pertaining only to the major 1,4-*trans*-PCB isomer were considered. An explanation of the mathematics applied to this process is provided in Chapter 2 and was a means to monitor monomer conversion during the (RAFT) polymerisation reactions.

The self-polymerisation process was physically observed as the material gradually changed colour and state; the original clear, colourless solution transformed into a pale yellow colour overnight. Thereafter, a severe change in the state of the material was observed; the viscosity gradually increased, becoming markedly thicker after 6 days, and by 12 days solidification was well underway. At two weeks the “tacky” material was not soluble in any NMR solvents. Hence, analysis halted at this point, but the sample was noted to have become a black, “tarry” solid by 30 days, adopting a very pungent, sharp odour, which could be attributed to the release of HCl. It is thought that crosslinking of the polymer chains had naturally occurred, rendering the material insoluble.

A radical stabiliser was thus adopted to enable adequate storage prior to polymerisation. This compound was required to be soluble in CB and, without reacting with the monomer itself, could prevent self-polymerisation. Phenothiazine (illustrated in Figure 3.3 as structure **3.1**) is a reported stabiliser of methacrylic acid<sup>14</sup> and has already been shown to inhibit CB polymerisation,<sup>6</sup> and so was ruminated in this instance. Inclusion of this additive was indeed found to inhibit degradation, as demonstrated in the comparative NMR spectrum in Figure 3.3 (**b**), whereby the traces are markedly purer. The polymeric signals at 2.4 – 2.6 ppm, for example, were noticeably absent until 43 days. Also, it was observed that the material did not become viscous (like the neat version) for approximately four months. Although the  $^1\text{H}$  NMR data suggest stability at ambient for over 43 days using phenothiazine, a more cautious

deduction would be that this compound stabilises CB reliably for up to two weeks. This is construed more from the physical observations noted during the trial; the considerable darkening of the material after this time implies that changes were happening to the solution which were not revealed by  $^1\text{H}$  NMR.

Stabilised CB was purified by vacuum distillation immediately prior to polymerisation, removing the phenothiazine stabiliser. CB was thereafter successfully polymerised; when a destabilised sample was stood at ambient self-polymerisation occurred at approximately the same rate as observed in previous trials (with uninhibited monomer), confirming successful removal of the stabiliser. Overall, the stabilisation regime, with phenothiazine, allowed for a continuous supply of monomer, which subsequently enabled polymerisation reactions to be undertaken as and when necessary, and occasionally on large scale (up to 100 g).

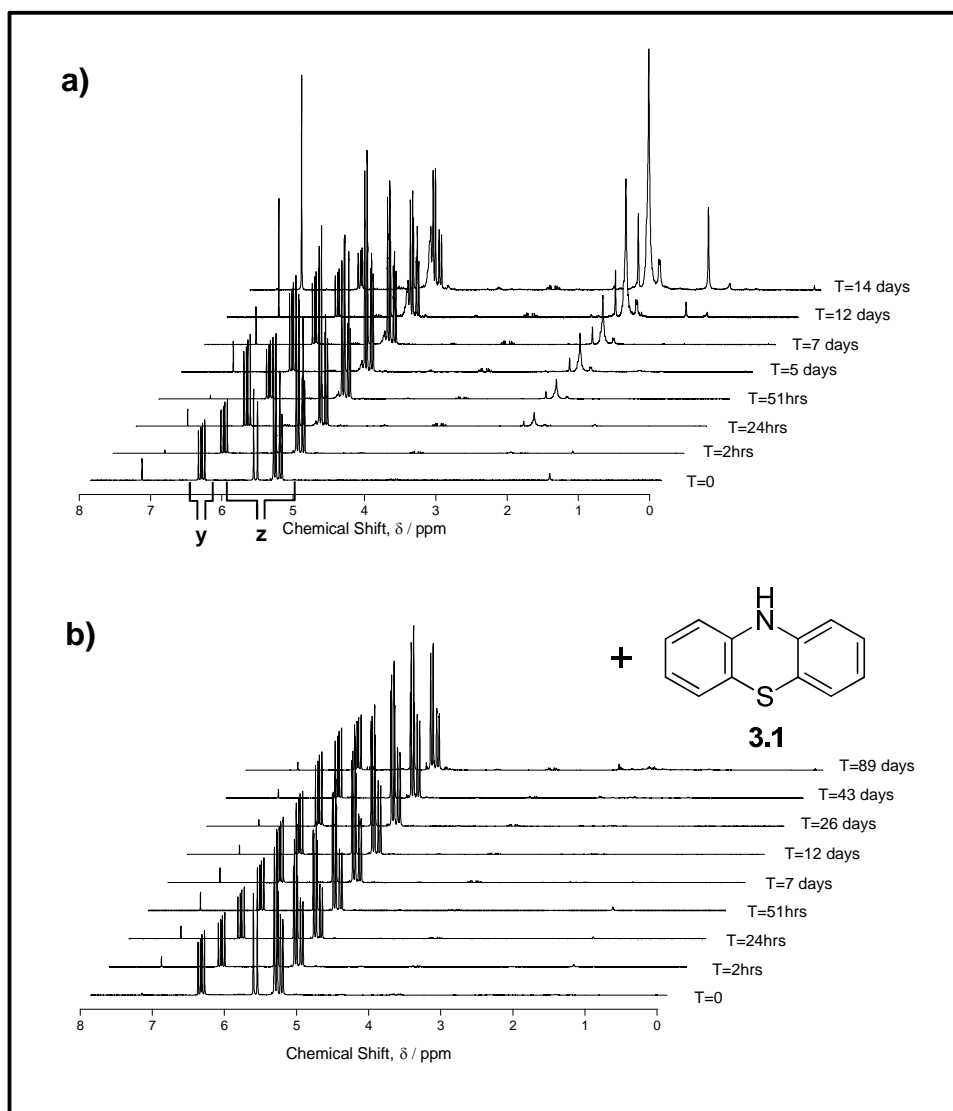


**Figure 3.3. Comparative  $^1\text{H}$  NMR spectra (in  $\text{CDCl}_3$ ) showing the self-polymerisation of CB (a) neat and (b) with 0.1 % (w/w) phenothiazine (3.1), under ambient conditions.**

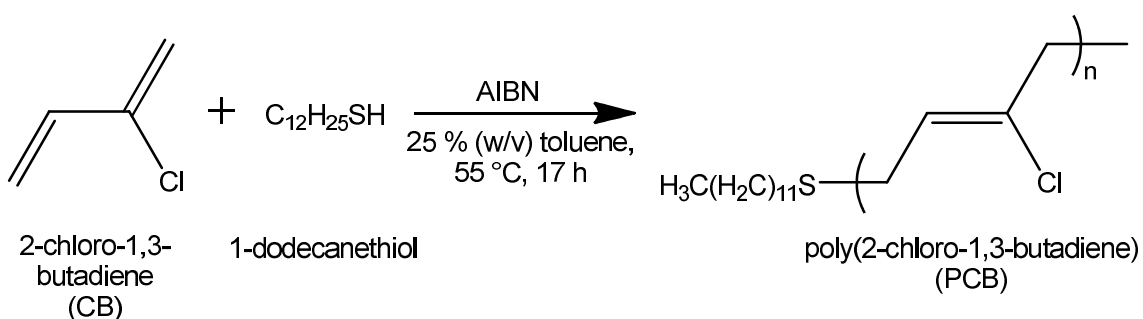
**Table 3.3. Approximate percentage degradation\* of uninhibited CB (a) by comparison of <sup>1</sup>H NMR integrals relating to vinyl and alkene protons in CB and PCB.**

Time	Integral y <sup>†</sup>	Integral z <sup>‡</sup>	% Degradation
2hrs	1	4.0561	13
24hrs	1	4.2989	23
51hrs	1	4.4566	31
5 days	1	4.6254	38
7 days	1	4.8566	46
12 days	1	6.0339	67
14 days	1	7.1382	75

\*The mathematics adopted here is the same as that used to calculate monomer conversion during polymerisation reactions by <sup>1</sup>H NMR spectroscopy, as explained in Chapter 2. For simplicity, only the protons of the major 1,4-*trans*-PCB isomer were considered. <sup>†</sup>Represents the sole vinyl proton of CB. <sup>‡</sup>Represents the vinyl proton of PCB plus the four alkene protons of CB.

### 3.2. Synthesis of poly(2-chloro-1,3-butadiene) *via* uncontrolled polymerisation

Initially, the polymerisation of CB proceeded with a thiol chain transfer agent (CTA). 1-Dodecanethiol (see Scheme 3.3) was adopted as a mediator,<sup>15-17</sup> where it would restrict the growth of polymer chains.<sup>18</sup> This type of CTA does not function the same as reversible addition-fragmentation chain transfer (RAFT) reagents, as thiols are unable to accurately predetermine the final polymer chain length (calculated using the molar ratio of monomer:CTA in RAFT).<sup>19</sup> These uncontrolled (yet constrained) polymerisations were undertaken in the first instance to yield low molecular weight PCB readily for cross-linking studies (see Chapter 4), whilst also assessing what this system could achieve (without looking to RAFT for full control).



**Scheme 3.3. The uncontrolled polymerisation of 2-chloro-1,3-butadiene (CB) using 1-dodecanethiol CTA (the main 1,4-*trans* polymer isomer configuration is shown).**

The adopted procedure was generally based on the work published by Oba and co-workers.<sup>15</sup> CB was polymerised herein in the presence of 1-dodecanethiol in a toluene solution and initiator was added when the appropriate temperature was reached. Termination then proceeded several hours later when the inhibitor was introduced (see Section 2.2.2 for experiment details).

### 3.2.1. The effect of monomer purity

As indicated in Section 3.1.5, CB was typically distilled prior to being polymerised, but one trial was undertaken to observe the effect that crude monomer had on the final polymer. In this instance, a portion of CB was reacted immediately after the drying stage (over  $\text{MgSO}_4$ ) and the distillation step was omitted. Figure 3.4 shows comparative GPC traces for PCB isolated after reacting crude and pure CB.

The main peak at approximately 23 – 25 minutes corresponds to PCB, but also present are high molecular weight impurity peaks at 17 and 20.5 minutes. This occurs only for that polymer furnished from impure CB. GPC analysis indicated that the size of these impurities ranged from 60,000 – 70,000 g/mol ( $M_n$ , relative to PSt). On the other hand, where pure CB was polymerised, no such impurities resolved.

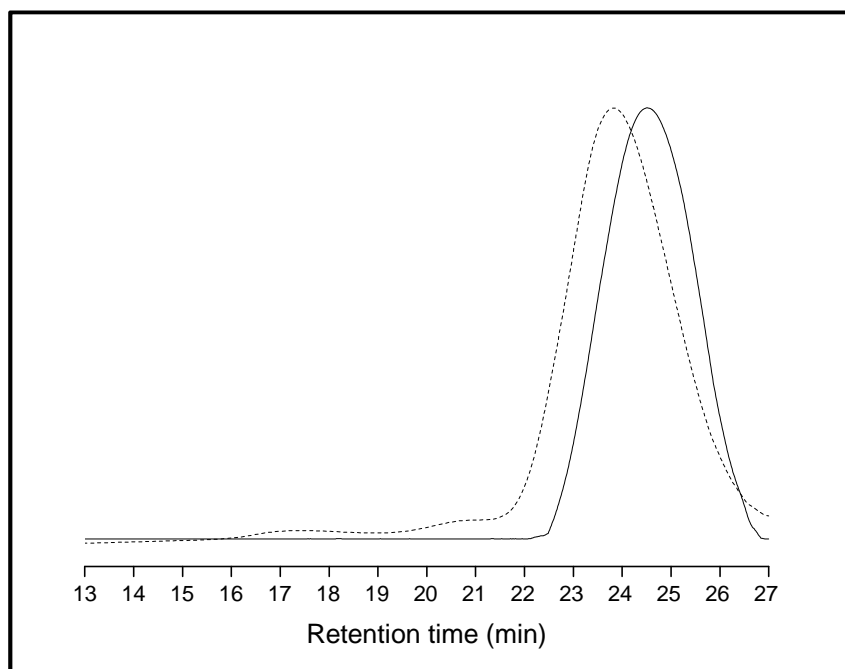


**Figure 3.4. Comparative GPC data (normalised RI response) for poly(2-chloro-1,3-butadiene) (PCB) originating from pure (—) and crude (---) monomer.**

These impurities in PCB were not identified, but it is feasible that they arose from the corresponding crude monomer (as the reaction conditions were comparable). It is likely that a small amount of self-polymerisation (of CB) occurred during the initial synthesis (due to a relatively high reaction temperature being maintained for two hours); these baseline impurities in the PCB GPC trace (shown by the dashed line in Figure 3.4) could be the result of this. The  $^1\text{H}$  NMR spectrum of crude CB shows a minimal amount of baseline impurities which disappear on distillation; any polymer would certainly be removed upon purification and would not be subsequently carried through to the final PCB product. Crucially, this experiment confirmed that the monomer required purification ahead of each polymerisation reaction so that polymer purity was not compromised.

### 3.2.2. Polymerisation

Several reactions were undertaken at 55 °C, using 1-dodecanethiol CTA and AIBN initiator, in toluene, whereby the concentration of the CTA was altered to establish the capability of this polymerisation system, as a whole. Table 3.4 summarises the results from a representative portion of these reactions.

**Table 3.4. Experimental data for the (uncontrolled) polymerisation of CB.**

Experiment	$[\text{M}]_0/[\text{CTA}]_0/[\text{AIBN}]_0$	Time (h)	$M_n^{\text{GPC}^*}$ (g/mol)	$\bar{D}$
1	1/0.03/0.01	17	3300	2.10
2	1/0.05/0.01	26	3000	2.00
3	1/0.06/0.01	20	2800	2.00
4	1/0.07/0.01	19	2000	1.80
5	1/0.09/0.01	15	2100	1.60
6	1/0.10/0.01	17	2100	1.55

Percentage solids varied between 76 – 84 % (w/w) throughout. <sup>\*</sup>Relative to polystyrene (PSt) standards.

A thiol CTA can be introduced as a regulator as it functions by simply capping the polymer chains to shorten them. In this short study, the CTA concentration was varied to assess its effect on the conventional free radical polymerisation of CB. Thereafter, it would be necessary to progress to more specialised, controlled systems capable of synthesising predefined polymers (oligomers) of CB over a wide range of molecular weights (*i.e.* RAFT). Currently, cross-linking the commercial high molecular weight (rubber) PCB yields insoluble material, thus rendering solution-state analytical techniques, such as NMR and GPC, impossible. In contrast, the use of oligomers would enable these tools to characterise the cross-linking reaction (because branched material, rather than cross-linked, would be produced). For this first set of experiments, the aim was to yield oligomeric PCB simply and readily, through the use of a simple thiol reagent.

A particularly narrow range of molecular weights was attained with this system, only achieving approximately 2,000 – 3,000 g/mol PCB, irrespective of the initial concentration of CTA employed. The dispersity (or distribution,  $\mathcal{D}$ ) of the polymer molecular weight was broad, between 1.5 and 2.0. An efficient controlled polymerisation would instead have yielded polymers with  $\mathcal{D}$  values typically around <1.2, so it was clear that this system was not accurately controlling the polymerisation of CB, as shown by the irregular polymer chain lengths. It is necessary to stress, however, that the calibration of the GPC with PSt standards renders  $M_n^{\text{GPC}}$  a relative value only.

Ideally, the polymerisation system eventually adopted for CB would successfully yield well-defined polymers over a wide range of predetermined molecular weights. Hence, the research progressed to RAFT polymerisation for the first time for CB monomer, as discussed in Section 3.3.

### **3.2.3. Spectroscopic characterisation of poly(2-chloro-1,3-butadiene)**

There are four possible isomer configurations in PCB, as shown in Figure 3.5, which result from the different ways in which CB monomer can react through the two carbon-carbon double bonds. The composition of each of these isomers present in the commercial rubber has been assigned mainly using FTIR, whereby 1,4-*trans* was deemed the major conformation (78 – 96 %), followed by 1,4-*cis* (4 – 18 %), then 3,4- (0.2 – 2 %) and 1,2- (0.3 – 2 %).<sup>20</sup> This section describes the characterisation of PCB synthesised *via* the uncontrolled route using FTIR and NMR (<sup>1</sup>H and <sup>13</sup>C) spectroscopy, whereby the potential presence of all four isomers in the polymer rendered the spectra relatively complex.

A typical FTIR spectrum of PCB is provided in Figure 3.6. Key peaks pertaining to certain bonds in the polymer chain are listed in Table 3.5, where assignment has been aided by

literature and the usual correlation tables.<sup>21-24</sup> Of particular importance is the  $1659\text{ cm}^{-1}$  peak, corresponding to the carbon-carbon double bond in the 1,4-*trans* PCB isomer. This, being a considerable, well-defined signal, has aided previous studies in assigning 1,4-*trans*-PCB as the principal isomer present in the commercial material.<sup>20</sup> Notably, there are peaks present which are responsible to all of the individual isomers. In the literature, the 1,2-isomer is defined by an inconsiderable peak at approximately  $925\text{ cm}^{-1}$ ,<sup>20</sup> which is present in this spectrum. As discussed in more detail in Chapter 4, facile isomerism of 1,2-PCB by allylic rearrangement<sup>10</sup> causes the disappearance of this peak and explains why this is present in PCB in the minority.<sup>20</sup>

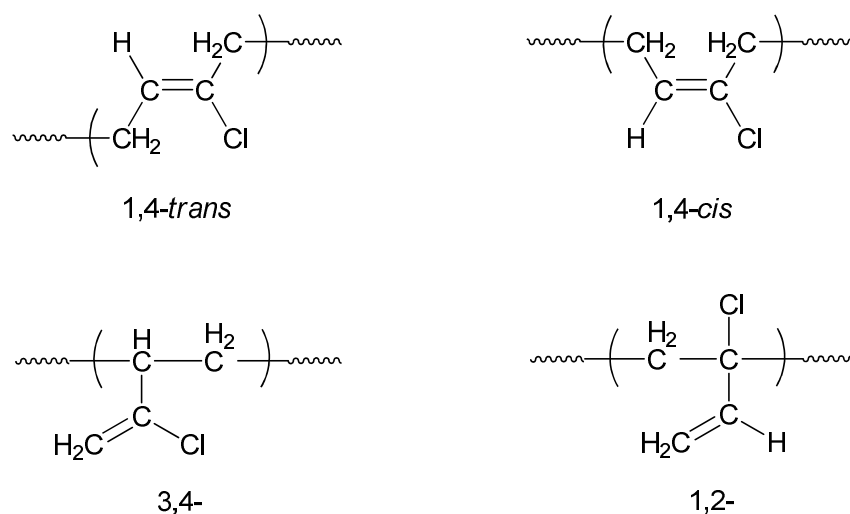


**Figure 3.5. The various isomers possible in PCB.**

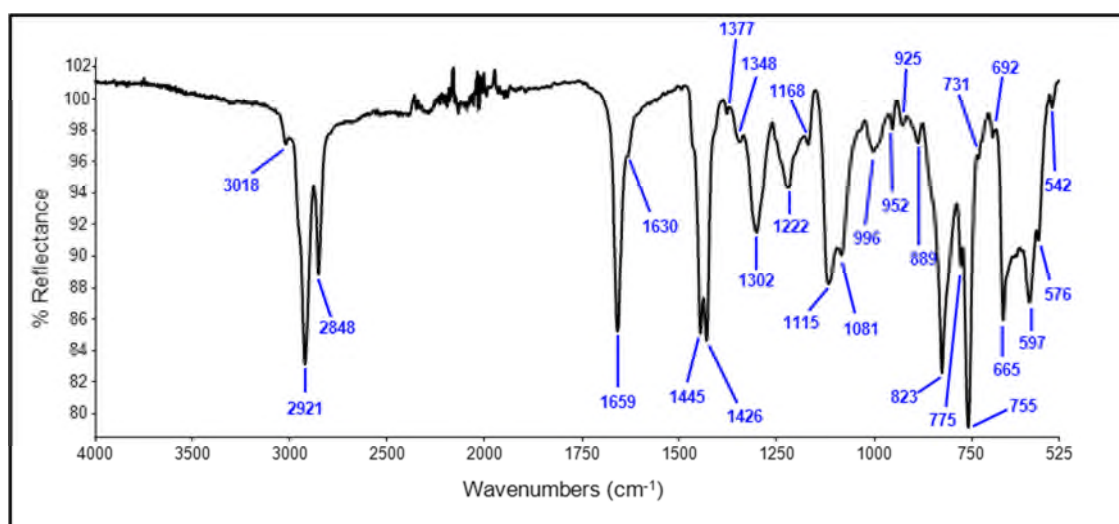


**Figure 3.6. FTIR spectrum of PCB.**



Table 3.5. FTIR peaks assigned in PCB, as aided by the literature.<sup>21-24</sup>

FTIR peak/s (Wavenumbers, cm <sup>-1</sup> )	Assignment
2921, 2848	CH <sub>2</sub> asymmetric stretching
1659	<i>trans</i> -1,4-PCB C=C stretching
1630	<i>cis</i> -1,4-PCB C=C stretching
1445, 1426	CH <sub>2</sub> deformation
1302	CH <sub>2</sub> wagging
1115, 1081	C—C stretching
925	1,2-PCB CH=CH <sub>2</sub> stretching
889	3,4-PCB C=CH <sub>2</sub> stretching
823	CH <sub>2</sub> rocking
665	C—Cl stretching

The PENDANT <sup>13</sup>C NMR spectrum of PCB is shown in Figure 3.7. This technique is not sensitive to the varied configuration of the monomer repeat units, which can, in particular, cause signals to split.<sup>13</sup> An extensive polymer backbone contributes negative CH<sub>2</sub> signals around 20 – 40 ppm and vinyl carbons are positive at 120 – 130 ppm. The one positive peak at 14 ppm relates to the sole methyl group of the dodecyl chain end. This leaves the remaining complicated region, at 130 – 140 ppm, to the terminal alkene and quaternary carbon environments.

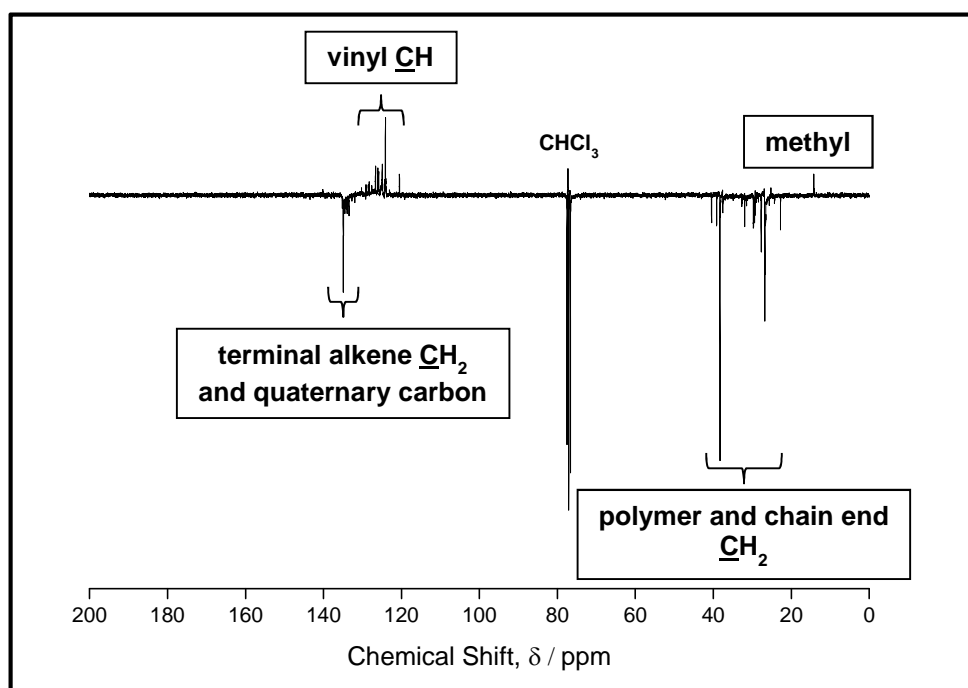
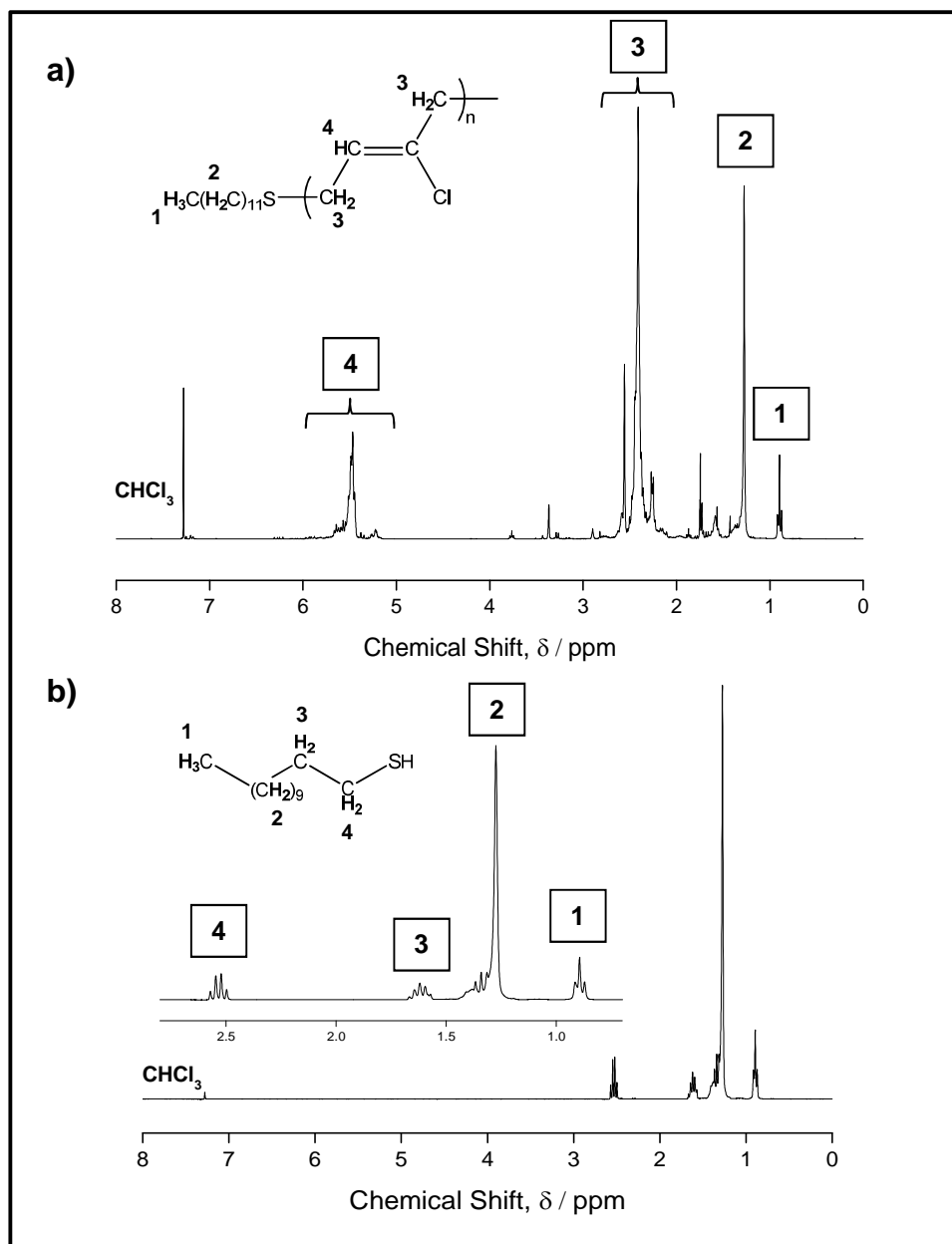


Figure 3.7. PENDANT <sup>13</sup>C NMR spectrum of PCB.

Figure 3.8 (a) shows the PCB  $^1\text{H}$  NMR spectrum, where vinyl protons were observed at 5 – 6 ppm and the macromolecular backbone was represented at 2.5 ppm. Signals pertaining to the 1-dodecanethiol CTA end group are also labelled (in a) and are shown more clearly for the neat reagent (in b). The NMR spectra for PCB are complex (due to the potential four isomers present), but literature was available to aid interpretation.<sup>13</sup>



**Figure 3.8.**  $^1\text{H}$  NMR spectra of (a) PCB, indicating the major 1,4-*trans* isomer, and (b) 1-dodecanethiol.

The different isomers in PCB have their own influence on the  $^1\text{H}$  spectrum and minor signals are assigned in Figures 3.9 (a and b). Where the broad peak at 5 – 6 ppm represents the majority of the vinyl protons, the lesser peaks surrounding it (x, y and z) are attributed to the 1,2-isomer, the minor component of the polymer.<sup>20</sup> The polymer backbone region in the  $^1\text{H}$

NMR spectrum is even more intricate because the methylene protons of all isomers contribute to this. There are a considerable number of CH<sub>2</sub> units in the polymer, making definitive assignment difficult. That said, a previous report<sup>13</sup> has characterised the 1,4-*trans* isomer signals and these are indicated in plot **b**. Notably, the peak at 2.4 ppm (denoted as **w**) is more significant because protons from the other isomers also contribute to this.

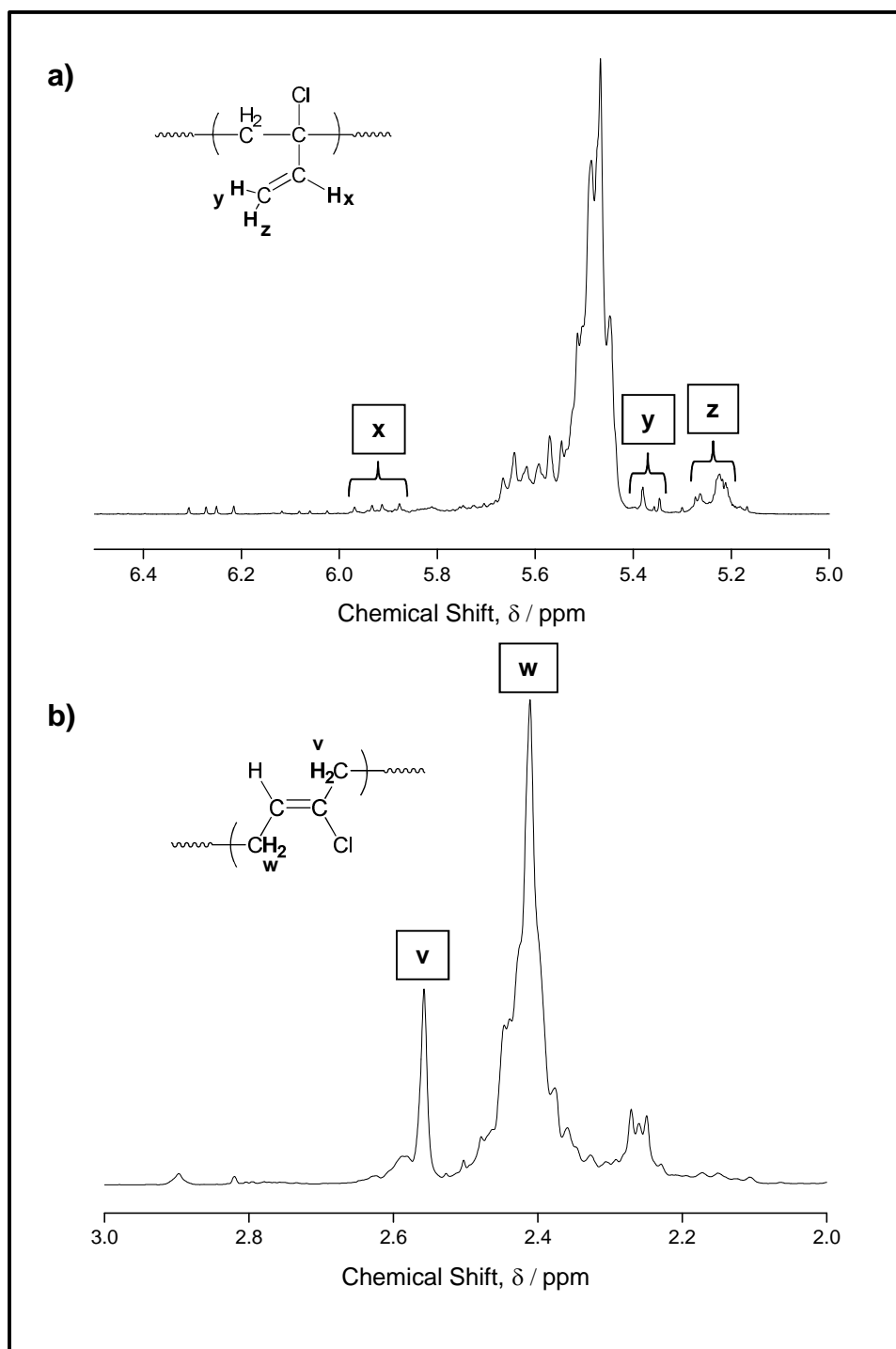
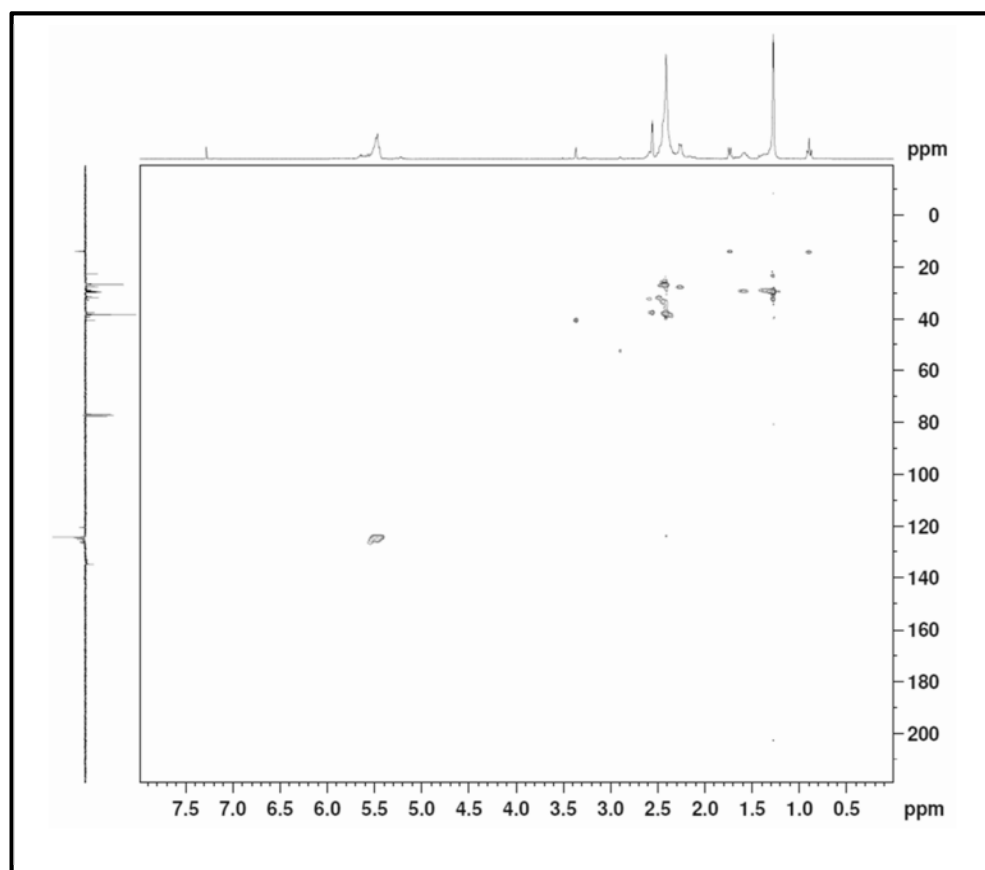


Figure 3.9. <sup>1</sup>H NMR spectra of PCB, highlighting the minor signals specific to the 1,2-isomer (a),<sup>13</sup> and the major polymer backbone signals (CH<sub>2</sub>, b).

Verification of the majority of these assignments, for both  $^1\text{H}$  and  $^{13}\text{C}$  NMR spectra, came from heteronuclear single quantum correlation (HSQC) data whereby the correlations between carbon and proton atoms are presented. Figure 3.10 shows the HSQC spectrum, with  $^1\text{H}$  data on the x-axis and the  $^{13}\text{C}$  on the y-axis. Where there is correlation between the two entities, a contour dot is yielded. For example, directly underneath the  $^1\text{H}$  methyl triplet at 0.9 ppm is a signal which aligns with the methyl  $^{13}\text{C}$  phased upwards on the y-axis at 14 ppm. This relationship confirms that these signals each belong to a methyl group. Similarly, there is correlation between the  $\text{CH}_2$  protons at 1.3 and 2.5 ppm in the  $^1\text{H}$  spectrum and the  $\text{CH}_2$  carbons around 20 – 40 ppm in the  $^{13}\text{C}$  spectrum. The positive signals around 120 – 130 ppm in the PENDANT spectrum are confirmed to be alkene as they correlate to the distinctive vinyl protons at 5.5 ppm in the  $^1\text{H}$  spectrum. These data corroborate the previously discussed analyses.



**Figure 3.10. HSQC NMR spectrum for PCB.**

### 3.3. Synthesis of poly(2-chloro-1,3-butadiene) *via* RAFT polymerisation

It was initially intended to control the polymerisation of CB in order to tailor the polymer for application in cross-linking studies (see Section 4.1). Low molecular weight polymer (oligomers) was required to represent PCB rubber in reactions with cross-linking additives.

PCB rubber is a high molecular weight polymer, which is difficult to process and is rendered insoluble once cross-linked. As a result, monitoring the cross-linking is extremely challenging as the standard analytical techniques often adopted, such as NMR spectroscopy, are not possible. It is known, for instance, that PCB rubber swells rather than dissolves in typical NMR solvents like  $\text{CDCl}_3$ .<sup>10</sup> Hence, the analytical methods were limited solely to FTIR spectroscopy (solid-state NMR was unavailable at sufficiently high resolution). Thus, lower molecular weight oligomers were considered because, when mixed with cross-linking additives, they would become branched (rather than fully cross-linked) and thus remain soluble, which would, in turn, render other analyses possible.

PCB is synthesised in industry by conventional free radical polymerisation using a thiol chain transfer agent (CTA) to regulate the molecular weight (see Section 3.2).<sup>15</sup> Controlling the synthesis of PCB using reversible addition-fragmentation chain transfer (RAFT) technology had, at the time of these studies, still eluded polymer chemists, in that no reports of such existed. The only publication involving this monomer in a controlled-radical reaction adopted NMP, where CB was copolymerised with a phosphonated diene.<sup>25</sup>

Controlled polymerisation techniques, such as ATRP, NMP and RAFT, enable a degree of control to be asserted over the polymer molecular weight, molecular weight distribution ( $M_w/M_n$ , dispersity,  $D$ ) and macromolecular architecture, which conventional free radical processes do not.<sup>26</sup> The RAFT technique is now often preferred to its predecessors, NMP and ATRP, because it is generally accepted as the most convenient and versatile of them all.<sup>27-29</sup>

The key feature of any given RAFT reaction is the CTA, which largely governs the degree of control that the system has over the polymerisation. This reagent is more sophisticated than the conventional thiol varieties; an appropriate CTA was sought to successfully control the synthesis of PCB using RAFT chemistry. Herein, the justification for each CTA trialled and the results obtained are described. Other reaction variables, such as the initiator and reaction medium, also influence the polymerisation and these are discussed where necessary.

### **3.3.1. Selection of chain transfer agents (CTAs)**

Four different RAFT CTAs have been investigated for CB polymerisation; *S*-1-dodecyl-*S'*-( $\alpha,\alpha'$ -dimethyl- $\alpha''$ -acetic acid)trithiocarbonate (DDMAT), *S*-(thiobenzoyl)thioglycolic acid (TBTA), 2-cyano-2-propylbenzodithioate (CPD) and cyanomethyl methyl(phenyl)carbamdithioate (CMPCD) (see Figure 3.11 for structures). These were selected because they have previously been successful in the polymerisation of 2-methyl-1,3-butadiene,<sup>30</sup> styrene,<sup>31</sup> methyl methacrylate<sup>32</sup> and vinyl chloride,<sup>33</sup> respectively.

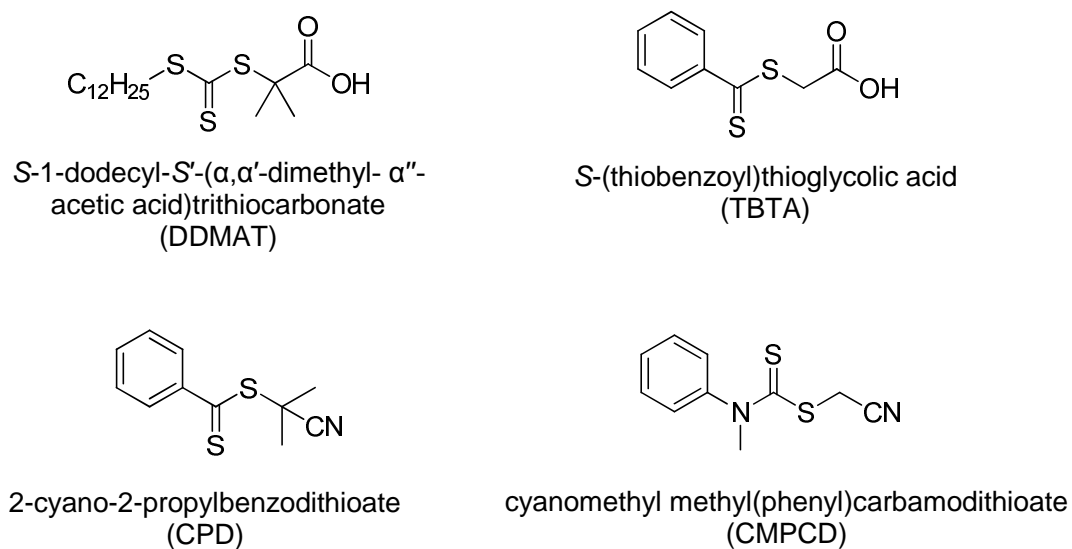


**Figure 3.11. Structures of the CTAs trialled in the RAFT polymerisation of CB.**

Polymerisation reactions were performed with each CTA, initially employing xylene and tetrahydrofuran (THF) solvents as the reaction media separately in each case. It was decided that bulk reactions would be carried out only on the most promising CTA system/s; the volatility and instability of the monomer would render bulk conditions (at 60 °C) more challenging, given the propensity of the monomer to evaporate at this temperature and the high viscosities which are anticipated at high conversions.

Certain CTA/solvent combinations adopted herein have also been reported elsewhere,<sup>34</sup> as in the work of Abreu *et al.* with CMPCD in THF.<sup>33</sup> Where xylene has been adopted in these studies, the commercial monomer solution (50 % w/w) was used; otherwise, CB was synthesised in-house and purified prior to polymerisation.  $\alpha,\alpha'$ -Azobisisobutyronitrile (AIBN) was selected as the initiator owing to its facile decomposition to generate free radicals at 60 °C, which is a suitable reaction temperature given that the boiling point of CB monomer just exceeds this (62 °C).

The kinetics of each reaction were assessed, whereby the evolution of polymer molecular weight over time and change in  $\bar{D}$  were monitored by GPC and the monomer conversion was calculated from <sup>1</sup>H NMR spectra. Herein, the results for each CTA in xylene and THF are discussed in turn, along with an account of the literature which justify trialling such conditions.

#### 3.3.1.1. S-(Thiobenzoyl)thioglycolic acid (TBTA)

S-(Thiobenzoyl)thioglycolic acid (TBTA) is a dithiobenzoate CTA with carboxylic acid functionality on the R group (Z(C=S)SR), as shown in Chapter 1, Figure 1.7). Generally, this

CTA is not the most prolific in the literature, looking across the full scope of monomer applications, but it was readily available to instigate the RAFT studies of CB in this instance. TBTA is reported as a successful mediator in controlling the polymerisations of 4-acetoxystyrene,<sup>35</sup> styrene (St) and *n*-butyl acrylate (nBA),<sup>31</sup> in particular.

Kanagasabapathy *et al.* compared TBTA to eleven other dithiobenzoate and dithiocarbamate derivatives in the polymerisation of 4-acetoxystyrene; TBTA offered the closest correlation between experimental ( $M_n^{\text{GPC}}$ ) and theoretical ( $M_n^{\text{th}}$ ) molecular weights.<sup>35</sup> In these reported experiments, a high reaction temperature (90 °C *versus* 60 °C) enhanced the rate of polymerisation by increasing the value of the transfer constant of the CTA.<sup>35</sup>

In similar work around the same time, Farmer and Patten<sup>31</sup> compared three dithiobenzoate CTA derivatives, including TBTA, in the RAFT polymerisations of St, methyl methacrylate (MMA) and nBA (**3.2**, **3.3**, **3.4**, respectively, in Figure 3.12, which also features the structures of the CTAs in the literature). None of the CTAs were able to control the polymerisation of MMA, although all of the CTAs were successful, to some degree, in controlling the polymerisations of nBA and St.<sup>31</sup> Computational studies were performed by the authors,<sup>31</sup> whereby semiempirical calculations elucidated the relative heats of reaction of the chain transfer equilibria ( $\Delta H^\ominus$ ) between the three CTAs and the dimers of the three respective monomers. This model was used to observe the relationship between molecular weight control and the stability of the CTA leaving group radical (which mediates chain transfer). A lack of control exhibited by all CTAs for MMA corroborates the large endothermic (positive  $\Delta H^\ominus$ ) results calculated for these systems (*i.e.*  $\gg 25$  kcal/mol). Results for nBA were all closer to thermoneutral, as was the reaction of CTA **3.6** for St ( $\Delta H^\ominus = 4$  kcal/mol,  $D = 1.04$ ). Conversely, TBTA gave a more endothermic enthalpy of equilibration for styrene ( $\Delta H^\ominus = 14$  kcal/mol) and a higher  $D$  value (1.38). These results infer superior control was achieved by **3.6**, which was attributed to its secondary *S*-thiobenzoyl- $\alpha$ -thiocarbonyl leaving group radical ( $\text{Bz}(\text{C}=\text{S})\text{SCH}_2(\text{CH}_3)\bullet$ ). This displays more steric hindrance and is electronically more stable than the primary radical equivalents of CTAs **3.5** and **3.7** ( $\text{Bz}(\text{C}=\text{S})\text{SCH}_2\bullet$ ).<sup>31</sup> This proves that the structure of the CTA can directly influence the degree of control achievable in a RAFT polymerisation.

In summary, according to the literature, TBTA is able to control the polymerisations, to certain degrees, of 4-acetoxystyrene,<sup>35</sup> St and nBA.<sup>31</sup> Although an alternative CTA (**3.6** in Figure 3.12) was slightly more effective for nBA, TBTA was still successful. Indeed, the one definite negative result was for MMA.<sup>31</sup> Interestingly, all of these monomers are of the more-activated class (MAMs),<sup>26</sup> so the choice of CTA is not simply dictated by which class the monomer belongs to; a range of polymerisation conditions contributes to the efficiency of the CTA and system as a whole.

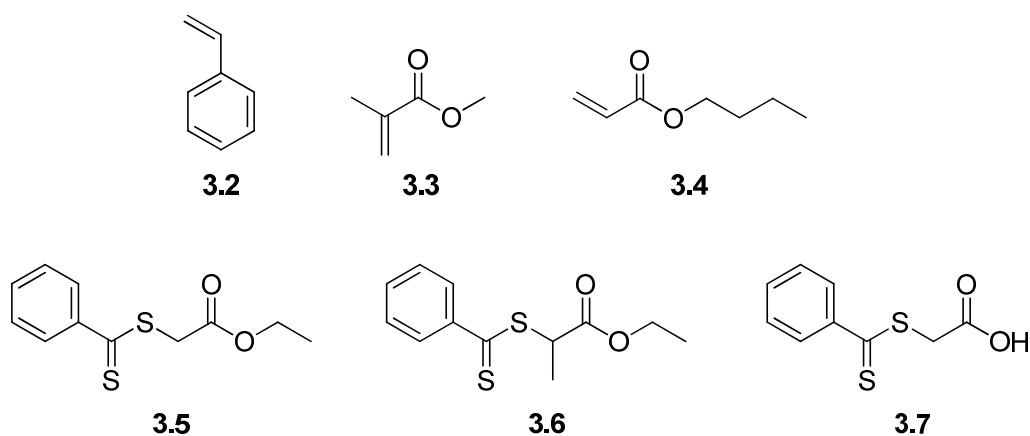
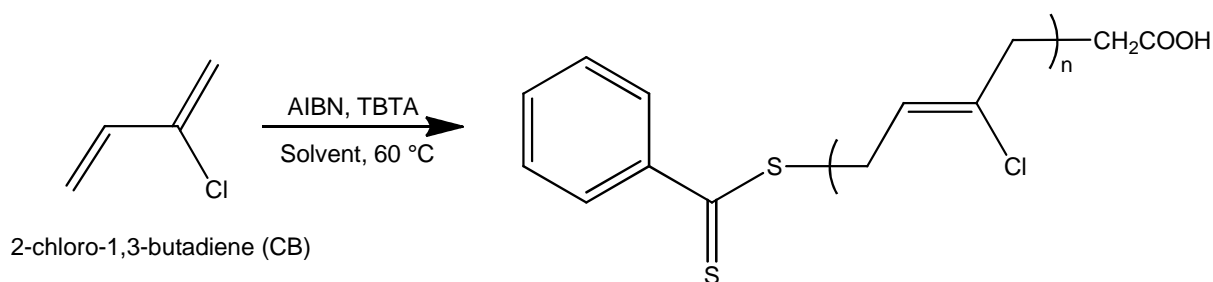


**Figure 3.12.** Styrene, St (3.2), methyl methacrylate, MMA (3.3), and *n*-butyl acrylate, nBA (3.4): the monomers studied using ethyl *S*-(thiobenzoyl)thioacetate (3.5), ethyl *S*-(thiobenzoyl)-2-thiopropionate (3.6) and *S*-(thiobenzoyl)thioglycolic acid, TBTA (3.7), RAFT CTAs in work by Farmer and Patten.<sup>31</sup> TBTA was studied herein for CB.



**Scheme 3.4.** The RAFT polymerisation of 2-chloro-1,3-butadiene (CB) using *S*-(thiobenzoyl)thioglycolic acid, TBTA, CTA (the main 1,4-*trans* polymer isomer configuration is shown).

Considering the literature, and the fact that TBTA was commercially available, TBTA was carried forward into studies for CB (see Scheme 3.4 for overall reaction). Figure 3.13 illustrates how molecular weight and  $\bar{D}$  changed over time for both xylene (a) and THF (b) solvent systems. At first glance, it can be seen that both polymerisations attained high monomer conversion (>95 % in THF and xylene), but in neither case did the growth of  $M_n$  follow a linear trend line nor adhere to the theoretical molecular weight ( $M_n^{\text{th}}$ , as indicated by a dashed line). In fact, both plots reside above  $M_n^{\text{th}}$  and relatively high molecular weight (~2500 – 4000 g/mol) was achieved very early on in each reaction. Linear growth of  $M_n$  did occur in xylene after 50 % conversion, but uniformity was almost completely absent in THF, with  $M_n$  seeming to decrease slightly after ~70 % conversion. This latter change is fairly negligible, with the polymer molecular weight seeming to decline from 7000 g/mol to 5500 g/mol, which can be attributed to termination in the final stages of polymerisation of the remaining small number of active polymer chains. Such a hypothesis is supported by the sudden increase in  $\bar{D}$  at this point of the reaction, as shown by the broad, tailing GPC traces



(in Figure 3.14). It is important to note that these  $M_n^{\text{GPC}}$  values are calculated against PSt standards and so only provide guidance for the absolute molecular weight.

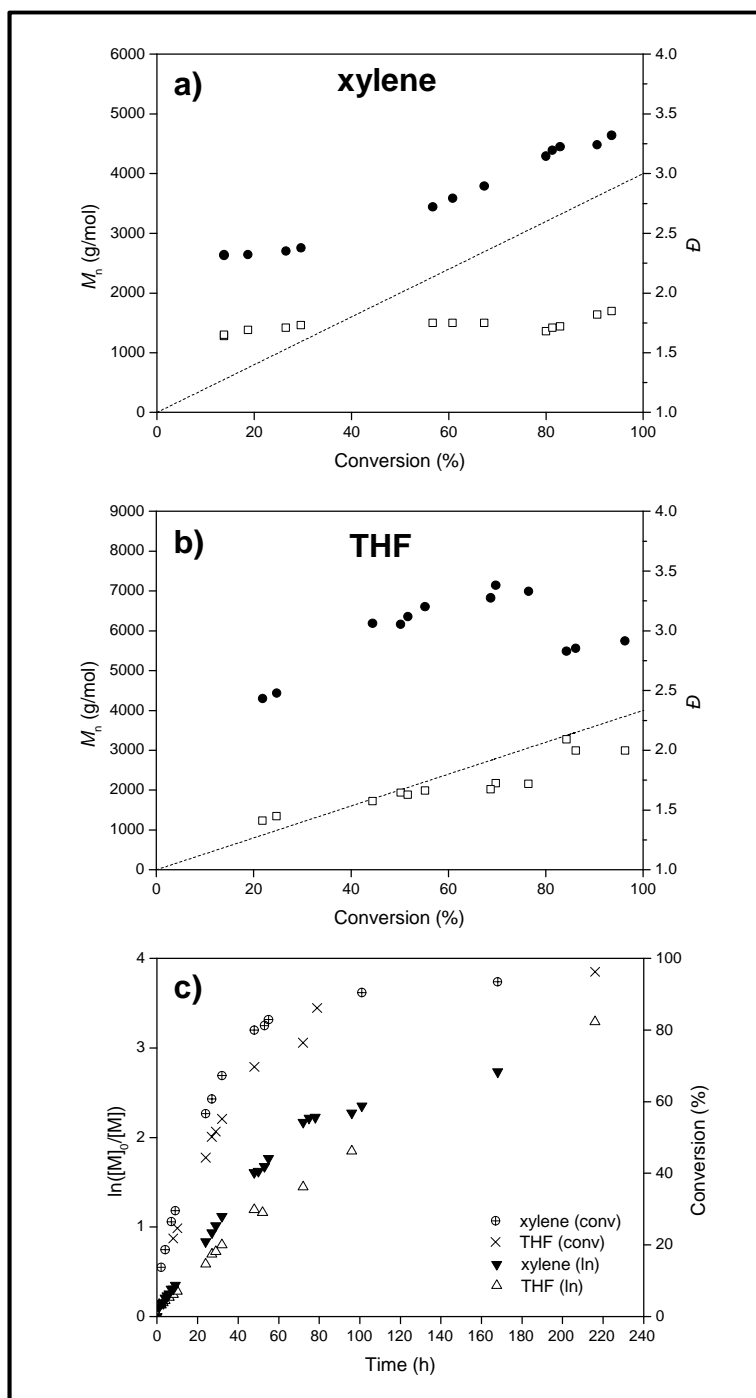


**Figure 3.13. Kinetic plots for the polymerisation of CB, in THF and xylene (50 % w/w each), under the following conditions:  $[AIBN]_0/[TBTA]_0/[CB]_0 = 0.2/1/45$  at 60 °C.**

**Where  $\bullet = M_n$ ,  $\square = D$ , --- =  $M_n^{\text{th}}$ .**

The evolution of the GPC traces over the course of each reaction is shown in Figure 3.14. In neither case did the peak have a symmetrical Gaussian shape; eventually high molecular weight impurities formed (at a retention time of 21 minutes) in the xylene system and,

although there was improvement, considerable tailing occurred in THF. These, in turn, afforded the broad molecular weight distributions and confirm that neither of these systems was able to control the polymerisation efficiently. A narrow dispersity (low  $\mathcal{D}$  value, ideally  $<1.2$ ) is characteristic for successful RAFT systems, which would be illustrated by narrower, more unimodal polymer peaks in the GPC traces.

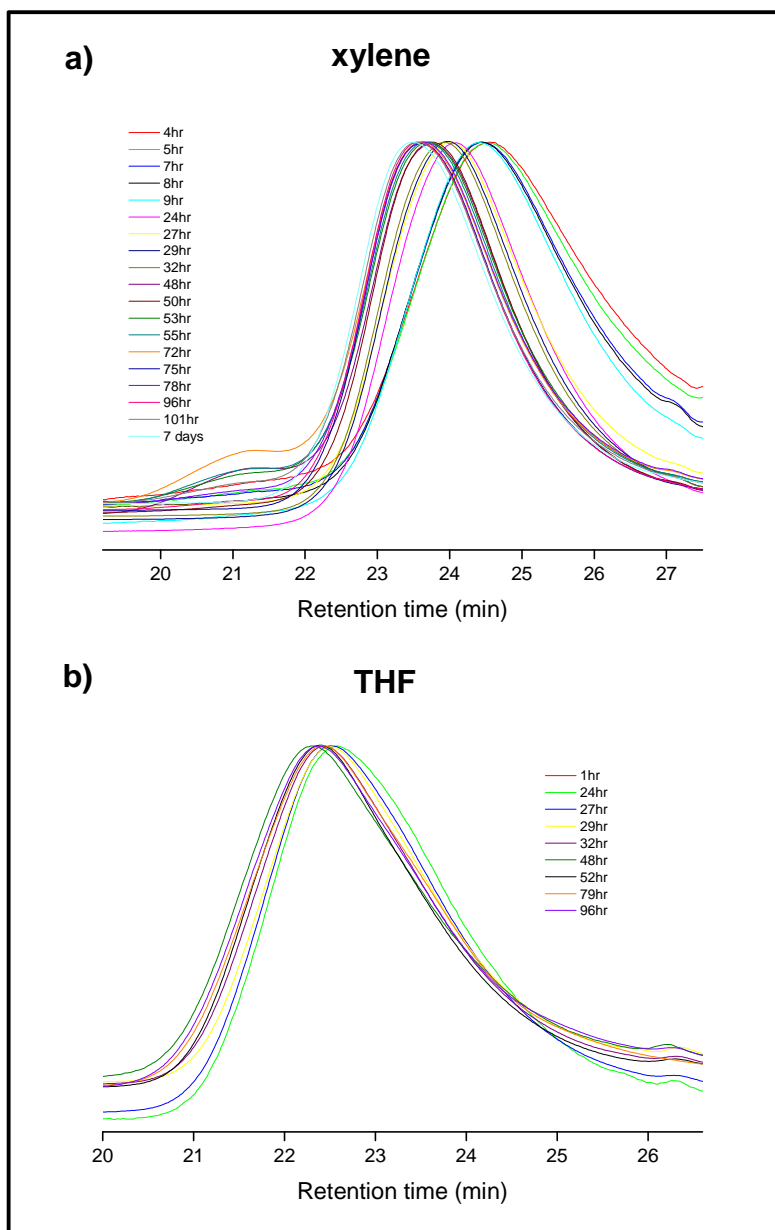


**Figure 3.14. GPC traces (normalised RI response) showing polymer formation over time for the TBTA polymerisation systems in xylene (a) and THF (b).**

It is clear that TBTA offered some degree of control over the polymerisation of CB, but the target molecular weight was exceeded and  $\mathcal{D}$  was larger than desired. There is some difference between the two solvent systems in that a higher molecular weight was reached in THF. Despite this, the initial apparent rate constant ( $k_{app}$ ) for the THF system is lower than that for xylene ( $0.022 \text{ h}^{-1}$  versus  $0.033 \text{ h}^{-1}$ , see Figure 3.13, c), implying a slower reaction in

the former. Whereas the rate reached a plateau by ~80 h in xylene, the plot for THF is approximately linear throughout, all the way to 220 h. The THF polymerisation was slower overall, reaching 96 % conversion only after 9 days; conversely, a similar point was reached in xylene after 7 days. In both cases, though, this is a very long time for any polymerisation to proceed and certainly explains the broad distributions.

According to Farmer and Patten, TBTA was not able to control the polymerisation of MMA, but was successful for St, nBA,<sup>31</sup> and, in a separate study, 4-acetoxystyrene.<sup>35</sup> Clearly, CB does not behave exactly the same as MMA in RAFT, as there was undoubtedly some degree of control experienced for CB by TBTA. However, experimental results infer that this system was not perfectly controlled, as in the respective reports for the other monomers, and so the RAFT behaviour of CB cannot directly compare to St, nBA or 4-acetoxystyrene, either. One possible correlation is that, in the work of Kanagasabapathy *et al.*, control over the polymerisation was possible in various (aromatic) solvents; the THF and xylene systems, here, offered fairly similar results for CB. So far, results are implying that solvent has a fairly negligible effect in RAFT, at least in comparing THF and xylene conditions.

TBTA is not a common RAFT CTA across the literature and publications reporting the use of such are scarce. It may be that, in the rapid evolution of RAFT chemistry, more complex CTAs have been designed specifically for their applications, leaving this simple molecule behind. For these initial experiments into the RAFT polymerisation of CB, this CTA was readily available and inexpensive so as to kick-off the research.

### 3.3.1.2. Cyanomethyl methyl(phenyl)carbamdithioate (CMPCD)

Cyanomethyl methyl(phenyl)carbamdithioate (CMPCD) was of particular relevance to these studies because of its application in the RAFT polymerisation of vinyl chloride (VC, Figure 3.15),<sup>33</sup> a related mono-vinyl chlorinated monomer. VC and CB are structurally similar (*i.e.* the electron-withdrawing chlorine atom bound to a vinyl group), it was necessary to observe if CMPCD CTA could effectively control the polymerisation of CB in the same way. However, the sole vinyl group of VC and the butadiene of CB are very different in terms of reactivity and this would undoubtedly cause the CTA/monomer compatibilities/reactivities to differ.

Abreu *et al.*<sup>33</sup> used computational studies to select CMPCD, which deemed such dithiocarbamates suitable for less-activated monomers (LAMs). VC, for instance, was calculated to have poorly stabilised propagating radicals,<sup>33</sup> which become poor leaving groups for other types of CTAs, such as dithioesters, and, as a consequence, inhibition or retardation of the polymerisation can occur.<sup>26</sup> For CMPCD, the Z-group (CH<sub>2</sub>CN) is a lone

pair donor and can stabilise through resonance with the thiocarbonyl functionality, thus encouraging fragmentation.<sup>26</sup>

The report for the synthesis of poly(vinyl chloride) (PVC) compares AIBN and diisobutryl peroxide (DIBPO) initiators, then dichloromethane (DCM), cyclohexanone and tetrahydrofuran (THF) solvents. Higher monomer conversions (up to 91 %) were achieved with DIBPO, as well as enhanced control, which was illustrated by relatively low  $\bar{D}$  values (lowest 1.4) and the  $M_n^{\text{GPC}}$  results matching the  $M_n^{\text{th}}$  more closely. Systems incorporating AIBN were unable to achieve such low dispersities and monomer conversions barely reached 40 %. Abreu *et al.* claim that the peroxide isopropyl radicals added more quickly to the monomer and CTA (than the cyanoisopropyl radicals from the thermal decomposition of AIBN), which helps to explain these superior results. Addition of cyanoisopropyl radicals to the CTA is also reversible, whilst it is irreversible for isopropyl radicals, thus any induction period is eliminated and the reaction rate increases, enhancing initiation efficiency.<sup>33</sup>

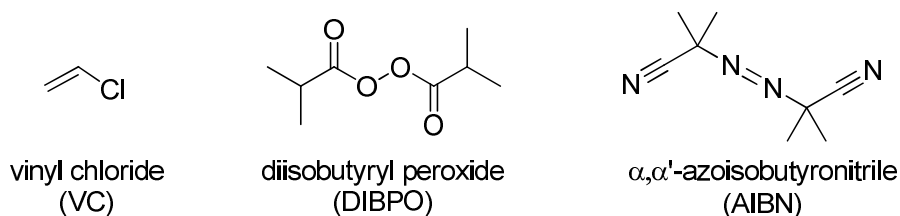
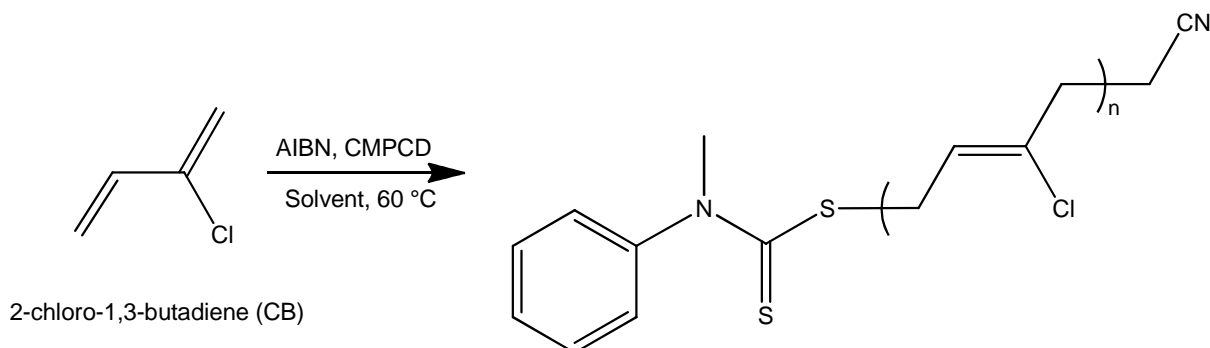


**Figure 3.15. Structures of vinyl chloride, VC, diisobutryl peroxide, DIBPO and  $\alpha, \alpha'$ -azoisobutyronitrile, AIBN.**

No polymerisation was observed in DCM and the cyclohexanone system generated a high  $\bar{D}$  value. Thus, THF (50 % w/w), DIBPO and CMPCD, at 42 °C, formed the final system. PVC up to 7000 g/mol, with  $\bar{D} \sim 1.4$ , was synthesised.<sup>33</sup> Despite the success of DIBPO for VC, it was not possible to source this initiator for these RAFT studies and so AIBN was employed, with polymerisations taking place at the typical 60 °C (Scheme 3.5).



**Scheme 3.5. The RAFT polymerisation of 2-chloro-1,3-butadiene (CB) using cyanomethyl methyl(phenyl)carbamdithioate, CMPCD, CTA (the main 1,4-*trans* polymer isomer configuration is shown).**

Figure 3.16 shows the change in molecular weight and  $\bar{D}$  with monomer conversion for both reactions (plot **a** for xylene, plot **b** for THF); this was the only system tested where the molecular weight decreased over the course of the polymerisations for both solvents. This is not typical behaviour for controlled reactions and, in the case of the xylene system, is attributed to the formation of low molecular weight species over time (Figure 3.17, **a**).

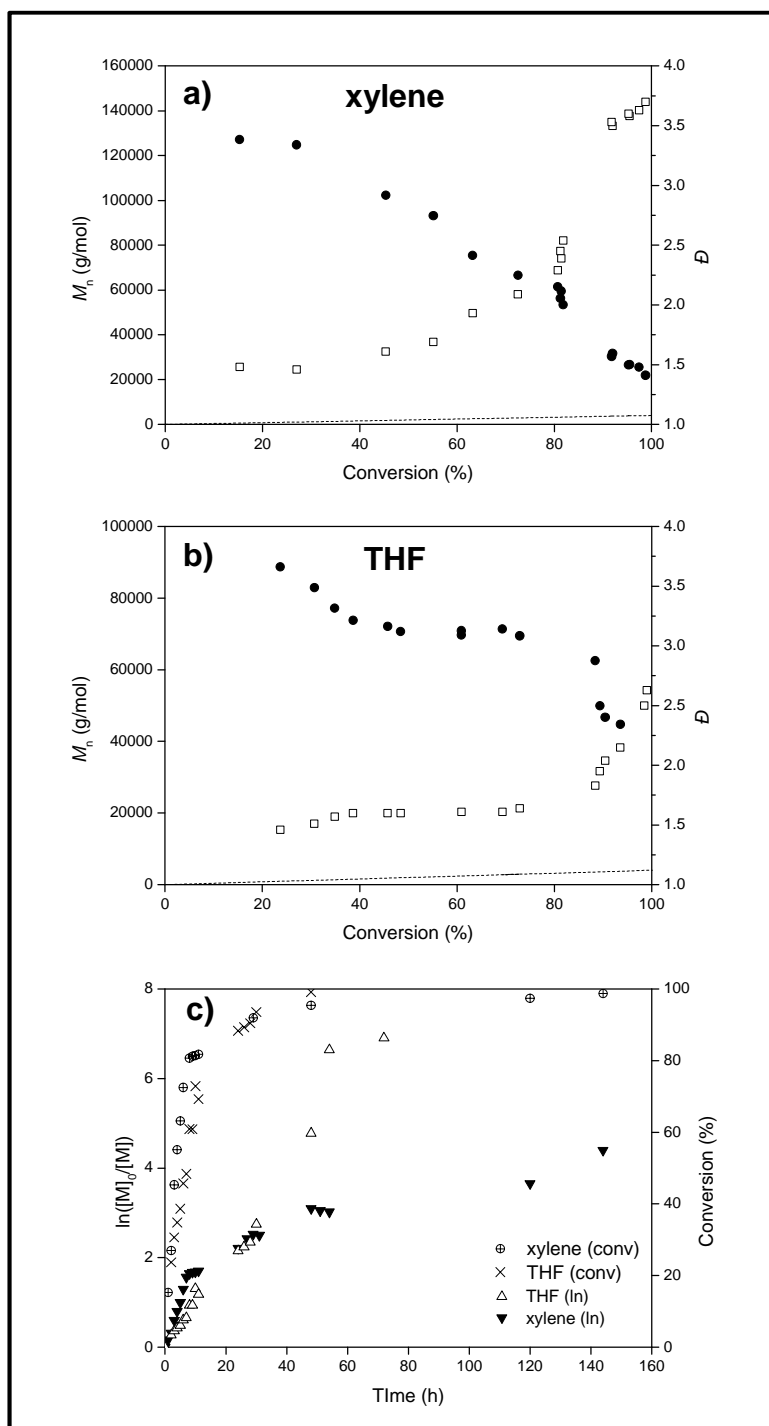
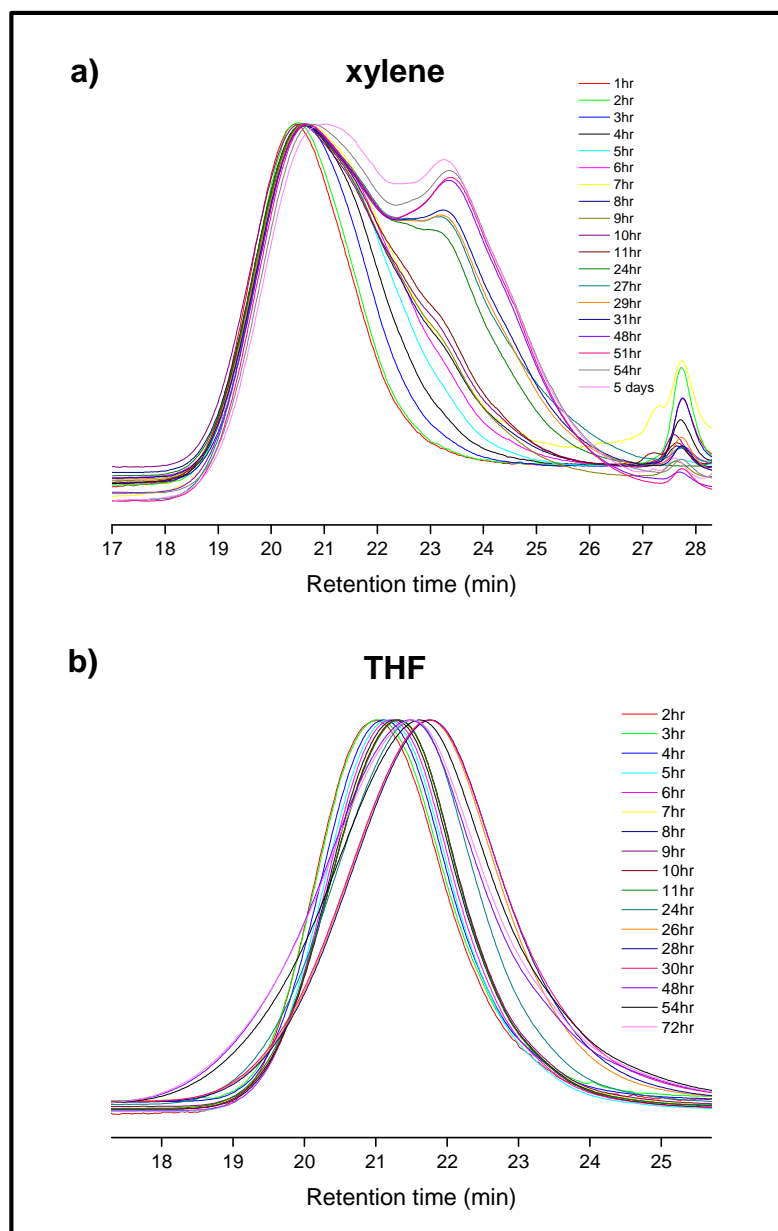


Figure 3.16. Kinetic plots for the polymerisation of CB, in THF and xylene (50 % w/w each), under the following conditions:  $[AIBN]_0/[CMPCD]_0/[CB]_0 = 0.2/1/45$  at 60 °C.

Where  $\bullet = M_n$ ,  $\square = \bar{D}$ ,  $---$  =  $M_n^{th}$ .

High molecular weight polymer formed early on in the reaction, followed by a distinct bimodal distribution appearing after 24 hours, causing a severe increase in  $\bar{D}$ . This secondary peak formed at higher retention time and the  $M_n^{\text{GPC}}$  was taken across the overall peak area, thus generating a seemingly lower  $M_n$  value each time. The severe lack of control was evident as both  $M_n$  plots stray far from the theoretical molecular weight trend line ( $M_n^{\text{th}}$ , ---), which almost cannot be seen at all, lying at the foot of each graph.



**Figure 3.17. GPC traces (normalised RI response) showing polymer formation over time for the CMPCD polymerisation systems in xylene (a) and THF (b).**

This CMPCD system was undoubtedly improved by introducing THF, *i.e.* the reaction medium adopted by Abreu *et al.* for VC.<sup>33</sup> Here, the GPC traces remained unimodal throughout the course of the polymerisation. The polymer peak did broaden considerably over time, however, so that  $\bar{D}$  reached  $\sim 2.5$ . Also, despite some improvement, the average

molecular weight still decreased over time as the peak shifted and eluted at increasingly higher retention times, yet again. Clearly, low molecular weight species were still forming, but not to such a degree as in the xylene reaction, to generate bimodal peaks. These new species were also closer (in retention time and molecular weight) to the majority of chains in THF because, overall, the chains were smaller (at higher retention time) than in xylene.

Adopting the more polar, non-aromatic solvent (THF) significantly improved this polymerisation system and offered more control, given the preferred unimodal peak shape in the GPC traces. This solvent/CTA combination was selected according to its applicability to VC,<sup>33</sup> but unfortunately it was not possible to directly compare results for the different monomers due to the use of AIBN *versus* DIBPO. The dispersity of the polymer increased over time from when AIBN was employed for VC, but  $\bar{D}$  values reached  $\sim 2.5$  here for CB. Also, the kinetic behaviour for VC was typical for a RAFT polymerisation in that molecular weight increased linearly over time; for CB this was not the case and high molecular weight polymers formed early on in the reactions (as is typical of conventional, uncontrolled free radical polymerisation). The rate constants obtained in the contrasting medium for each of these experiments differ by a factor of six;  $k_{app}$  in xylene being highest at  $0.174 \text{ h}^{-1}$ , whereas  $k_{app} = 0.034 \text{ h}^{-1}$  in THF (see Figure 3.16, **c**, semi-logarithmic plot). These  $k_{app}$  values infer that the THF reaction was slower at the start, but the gradient for this plot is steeper overall, whereas that for xylene is more gradual. Despite this difference, they both seem to follow a stepwise 'S' shaped function, (which is more pronounced in the xylene system), where an initial steep slope is followed by a moderate plateau and then a second incline. The THF reaction shows a final plateau as the polymerisation reached completion, from 60 hours; xylene has a longer initial plateau at 50 – 120 hours. This 'staggered' behaviour was not observed by Abreu *et al.* for VC using CMPCD.<sup>33</sup>

The differing reactivities of VC and CB must have contributed to the contrasting results; CMPCD is clearly more appropriate for VC than CB. Abreu *et al.* define VC as a less-activated monomer (LAM),<sup>33</sup> which is why the dithiocarbamate is apparently suitable. The extra double bond in the CB structure most likely renders this more-activated (a MAM), although this is not yet official (due to the general lack of controlled polymerisation reports).

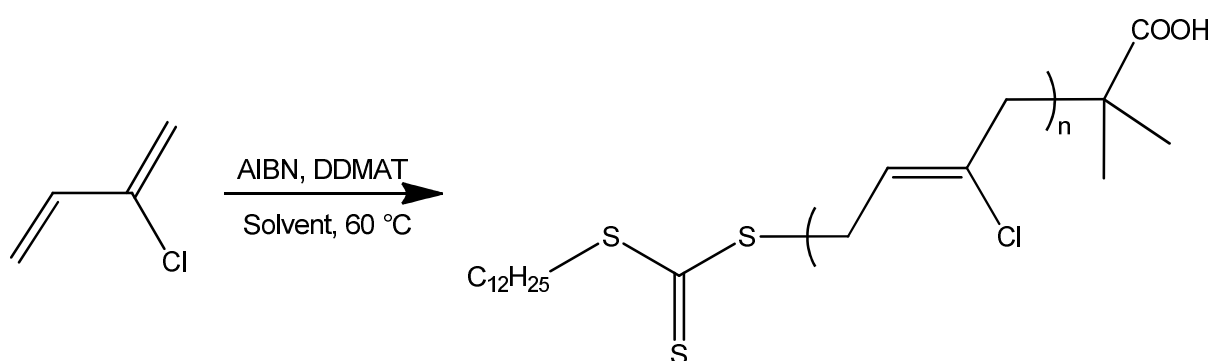
### 3.3.1.3. S-1-Dodecyl-S'-( $\alpha,\alpha'$ -dimethyl- $\alpha''$ -acetic acid)trithiocarbonate (DDMAT)

S-1-Dodecyl-S'-( $\alpha,\alpha'$ -dimethyl- $\alpha''$ -acetic acid)trithiocarbonate (DDMAT) was the first reported RAFT CTA for the controlled radical polymerisation of 2-methyl-1,3-butadiene (isoprene);<sup>30</sup> NMP has been used to synthesise predefined poly(2-methyl-1,3-butadiene) (which is more commonly known as polyisoprene).<sup>36</sup> The few attempts to apply ATRP to this monomer have

generated poor results overall, in particular affording low yields and insufficient control.<sup>37, 38</sup> At the time of this initial RAFT report (2007), DDMAT had to be synthesised,<sup>39</sup> but the growing popularity of RAFT over recent years has led to more CTAs becoming commercially available and hence it was possible to purchase DDMAT for the experiments herein. The rare publication on the RAFT polymerisation of 2-methyl-1,3-butadiene<sup>30</sup> was significant because there is a lack of RAFT reports generally on simple butadiene derivatives. This could imply difficulty with such processes, or just reflect a lesser demand. Despite the clear difference between the structures and inherent reactivities of CB and 2-methyl-1,3-butadiene, this particular work was novel and interesting for consideration with CB.

The DDMAT CTA, with an *S*-alkyl *Z* group, was considered to be a reasonable candidate for controlling the polymerisation of CB, owing to the potential of this monomer to be considered as a MAM (*versus* VC, as discussed in Section 3.3.1.2). Trithiocarbonates can control the polymerisations of such monomers and reduce the likelihood of retardation occurring.<sup>26</sup> Indeed, Jitchum and Perrier<sup>40</sup> also found that a trithiocarbonate CTA offered superior control to other CTAs in the RAFT polymerisation of 2-methyl-1,3-butadiene. These researchers elected 2-ethylsulfanylthiocarbonylsulfanylpropionic acid ethyl ester (ETSPE), over a dithiobenzoate derivative; ETSPE was not available for this work.

The reaction conditions of Germack and Wooley, with DDMAT, included *tert*-butyl peroxide (initiator) at 125 °C, in bulk. This system was able to yield up to 5000 g/mol polymer with a narrow molecular weight distribution ( $\mathcal{D} = 1.2$ ) after 25 hours. However, the monomer conversion obtained for this was low (<30 %).<sup>30</sup> The target molecular weight was 13,000 g/mol, but it is not clear if this was successfully attained. DDMAT has also been applied to methyl acrylate (MA),<sup>41</sup> *tert*-butyl acrylate (tBA),<sup>42</sup> and *N*-isopropylacrylamide (NIPAM)<sup>43</sup>.



**Scheme 3.6. The RAFT polymerisation of 2-chloro-1,3-butadiene (CB) using S-1-dodecyl-S'-( $\alpha,\alpha'$ -dimethyl- $\alpha''$ -acetic acid)trithiocarbonate, DDMAT, CTA (the main 1,4-*trans* polymer isomer configuration is shown).**

The previous scheme (3.6) depicts the CB polymerisation undertaken with DDMAT. There were concerns over the practicality and safety of the high temperatures adopted by Germack



and Wooley for 2-methyl-1,3-butadiene, (125 °C), and so 60 °C was maintained for these systems (with CB).

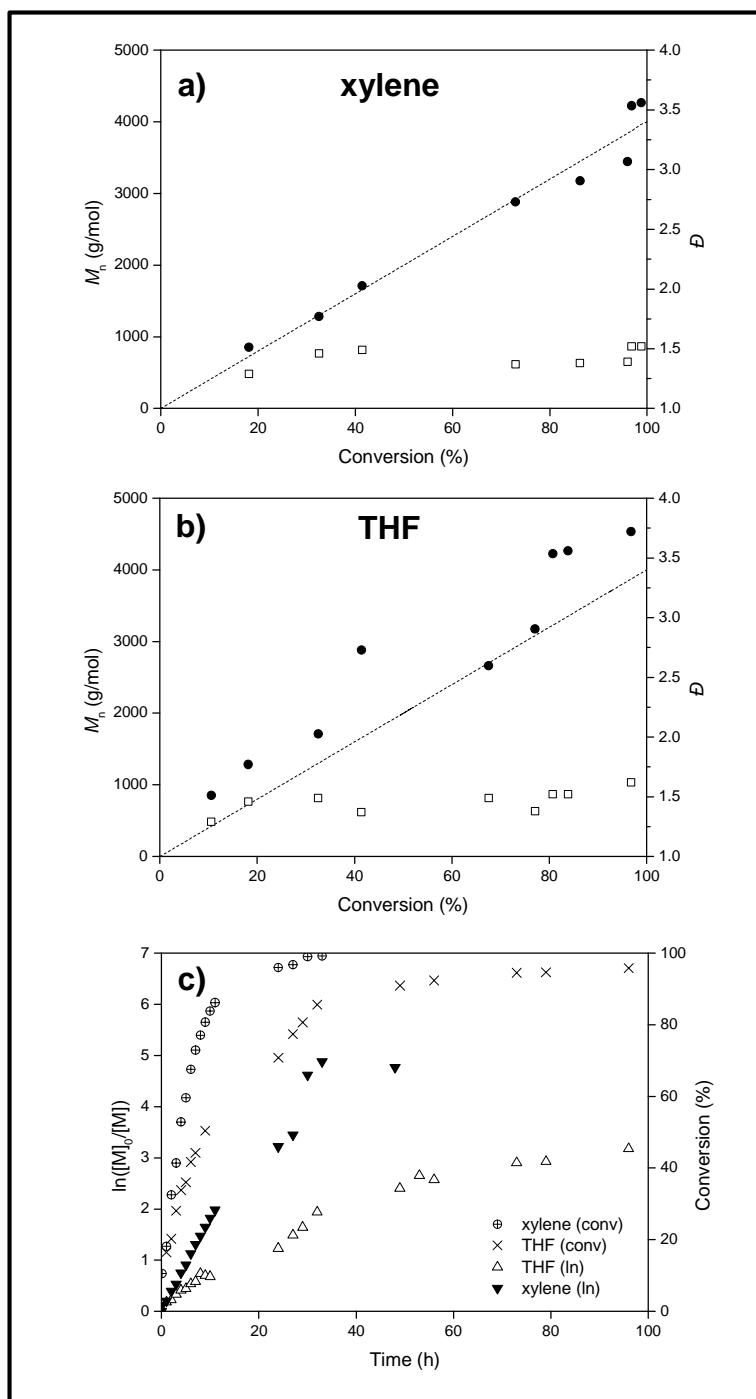


**Figure 3.18. Kinetic plots for the polymerisation of CB, in THF and xylene (50 % w/w each), under the following conditions:  $[AIBN]_0/[DDMAT]_0/[CB]_0 = 0.2/1/45$  at 60 °C.**

**Where ● =  $M_n$ , □ =  $D$ , --- =  $M_n^{th}$ .**

As shown in Figure 3.18, in each case, molecular weight increased with monomer conversion and reached the target 4000 g/mol at high conversion (>90 % in xylene, 80 % in THF). Evolution in both systems followed the theoretical molecular weight line ( $M_n^{th}$ , ---),

although the THF plot (b) was slightly less uniform. This is the best-fitting trend so far experienced amongst the CTAs tested. However, the values of  $\bar{D}$  in both cases were  $>1.2$  throughout the polymerisations and reached 1.5, which suggests that DDMAT did not have complete control over these polymerisations, under these conditions. In terms of the kinetics, the reaction proceeded faster in xylene, whereby 96 % conversion was achieved after 24 hours, but the THF reaction took 73 hours to reach the same point. The initial apparent rate constant,  $k_{app}$ , of the THF reaction is once again slightly higher than that for xylene ( $0.050 \text{ h}^{-1}$  versus  $0.042 \text{ h}^{-1}$ ). In Figure 3.18 (c), the semi-logarithmic plots follow the same trend, with an initial incline followed by a plateau in the rate, although THF has a much shallower gradient overall, implying that it is slower, despite the higher  $k_{app}$  at the start of the reaction.

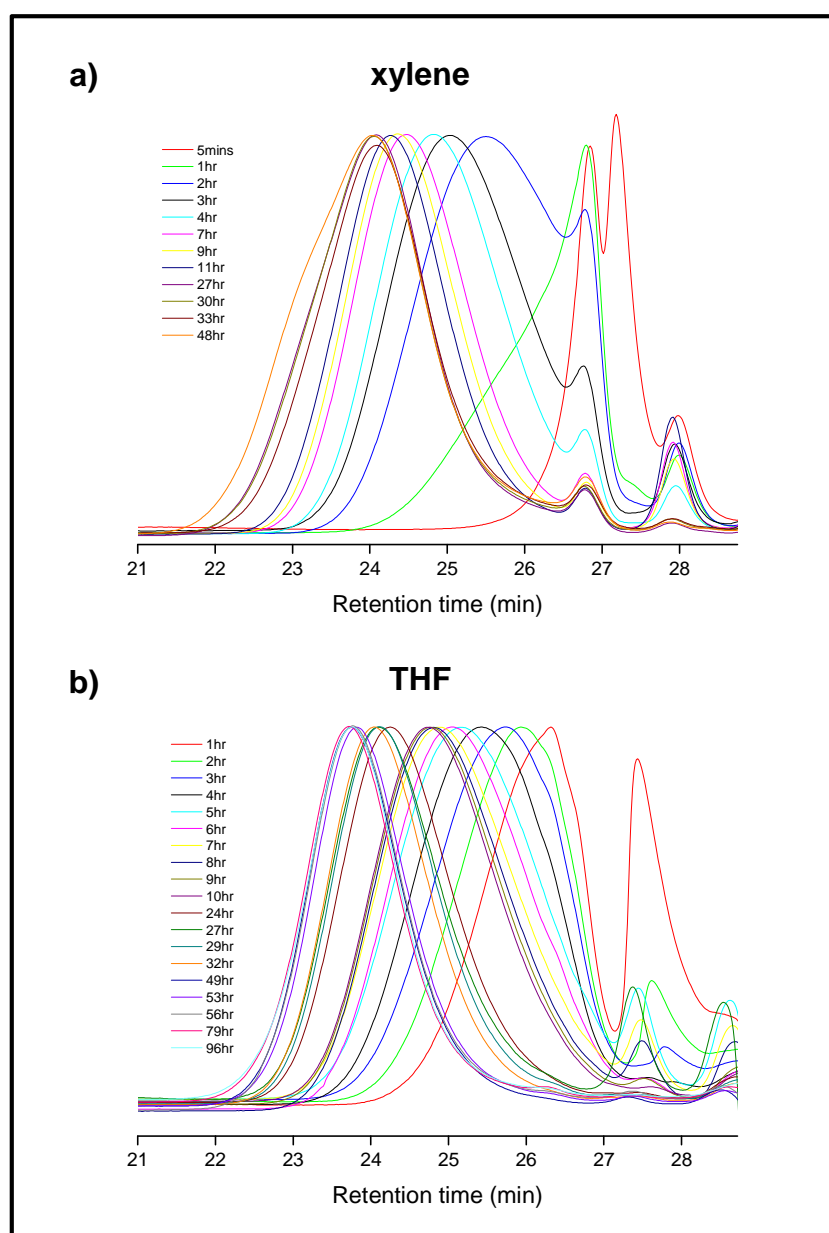


**Figure 3.19. GPC traces (normalised RI response) showing polymer formation over time for the DDMAT polymerisation systems in xylene (a) and THF (b).**

Although the  $M_n$  and  $\bar{D}$  results for these systems seem to be comparable, the GPC results do demonstrate a slight difference (see Figure 3.19). For instance, the polymer peak shapes at the start of each reaction, whilst broad for both, were more multi-modal in the case of xylene. THF afforded unimodal polymer peaks which were generally more uniform; this arguably demonstrates slightly more control over the growth of polymer chains.

The successful application of DDMAT to 2-methyl-1,3-butadiene<sup>30</sup> was reasonable justification for trials here and, accordingly, this CTA gave some promising results for the RAFT polymerisation of CB. Molecular weight increased linearly with conversion and  $M_n^{\text{th}}$  was achieved in good time. However, the  $\bar{D}$  values were still not  $<1.2$  in either xylene or THF, which demonstrates a loss of control over the growth of the polymer chains. GPC polymer peak shapes were more monomodal in THF, though, which is most likely attributed to a slightly slower polymerisation overall.

#### 3.3.1.4. 2-Cyano-2-propylbenzodithioate (CPD)

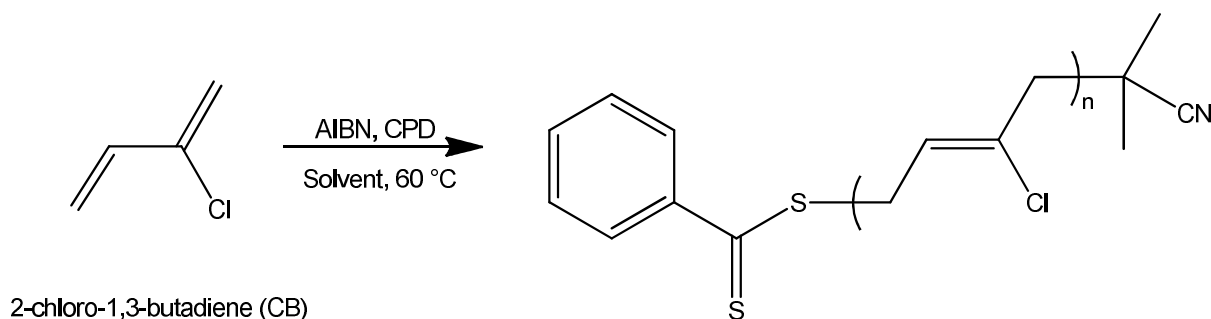
2-Cyano-2-propylbenzodithioate (CPD) is a dithiobenzoate CTA, where  $Z = \text{phenyl}$  and  $R = \text{C}(\text{Me})_2\text{CN}$  in the generic  $Z(\text{C}=\text{S})\text{SR}$  structure (the structure of CPD is shown in Figure 3.11). This RAFT CTA has been successful in controlling the polymerisation of MMA<sup>44, 45</sup> and other (meth)acrylates,<sup>34, 46</sup> which are defined as more-activated monomers (MAMs)<sup>26</sup>. Often in previous reports, CPD has been selected after a rigorous screening process, where it has performed more effectively against alternative CTAs, such as other dithiobenzoate, dithiocarbamate and trithiocarbonate derivatives, affording narrower molecular weight distributions in the furnished polymers.<sup>44, 45, 47</sup> As many of these reported reactions used AIBN as the initiator and aromatic hydrocarbon solvents (such as toluene or benzene) for the reaction media,<sup>44-48</sup> this gave substance to employing similar conditions in these studies. Interestingly, CPD has also been successful in the RAFT polymerisation of 2-(dimethylamino)ethyl methacrylate (DMAEMA) with AIBN in THF (50 % w/w).<sup>34</sup> Thus, studying the effects of xylene and THF in the RAFT polymerisation of CB, with CPD, is further justified.

Interestingly, CPD was also found to be successful for Weber *et al.*<sup>47</sup> to polymerise 2-isopropenyl-2-oxazoline (iPOx) for the first time using RAFT. Here, this CTA outperformed another trithiocarbonate and a dithiocarbamate, affording lower dispersities ( $\bar{D} = 1.2 - 1.4$ ), to furnish low molecular weight polymer in toluene, using AIBN as the initiator.

The reason behind the success of CPD in these reported RAFT polymerisations seems to be the effectiveness of the R group ( $\text{C}(\text{Me})_2\text{CN}$ ). It is known that the R group is specifically required to be a good leaving group and have a proficient corresponding reinitiating radical.<sup>45</sup>

Authors mainly attribute the efficiency of this CTA in RAFT to the cyanoalkyl R group. For instance, in NMR studies elucidating the early stages of the RAFT mechanism, it was found that the “superior”<sup>48</sup> tertiary leaving group of CPD caused faster fragmentation rates of radical intermediates. Also, results of molecular orbital calculations have shown that the cyanoalkyl R group radical has a lower rate constant than other dithiobenzoates, such as cumyl dithiobenzoate, which helps to prevent retardation occurring in the polymerisation. This was the rationale for adopting CPD in certain RAFT polymerisations of St and MMA in the same work.<sup>44</sup>

Given the positive conclusions drawn from the literature, CPD was thereafter investigated in the RAFT polymerisation of CB, employing THF and xylene as solvents, with AIBN as the initiator at 60 °C, as in previous experiments. Scheme 3.7 shows the overall reaction.



**Scheme 3.7. The RAFT polymerisation of 2-chloro-1,3-butadiene (CB) using 2-cyano-2-propylbenzodithioate, CPD, CTA (the main 1,4-*trans* polymer isomer configuration is shown).**

As with the trithiocarbonate CTA (DDMAT, Section 3.3.1.3), this CPD system demonstrated a linear increase in polymer molecular weight with monomer conversion in both xylene and THF media (see Figure 3.20). In xylene, however, the molecular weight far exceeded the target, reaching as high as 23,000 g/mol, where  $M_n$  data points do not at all follow the theoretical line (---,  $M_n^{\text{th}}$ ; Figure 3.20, **a**). This trend was also observed with the other dithiobenzoate CTA, TBTA (Section 3.3.1.1), where  $M_n^{\text{th}}$  was also exceeded. However, the molecular weight did not rise as dramatically in the case of TBTA and there is a more considerable difference between solvent systems here (for CPD). Noticeably, the molecular weight dispersity ( $\mathcal{D}$ ) in the xylene system for CPD is <1.25 up to 40 % conversion, at which point the target 4000 g/mol was achieved. Thereafter,  $\mathcal{D}$  values increased >1.5 eventually.

Overall, there was enhanced control over this polymerisation by replacing xylene with THF. In this latter case, the target molecular weight was reached after ~60 % conversion and a plateau appeared around 5000 g/mol at ~80 % conversion. This is coupled with a better fit of the  $M_n^{\text{GPC}}$  plot with  $M_n^{\text{th}}$ , as shown in Figure 3.20, **b**. There was a marked improvement also

in  $\mathcal{D}$  values, which do not exceed 1.3 throughout the course of the THF reaction, up to 97 % conversion (see Figure 3.20, **b** for the THF results).

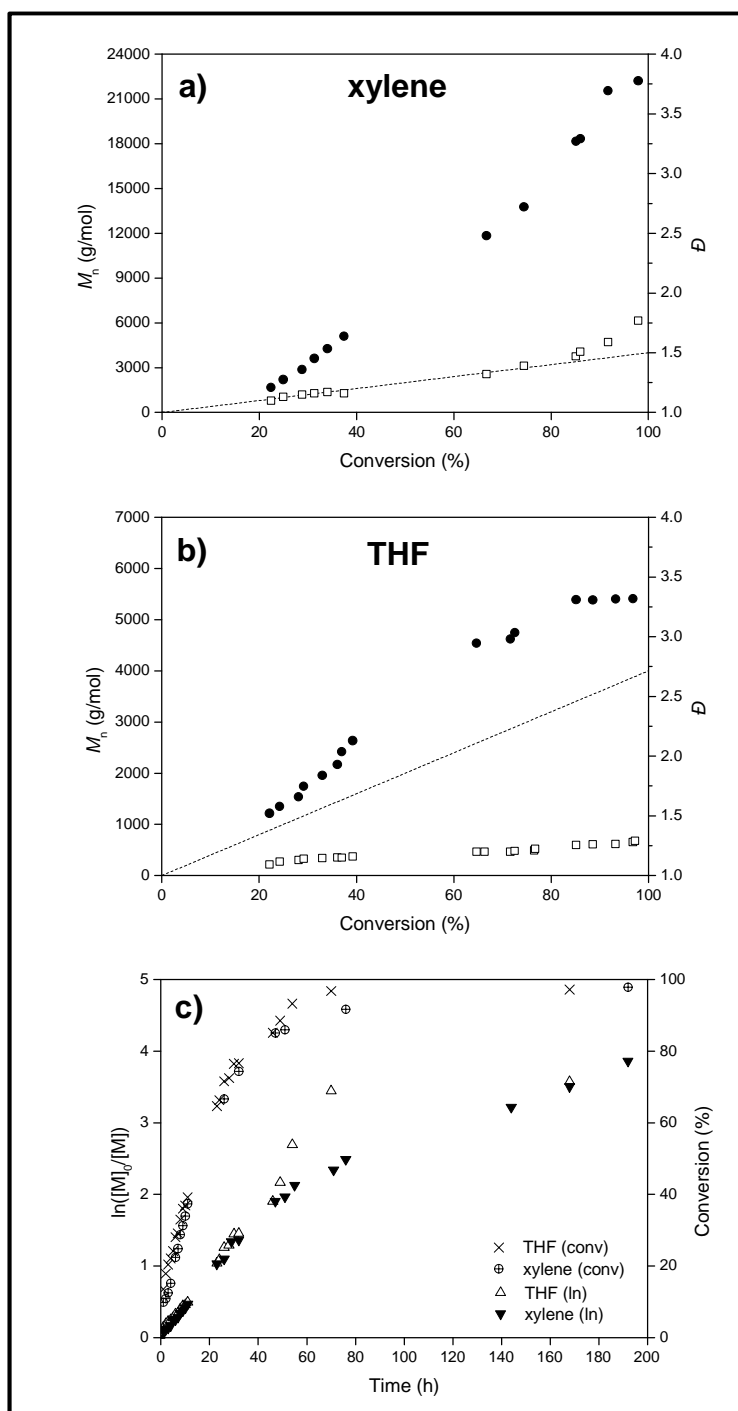


**Figure 3.20.** Kinetic plots for the polymerisation of CB, in THF and xylene (50 % w/w each), under the following conditions:  $[AIBN]_0/[CPD]_0/[CB]_0 = 0.2/1/45$  at 60 °C.

Where  $\bullet = M_n$ ,  $\square = \mathcal{D}$ ,  $--- = M_n^{th}$ .

Figure 3.21 illustrates the GPC traces for polymer formation over the course of each reaction. Here, it is possible to see that shoulders eventually appear on the main polymer peaks in the xylene system. In contrast, samples analysed between roughly ten hours and

32 hours in the THF reaction afforded unimodal polymer peaks (with a slight high molecular weight shoulder forming eventually after two days). Hence, terminating the THF polymerisation at 24 hours (66 % conversion), for instance, would yield polymer with  $M_n^{\text{GPC}} = 4400$  g/mol,  $\mathcal{D} = 1.20$  and a unimodal distribution. In contrast, the last unimodal peak in the xylene system correlates with that obtained at 11 hours, where the polymer would give  $M_n^{\text{GPC}} = 5100$  g/mol,  $\mathcal{D} = 1.16$ , where the monomer conversion was low (37 %).

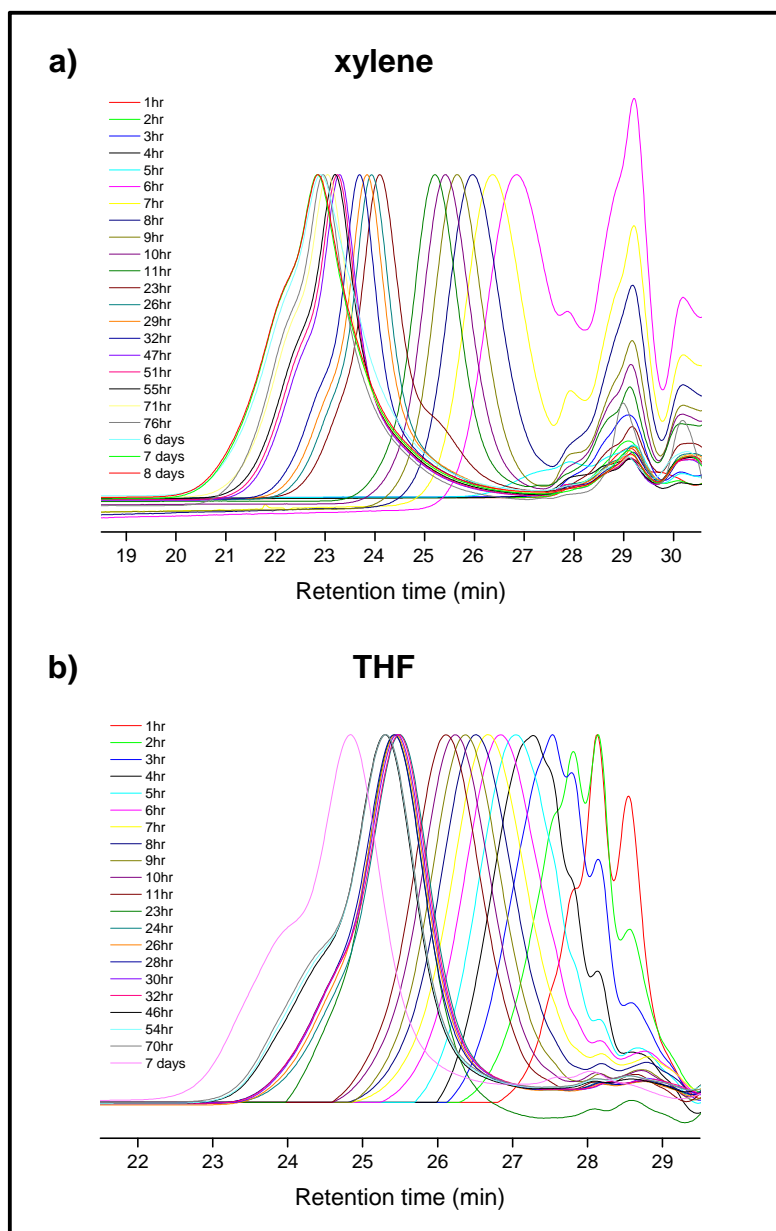


**Figure 3.21. GPC traces (normalised RI response) showing polymer formation over time for the CPD polymerisation systems in xylene (a) and THF (b).**

The polymerisations were similar in terms of kinetics, affording initial apparent rate constants ( $k_{\text{app}}$ ) of  $0.042$  h<sup>-1</sup> and  $0.050$  h<sup>-1</sup> for xylene and THF, respectively. However, the semi-logarithmic plot for THF is linear for longer, whereas that for xylene has two distinct regimes, as the gradient is more shallow after 60 h (see Figure 3.20, c). This trend in the kinetics, with

two periods in the reaction proceeding at contrasting rates, was also seen in the RAFT polymerisation of VC in THF with CMPCD.<sup>33</sup>

It is clear that CPD is capable of controlling the polymerisation of CB in THF, with experimental  $M_n$  values matching  $M_n^{\text{th}}$  and narrow dispersity ( $\mathcal{D} < 1.3$ ) throughout the reaction. The success of CPD adds further weight to the argument that CB lies in the more-activated category (MAM, as defined originally by Moad *et al.*)<sup>26</sup> and, on the whole, behaves similarly to (meth)acrylates,<sup>32, 34, 45, 46</sup> to which CPD has previously been applied.

### **3.3.2. DDMAT and CPD RAFT polymerisation reactions in bulk**

For comparative purposes, the RAFT polymerisation of CB was also conducted in bulk conditions (*i.e.* not employing any additional solvent medium). The previous sets of results for the four CTAs in solution inferred that DDMAT and CPD CTAs offered the greatest control, in general (irrespective of solvent). Both CTAs enabled the target molecular weights to be met at high conversions (in each solvent for DDMAT, only in THF for CPD). Also, both CTAs performed more effectively in THF, than in xylene, as these conditions realised more uniform, unimodal polymer peaks in the GPC. However, the distinction between the two CTAs resides with the molecular weight distributions, whereby the values of  $\mathcal{D}$  obtained for CPD in THF remained  $< 1.3$  throughout the polymerisation, which is an excellent result. Conversely,  $\mathcal{D}$  for DDMAT reached up to 1.6.

The other CTAs, TBTA and CMPCD, were unable to control the polymerisation of CB in solution, in that the evolution of molecular weight did not follow the  $M_n^{\text{th}}$  trend line in any case. Molecular weight distributions were also broad and, in the case of CMPCD, the gradual formation of low molecular weight species caused bimodal GPC peak shapes, thus affecting an apparent decrease in molecular weight. It was therefore decided to only investigate the bulk RAFT polymerisations of CB with DDMAT and CPD CTAs.

In the same way as with the previous reactions in THF, the monomer was synthesised, dried and distilled beforehand. In each case, CB was able to dissolve the reagents (AIBN and the CTAs) in the bulk, so that the reaction media were homogeneous. The two reactions were undertaken in parallel at 60 °C and aliquots were taken periodically to assess  $M_n$ ,  $\mathcal{D}$  and conversion, as was typical throughout these RAFT investigations.

Figures 3.22 and 3.23 display the kinetics results and GPC traces, respectively, for each system (or CTA). It should be noted that the two reactions targeted different molecular weights ( $M_n^{\text{th}}$ ): 10,000 g/mol for CPD and 4000 g/mol for DDMAT. Considering this, the first observation is that both systems approximately reached their  $M_n^{\text{th}}$ : DDMAT at  $> 95$  %

conversion and CPD at 72 %. However, the CPD reaction continued past this point so that the  $M_n^{\text{th}}$  was exceeded and  $\sim 20,000$  g/mol was eventually obtained by the end of the polymerisation. This is complimented by the higher  $\mathcal{D}$  values of the CPD system, in that 1.15 – 1.45 was observed up to 75 % conversion, but  $\mathcal{D}$  exceeded 2.7 at >95 %. The reaction was thus fairly controlled initially, but control was eventually lost and termination reactions prevailed. Conversely, the  $\mathcal{D}$  values decreased over time in the DDMAT system, which is more fitting for a controlled-radical polymerisation.<sup>49, 50</sup> The value of  $\mathcal{D}$  decreased from 1.4 to 1.25 from 50 to 95 % conversion. Although both reactions reached high conversion (>90 %), this was achieved more readily for DDMAT after just eight hours; at a similar point in the CPD reaction, only 75 % monomer was consumed. Hence, the faster polymerisation was that employing DDMAT, which yielded a higher initial apparent rate constant,  $k_{\text{app}}$ , of  $1.248 \text{ h}^{-1}$ , whereas that for CPD was  $0.247 \text{ h}^{-1}$ .

The results of the periodic GPC analyses are displayed subsequently in Figure 3.23 for DDMAT and CPD, respectively. Here, the evolution of the polymer peaks over time compliments the dispersity results for each system. For instance, the gradual decrease of the  $\mathcal{D}$  values for the DDMAT system is demonstrated by narrowing of the peak (graph **a**); initially the peak is quite broad, but this is rectified as the RAFT equilibrium becomes established and all the radicals become incorporated into propagation reactions. In contrast, the GPC peak shape broadens over time for CPD (graph **b**) and a high molecular weight shoulder begins to appear after just four hours. This progresses until the molecular weight distribution is very broad at the end of polymerisation ( $\mathcal{D} > 2.7$  at >95 %).

In comparing the results of each of the bulk reactions with those previously in solution, it was concluded that swapping xylene solvent for THF vastly improved the DDMAT system overall (see Section 3.3.1.3). This conclusion was reached because of the more unimodal GPC peaks obtained in THF; the xylene system saw multi-modal peaks initially. For the equivalent bulk reaction, the GPC also shows unimodal peaks, although the dispersity is shown to decrease over time for this system. A reduction from 1.4 to 1.25 is a vast improvement on the solution systems for this CTA, where the value of  $\mathcal{D}$  increased up to 1.6 in THF. Hence, the bulk system is favoured over solution for DDMAT, overall, even outshining the respectable results obtained in THF.

The CPD system in THF was especially promising as this yielded monodisperse polymer of the target molecular weight at high conversion. Crucially,  $\mathcal{D}$  remained  $< 1.3$  over the course of the polymerisation. This was an improvement on the xylene system, where higher  $\mathcal{D}$  values were obtained (reaching 1.8) and the  $M_n^{\text{th}}$  was far exceeded. The corresponding bulk reaction saw intermediary results, which were lower than those in xylene, but still higher than those in THF; the increase in  $\mathcal{D}$  from 1.15 to 1.45 up to 75 % conversion in bulk is inferior to



the <1.3 values obtained in THF. Hence, the THF system for CPD is still favoured. One similarity between the THF and bulk CPD systems is that both see the polymer GPC peaks become partially bimodal over time, as high molecular weight shoulders form.

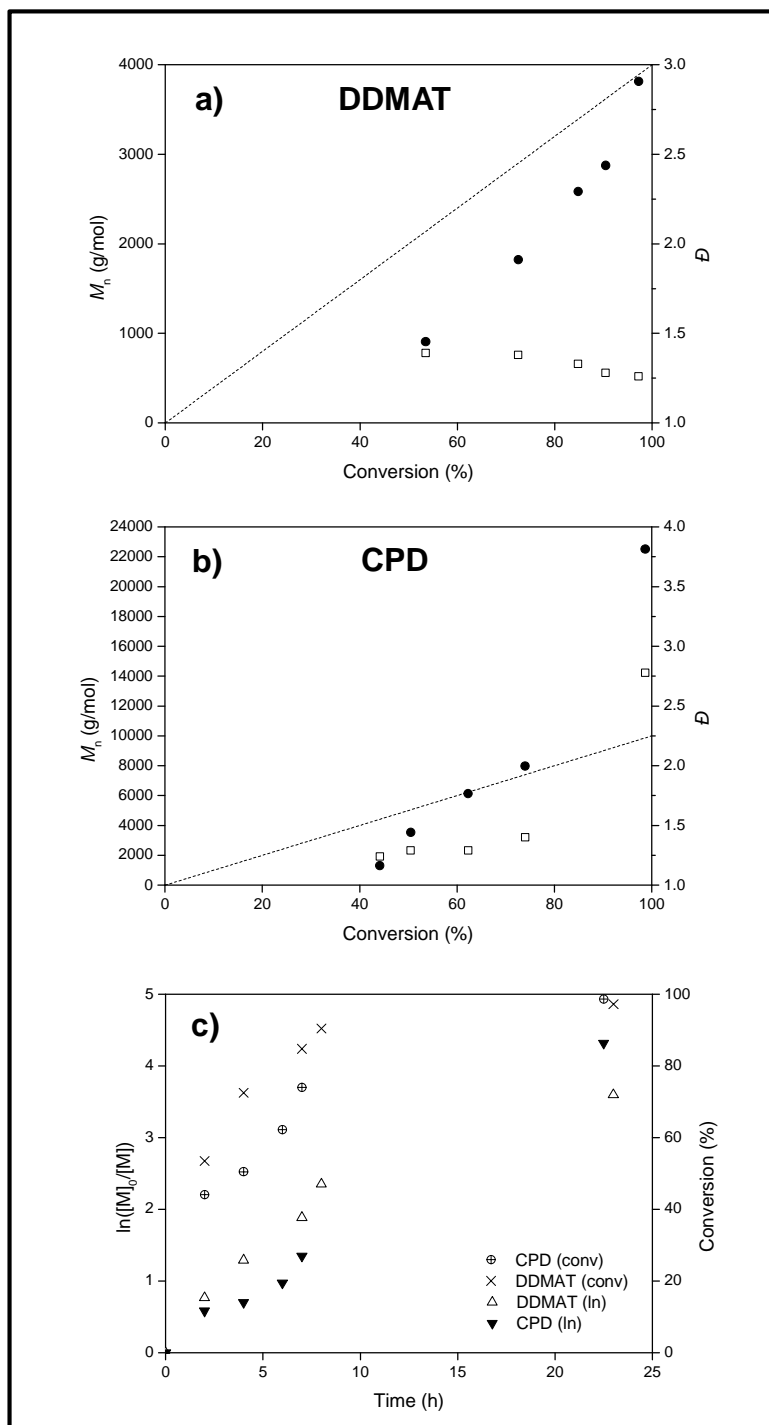
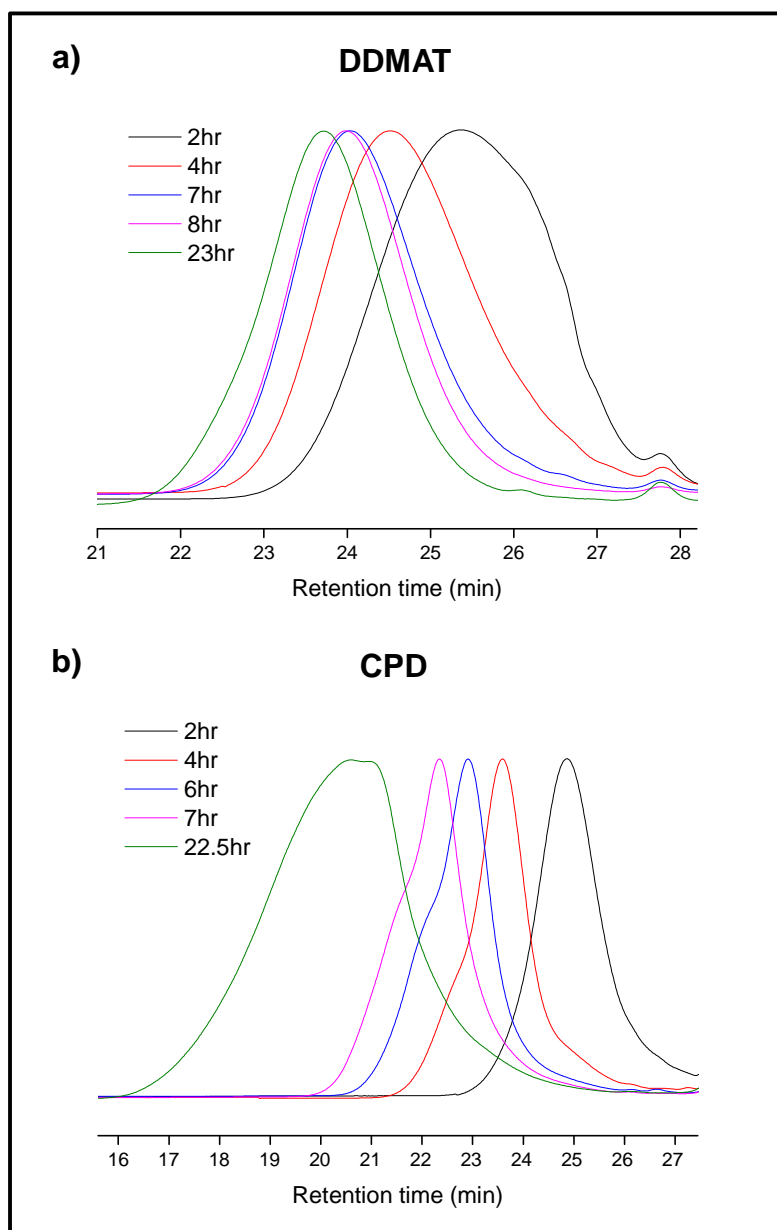


Figure 3.22. Kinetic plots for the polymerisation of CB in bulk at 60 °C for DDMAT and CPD under the following conditions:  $[AIBN]_0/[DDMAT]_0/[CB]_0 = 0.2/1/45$  and  $[AIBN]_0/[CPD]_0/[CB]_0 = 0.2/1/113$ . Where  $\bullet = M_n$ ,  $\square = \bar{D}$ ,  $---$  =  $M_n^{th}$ .



**Figure 3.23. GPC traces (normalised RI response) showing polymer formation over time for the polymerisation systems comprising DDMAT (a) and CPD (b).**

Unsurprisingly, both bulk polymerisations proceeded faster than their solution equivalents, with higher initial apparent rate constants and the reactions overall were shorter. As Table 3.6 clearly shows, the CPD bulk reaction proceeded at least five times faster and DDMAT was 25 times faster than in solution. In the bulk systems, a seven hour reaction afforded 74 % and 84 % conversion, respectively, for CPD and DDMAT. Significantly more time was required to reach this point in solution in both cases. For instance, DDMAT needed 30 hours in xylene and then 96 hours in THF respectively, to each achieve >95 % conversion. Similarly, >90 % monomer was consumed in the CPD system after 54 hours in THF and 76 hours in xylene, respectively. This is a typical trend in polymerisation reactions,<sup>35, 51-53</sup> whereby addition of solvent effectively reduces the concentration of monomer, causing a

decrease in the rate.<sup>52</sup> It is interesting that the solution results are comparable for the two CTAs, but in bulk conditions the magnitude of difference is more considerable in the case of DDMAT.

**Table 3.6. Comparison of initial apparent rate constants,  $k_{app}$ , in the RAFT polymerisations of CB employing DDMAT and CPD CTAs (obtained under solution and bulk conditions).**

CTA	Initial Apparent Rate Constant, $k_{app}$ ( $h^{-1}$ )		
	xylene	THF	bulk
<b>DDMAT</b>	0.042	0.050	1.248
<b>CPD</b>	0.042	0.050	0.247

So far, the conditions for an optimum RAFT polymerisation have been identified as the DDMAT/bulk system or CPD 50 % (w/w) in THF. Both systems see a linear increase in molecular weight, so that  $M_n^{th}$  was attained at high conversion for each. Despite the CPD/THF reaction proceeding for almost three days to reach 96 % monomer conversion, the molecular weight distributions (or dispersities) are far superior to any other, in that they remain <1.3 throughout. This infers that this polymerisation is indeed very well controlled and the polymer chains continue to grow at a uniform rate over this sustained period of time. These results separate this system from the others trialled here and make this system most favourable. The  $\bar{D}$  values of the DDMAT/bulk system are still respectable, in that this is the only case when they decrease over time. However, they majorly resided within the 1.4 – 1.25 range, which is inferior to the CPD/THF system. The results for the optimum CPD/THF system are subsequently summarised in Section 3.3.3.

### 3.3.3. Optimum system

Figure 3.24 summarises the experimental results from the most effective system, comprising CPD in THF (see Scheme 3.7 for overall reaction). Control over molecular weight is evident due to the low  $\bar{D}$  values and linear increase in molecular weight over time. Crucially, the final  $M_n^{GPC}$  is close to the target (4000 g/mol). The first order semi-logarithmic plot (in Figure 3.24)

is linear up to 95 % conversion, with an apparent rate constant,  $k_{app}$ , of  $0.050 \text{ h}^{-1}$ . Thus implying that the number of propagating radicals is constant over the course of the polymerisation.

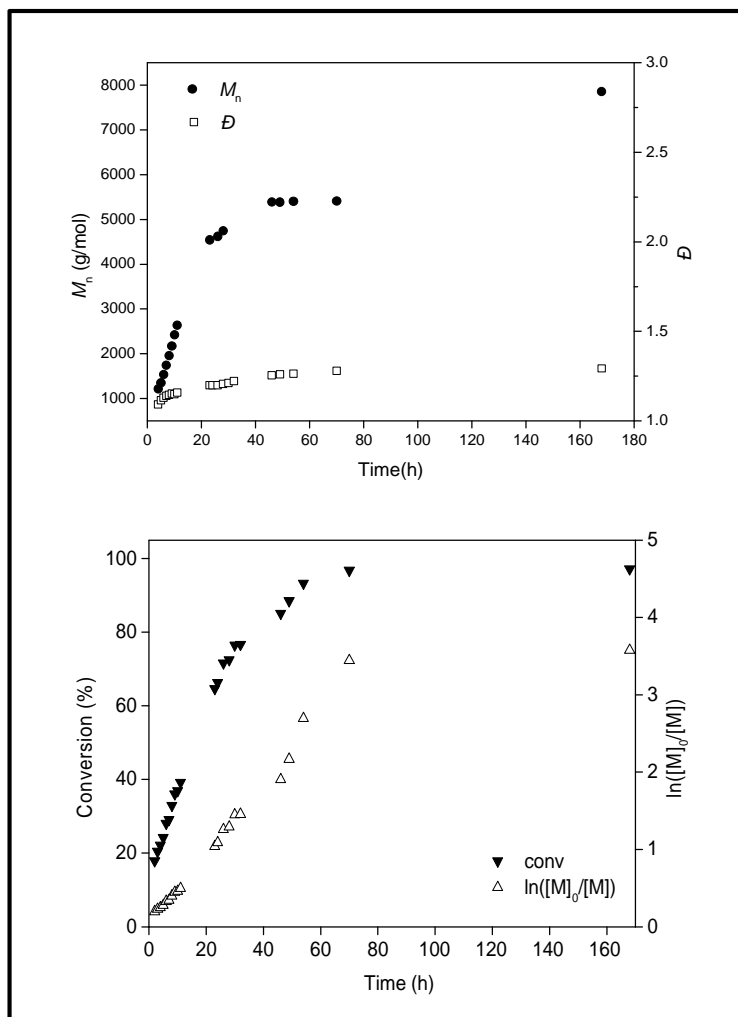


**Figure 3.24. Kinetic plots for the RAFT polymerisation of CB under the following conditions:  $[AIBN]_0/[CPD]_0/[CB]_0 = 0.2/1/45$  at  $60 \text{ }^\circ\text{C}$  in THF (50 % w/w).**

The CPD system was probed further in an attempt to furnish higher molecular weight PCB, whilst retaining a narrow molecular weight distribution. Varying the monomer to CPD ratio (*i.e.* modifying the target  $D_p$ ) enabled polymers of 20,000 g/mol and 50,000 g/mol ( $D_p \sim 230$  and 560, respectively) to be synthesised. Figure 3.25 shows that this system was successful in controlling the synthesis of PCB over a range of predetermined target molecular weights; low dispersities ( $D < 1.25$ ) resulted in each case. Higher molecular weights (than 50,000 g/mol) were not attempted but would certainly feature in future studies so as to give a full appreciation of what this system could achieve.

**Table 3.7. Comparison of theoretical ( $M_n^{\text{th}}$ ) and experimental ( $M_n^{\text{GPC}}$ ) molecular weights, and dispersities ( $\mathcal{D}$ ), obtained for the optimum CB RAFT system targeting different degrees of polymerisation ( $D_p$ ).**

Denotation in Figure 3.25	Reagent conditions [AIBN] <sub>0</sub> /[CPD] <sub>0</sub> /[CB] <sub>0</sub>	$M_n^{\text{th}}$	$M_n^{\text{GPC}}$	$\mathcal{D}$
		g/mol		
---	0.2/1/45	4000	4600	1.20
—	0.2/1/225	20,000	19,700	1.19
...	0.2/1/565	50,000	54,300	1.24

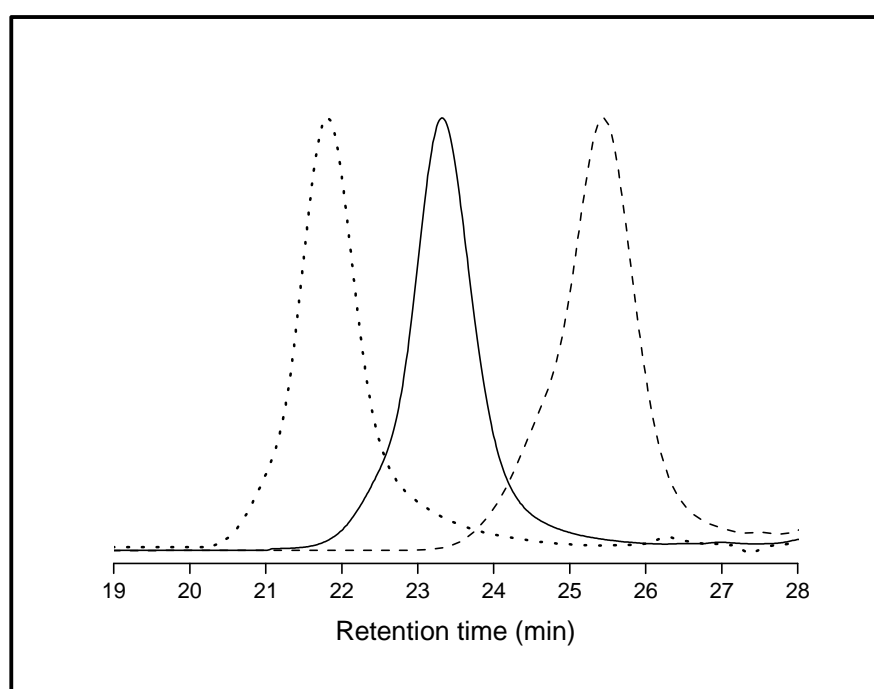


**Figure 3.25. GPC traces (normalised RI response) of PCB with varying molecular weights, synthesised by RAFT using CPD at 60 °C in THF (50 % w/w).**

Finally, to demonstrate that this polymerisation was truly controlled, a self-blocking experiment was performed. Here, polymer was isolated from a RAFT CPD reaction (termed macroCTA,  $M_n = 1500$  g/mol,  $\mathcal{D} = 1.16$ , 35 % conversion) and reacted with a further portion of CB monomer, in the presence of AIBN and THF (*N.B.* the macroCTA was isolated at low conversion to ensure that end group functionality was retained; chain end fidelity is vital, particularly in the production of block copolymers, and can be achieved, in combination with high monomer conversion, through the judicious choice of initiator concentration).<sup>54</sup> As Figure 3.26 shows, there was a near-monomodal increase in molecular weight after the reaction ( $M_n = 3900$  g/mol,  $\mathcal{D} = 1.27$ , 63 % conversion), illustrating successful control over chain extension. This is attributed to the CTA end groups being retained on the polymer (as

shown in Scheme 3.7). Only approximately 0.2 % of the macroCTA remains in the extended PCB-*b*-PCB (as calculated by GPC). To note, the relatively insignificant peaks at high retention time (~27.5 min) correspond to low molecular weight impurities outside of the calibration range (*i.e.* <162 g/mol, the lowest calibration PSt standard).

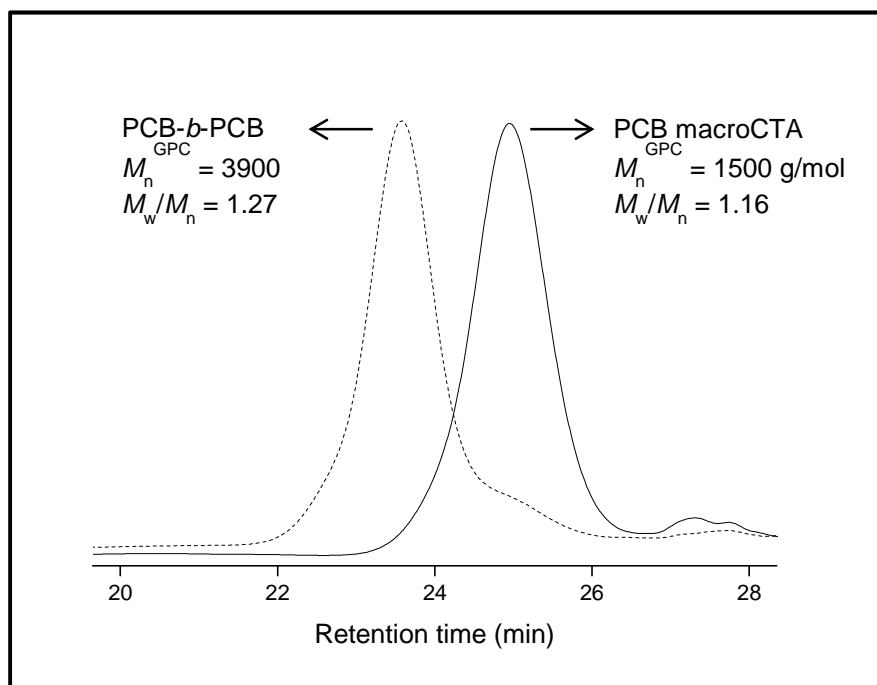


**Figure 3.26. GPC traces (normalised RI response) of the PCB macroCTA and the corresponding PCB-*b*-PCB following chain extension using CPD CTA.**

The success of CPD for CB<sup>55</sup> suggests that CB could lie in the more-activated monomer (MAM) class, along with MMA and other acrylates, as outlined by Moad *et al.*<sup>26</sup> That is, despite the lack of an aromatic ring, carbonyl or cyano group to conjugate the double bonds, which is a general feature in such.<sup>56</sup> CPD has been successful for a wide range of monomers, including 2-isopropenyl-2-oxazoline (*i*POx)<sup>47</sup> and 2-(dimethylamino)ethyl methacrylate (DMAEMA).<sup>34</sup> This implies that CPD is particularly versatile and it outperforms the others tested here. As in other reports, CPD is preferred to other trithiocarbonate and dithiocarbamate CTAs.<sup>47</sup> The stable tertiary cyanoalkyl R group is clearly a proficient leaving group in the RAFT polymerisation of CB, as previously found for other monomers.<sup>44, 48</sup>

Interestingly, the two most successful CTAs in this study – DDMAT and CPD – contribute tertiary R group radicals to the RAFT mechanism, which differ to the primary propagating radicals of CB. Moad *et al.* state that MAMs usually generate tertiary or secondary propagating radicals and are controllably polymerised using more active CTAs, such as aromatic dithioesters.<sup>26</sup> On the other hand, TBTA and CMPCD CTAs fragment to yield primary R group radicals. Hence, there seems to be a trend, at least shown by these results,

that the CTA and monomer must contribute contrasting types of radicals to the mechanism, for successful control. This would help to rationalise the success of CPD for CB.

Throughout the course of this study, it was observed that THF (as the solvent medium) offered more control over the polymerisations than xylene. There was generally better correlation between the experimental and theoretical molecular weights, and lower dispersity ( $\bar{D}$ ) values, for all CTAs except TBTA; overall, there was negligible difference between the solvent systems for TBTA. Despite the uncharacteristic decrease in average molecular weights over time for CMPCD, THF also still improved this system.

The reason for these differences caused by only a change in solvent is not obvious. In general, there is a shortage of literature reporting on, and justifying, the effects of solvent but a small number of studies have been undertaken.<sup>45, 52, 53, 57</sup> Overall, the polarity/aromaticity of the solvent has been deduced irrelevant,<sup>53</sup> as with other properties such as viscosity.<sup>57</sup> Instead, the ability of the solvent to dissolve the initiator<sup>57</sup> or CTA<sup>45</sup> has been deemed influential. In the latter case, Benaglia *et al.*<sup>45</sup> found that acetonitrile (ACN) and DMF were more capable of dissolving a pyridinium toluenesulfonate salt derivative of CPD (than benzene), which allowed higher conversions to be achieved. However, the authors do admit that solvent effects were relatively minor.<sup>45</sup> Solvent has been seen to affect the initiation stage of the free radical RAFT mechanism, though, in particular how readily the initiator decomposes.<sup>57</sup> For instance, in *N,N*-dimethylacetamide (DMAc), 2,2'-azobis(*N*-butyl-2-methylpropionamide) decomposed faster than in toluene. This correlated with achieving higher monomer conversions in the former system; all solvents tested were able to comparably control the molecular weight.<sup>57</sup>

Considering the conclusions regarding solvent effects in literature, THF prevailing over xylene in these studies may be due to a number of factors, including the solubilities of AIBN, the CTAs or the monomer itself. Perhaps, these results correlate with those of Durr *et al.*, in that the decomposition of AIBN is more efficient in THF. On the whole, however, reactions proceeded slightly slower in this solvent, which fortunately did not cause broader molecular weight distributions. Also, as for the work reported by Benaglia *et al.*,<sup>45</sup> the CTAs may be more soluble in THF and, thus, contribute to a more efficient addition-fragmentation mechanism. It may also just be a simple case of CB having a greater affinity for THF than xylene. The additional study into bulk polymerisation (Section 3.3.2) also enabled the conclusion that the 50 % (w/w) THF system was the favoured condition for CB, as this offered much lower  $\bar{D}$  values. This further substantiates the claim that solubility is key; THF is more capable of dissolving all of the reagents and allowing for controlled polymerisation, whereas CB as the sole solvent does not offer such control. Without further studies of this nature it is difficult to draw definitive conclusions as to the effect of solvent, on the whole.

### 3.4. Conclusion and future work

2-Chloro-1,3-butadiene (CB) monomer has been effectively synthesised through the dehydrochlorination of 3,4-dichloro-1-butene. A phase-transfer catalyst (PTC) was able to minimise the temperature and duration of the reaction and a minimum base concentration of 25 % (w/v) was proven necessary.<sup>8</sup> CB was stabilised by phenothiazine (0.1 % w/w), which enabled dependable storage for up to two weeks.

If more importance was placed on the monomer synthesis stage, attempts would have been made to further optimise the conditions for this reaction. For instance, higher concentrations of sodium hydroxide (than the typical 25 % w/v)<sup>8</sup> would be trialled to see the effects on product yield and reaction time. Given the overall capricious nature of the synthesis, the laboratory-scale process would certainly need to be fine-tuned so as to provide a more reliable procedure for future research.

PCB was initially synthesised using 1-dodecanethiol CTA and AIBN at 55 °C.<sup>15</sup> These conditions yielded polymers with molecular weights between 2000 – 3000 g/mol and broad dispersities ( $\bar{D} = 1.5 - 2.0$ ). These studies were a precursor to the investigations into RAFT for CB; more specialised conditions were deemed necessary for accurately managing polymer growth, to ultimately predefine the polymer over a wide range of molecular weights.

Controlled polymerisation of CB by RAFT has been successfully demonstrated for the first time employing 2-cyano-2-propylbenzodithioate (CPD) CTA, THF (50 % w/w) and AIBN at 60 °C, to yield homopolymers up to 50,000 g/mol with narrow molecular weight distributions ( $\bar{D} < 1.25$ ).<sup>55</sup> A successful self-blocking experiment has also verified that the CTA end group was retained and able to react further. The current capabilities of this CPD/THF system have not quite been fully assessed, though, as it is not known how high a molecular weight is truly achievable. Therefore, future work would include altering the monomer:CTA ratio to target even higher molecular weights (*i.e.* >50,000 g/mol) to evaluate the upper limit of this system.

The success of CPD in providing more control than the other CTAs tested [S-(thiobenzoyl)thioglycolic acid, TBTA, cyanomethyl methyl(phenyl)carbamodithioate, CMPCD, and S-1-dodecyl-S'-( $\alpha, \alpha'$ -dimethyl- $\alpha''$ -acetic acid)trithiocarbonate, DDMAT] is largely attributed to a “superior”<sup>48</sup> leaving group ( $R = C(\text{Me})_2\text{CN}$ ). Overall, CPD has shown great versatility as a CTA for other monomers such as methyl methacrylate (MMA)<sup>44, 45</sup> and other acrylates,<sup>34, 46</sup> which are all classified as more-activated monomers (MAMs).<sup>26</sup> The DDMAT CTA, a trithiocarbonate derivative, also performed relatively well for CB (see Section 3.3.1.3), affording polymer with molecular weights close to  $M_n^{\text{th}}$  at high conversion. This CTA, being a trithiocarbonate, is also known to effectively control the polymerisations of MAMs.<sup>26</sup> Hence, it is not a coincidence that these two CTAs are the most suitable (of those tested) for CB; for



the first time, it is possible to classify CB as a MAM, within the realm of RAFT chemistry. The less successful experimental results also support this theory, in that CMPCD (Section 3.3.1.2), a successful CTA for the RAFT polymerisation of vinyl chloride (VC), a less-activated monomer (LAM),<sup>33</sup> did not control the polymerisation in this instance.

It is possible that an alternative initiator, and/or concentration thereof, may be more suitable in the RAFT polymerisation of CB, although the boiling point of this monomer (62 °C) limits the reaction temperature. Ideally, a lower temperature system with the same, if not improved, capabilities would be sought for a more viable application in industry, perhaps to enable the synthesis of predefined PCB on a larger scale. It is also apparent that solvent has a vital role in RAFT; throughout these experiments, the THF systems have shown enhanced control (*versus* xylene), but these were also slower reactions. Bulk polymerisations (undertaken with DDMAT and CPD) proceeded more rapidly, but resulted in higher dispersities. It is thought that the solubility of the CTA<sup>45</sup> or initiator<sup>57</sup> caused the contrasting results obtained with the solvent systems investigated herein. Further research into RAFT of CB is necessary, whereby a broader range of solvents should be tested at varying concentrations. There are numerous reports of systems employing aromatic solvents, especially combined with the same CTAs trialled in this work,<sup>31, 45, 47</sup> and THF features fairly widely.<sup>33, 34</sup> Thus, it would be interesting to examine the effects of completely different types of solvent, such as DMF or ACN, which were investigated by Benaglia *et al.* in the controlled polymerisations of MMA.<sup>45</sup> It may be feasible for the optimum CPD system discovered here to be further improved with a lower concentration of solvent, especially given that reasonable results were obtained for DDMAT and CPD under bulk conditions. Hence, a concentration (at least of THF) residing between zero and 50 % (w/w) may afford monodisperse, predefined polymer in an optimum reaction time.

### 3.5. References

1. G. Odian, *Principles of Polymerization*, Wiley Interscience, New York, 1991.
2. C. M. Blow and C. Hepburn, eds., *Rubber Technology and Manufacture*, Butterworths, London, 1982.
3. W. Hofmann, *Rubber Technology Handbook*, Hanser, Munich, 1996.
4. M. Lynch, *Chem.-Biol. Interact.*, 2001, **135-136**, 155-167.
5. I. E. Muskat and H. E. Northrup, *J. Am. Chem. Soc.*, 1930, **52**, 4043-4055.
6. *US Pat.*, 4540838, 1985.
7. *US Pat.*, 4125564, 1978.
8. *EP Pat.*, 0001905, 1978.
9. *EP Pat.*, 0114643, 1984.
10. M. Orchin, F. Kaplan, R. S. Macomber, R. M. Wilson and H. Zimmer, *The Vocabulary of Organic Chemistry*, Wiley, New York, 1980.
11. L. M. Mascavage, F. Zhang-Plasket, P. E. Sonnet and D. R. Dalton, *Tetrahedron*, 2008, **64**, 9357-9367.
12. W. H. Carothers, I. Williams, A. M. Collins and J. E. Kirby, *J. Am. Chem. Soc.*, 1931, **53**, 4203-4225.

13. N. Makhiyanov and A. S. Khachaturov, *Polymer Science, Ser. A*, 2010, **52**, 209 - 219.
14. *US Pat.*, 2978501, 1961.
15. *US Pat.*, 5523355, 1996.
16. K. Itoyama, N. Hirashima, J. Hirano and T. Kadowaki, *Polym. J.*, 1991, **23**, 859-864.
17. K. Itoyama, N. Shimizu and S. Matsuzawa, *Polym. J.*, 1991, **23**, 1139-1142.
18. P. J. Flory, *Principles of Polymer Chemistry*, Cornell University Press, New York, 1953.
19. J. M. G. Cowie, *Polymers: Chemistry & Physics of Modern Materials*, Chapham & Hall, Bath, 1991.
20. R. C. Ferguson, *J. Polym. Sci., Part A: Gen. Pap.*, 1964, **2**, 4735-4741.
21. C. W. Evans, *Practical Rubber Compounding and Processing*, Applied Science Publishers, London, 1981.
22. G. Odian, in *Elastomers and Rubber Elasticity*, ACS Symposium Series, 1982, vol. 193, ch. 1, pp. 1-31.
23. T. Yoshida, *Mater. Trans.*, 2003, **44**, 2489-2493.
24. K. O. Calvert, in *Polymer Latices and their Applications*, ed. K. O. Calvert, Applied Science Publishers, London, 1982, pp. 1-10.
25. N. Ajellal, C. M. Thomas and J.-F. Carpentier, *Polymer*, 2008, **49**, 4344-4349.
26. G. Moad, E. Rizzardo and S. H. Thang, *Acc. Chem. Res.*, 2008, **41**, 1133-1142.
27. G. Moad, E. Rizzardo and S. H. Thang, *Aust. J. Chem.*, 2005, **58**, 379-410.
28. G. Moad, E. Rizzardo and S. H. Thang, *Aust. J. Chem.*, 2009, **62**, 1402-1472.
29. R. P. Babu and R. Dhamodharan, *Polym. Int.*, 2008, **57**, 365-371.
30. D. S. Germack and K. L. Wooley, *J. Polym. Sci., Part A: Polym. Chem.*, 2007, **45**, 4100-4108.
31. S. C. Farmer and T. E. Patten, *J. Polym. Sci., Part A: Polym. Chem.*, 2002, **40**, 555-563.
32. Y. K. Chong, J. Krstina, T. P. T. Le, G. Moad, A. Postma, E. Rizzardo and S. H. Thang, *Macromolecules*, 2003, **36**, 2256-2272.
33. C. M. R. Abreu, P. V. Mendonça, A. C. Serra, J. F. J. Coelho, A. V. Popov, G. Gryn'ova, M. L. Coote and T. Guliashevili, *Macromolecules*, 2012, **45**, 2200-2208.
34. W. Cai, W. Wan, C. Hong, C. Huang and C. Pan, *Soft Matter*, 2010, **6**, 5554-5561.
35. S. Kanagasabapathy, A. Sudalai and B. C. Benicewicz, *Macromol. Rapid Commun.*, 2001, **22**, 1076-1080.
36. D. Benoit, E. Harth, P. Fox, R. M. Waymouth and C. J. Hawker, *Macromolecules*, 2000, **33**, 363-370.
37. J. Li, J. El harfi, S. M. Howdle, K. Carmichael and D. J. Irvine, *Polym. Chem.*, 2012, **3**, 1495-1501.
38. J. Wootthikanokkhan, M. Peesan and P. Phinyocheep, *Eur. Polym. J.*, 2001, **37**, 2063-2071.
39. J. T. Lai, D. Filla and R. Shea, *Macromolecules*, 2002, **35**, 6754-6756.
40. V. Jitchum and S. Perrier, *Macromolecules*, 2007, **40**, 1408-1412.
41. L. Lu, N. Yang and Y. Cai, *Chem. Commun.*, 2005, 5287-5288.
42. A. M. Nyström and K. L. Wooley, *Tetrahedron*, 2008, **64**, 8543-8552.
43. B. Ebeling and P. Vana, *Macromolecules*, 2013, **46**, 4862-4871.
44. Y. K. Chong, J. Krstina, T. P. T. Le, G. Moad, A. Postma, E. Rizzardo and S. H. Thang, *Macromolecules*, 2003, **36**, 2256-2272.
45. M. Benaglia, E. Rizzardo, A. Alberti and M. Guerra, *Macromolecules*, 2005, **38**, 3129-3140.
46. E. T. A. van den Dungen, H. Matahwa, J. B. McLeary, R. D. Sanderson and B. Klumperman, *J. Polym. Sci. Part A: Polym. Chem.*, 2008, **46**, 2500-2509.
47. C. Weber, T. Neuwirth, K. Kempe, B. Ozkahraman, E. Tamahkar, H. Mert, C. R. Becer and U. S. Schubert, *Macromolecules*, 2012, **45**, 20-27.
48. J. B. McLeary, F. M. Calitz, J. M. McKenzie, M. P. Tonge, R. D. Sanderson and B. Klumperman, *Macromolecules*, 2004, **37**, 2383-2394.
49. B. M. Mandal, *Fundamentals of Polymerization*, World Scientific, Singapore, 2013.
50. *WO Pat.*, 9801478, 1997.
51. S. Perrier and P. Takolpuckdee, *J. Polym. Sci. Part A: Polym. Chem.*, 2005, **43**, 5347-5393.
52. R. P. Babu and R. Dhamodharan, *Polym. Int.*, 2008, **57**, 365-371.
53. M. R. Wood, D. J. Duncalf, P. Findlay, S. P. Rannard and S. Perrier, *Aust. J. Chem.*, 2007, **60**, 772-778.
54. G. Gody, T. Maschmeyer, P. B. Zetterlund and S. Perrier, *Nat. Commun.*, 2013, Article Number 2505.
55. N. Pullan, M. Liu and P. D. Topham, *Polym. Chem.*, 2013, **4**, 2272-2277.
56. D. J. Keddie, G. Moad, E. Rizzardo and S. H. Thang, *Macromolecules*, 2012, **45**, 5321-5342.
57. C. J. Dürr, S. G. J. Emmerling, A. Kaiser, S. Brandau, A. K. T. Habicht, M. Klimpel and C. Barner-Kowollik, *J. Polym. Sci. Part A: Polym. Chem.*, 2012, **50**, 174-180.

## **CHAPTER 4**

# **SPECTROSCOPIC ANALYSIS OF THE CROSS-LINKING OF POLY(2-CHLORO-1,3-BUTADIENE)**

## 4. Spectroscopic analysis of the cross-linking of poly(2-chloro-1,3-butadiene)

This chapter details the first of two industrially-driven studies concerning poly(2-chloro-1,3-butadiene) (PCB) which were each, in part, undertaken in collaboration with Robinson Brothers Ltd. (RBL), West Bromwich. Spectroscopic investigations into elucidating the cross-linking mechanism of PCB are discussed herein, whereby the subsequent chapter focusses on the latex development of this polymer (Chapter 5).

### 4.1. Cross-linking poly(2-chloro-1,3-butadiene)

The quest to elucidate the cross-linking mechanism of PCB was rationalised in the Introduction to this thesis (Section 1.2.2). Briefly, ethylene thiourea (ETU) is the industrial standard reagent for cross-linking PCB, affording optimal physical properties in the rubber product. However, concerns over the toxicity of this reagent have emerged within the European Union so that the applications of ETU, on the whole, will eventually be severely restricted if not completely banished. It is industrially relevant, therefore, to study the cross-linking reaction between PCB and ETU so that a replacement can be sought. Herein, a discussion into the cross-linking of PCB is provided, with the objective to elucidate the ETU mechanism, which is as yet unconfirmed in the literature.

These particular studies employed ~3000 g/mol PCB, which had been synthesised *via* uncontrolled free radical polymerisation (as detailed in Section 3.2). The original drive of the RAFT polymerisation studies (Section 3.3) was to furnish PCB especially for this purpose, however this was not feasible as the cross-linking experiments had to take place immediately at the start of the project so as to generate data readily for RBL. In general, these experiments were performed in test tubes or glass vials, the reagents mixed with polymer, and the resultant solutions heated at 160 °C to simulate cross-linking. Aliquots were taken periodically for the relevant analyses.

K. Berry (RBL) examined the cross-linking of PCB rubber with a similar variety of reagents in parallel to these particular investigations.<sup>1</sup> In stark contrast to the rubber ( $M_n$  ~500,000 g/mol from GPC analysis against PSt standards), the PCB synthesised in-house was more practical and easier to analyse by standard solution-based techniques, due to enhanced solubility. The rubber is more complicated to process, as it requires milling so as to incorporate the reagents and high pressure for the cross-linking reactions (employing a rheometer). Once fully cross-linked, the rubber is rendered totally insoluble, so that only physical tests can be conducted on the final product (such as tensile testing and rheology). Thus, oligomeric PCB was considered because the material would make the process more straightforward, overall. Also, a pseudo-infinite three-dimensional network would not be

created within the oligomers due to its considerably lower molecular weight and shorter chain lengths. It was therefore intended to utilise a range of different analytical techniques, such as FTIR, GPC and NMR, to monitor the reactions throughout. However, the NMR and GPC results failed to offer any additional information to that provided by FTIR, so the focus remained solely on the latter. Where necessary, the results from the rubber investigations of Berry<sup>1</sup> are presented to complement the observations here.

The FTIR spectrum of pure PCB ( $M_n \sim 3000$  g/mol) is presented in Figure 4.2, with the appropriate assignment of relevant peaks listed in Table 4.1, as aided by literature.<sup>2-5</sup> Notably, this spectrum compared well with the rubber material and as such was used extensively as a standard for comparing against results obtained during the various cross-linking reactions. Figure 4.1 shows the four isomers present in PCB, which contribute to the complex FTIR spectrum.

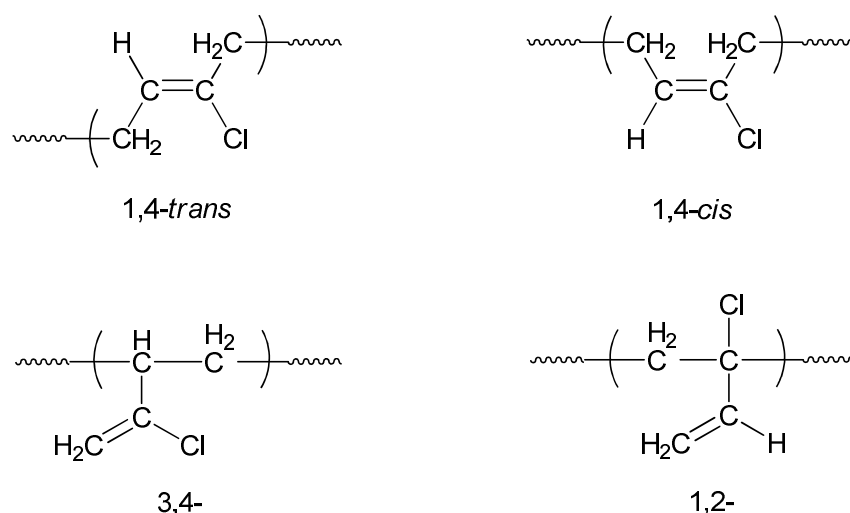


**Figure 4.1.** The four isomers of poly(2-chloro-1,3-butadiene) (PCB).

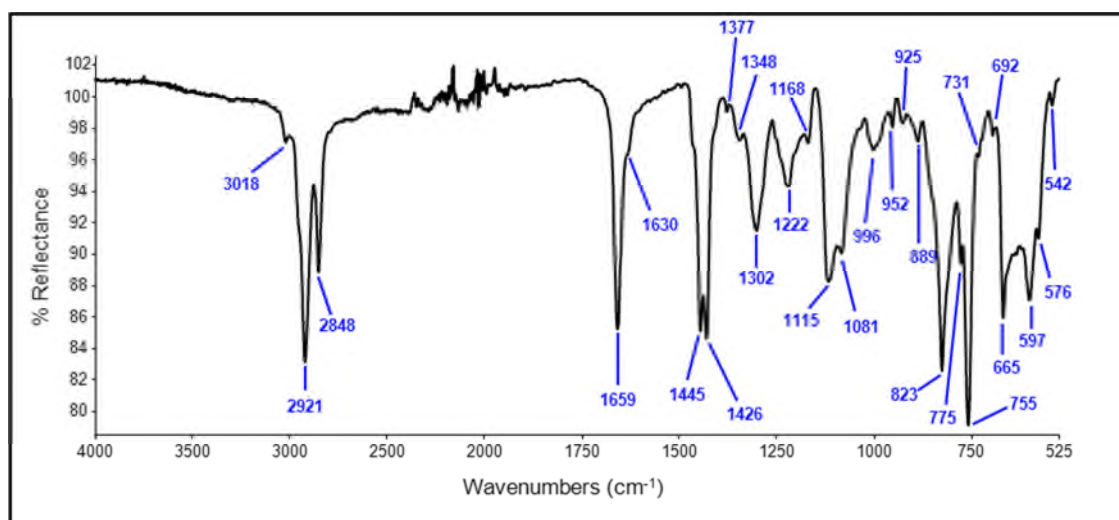


**Figure 4.2.** FTIR spectrum of PCB.

**Table 4.1. FTIR peaks assigned in PCB, as aided by the literature.<sup>2-5</sup>**

FTIR peak/s (Wavenumbers, cm <sup>-1</sup> )	Assignment
2921, 2848	CH <sub>2</sub> asymmetric stretching
1659	<i>trans</i> -1,4-PCB C=C stretching
1630	<i>cis</i> -1,4-PCB C=C stretching
1445, 1426	CH <sub>2</sub> deformation
1302	CH <sub>2</sub> wagging
1115, 1081	C—C stretching
925	1,2-PCB CH=CH <sub>2</sub> stretching
889	3,4-PCB C=CH <sub>2</sub> stretching
823	CH <sub>2</sub> rocking
665	C—Cl stretching

Table 4.2 provides an overview of all of the reactions undertaken with PCB. The weights of the various reagents are displayed in parts per hundred rubber (phr), as is typical in the rubber industry (but is comparable to % w/w, as measurements are by weight; the rubber material here represents 100 % w/w or 100 phr). To note, the ZnO employed in these reactions was “active” grade, *i.e.* a solid with a very small particle size and overall large surface area, which enabled a lesser quantity to be used and more easily mixed. A discussion of results from all of the cross-linking reactions undertaken in this study is provided in the following sections, tackling each relevant system in turn.

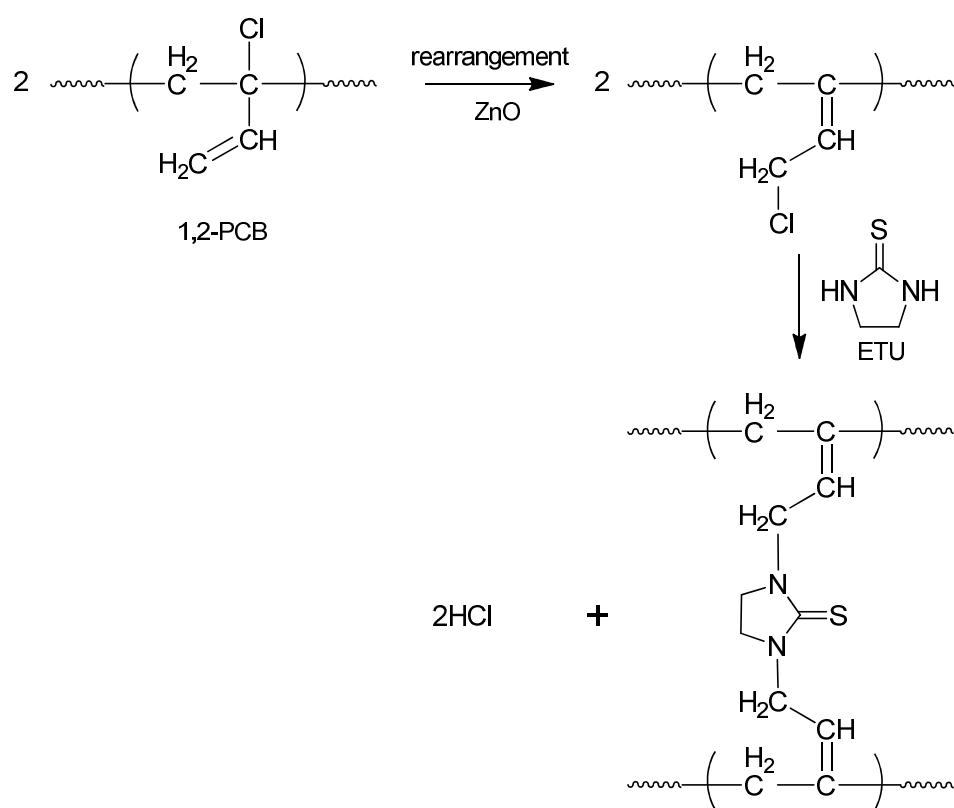
**Table 4.2. List of additives used in the cross-linking studies.\***

Additive name	Abbreviation	Level adopted (phr) <sup>†</sup>	Reason for study
Ethylene thiourea	ETU	2	Industrial standard for PCB
Zinc oxide	ZnO	1	Industrial standard for PCB
Piperazine	PIP	2	Model compound
1,4-Diaminobutane	DAB	2	Model compound
Dibutyl thiourea	DBTU	2	Model compound
1,8-Octanedithiol	ODT	2	Model compound
Tetrabutylthiuram disulfide	TbuT	2	Alternative industrial accelerator

\*All additives were tested individually and in conjunction with ZnO. <sup>†</sup>The term “phr” denotes parts per hundred rubber, *i.e.* relative to polymer; ZnO was adopted at 1 phr in all cases.

#### 4.1.1. Cross-linking PCB with ETU

It is not known exactly how ETU, the standard industrial PCB rubber accelerator, chemically cross-links the polymer chains. The most prominent theory in the literature is that of Kovacic,<sup>6</sup> who states that ETU 'slots in' between the polymer chains, as shown in Scheme 4.1. Allylic rearrangement of the chlorine atom of the 1,2-isomer is the initial step, which is generally accepted by several theoretical modellers who have studied the cross-linking of PCB.<sup>7-11</sup> The 1,2-isomer is defined principally by a small peak at 924 – 926 cm<sup>-1</sup> in the FTIR spectrum of PCB (see Figure 4.2 in Section 4.1). In the cross-linking experiment undertaken on low molecular weight PCB, it was found that this peak gradually diminished over time (within ten minutes), supporting the rearrangement theory.



**Scheme 4.1. The PCB/ETU cross-linking mechanism according to Kovacic.<sup>6</sup>**

The Kovacic theory also states that HCl is generated as a result of the bis-alkylation reaction (as illustrated in Scheme 4.1), as the amine hydrogen atoms of ETU and the chlorine from the polymer chain are expelled. It is interesting to note that thus far there have been no studies into cross-linking PCB whereby the by-products of the reactions have been elucidated; this novel approach was taken throughout these experiments. Considering this, the pH of the headspace of the PCB/ETU cross-linking reaction mixture was taken periodically to test for the possible emission of HCl gas. It was indeed found to become instantly acidic and remained so throughout the reaction; this result certainly supports the Kovacic theory.<sup>6</sup>

Observing distinct changes in the FTIR spectrum, (compared to the original PCB), a new peak appears at  $1548\text{ cm}^{-1}$ , as highlighted in Figure 4.3. This infers that a new chemical bond is formed during the reaction, but it is difficult to elucidate the exact nature of this peak using the standard spectroscopy correlation tables.<sup>12</sup> It was considered that a hydrochloride (HCl) salt may have been generated, given the confirmed presence of acid. To assess if this was the case, the reacted PCB was water washed and dried; a process that would remove all salt species from the polymer. However, the  $1548\text{ cm}^{-1}$  peak was retained in the treated PCB material. Hence, this peak could not represent a salt complex and the possibility of the ETU cross-linking alone yielding a salt was dismissed. As this fundamental peak clearly represents a new chemical composition in the polymer, this helps to further substantiate the Kovacic mechanism.

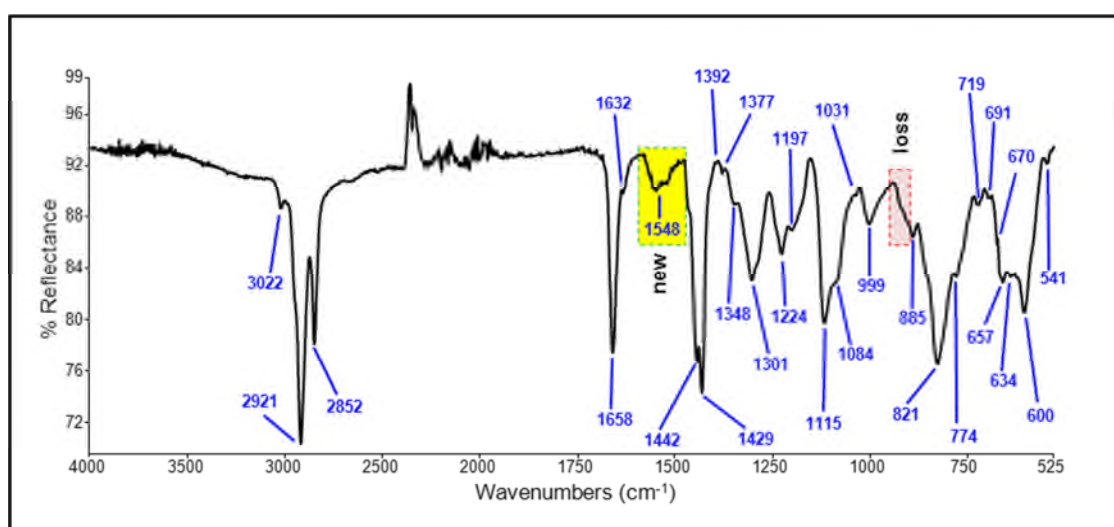


**Figure 4.3. Representative FTIR spectrum collected during the PCB/ETU reaction, highlighting a new peak at  $1548\text{ cm}^{-1}$ .**

#### **4.1.2. Cross-linking PCB with ZnO**

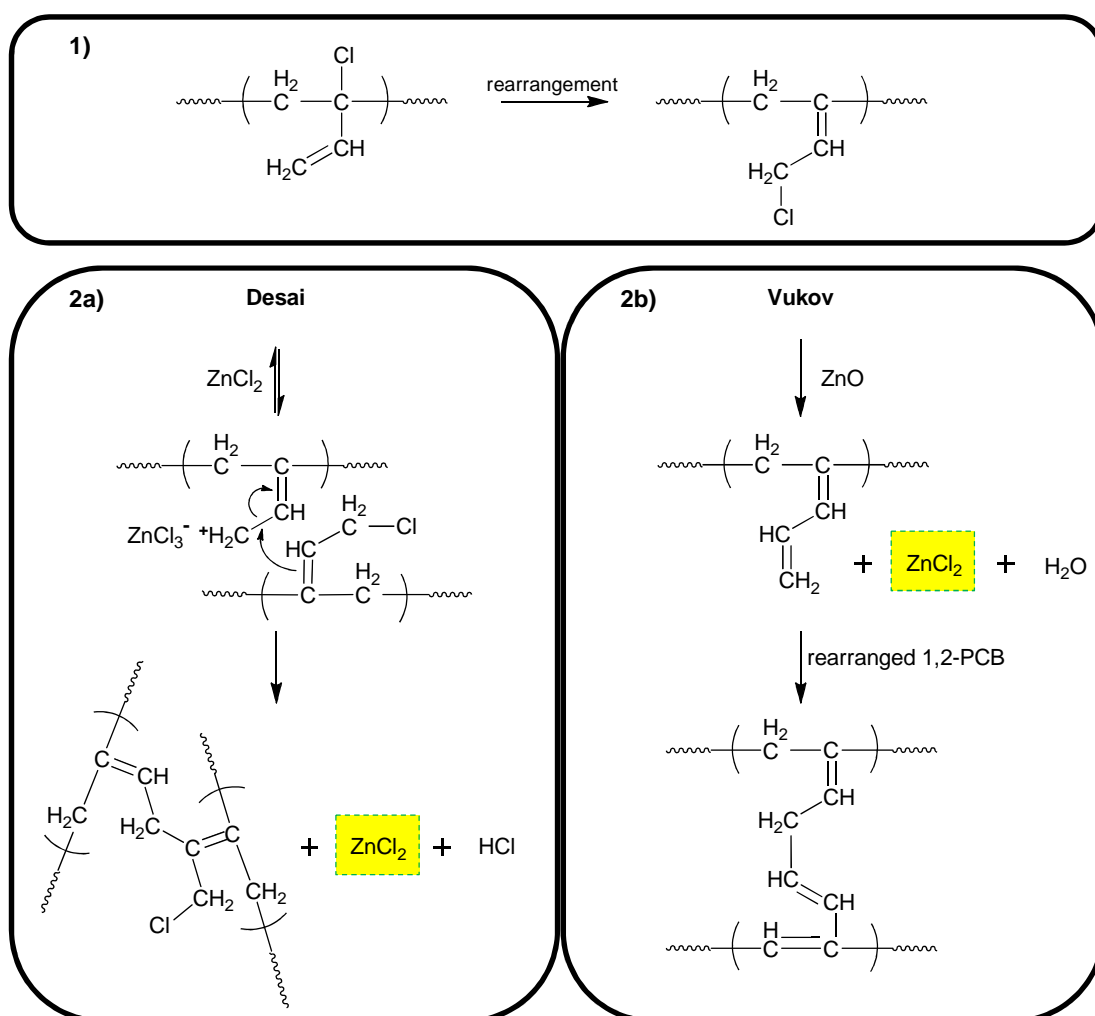
It is known that ZnO can cross-link PCB (rubber) by itself, which is unique for a metal oxide in this context as such components are usually only adopted to accelerate the reaction.<sup>13</sup> Although the mechanism by which ZnO can cross-link is also focus of some speculation, rearrangement of the 1,2-PCB chlorine is generally recognised as the initial step, regardless of the presence of this reagent.<sup>7-11</sup> Hence, it is not surprising that herein a reduction of the  $925\text{ cm}^{-1}$  peak in the FTIR spectrum was observed; rearrangement occurred within just five minutes, which was faster than with ETU (Section 4.1.1).

One of the published theories concerning a possible ZnO mechanism is that whereby an ether linkage transpires, as shown in Scheme 4.2.<sup>14</sup> Observing the FTIR spectra, this type of





this substance is actually a reactant facilitating cross-linking, but is not consumed in the overall reaction itself. Notably, the Desai mechanism states that  $\text{ZnCl}_3^-$  forms during an intermediary stage of the reaction, however this is not possible to exist, chemically. To test for the formation of  $\text{ZnCl}_2$  in the PCB/ $\text{ZnO}$  reaction, the FTIR spectrum of the neat  $\text{ZnCl}_2$  was compared to those obtained over the course of the reaction. The representative spectrum in Figure 4.5 (B) does not match; the distinctive peaks at  $1615\text{ cm}^{-1}$  and  $1404\text{ cm}^{-1}$  are not visible in the reaction spectrum (A), although it is possible that they could be masked slightly by the polymer. There is also no comparison in the FTIR spectrum with that of  $\text{ZnO}$ , which is also shown in Figure 4.5 (C). This infers that  $\text{ZnCl}_2$  is not formed at any time during the reaction of PCB with  $\text{ZnO}$ , which discounts the theories of Desai<sup>7</sup> and Vukov,<sup>15</sup> where  $\text{ZnCl}_2$  is a distinct by-product. Further evidence for the invalidation of the mechanism provided by Vukov<sup>15</sup> is the lack of a signal pertaining to a diene being observed; a strong peak at  $\sim 1600\text{ cm}^{-1}$  would confirm  $\text{C}=\text{C}$  formation<sup>12</sup> and would be clear in the PCB spectrum.



**Scheme 4.3. The Desai<sup>7</sup> (2a) and Vukov<sup>15</sup> (2b) mechanisms of cross-linking PCB, where both are preceded by allylic rearrangement of 1,2-PCB (step 1).**

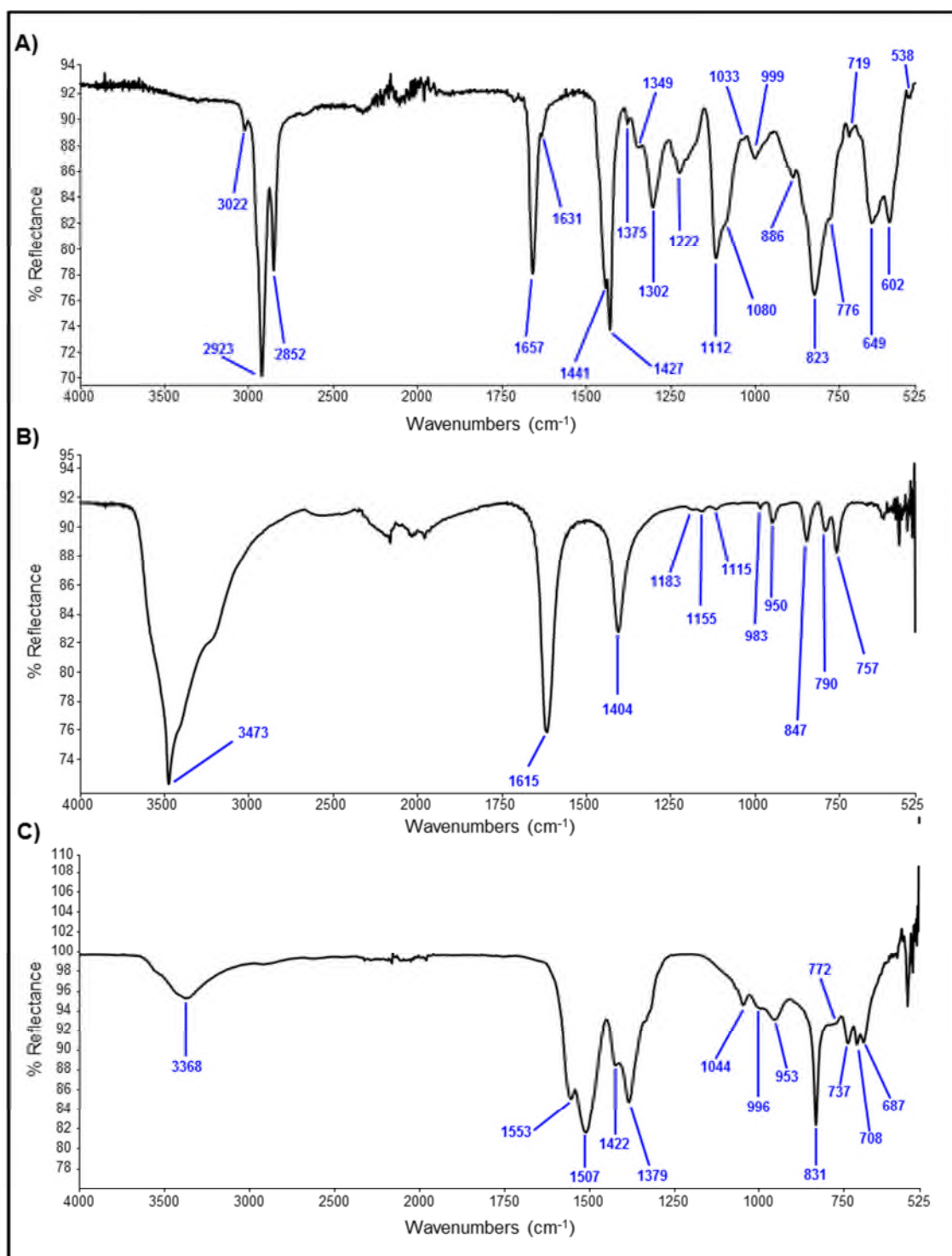


**Figure 4.5. Representative FTIR spectrum collected during the PCB/ZnO reaction (A) versus FTIR spectra of ZnCl<sub>2</sub> (B) and ZnO (C).**

#### **4.1.3. Cross-linking PCB with ETU and ZnO**

ETU and ZnO were combined for a PCB reaction, which would simulate the actual industrial rubber cross-linking system. In this instance, the FTIR peak representing the 1,2-isomer

( $\sim 925\text{ cm}^{-1}$ ) disappeared after just five minutes, considerably quicker than the ETU reaction, but marginally slower than that employing just ZnO. Once again, allylic rearrangement of 1,2-PCB is confirmed and occurs faster than ETU alone because of the presence of the metal oxide. However, there is a delay when ZnO and ETU are present together, compared to when ZnO is by itself, which must be a consequence of competing reactions taking place.

The FTIR spectrum of the reaction mixture collected after 30 minutes is provided in Figure 4.6 (B). This shows a distinct new peak at  $1545\text{ cm}^{-1}$  which is not attributed to any of the starting materials and, indeed, is absent at the start of the reaction. Interestingly, this is comparable to the new peak formed during the ETU reaction, at  $1548\text{ cm}^{-1}$  (shown in Figure 4.3 of Section 4.1.1). In that case, the peak was not removed upon water-washing and was thus not deemed to represent a salt. This was also the case for the PCB/ETU/ZnO mix and so the new chemical bond forming due to ETU occurs irrespective of whether ZnO is present or not.

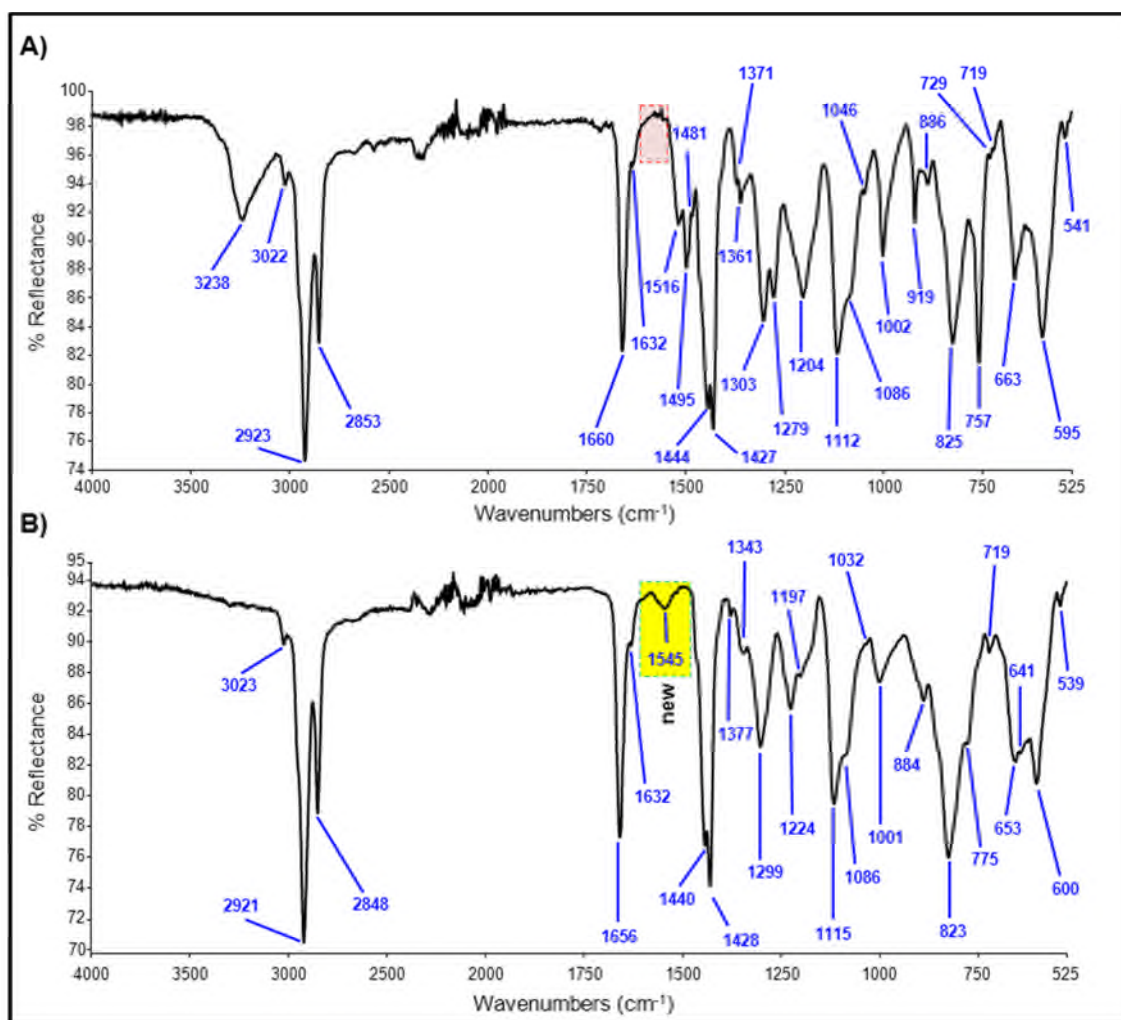
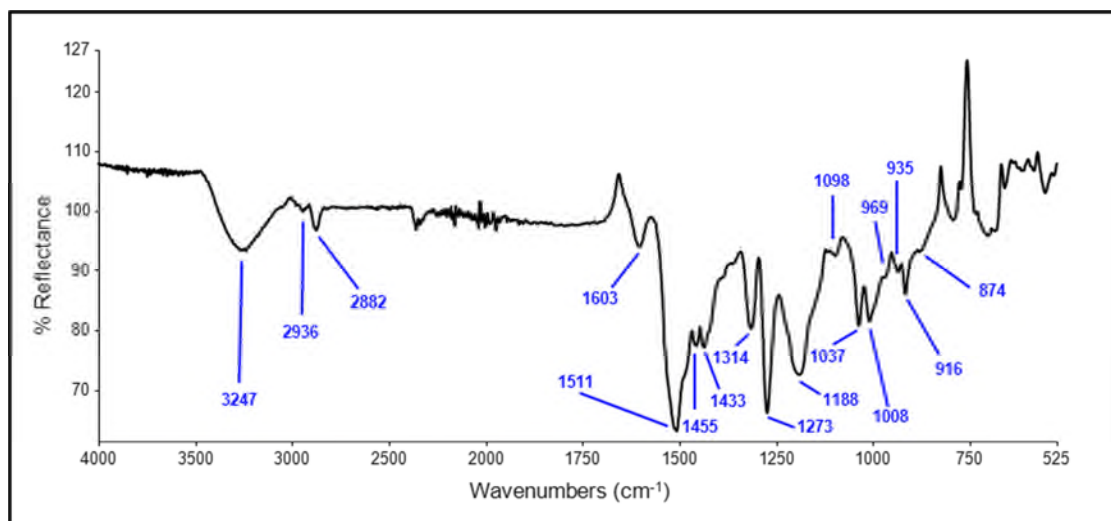


Figure 4.6. FTIR spectra collected at the start (A) and during (B) the PCB/ETU/ZnO reaction, with emphasis on the new peak formed at  $1545\text{ cm}^{-1}$ .

The headspace of the PCB/ETU/ZnO reaction was also found to be acidic, in the same way as in the individual PCB/ETU reaction. Thus, it is apparent that the chemistry taking place in the individual reaction (of ETU with PCB) is also occurring in the combined system. The one distinction in this case, however, was the gradual formation of an off-white solid precipitating out of solution. This substance was not produced in either of the respective individual reactions and does not correlate to the reactants themselves. The FTIR spectrum of the formed solid is shown in Figure 4.7, whereby the polymer background has been subtracted (hence the presence of a small number of 'negative' peaks).



**Figure 4.7. FTIR spectrum of the solid by-product from the PCB/ETU/ZnO reaction, whereby the polymer background (neat PCB) has been subtracted.**

A number of experiments were performed in an attempt to establish the identity of this compound. To verify that ETU was not forming a salt in the presence of ZnO, the raw materials, ETU and HCl, were reacted together under the same conditions (*i.e.* temperature) in the absence of polymer; the FTIR spectrum of the resulting substance did not corroborate with that of the new solid from the cross-linking reaction. A reaction between ETU and ZnO also failed to yield a solid with a similar FTIR spectrum to this new material. However, adding HCl to an ETU/ZnO mix, reacting and then washing with methanol (to remove excess ETU) did yield a (dried) solid with a comparable FTIR spectrum. It was then considered that the well-known leaching reaction of ZnO by HCl could be occurring, which generates zinc chloride ( $\text{ZnO} + 2\text{HCl} \rightarrow \text{ZnCl}_2 + \text{H}_2\text{O}$ ) and is vital for recycling zinc industrially.<sup>4</sup> This subsequently implied that  $\text{ZnCl}_2$  formed *in situ* within the PCB/ETU/ZnO system and was then able to react with ETU. Hence, a final test reaction between ETU and  $\text{ZnCl}_2$  was performed, which furnished a solid compound with a comparable FTIR spectrum to that from the cross-linking reaction. The FTIR spectra of the products of these relevant reactions are shown in Figure 4.8, for comparison against Figure 4.7, the FTIR of the original, enigmatic solid, which is itself as yet still unassigned.

It has thus been deduced that  $\text{ZnCl}_2$  is a by-product of the reaction between PCB, ETU and  $\text{ZnO}$ . This supports the theory of Pariser,<sup>16</sup> whereby  $\text{ZnCl}_2$  is generated, as shown in Scheme 4.4 at the end of this sub-section. Notably, the theories of Vukov<sup>15</sup> and Kovacic<sup>6</sup> also state that  $\text{ZnCl}_2$  is formed during cross-linking, although these studies focussed on the independent reagents,  $\text{ZnO}$  and ETU, respectively (not in conjunction with one another). It has already been established that  $\text{HCl}$  is also a by-product, which was also hypothesised by Kovacic<sup>6</sup> and Vukov.<sup>15</sup> To note, the mechanism of Vukov is based on the formation of a diene and carbon-carbon cross-links forming the chemical bridge between polymer chains.<sup>15</sup> This has not as yet been proven in these studies. Thus far, it is postulated that a combination of reactions is occurring when ETU and  $\text{ZnO}$  are working in unison, given that there is some degree of evidence for all of the stated theories.

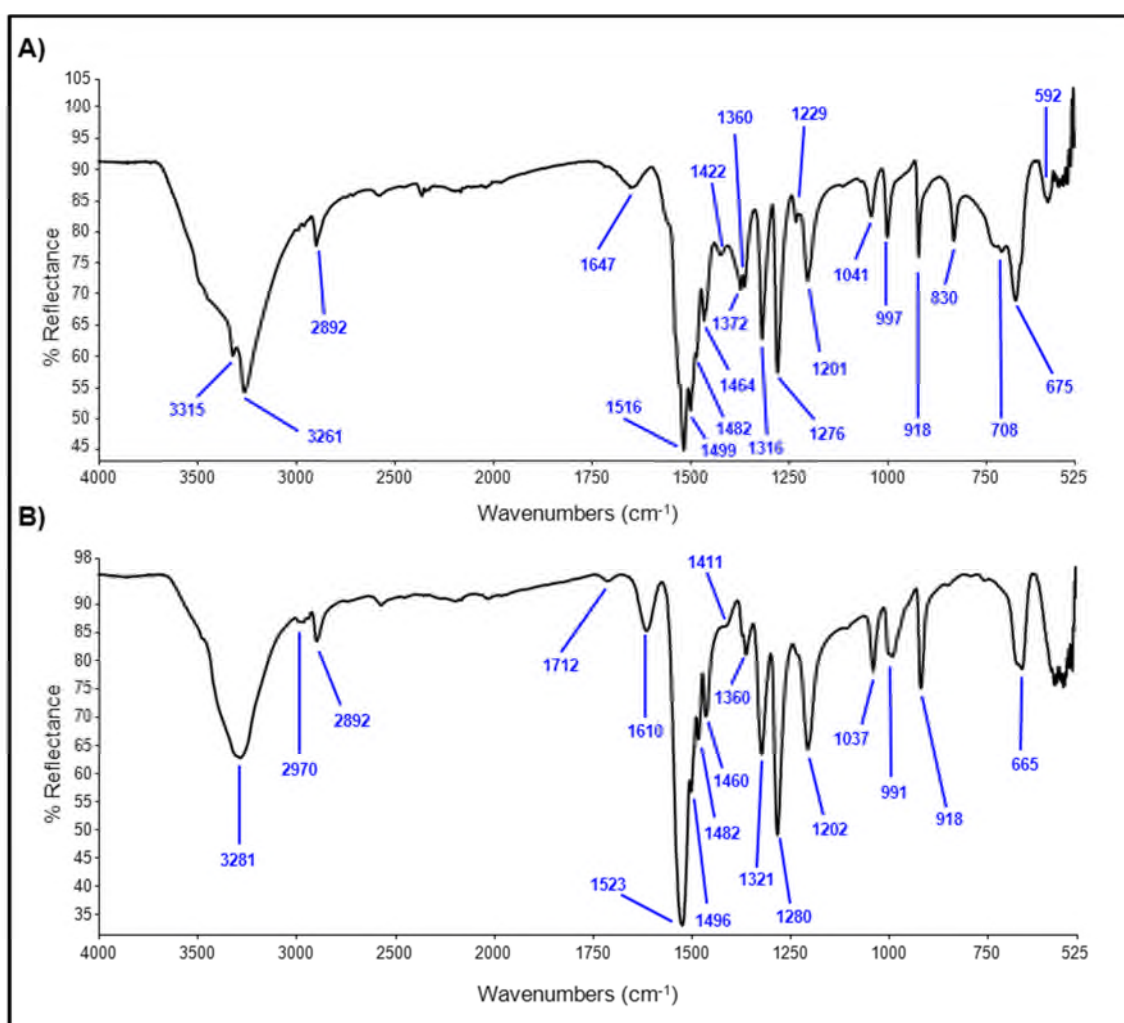


**Figure 4.8. FTIR spectra of the solid products from (A) the ETU/ $\text{ZnO}$ / $\text{HCl}$  test reaction and (B) the ETU/ $\text{ZnCl}_2$  test reaction.**

Ethylene urea (EU) is also generated during the Pariser reaction (Scheme 4.4).<sup>16</sup> Hence, it was also necessary to test for the formation of EU in the PCB/ETU/ $\text{ZnO}$  system. The distinguishing feature of the EU FTIR spectrum is the carbonyl peak at  $1642\text{ cm}^{-1}$ , as shown



in Figure 4.9, plot **A**. However, this signal did not appear during this reaction (see previous representative spectrum for the reaction mixture in Figure 4.6). Given the distinguishable nature of such a peak,<sup>12</sup> a C=O stretch would certainly be expected if EU had indeed been formed. Interestingly, this was proven instead by Berry in analogous experiments with the high molecular weight PCB rubber.<sup>1</sup> Figure 4.9, **B** shows the FTIR spectrum obtained when the rubber was reacted in a similar way with ETU/ZnO and purified by methanol soxhlet extraction, yielding solid extracts. There are clear similarities between the spectrum for the extracts and that for EU, as in the distinct peaks in the carbonyl region. Berry verified further that EU was a by-product using TLC and GC-MS.<sup>1</sup>

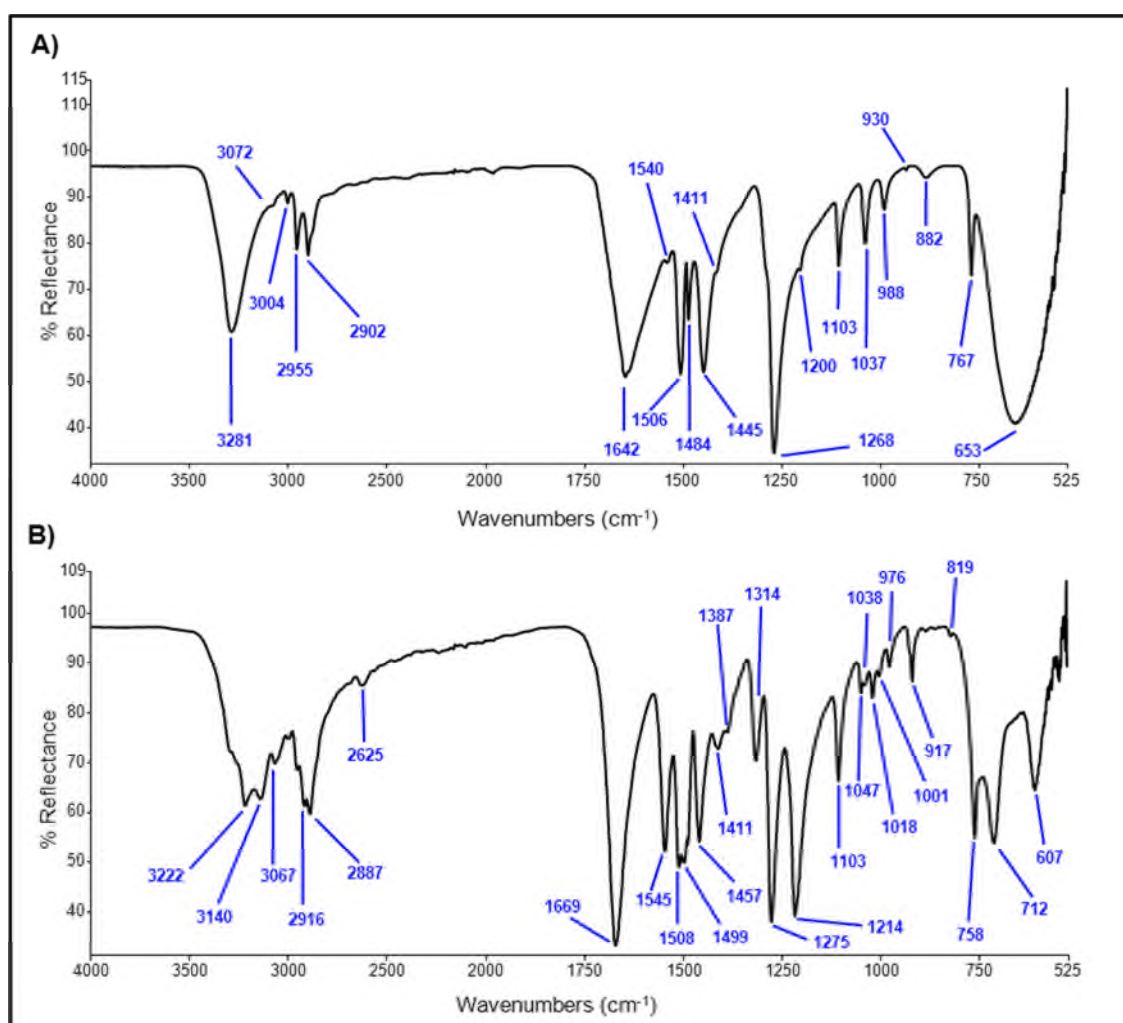
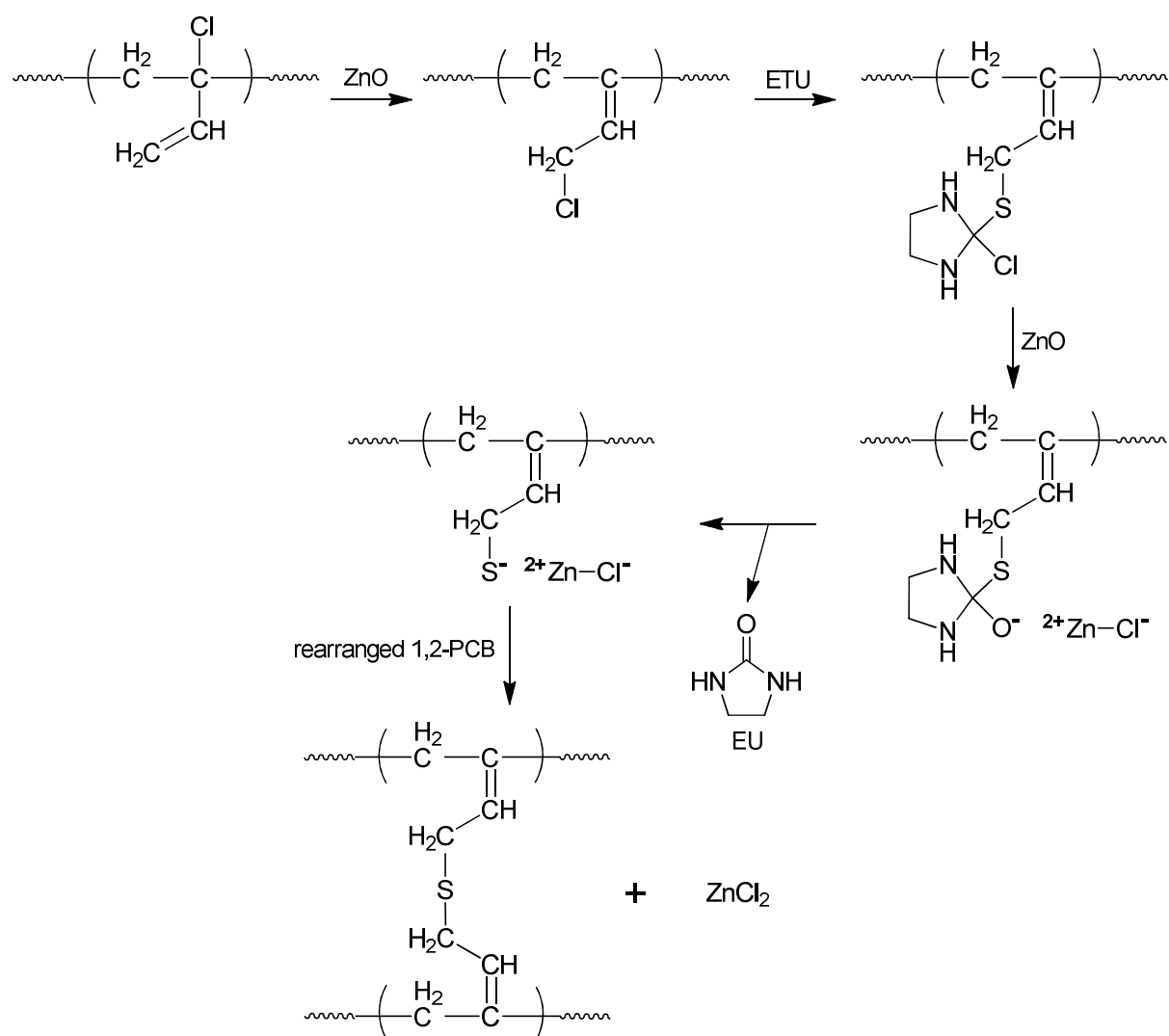


**Figure 4.9. FTIR spectra of (A) ethylene urea (EU) and (B) solid extracts from the PCB rubber ETU/ZnO reaction performed by Berry,<sup>1</sup> each displaying carbonyl peaks in the 1670 – 1640  $\text{cm}^{-1}$  region.**

It is not clear why there are discrepancies between the results of Berry<sup>1</sup> and those obtained here, or why EU formed in the rubber mix but not with low molecular weight PCB. Although the reactions were designed to imitate each other, there is no doubt that reacting the two types of contrasting materials yielded some inconsistencies; EU may not have formed here

due to a less efficient system or ineffective mixing of reagents. For instance, the experiments undertaken by Berry involved mechanical milling the rubber to incorporate the additives; curing was undertaken at the same temperature (160 °C) but adopting a rheometer; the ZnO adopted for the rubber was also not “active” grade. Despite the different techniques employed with the rubber and low molecular weight PCB, the results from each set of studies largely correlated with each other, with the exception of this single occurrence regarding EU. Thus, it is vital to include the results of Berry in this instance,<sup>1</sup> as they add to a more comprehensive picture. Whilst formation of EU looks fairly certain from the rubber trials, and supports the theory of Pariser,<sup>16</sup> the fact that this is not replicated here does cast some shadow on this finding. Evidence towards Pariser is, therefore, only partially credible at this point.



**Scheme 4.4. The mechanism of cross-linking PCB with ETU and ZnO, as originally proposed by Pariser and adapted from the literature.<sup>16</sup>**



#### 4.1.4. Cross-linking PCB with model compounds and other standard accelerators

In order to yield further information as to the nature of the ETU reaction, several model compounds and a further standard rubber accelerator were employed in analogous reactions. These compounds are illustrated in Table 4.3 and all exhibit some chemical functionality that can be compared with ETU. The tests were principally conducted to examine the roles of certain relevant functionalities, such as thiols (*i.e.* the sulfur atom) and amines.

**Table 4.3. Model compounds and accelerators adopted in PCB cross-linking studies.**

Full Name	Abbreviation	Structure
Dibutyl thiourea*	DBTU	
1,4-Diaminobutane*	DAB	$\text{H}_2\text{N}(\text{CH}_2)_4\text{NH}_2$
1,8-Octanedithiol*	ODT	$\text{HS}(\text{CH}_2)_8\text{SH}$
Piperazine*	PIP	
Tetrabutylthiuram disulfide†	TbuT	

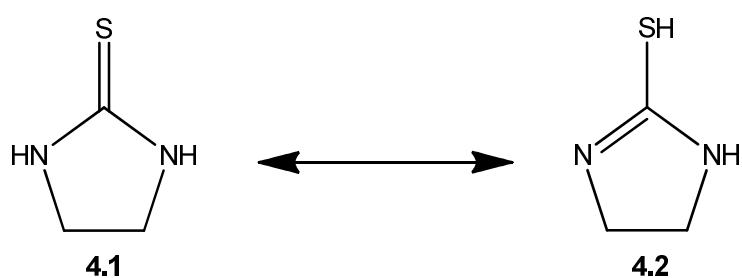
\*Model compound. †Industrial rubber accelerator.

##### 4.1.4.1. Cross-linking PCB with model compounds

Various model compounds were assessed in an attempt to establish which functionality of the ETU molecule could be the site of cross-linking, *i.e.* at the sulfur, carbon or nitrogen atoms. A range of amines and thiols were assessed, namely piperazine (PIP), 1,4-diaminobutane (DAB), dibutylthiourea (DBTU) and 1,8-octanedithiol (ODT) (as shown in Table 4.3). These are a diverse range of molecules, comprising a cyclic diamine (PIP), linear diamine (DAB), linear dithiol (ODT) and a non-cyclic molecule with the same N-C=S functionality as ETU (DBTU). The PCB rubber studies of Berry also incorporated these compounds.<sup>1</sup>

All of the model compounds were reacted with low molecular weight PCB under the same conditions as previously with ZnO and ETU (separately and together). Firstly, it was observed in each of these cases that the  $925\text{ cm}^{-1}$  peak, assigned to the 1,2-isomer,

disappeared within a few minutes. This correlates with data obtained during the ETU reaction (and throughout the studies so far), and validates allylic rearrangement of the chlorine atom in the 1,2-isomer. Interestingly, aside from this change, the FTIR spectra from the ODT reaction showed no other variations over the course of the reaction. No new peaks were formed, nor did any disappear, which infers that no noticeable chemical reaction (cross-linking) took place. Also, the pH of the reaction mixture headspace remained neutral throughout, indicating that no acidic or alkaline vapours were expelled. These findings indicate that cross-linking did not occur in the case of ODT and therefore it is highly probable that the sulfur atom of ETU would not be the primary site for reaction. This supports the claim of Kovacic, where reaction is instead through the nitrogen atoms,<sup>6</sup> and correlates with the work of Berry, whose rheological data proved that (di)thiol model compounds were not able to cross-link the rubber.<sup>1</sup> Although ODT contains a carbon-sulfur single bond, whereas that of ETU is unsaturated, this was still considered an adequate representative molecule given that the major tautomeric form of ETU is the thiol, mercaptoimidazoline (**4.2**), as depicted in Scheme 4.5.



**Scheme 4.5. The tautomeric forms of ethylene thiourea (ETU, 4.1), where mercaptoimidazoline (4.2) is present at 58 %.<sup>17</sup>**

The reaction of piperazine with PCB is an intriguing one; the headspace of this reaction was observed to be alkaline throughout, which contrasts directly to the acidic environment that ETU created. However, it is most likely that any excess amine (from PIP) could have contributed to this alkalinity, masking any acidic products formed. New FTIR peaks at  $1535\text{ cm}^{-1}$  and  $1565\text{ cm}^{-1}$  developed during the PIP reaction (as shown in Figure 4.10, **A**). These are in the same region as the new peak formed in the ETU reaction, but they are more distinct in this case. This could infer that PIP reacts differently with PCB to ETU. Given the alkaline (not acidic) nature of the reaction medium, the possibility of salt formation was again considered and the final reacted mixture was water-washed; these key peaks vanished (Figure 4.10, **B**) and did not appear in the water washings themselves. Thus, instead of new chemical bonds being created, a piperazine hydrochloride salt was believed to form, as proven by the effectual displacement by water. This contrasts with the results of ETU (Section 4.1.1), which was not found to form a salt; the reaction pathway of PIP may be different, where it facilitates cross-linking *via* a salt intermediate.

To test this new HCl salt formation theory, a sample of PIP was heated with a small amount of HCl at the same temperature (160 °C). The resultant FTIR spectrum of the material was compared to that of neat PIP. As Figure 4.11, **B** shows, there is a distinct new peak (1542  $\text{cm}^{-1}$ ) in the acidified version, which is not associated with the raw material. This correlates with one of the new peaks obtained in that region during the cross-linking experiment (see Figure 4.10, **A**). As piperazine does appear to form a salt with HCl, it can be concluded, therefore, that this is most likely also happening in the reaction with PCB.

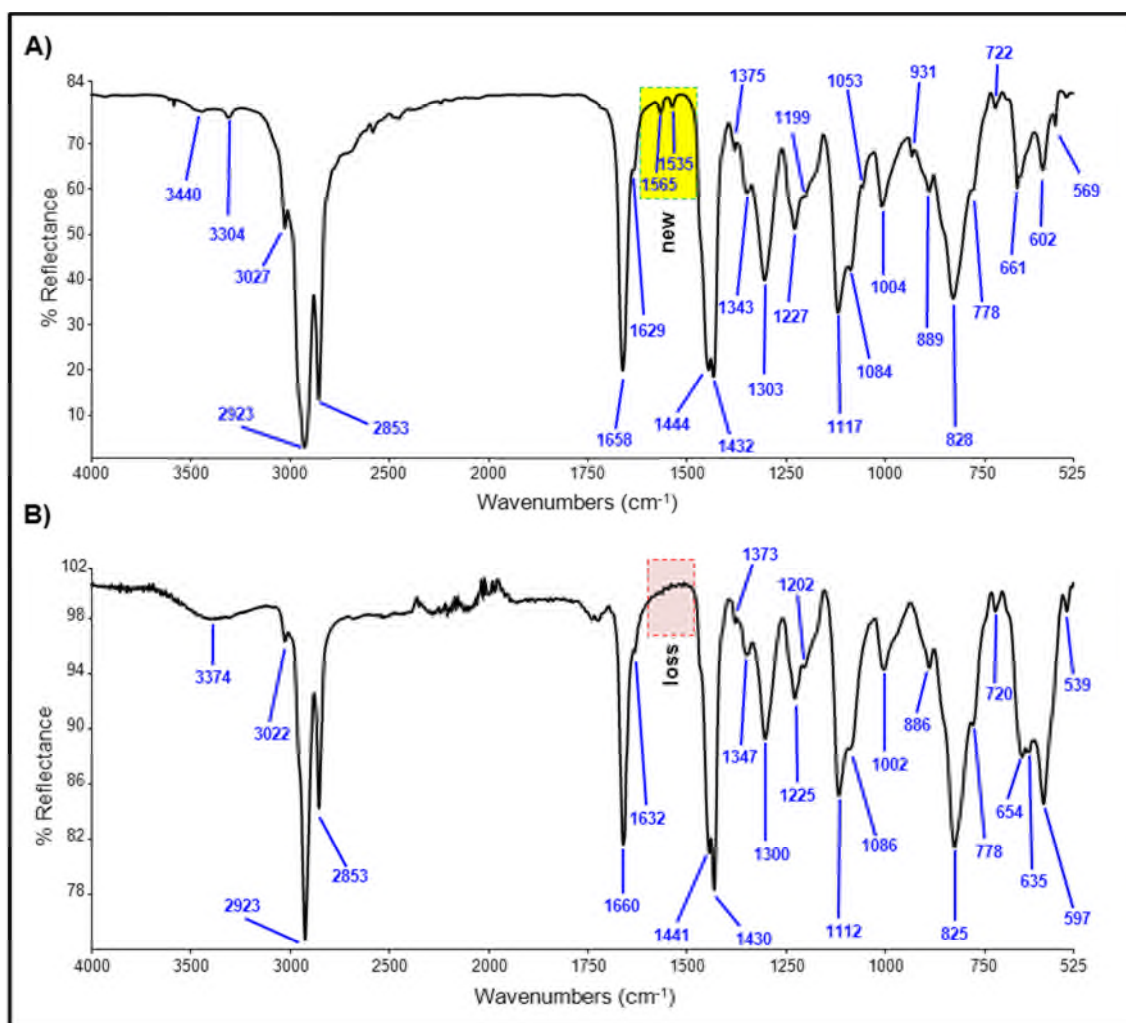


**Figure 4.10. FTIR spectra collected during the PCB/PIP reaction (A) and that of the water washed, dried final material (B), where the peaks at 1565  $\text{cm}^{-1}$  and 1535  $\text{cm}^{-1}$  were eradicated.**

Similarly, the reactions of PCB with diamines, DAB and DBTU, formed new FTIR peaks in the same 1550 – 1530  $\text{cm}^{-1}$  region as those obtained with PIP, so it was deemed that HCl salts were also forming in these reactions. No other significant observations were made. The fact that diamines DAB, DBTU and PIP all form hydrochloride salts during these cross-linking reactions with PCB, whereas ETU does not, may imply contrasting reaction mechanisms, *i.e.* the former involving salt intermediates. Alternatively, this may just reflect the degree of

basicity of the molecules. For instance, PIP ( $pK_a = 9.79$ )<sup>18</sup> is more basic than ETU ( $pK_a = 2.70$ )<sup>19</sup>, and so extraction of the HCl proton is more favourable and thus salt formation is more liable. The presence of the carbon-sulfur double bond of ETU is clearly influential, but it cannot necessarily react directly, as indicated by the inability of ODT to cross-link PCB.

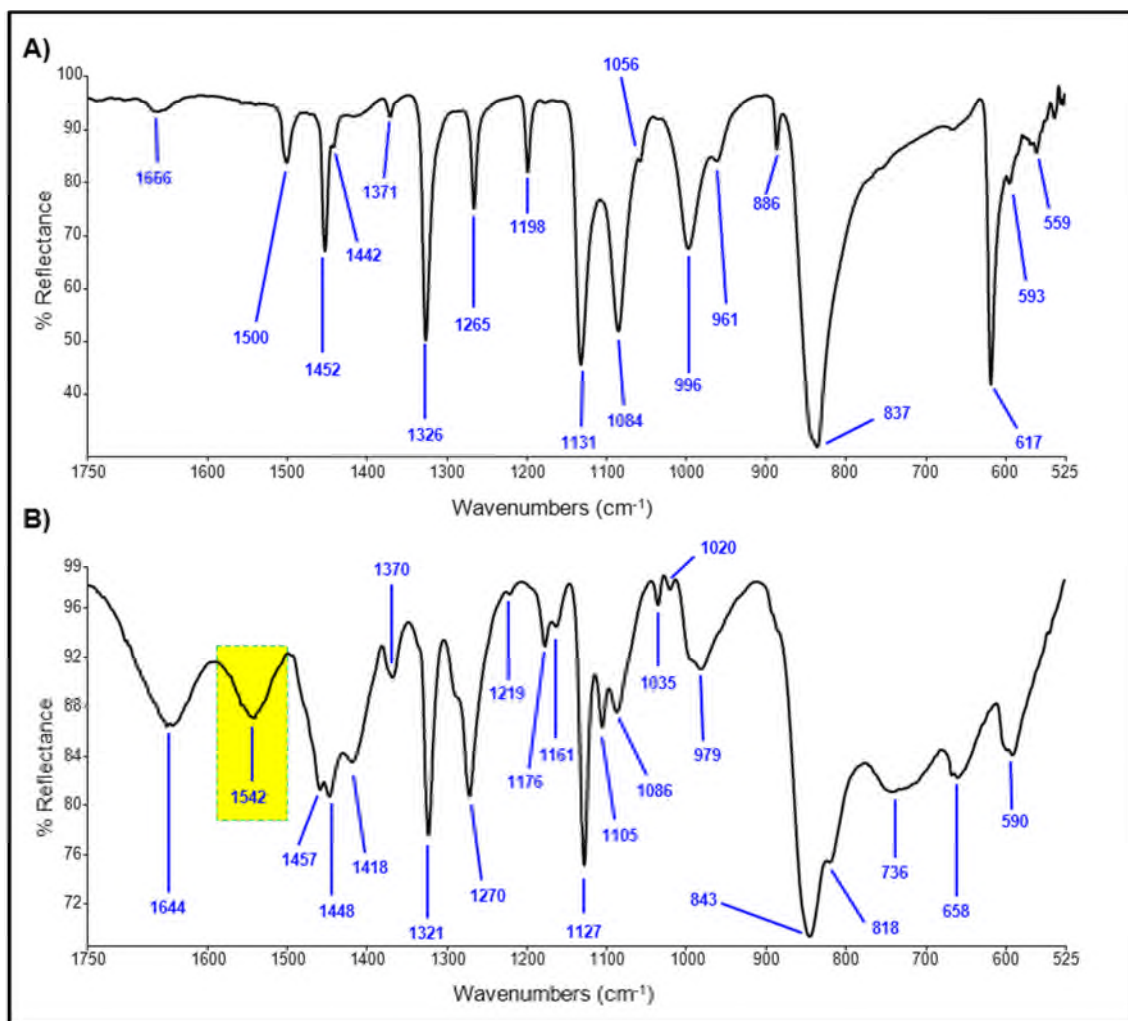


**Figure 4.11. FTIR spectra, displayed in the 1750 – 525  $\text{cm}^{-1}$  region, of PIP (A) and acidified PIP (B); the highlighted 1542  $\text{cm}^{-1}$  peak confirms salt formation.**

#### 4.1.4.2. Cross-linking PCB with model compounds combined with ZnO

Owing to the fact that the typical industrial cross-linking reagents for PCB include ETU and ZnO, PIP, DAB, ODT and DBTU were each reacted with ZnO (with PCB). The 1,2-isomer FTIR peak ( $925 \text{ cm}^{-1}$ ) disappeared for all of the reactions. Allylic rearrangement was generally observed to occur more quickly when ZnO was present. For example, the  $925 \text{ cm}^{-1}$  peak would disappear within five minutes (with ZnO), rather than ten minutes (without ZnO) in all cases. Thus, ZnO was confirmed to accelerate each reaction, which is already an established role within cross-linking in the literature, because it preferentially reacts with the

1,2-PCB isomer.<sup>13</sup> This is reportedly accredited to the zinc dication,  $Zn^{2+}$ , which can complex with sulfur-containing cross-linking additives,<sup>13</sup> as discussed in Section 1.2.1.2.

The new FTIR peaks initially formed during cross-linking by the model compounds alone were also apparent in these reactions. For instance,  $1569\text{ cm}^{-1}$  and  $1528\text{ cm}^{-1}$  peaks formed for PCB/DAB/ZnO and PCB/DBTU/ZnO yielded a peak at  $1552\text{ cm}^{-1}$ . For PCB/PIP/ZnO, a new peak at  $1570\text{ cm}^{-1}$  appeared initially, which is shifted slightly compared to those in the individual PIP reaction (see Figure 4.10), but this broad band may mask other minor peaks. The main difference in all of these cases, however, is that these new peaks all disappear over time when ZnO is present, as illustrated in Figure 4.12 for PCB/DAB/ZnO.

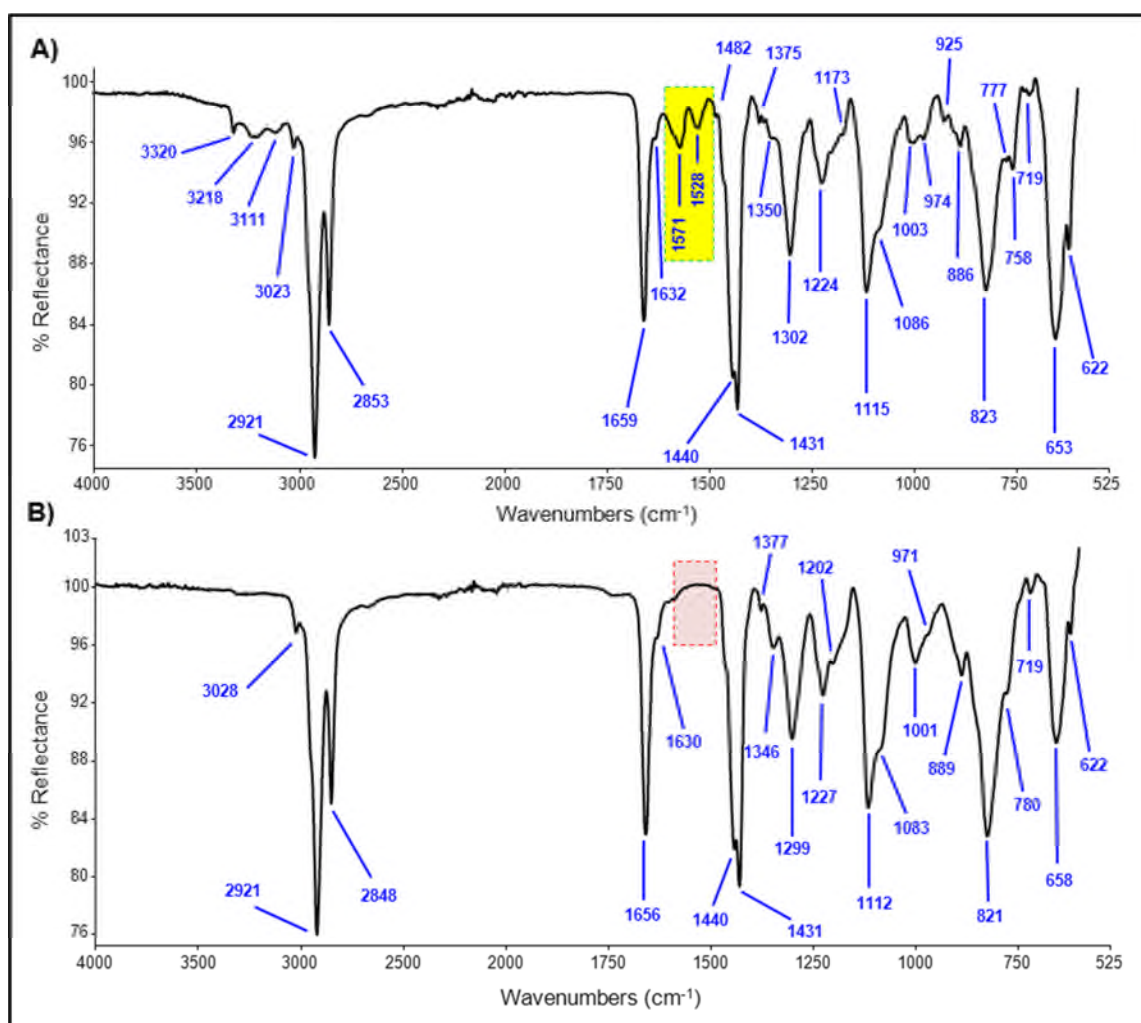


**Figure 4.12.** FTIR spectra collected during the PCB/DAB/ZnO reaction, at five minutes (A) and 60 minutes (B), where distinct changes occur in the  $1600 - 1500\text{ cm}^{-1}$  region.

To note, mono derivatives of these respective amines and thiols were not tested as the rubber studies undertaken by Berry yielded negative results.<sup>1</sup> It was found that they blocked active sites on the polymer chain and could not facilitate cross-linking.<sup>1</sup> The PCB/ODT/ZnO reaction immediately formed a new peak at  $1569\text{ cm}^{-1}$  in the spectrum (Figure 4.13, A) which

diminished over the course of the reaction (Figure 4.13, **B**), in the same way as in the equivalent PIP and DAB reactions. Clearly some kind of chemical reaction was taking place in this PCB/ODT/ZnO system, given the new FTIR peak which does not appear when ODT is adopted by itself (Section 4.1.4.1). If the Kovacic mechanism is to be believed, bis-alkylation would enable the dithiol to slot in between PCB chains,<sup>6</sup> if linkage occurred through the sulfur atoms. This may be the case, but clearly can only occur when ZnO is present. The ZnO, through  $Zn^{2+}$ , could activate the polymer chain, creating active sites at which the thiol groups react. In this case, C–S bonds would form, thus producing peaks in the 700 – 600  $cm^{-1}$  region of the FTIR spectrum, although these are notoriously difficult to elucidate,<sup>12</sup> unless Raman spectroscopy is available. The spectrum shown in Figure 4.13 indicates a large peak in this region, but this is present at the same relative intensity at the start and end of the reaction, so cannot represent new C–S bonds gradually forming. However, given that this peak is so considerable, it may be masking any other minor signals. Hence, it is not possible to ascertain if a new C–S bond is created and, moreover, if Kovacic can be accredited.

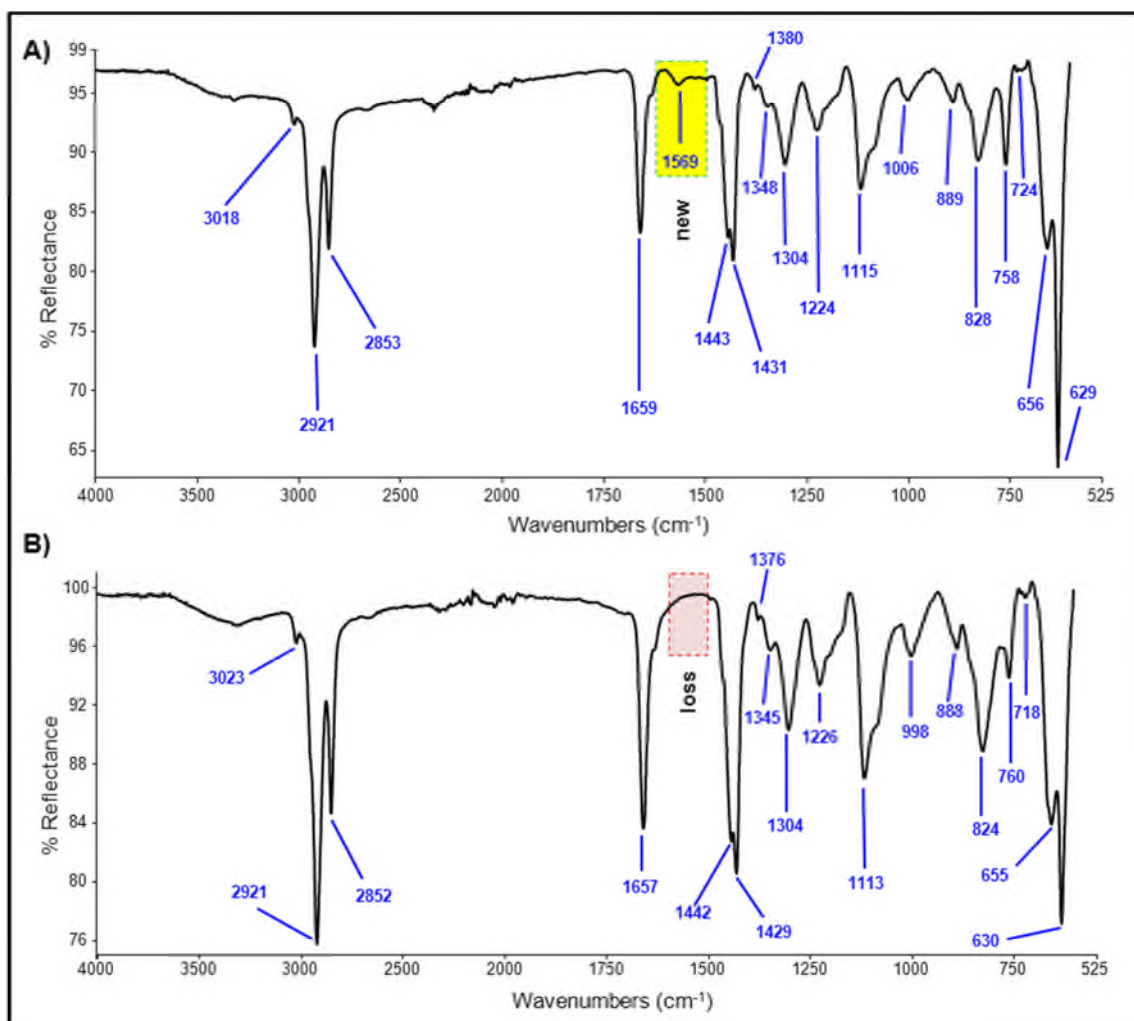


**Figure 4.13.** FTIR spectra collected at the start of the PCB/ODT/ZnO reaction (A), and after 10 minutes (B), where the 1569  $cm^{-1}$  peak disappears.



#### 4.1.4.3. Cross-linking PCB with tetrabutylthiuram disulfide (TbuT)

To again imitate the studies of Berry,<sup>1</sup> a set of reactions were further performed on PCB with a thiuram-based standard rubber accelerator, tetrabutylthiuram disulfide (TbuT). This particular compound is a known cross-linker, both in the raw form and when complexed with the  $Zn^{2+}$  dication.<sup>2, 3</sup> On reacting PCB with TbuT and monitoring the reaction periodically by FTIR, no new peaks in the spectrum were observed to form, which would otherwise indicate new bond formation. However, as Figure 4.14 shows, the signal at  $1486\text{ cm}^{-1}$ , ascribed to the carbon-nitrogen bond of the N-C=S functionality,<sup>12</sup> diminishes completely after 30 minutes. Hence, the structure of TbuT is clearly being altered in some way, although it is difficult to visualise exactly how from these data alone. Also, the peak for the 1,2-isomer, at  $924\text{ cm}^{-1}$ , disappears within this time, as is common throughout all of the reactions undertaken with PCB thus far.

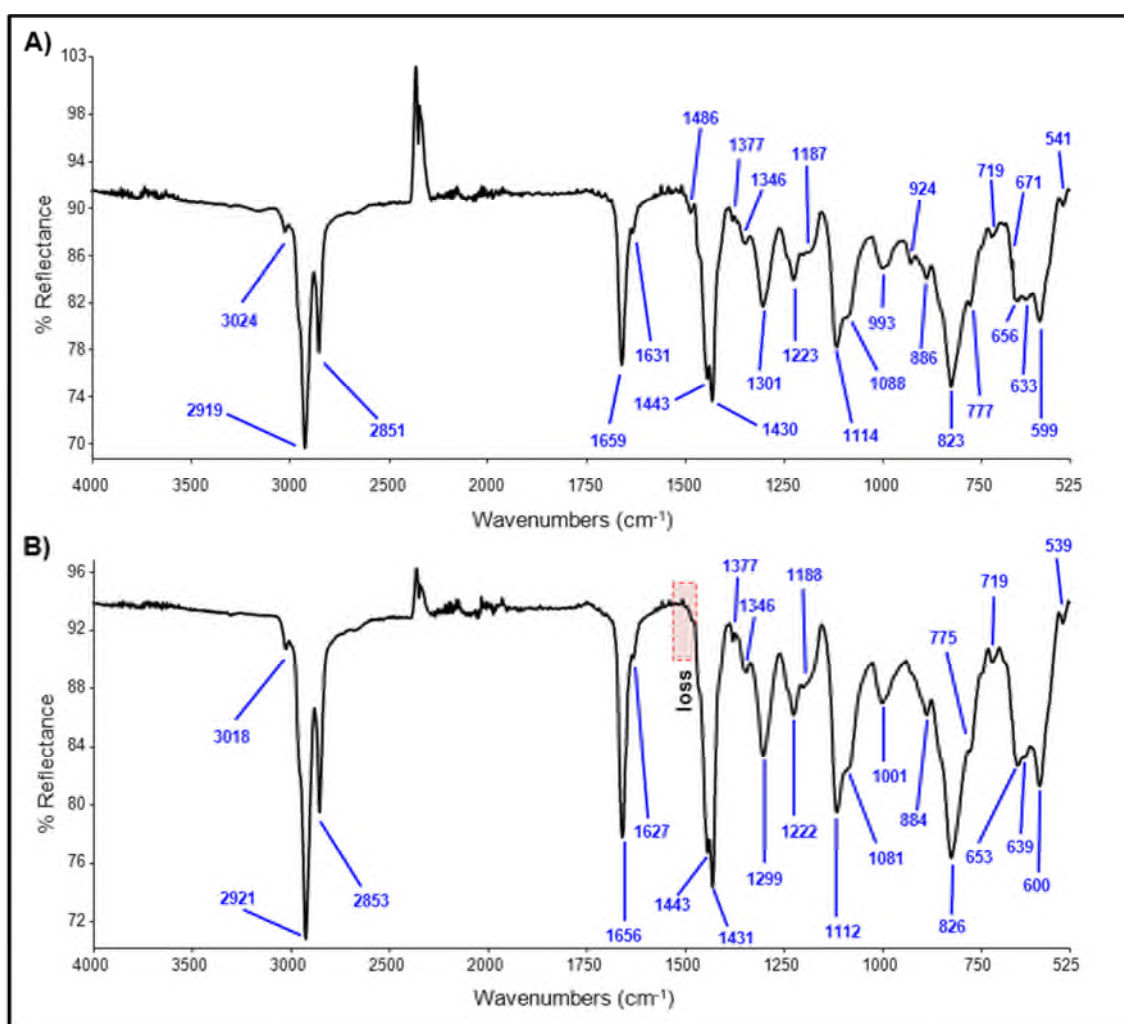


**Figure 4.14. FTIR spectra collected during the PCB/TbuT reaction, where the  $1486\text{ cm}^{-1}$  peak at the start (A) disappears within 30 minutes (B).**

#### 4.1.4.4. Cross-linking PCB with tetrabutylthiuram disulfide (TbuT) combined with ZnO

In the same manner as the investigations with ETU and model compounds, TbuT was also reacted with PCB in conjunction with ZnO. Firstly, the aforementioned key peaks (in Section 4.1.4.3), namely those at  $924\text{ cm}^{-1}$  and  $1486\text{ cm}^{-1}$ , both also diminished in this case, albeit at a faster rate. Thus, whatever the nature of the reaction, it was being accelerated by the presence of the metal oxide, although it is not known how the ZnO was affecting the  $1484\text{ cm}^{-1}$  peak exactly. Acceleration was also found to occur between ETU and the model compounds (separately) with ZnO.

Figure 4.15 shows the FTIR spectrum of the PCB/TbuT/ZnO mixture at the end of the reaction. A new minor peak is visible at  $1560\text{ cm}^{-1}$ , which does not feature in the raw material or during the PCB/TbuT reaction (Section 4.1.4.3). One notion was that this peak could be assigned as a carbon-sulfur double bond, especially given the weakness of the band,<sup>12</sup> but the absence of such in the TbuT raw material spectrum raises doubt (given that the structure comprises two C=S bonds). Hence, despite a precarious assignment, it at least can be established that TbuT is most definitely reacting in such a way that the structure is being altered.

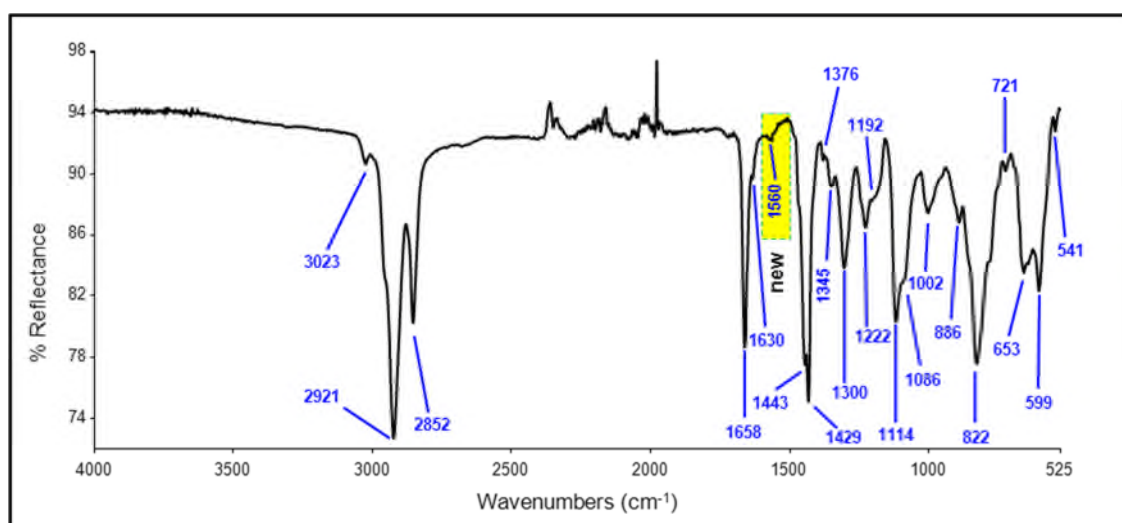


**Figure 4.15. FTIR spectrum collected at the end of the PCB/TbuT/ZnO reaction, highlighting a new peak at  $1560\text{ cm}^{-1}$ .**

Given the absence of the  $1560\text{ cm}^{-1}$  peak in the PCB/TbuT reaction (Section 4.1.4.3), the additional ZnO must be acting as more than an accelerator and is actually facilitating chemical changes. The concept of ZnO activating the PCB chain is thus being further substantiated; by involving ZnO (or  $\text{Zn}^{2+}$ ), it is possible that the sulfur atom could form some part of the cross-link, which would be a somewhat novel theory for PCB. It is interesting that a similar, as yet unassigned peak develops during the PCB/ETU/ZnO reaction, at  $1545\text{ cm}^{-1}$ , which may be a sulfur-based bond. However, this peak also forms with ETU in the absence



of ZnO. This disparity may be due to contrasting reactivities of TbuT and ETU, and the sulfur atoms being potentially more/less available to react. For instance, the structure of TbuT (shown in Table 4.3) contains a disulfide bridge between the thiocarbonyl groups, whereas the sole sulfur of ETU is directly bonded to the five-membered ring. Cleavage of the central TbuT sulfur-sulfur bond may occur (facilitated by  $Zn^{2+}$ ) and the reaction would then proceed through the liberated sulfur atoms ( $S^{\cdot-}$ ). This cannot happen to the sulfur of ETU ( $C=S$ ), so the reaction would not proceed in the same way; the reaction of PCB with ETU clearly does not need ZnO to activate some new type of sulfur-based bond.

#### 4.1.5. Conclusions for the current cross-linking mechanism of poly(2-chloro-1,3-butadiene)

Considering the collective data presented herein for the PCB cross-linking studies, it is now possible to postulate which mechanisms are occurring. Firstly, allylic rearrangement of the 1,2-PCB isomer (depicted in Scheme 4.6) has been demonstrated in every reaction of PCB with ETU, model compounds and TbuT, and each in combination with ZnO. The FTIR spectra have all shown a reduction in the FTIR peak at approximately  $925\text{ cm}^{-1}$ , which represents this isomer. Furthermore, this peak diminishes more rapidly when ZnO is present, indicating that ZnO accelerates rearrangement. From this, it may also be assumed that the metal oxide is capable of accelerating the entire cross-linking reaction (as rearrangement is renowned as the first stage), depending on which step is rate-determining.<sup>7-11</sup> To elucidate the stages after this, ETU and other (sulfur- and nitrogen-containing) compounds were assessed, on their own and in conjunction with ZnO, and these results are summarised in the following sub-sections.



**Scheme 4.6. Allylic rearrangement of the 1,2-PCB isomer.**<sup>7-11</sup>

##### 4.1.5.1. Cross-linking of PCB by ETU compared with other compounds

The reaction involving ETU was found to expel HCl vapours, which directly correlates with the Kovacic mechanism, as bis-alkylation yields HCl.<sup>6</sup> In this case, the HCl was not found to form a salt with ETU. Conversely, the model compound piperazine (PIP), a six-membered

cyclic diamine, was found to form a hydrochloride salt. These contrasting trends infer different reaction pathways for ETU and PIP, where the mechanism of the latter may be *via* a salt intermediate. The carbon-sulfur double bond of ETU is presumably rendering the nitrogen atoms of the molecule less basic, thus preventing them from forming a salt.

It has been deduced that the sulfur of ETU cannot react with the polymer chain directly in the absence of ZnO. The lack of reaction by 1,8-octanedithiol (ODT) with PCB helps to prove this and in turn supports the claim of Kovacic. However, ODT was capable of reacting in the presence of ZnO. It is therefore apparent that ZnO not only accelerates the reaction rate, but also helps to facilitate a reaction through sulfur, that is, the thiol group of ODT (*versus* C=S of ETU, which is admittedly chemically different).

The existing theories concerning cross-linking by ZnO alone have, on the whole, been disproved. An ether linkage was not substantiated, nor was the formation of ZnCl<sub>2</sub>, which would otherwise verify the claims detailed by Aprem,<sup>14</sup> Desai<sup>7</sup> and Vukov,<sup>15</sup> respectively. Likewise, it was not possible to prove diene cross-links (Vukov),<sup>15</sup> as new carbon-carbon double bonds were not found to form during the ZnO reaction.

The studies undertaken with tetrabutylthiuram disulfide (TbuT) showed that the N-C=S functionality was disrupted in some way during cross-linking. An FTIR peak pertaining to this part of the structure of the molecule diminished over time, most readily when ZnO accompanied the mixture. The presence of ZnO also enabled a new type of bond to form, as demonstrated by a new FTIR peak (1560 cm<sup>-1</sup>), which was understood to represent a C-S bond. This evidence therefore suggests that ZnO is altering the accelerator composition and enabling cross-linking through sulfur (which is not possible in the absence of ZnO).

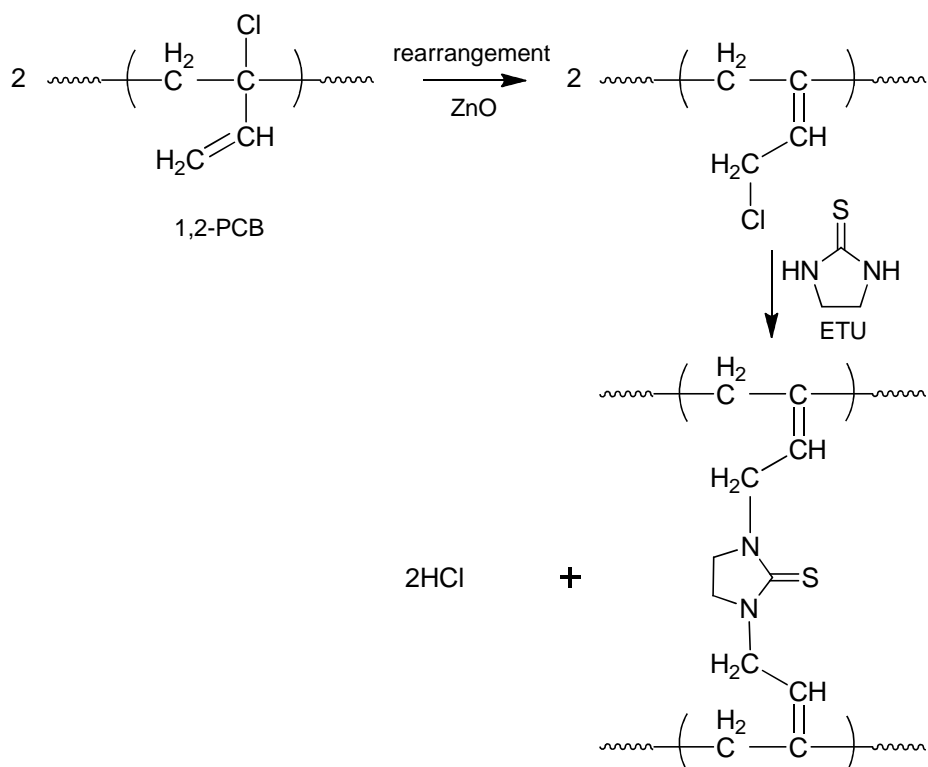
#### 4.1.5.2. The ETU/ZnO mechanism of cross-linking PCB

There is strong evidence that there is not one single ETU/ZnO cross-linking mechanism for PCB. It is most likely that the ETU bis-alkylation mechanism of Kovacic<sup>6</sup> is indeed in effect, as indicated, for instance, by the acidic environment ETU generates. Additionally, the Pariser mechanism (shown previously in Scheme 4.4),<sup>16</sup> which is the only report of the effect of ETU and ZnO in unison, has been partially proven through the formation of ZnCl<sub>2</sub> and EU. Low molecular weight PCB was reacted with ETU and ZnO, whereby a white solid was furnished. This was elucidated as the product of an ETU/ZnCl<sub>2</sub> reaction, thus proving that ZnCl<sub>2</sub> had formed *in situ* (*via* HCl and ZnO). EU was discovered separately by Berry with PCB rubber.<sup>1</sup>

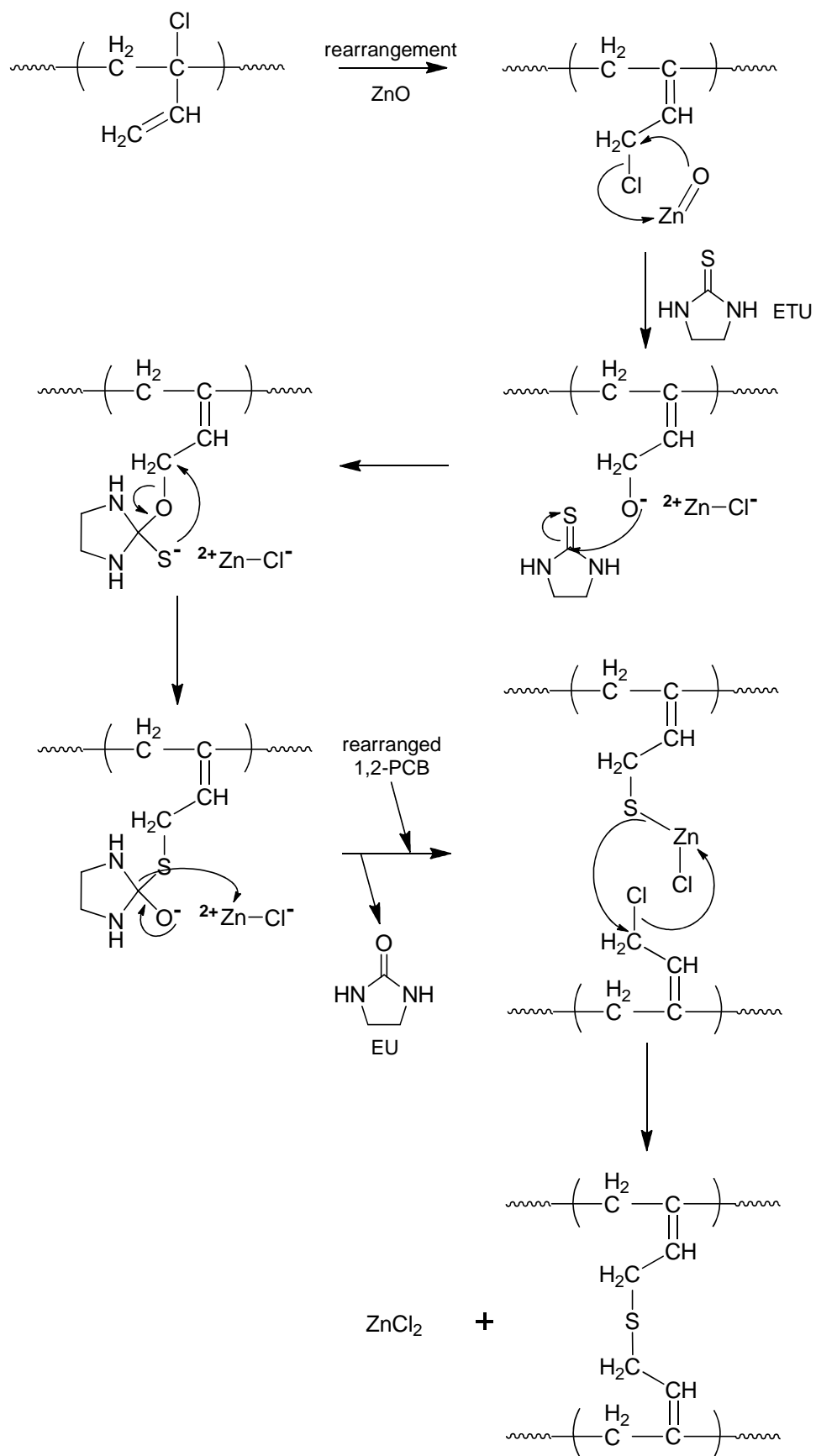
Although the same species are produced as those proposed by Pariser,<sup>16</sup> it is not possible that the reaction mechanism proceeds in exactly the same manner. Crucially, it is unlikely

that sulfur reacts directly with the polymer chain, as ODT could not react on its own and (di)thiols were unable to cross-link the rubber by themselves.<sup>1</sup> However, the addition of ZnO changed the reactivity of the systems, enabling ODT to react and facilitating changes with TbuT, where new carbon-sulfur bonds were deemed to form in the latter. Thus, it is believed that ZnO activates the polymer chain towards reaction with sulfur.

Schemes 4.7 and 4.8 display the two mechanisms which have been proven to occur in the cross-linking of PCB with ETU and ZnO, including that of Kovacic<sup>6</sup> and a novel proposal.<sup>20</sup> All three are proposed as simultaneously occurring mechanisms, hence the complications which have arisen during the elucidation, overall. The first step for each is rearrangement of the 1,2-isomer. In the case of the new mechanism (4.8), the polymer chain becomes activated by ZnO, where the PCB chlorine atom is replaced by oxygen. This makes it possible for the sulfur-containing species to interact and effectively displace oxygen, thus generating EU. As a result, a new carbon-sulfur bond forms as the cross-link and ZnCl<sub>2</sub> is released. The last stage of this mechanism is comparable to Pariser (see Scheme 4.4),<sup>16</sup> but, vitally, ZnO has here been found to react before ETU. The newly-suggested mechanism (4.8) was realised during this project which ran alongside that of Berry,<sup>1</sup> whereby the rubber and oligomeric PCB studies (the former undertaken at RBL; the latter at Aston University) complemented each other. Without the aid of these particular studies described here, especially regarding the observation of by-products, it would not have been possible to make such a discovery.



**Scheme 4.7. The Kovacic mechanism of cross-linking PCB with ETU and ZnO in unison.<sup>6</sup>**



**Scheme 4.8. The new mechanism of cross-linking PCB by ETU and ZnO in unison,<sup>20</sup> which is similar to that of Pariser.<sup>16</sup>**

#### **4.1.6. Towards a safer accelerator system for cross-linking poly(2-chloro-1,3-butadiene)**

This PhD project, and that of Berry,<sup>1</sup> was supported by Robinson Brothers Ltd. (RBL), who were funded by a European project entitled SafeRubber.<sup>21</sup> Involving several companies and academic institutions, the principal objective of SafeRubber was to identify and produce an alternative PCB rubber cross-linker to the hazardous reagent ETU.<sup>22-25</sup> Achieving this was primarily undertaken through RBL and Aston collaborating to elucidate the current cross-linking mechanism, which would then shed light on how an alternative molecule should function. To complete this section on cross-linking, it is appropriate to now summarise how the project has achieved this aim, on the whole.

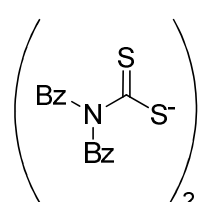
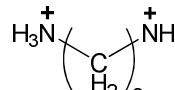
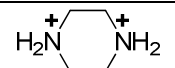
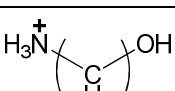
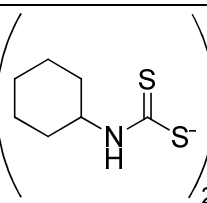
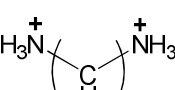
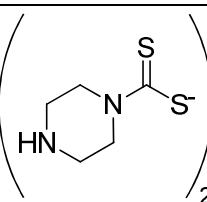
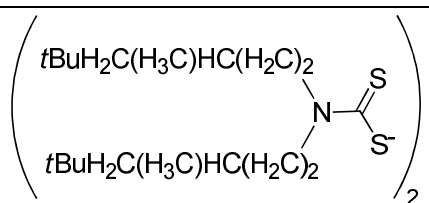
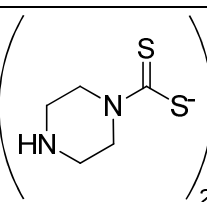
As concluded in the previous section (4.1.5.2), the bis-alkylation mechanism of Kovacic<sup>6</sup> and a modified Pariser mechanism<sup>20</sup> have been deemed to occur in the standard industrial ETU/ZnO cross-linking system for PCB. In the latter, ZnO was deemed crucial in activating the polymer chain towards cross-linking through sulfur and in facilitating prompt rearrangement of the 1,2-isomer.

Interestingly, during these studies it was found that DBTU and model diamine compounds, PIP and DAB, caused cross-linking, as did the thiuram-based accelerator, TbuT. PIP, DAB and DBTU formed hydrochloride salts when ZnO was absent; in the presence of the metal oxide, no such salts existed as the FTIR peaks originally pertaining to such, in the 1600 – 1500 cm<sup>-1</sup> region, disappeared over time. The N–C=S functionality of TbuT was disrupted during the reaction with PCB, with and without ZnO; a carbon-sulfur bond was believed to form when ZnO was present. All of these combined data inspired the prospect that the alternative cross-linker (to ETU) should comprise a diamine, which would function by removing the chlorine atom of the polymer and thus activate the chain. Additionally, a sulfur-based compound would provide the cross-link atom/s.

A collection of potential new accelerators (PNAs) was devised by the SafeRubber consortium (RBL and the various European project partners) and are listed in Table 4.4. These molecules each comprised a cross-linker (sulfur-containing) component and an amine-based activator. The theory behind this concoction was that the diamine would separate from the complex during curing (*i.e.* on heating), activate the polymer chain and then the sulfur-compound would be able to react with the polymer chain in a similar manner to ETU, *via* sulfur (see Scheme 4.8 in Section 4.1.5.2). It was the role of the University of Milano-Bicocca, Italy, to screen these various molecules regarding their potential hazardous properties using select computer-simulated models. Quantitative structure-property (QSPR) and quantitative structure-activity relationship (QSAR) data correlated each structure with specific processes, such as chemical reactivities, and concluded on their suitability to this

particular role (in cross-linking PCB). In this case, all of the listed compounds gave promising results and were deemed not mutagenic or carcinogenic in nature, and were not possible (human) skin sensitizers.

**Table 4.4. List of original potential new accelerators (PNAs) for cross-linking PCB, designated by the SafeRubber consortium.**

Abbreviation	Cross-linker	Activator
PNA-1		
PNA-2		
PNA-3*		
PNA-4		
PNA-5		
PNA-6		
PNA-7		

\* PNA-3 comprises only one cross-linker molecule and one activator molecule.

These compounds were comprehensively tested by Berry at RBL to assess their ability in curing PCB rubber;<sup>1</sup> the most promising tensile and rheological data resulted from PNA-5, which afforded similar results to the ETU system for PCB. Structurally, PNA-5 comprises a 1,3-diaminopropane linear chain and a piperazine-based dithiocarbamate. The N-C=S functionality compares to that in the TbuT structure when it forms a complex with the Zn<sup>2+</sup>

dication, as shown in Figure 4.16. This, along with the piperazine ring, appears to be a good combination of the molecules tested in these studies (PIP, TbuT and alkyl diamines) which were all found to successfully cross-link PCB oligomer (and rubber) without the need for ZnO.

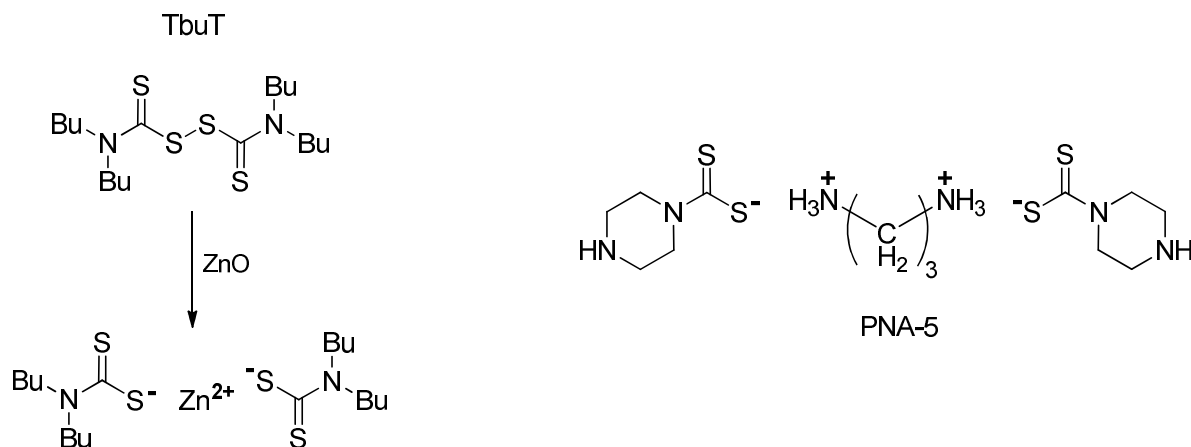


**Figure 4.16. Comparison of Zn<sup>2+</sup>-complexed TbuT and PNA-5 structures, where Bu denotes a linear butyl group.**

The FTIR spectrum of pure PNA-5 is provided in Figure 4.17 (A). NH<sub>3</sub><sup>+</sup> bending is highlighted at 3169 cm<sup>-1</sup> and the N-C=S functionality is confirmed by the peak at 1458 cm<sup>-1</sup>.<sup>12</sup> This new compound was adopted in analogous cross-linking experiments to the studies of Berry,<sup>1</sup> incorporating the low molecular weight PCB. Distinct changes in the FTIR spectrum during the reaction are illustrated in Figure 4.17 (B) where new peaks were afforded at 1537 cm<sup>-1</sup> and 1565 cm<sup>-1</sup>. Variations within this particular region (1600 – 1500 cm<sup>-1</sup>) were observed throughout the studies herein, with ETU, model compounds and TbuT. Notably, the 1458 cm<sup>-1</sup> peak in the raw material was not observed in the curing mixture at any point during the ‘cross-linking’ reaction, so it was not possible to determine what befell the N-C=S bond. It is possible that this peak, being relatively insignificant, has been masked by parent polymer peaks, in this instance.

PNA-5 was also reacted with PCB in combination with ZnO. In the work of Berry,<sup>1</sup> the rubber material afforded similar rheological properties to that cured with ETU/ZnO. Here, in the low molecular weight PCB, the FTIR indicated that new peaks formed at 3209 cm<sup>-1</sup> and 3175 cm<sup>-1</sup>, which are located in the same region as the NH<sub>3</sub><sup>+</sup> bending of the PNA-5 raw material (see Figure 4.17, A), which implies that the nitrogen atoms are potentially being involved in the reaction. Also, the 1574 cm<sup>-1</sup> peak is a new addition and is again situated in that same area where changes have been noticeable throughout these studies. An *in situ* spectrum is displayed in Figure 4.18 with these peaks highlighted.

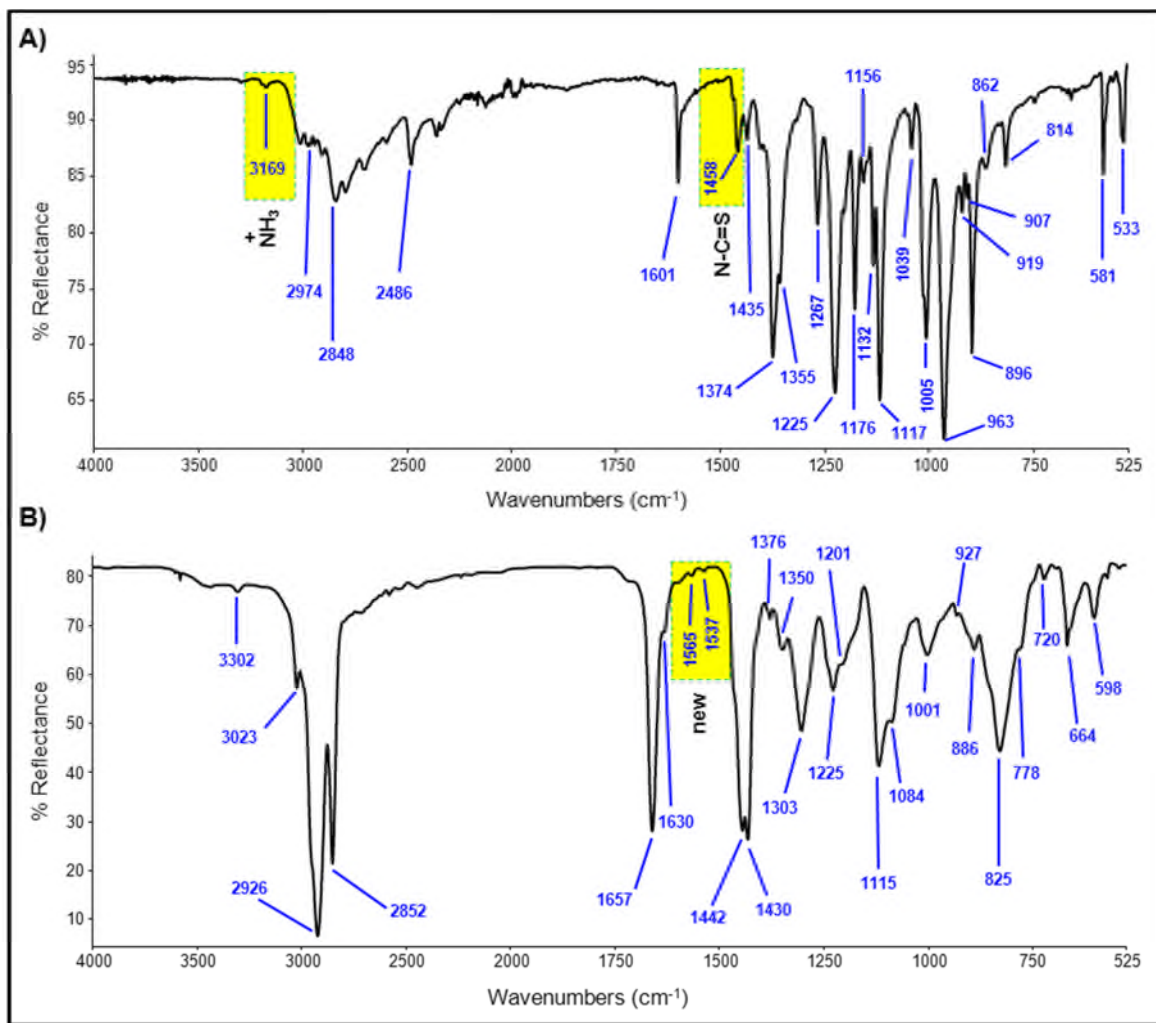


Figure 4.17. FTIR spectrum of PNA-5 (A) and representative spectrum collected during a PCB/PNA-5 cross-linking reaction (B).

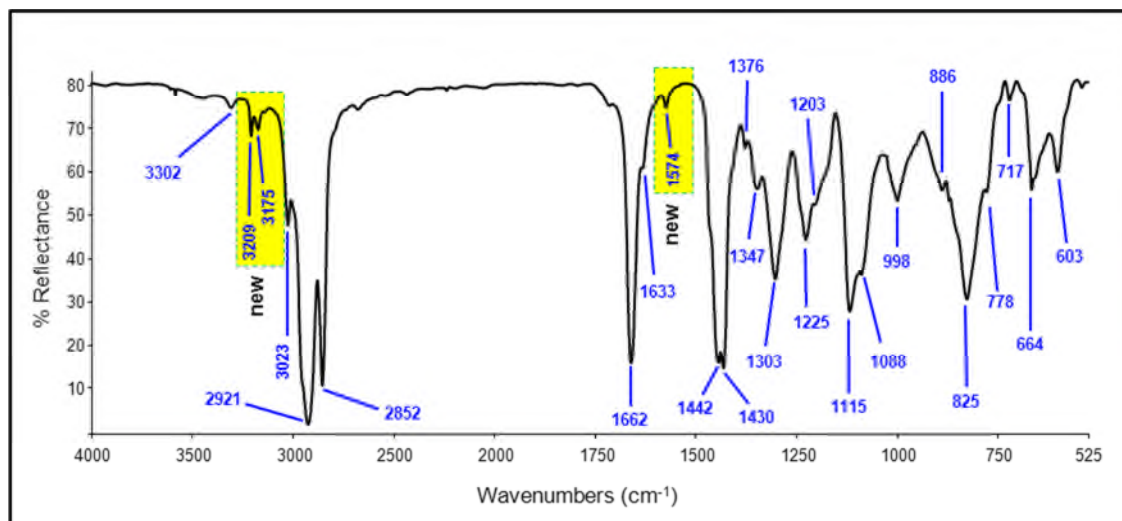
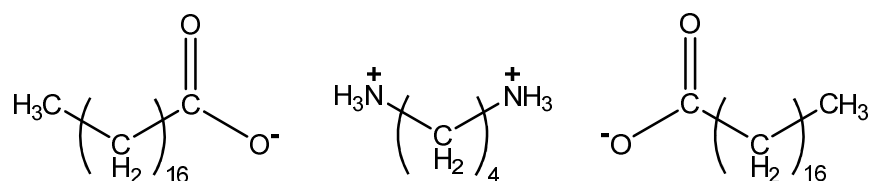


Figure 4.18. Representative FTIR spectrum collected during the PCB/PNA-5/ZnO cross-linking reaction, with newly formed peaks highlighted.



A secondary aim of the SafeRubber<sup>21</sup> project was to reduce the level of ZnO in the industrial PCB cross-linking formulation, as this reagent also poses environmental hazards. Hence, a multi-functional additive (MFA) was adopted in place of ZnO to further optimise the PNA-5 system. As defined in the Introduction Chapter (Section 1.2.1.3), MFAs comprise a fatty acid-diamine complex; this type of compound can activate cross-linking and aid the processing of the rubber material.<sup>26</sup> Crucially, many MFAs are non-toxic and are already well-known to industry. In particular, 1,4-MFA (Figure 4.19) is based on a 1:2 stoichiometric ratio of 1,4-diaminobutane (DAB) and stearic acid (C<sub>18</sub> saturated fatty acid).



**Figure 4.19. Structure of 1,4-MFA.**

1,4-MFA was found to cross-link PCB rubber by Berry, independently and in combination with PNA-5, whereby the latter afforded similar tensile results as the rubber cured by the original ETU/ZnO system.<sup>1</sup> Hence, the initial objective to replace ETU was successfully met and the additional bonus of eradicating ZnO was made possible. Thus, a new, safer accelerator system for PCB has been successfully devised through the combined efforts of Aston University, RBL and the various SafeRubber partners.<sup>21</sup> The PNA-5/1,4-MFA system is undergoing further comprehensive tests with PCB rubber, so that this combination will potentially be adopted worldwide in the future.

## 4.2. References

1. K. I. Berry, The Quest for a Safer Accelerator for Polychloroprene Rubber, PhD Thesis, Aston University, Birmingham, 2013.
2. C. W. Evans, *Practical Rubber Compounding and Processing*, Applied Science Publishers, London, 1981.
3. G. Odian, in *Elastomers and Rubber Elasticity*, ACS Symposium Series, 1982, vol. 193, ch. 1, pp. 1-31.
4. T. Yoshida, *Mater. Trans.*, 2003, **44**, 2489-2493.
5. K. O. Calvert, in *Polymer Latices and their Applications*, ed. K. O. Calvert, Applied Science Publishers, London, 1982, pp. 1-10.
6. P. Kovacic, *Ind. Eng. Chem. Res.*, 1955, **47**, 1090-1094.
7. H. Desai, K. G. Hendrikse and C. D. Woolard, *J. Appl. Polym. Sci.*, 2007, **105**, 865-876.
8. P. E. Mallon, W. J. McGill and D. P. Shillington, *J. Appl. Polym. Sci.*, 1995, **55**, 705-721.
9. Y. Miyata and M. Atsumi, *Rubber Chem. Technol.*, 1989, **62**, 1-12.
10. I. Kuntz, R. L. Zapp and R. J. Pancirov, *Rubber Chem. Technol.*, 1984, **57**, 813-825.
11. Y. Miyata and M. Atsumi, *J. Polym. Sci. Part A: Polym. Chem.*, 1988, **26**, 2561-2572.
12. R. M. Silverstein, G. C. Bassler and T. C. Morrill, *Spectrometric Identification of Organic Compounds*, Wiley, Singapore, 1991.
13. G. Heideman, R. N. Datta, J. W. M. Noordermeer and B. v. Baarle, *J. Appl. Polym. Sci.*, 2005, **95**, 1388-1404.

14. A. S. Aprem, K. Joseph and S. Thomas, *Rubber Chem. Technol.*, 2005, **78**, 458-488.
15. R. Vukov, *Rubber Chem. Technol.*, 1984, **57**, 284-290.
16. R. Pariser, *Kunststoffe*, 1960, **50**, 623-627.
17. L. Krause and M. A. Whitehead, *Mol. Phys.*, 1973, **25**, 99-111.
18. D. D. Perrin, *Aust. J. Chem.*, 1964, **17**, 484-488.
19. L. Zhou, X. Liu, S. Kang, F. Zhang and C. Pan, *Food Chemistry*, 2013, **138**, 1355-1359.
20. K. I. Berry, M. Liu, K. Chakraborty, N. Pullan, A. West, C. Sammon and P. D. Topham, *Rubber Chem. Technol.*, 2014, Accepted.
21. SafeRubber, <http://www.saferubber.eu/>, Accessed 11/03/2014.
22. D. M. Smith, *Occup. Med.*, 1976, **26**, 92-94.
23. D. M. Smith, *Br. J. Ind. Med.*, 1984, **41**, 362-366.
24. R. S. Chhabra, S. Eustis, J. K. Haseman, P. J. Kurtz and B. D. Carlton, *Fundam. Appl. Toxicol.*, 1992, **18**, 405-417.
25. J. Ashby, *Mutagenesis*, 1986, **1**, 3-16.
26. G. Heideman, J. W. M. Noordermeer and R. N. Datta, *Rubber Chem. Technol.*, 2006, **79**, 561-588.

## **CHAPTER 5**

# **POLY(2-CHLORO-1,3-BUTADIENE) LATEX DEVELOPMENT**

## 5. Poly(2-chloro-1,3-butadiene) latex development

The second industrial component of this PhD project concerned the development of poly(2-chloro-1,3-butadiene) (PCB) latex films. It was the overall aim of Robinson Brothers Ltd. (RBL) to eventually replace the standard thiourea/guanidine-based accelerator system in the manufacture of PCB latex rubber with safer, non-toxic reagents. This is a similar concept to that for the cross-linking studies performed on PCB oligomers and rubber (detailed previously in Chapter 4), where ethylene thiourea (ETU) was the primary concern.

### 5.1. Introduction

PCB latex is a diverse material, being adopted in coatings, adhesives and automotive parts, for example,<sup>1, 2</sup> (as previously reviewed in Section 1.3.3.2). One of the most important applications, however, is in the manufacture of latex gloves. Natural rubber (NR) has been prominent in this field, historically, but the focus has shifted to other materials owing to the fact that residual proteins within NR can leach out of the material and cause skin allergies amongst users.<sup>3</sup> PCB latex rubber has been deemed a suitable alternative material, as harmful proteins are absent in the first place and so the material is safer overall; PCB gloves are less likely to afford skin dermatitis or cause skin sensitivity.<sup>3</sup>

The safety of latex gloves is of paramount importance as such items are widely used in the public services and scientific professions, ultimately acting as a protective barrier to the skin.<sup>2</sup> Certain chemicals used in the production of latex rubber are the primary offenders in terms of causing skin problems amongst glove wearers; it is not the latex rubber itself which causes direct harm to the skin.<sup>4</sup> A review by Rose *et al.* highlights accelerator compounds as generally the most harmful type of additives within a latex formulation,<sup>5</sup> whereby the (human) patch test studies of Geier *et al.* have revealed that thiuram derivatives most regularly cause problems.<sup>6</sup>

Table 5.1 illustrates the main reagents employed throughout these latex studies, which were incorporated as aqueous dispersions. As detailed in Section 1.3.3.1, accelerators are responsible for linking polymer chains and creating the cross-linked network. Fillers are responsible for providing abrasive resistance in the final material and surfactants are wholly involved in stabilising the system. Antioxidants are present to aid in preventing degradation of the final rubber material, such as by UV, heat, *etc.*<sup>2</sup> To note, this part of the project utilised commercially available, pre-prepared PCB in the form of an emulsion; it was not necessary to synthesise polymer for these studies.

**Table 5.1. Individual components in the PCB latex formulations.**

Reagent	Dispersion level (% w/w)	Function
ZnO	50	accelerator
Aquanox 2246	45	antioxidant
Kaolin clay	40	filler, processing aid
Darvan <sup>®</sup> SMO	30	surfactants
Darvan <sup>®</sup> WAQ	25	

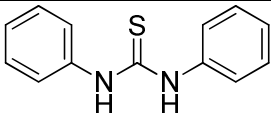
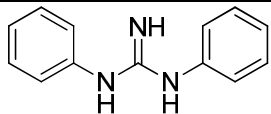
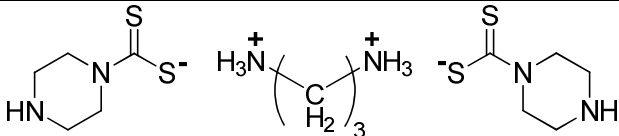
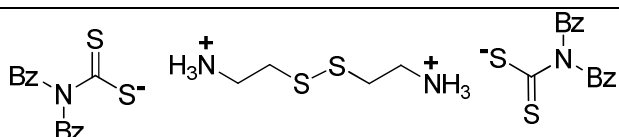
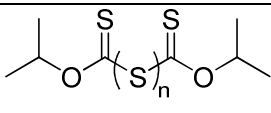
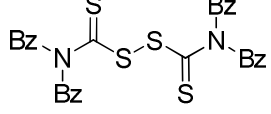
For these experiments, the reagents listed in Table 5.1 were added to the PCB emulsion, along with the appropriate accelerator compounds, and the dipping procedure described in Chapter 2 (Section 2.2.6) was employed to produce the PCB latex films. During this process a mould, or 'former', was submerged into the latex formulation and a coating materialised on the surface. Subsequent leaching, drying and thermal cross-linking (curing) stages were then undertaken to generate the final films. The focus of these studies was the accelerator system within the PCB formulation, whereby several variations were employed. Table 5.2 lists the accelerators which were trialled, alongside their adopted abbreviations and chemical structures.

This eclectic mix of accelerators includes DPG and DPTU, which together form the standard guanidine/thiourea system typically employed in the industrial production of PCB latex gloves;<sup>7</sup> crucially, these molecules have been identified as skin allergens by Geier *et al.*<sup>6</sup> Also included in the research was the molecule which transpired from the SafeRubber consortium (PNA-5, see Chapter 4),<sup>8</sup> a thiuram disulfide (TBzTD), a xanthogen polysulfide (DIXP) and a completely novel compound (PNA-8) which was developed at RBL. Various combinations of these compounds were assessed in the PCB formulations, whereby ZnO was also present as an activator (of polymer chains towards cross-linking). Each accelerator system is rationalised in the corresponding results section and each batch (or experiment) is denoted by an individual character, namely 'A', 'B', 'C', *etc.*

On the whole, there is scarce literature concerning studies specifically on PCB latex materials. A recent report by Rattanasom *et al.* describes ultrasonication as an effective method to disperse additives optimally within the formulation, but it does not focus on the nature of the accelerators.<sup>9</sup> It is suspected that the lack of relevant literature is associated with the sensitivity of such information within industry and companies not wishing to disclose their technology to competitors. The research described in this chapter was an entirely new

venture for the industry sponsor of the project, RBL, and was anticipated to initiate a new area of interest for their line of rubber additive products.

**Table 5.2. Accelerators adopted in the PCB latex formulations.**

Accelerator name	Abbreviation	Structure
Diphenyl thiourea	DPTU	
Diphenyl guanidine	DPG	
Piperazine-1-carbodithioic acid 1,3-diaminopropane complex	PNA-5	
2,2'-Dithio di(ethylammonium)-bis(dibenzylthiocarbamate)	PNA-8	
Diisopropyl xanthogen polysulfide	DIXP	
Tetrabenzylthiuram disulfide	TBzTD	

## 5.2. PCB latex films from the standard DPTU/DPG accelerator system

PCB latex films were synthesised in the first instance using the 'industry-standard' accelerator system. It was intended that the physical (tensile) test results from these films would yield benchmark data which would be subsequently targeted. A binary organic accelerator system comprising a thiourea derivative, DPTU, and a guanidine, DPG, was adopted, with the addition of ZnO. These are the three accelerator components which are used for preparing industrial PCB latex gloves.<sup>7</sup> Table 5.3 lists the reagents in the formulation in their entirety. Given that this work incorporated reagents as aqueous dispersions or emulsions, several precise calculations were necessary to ensure that the final formulation contained the appropriate minimum quantity of solids (total solids content, TSC). Throughout this work, 40 % TSC was adopted, which is within the range recommended by Feast for PCB latex (35 – 60 %).<sup>10</sup> An exemplar table is provided in Section 2.2.5, which illustrates the exact adjustments made for the 'optimum' formulation developed during this project. For

simplicity, the universal units of parts per hundred rubber (phr) are given for each experiment throughout this chapter.

**Table 5.3. Formulation details for the compounding of PCB/DPTU/DPG latex films (A).**

Reagent		PCB latex	Darvan <sup>®</sup> WAQ	ZnO	Aquanox 2246	Kaolin clay	Darvan <sup>®</sup> SMO	DPTU	DPG
Dispersion level (% w/w)		50	25	50	45	40	30	50	40
Quantity (phr)	A	100	0.3	5	1.5	10	1	2	2

The hazardous nature of certain sulfur- and nitrogen-containing accelerators has already been discussed in the Introduction Chapter, regarding the curing of pure rubber and of latexes (Sections 1.2.2.1 and 1.3.3.2, respectively). In general, thiurams have been identified as the most harmful allergens associated with rubber latex gloves.<sup>6</sup> Thiourea compounds have also been highlighted as potential carcinogens, with particular emphasis on ethylene thiourea (ETU),<sup>11-13</sup> which includes the possible risk to the unborn fetuses of pregnant women handling this chemical.<sup>14</sup> Additional reference has been made, in the review by Ashby,<sup>15</sup> to the toxicity of other types of thiourea, such as diethyl thiourea and *N,N*-dicyclohexyl thiourea. Given that DPTU is a thiourea derivative, and that both DPTU and DPG feature in the latex allergen list of Geier,<sup>6</sup> there are concerns over PCB latexes formulated using this standard accelerator system. This is the drive for these experiments, as these compounds should be replaced. It was precautionary that this particular PCB latex (involving DPTU/DPG, denoted as films **A** throughout) was compounded by a male co-worker (M. Liu, RBL), given the potential damaging effect that thioureas can have on unborn fetuses in the womb;<sup>14</sup> the preparation (cutting) of the test dumbbells and subsequent analysis was undertaken by the author. Table 5.4 illustrates the tensile results obtained for these standard PCB films, as obtained through the use of a tensometer (details of which are provided in the Experimental Chapter, Section 2.3.4).

The physical testing of the PCB rubber latex films required each sample to be cut into the shapes of dumbbells, of a predefined size (as depicted in Figure 5.1), which were then individually affixed in the tensometer and stretched until they ruptured. Ultimate tensile strength (UTS) data reflect how resistant the material is to abrasion and tear;<sup>16</sup> a high UTS result is suggestive of a rigid, strong rubber with superior resilience. Elongation at break describes the overall extension of the dumbbell which was achieved before it ruptured, which

is typically expressed as a percentage of the original length.<sup>7</sup> Modulus in this instance refers to the Young's modulus ( $E$ ) and is a measure of the stiffness of a material,<sup>17</sup> whereby the stress required to enforce a certain strain upon it is determined; this is normally the force required to extend the sample to a certain percentage of the initial dimension (e.g. 300 %).<sup>7</sup> Overall, modulus portrays how soft a material is, whereby less force is required to stretch softer materials (thus yielding lower MPa values). The latex dumbbells were analysed to obtain these results, whereby mean values for the UTS, elongation at break and 300 % modulus, respectively, were calculated from ten data points. It was imperative to analyse a standard PCB latex film, which would act as a control and generate data for comparison against other films. Hereafter, the tensile test results of the new films are compared against those in Table 5.4, to give an indication of their relative 'quality'. It was noted that these PCB/DPTU/DPG films were homogeneous, cream-coloured and smooth to the touch.

**Table 5.4. Tensile results for the PCB/DPTU/DPG latex films (A).\***

Accelerator system		UTS (MPa)	Elongation at break (%)	300 % Modulus (MPa)
DPTU/DPG	A	23.7 ±1.8	861 ±22	2.40 ±0.28

\*Mean results were obtained from ten data points in each case. The error given is one standard deviation.



**Figure 5.1. Image of the final PCB/DPTU/DPG latex film (A), which has been cut into dumbbells prior to tensile testing.**

### 5.3. Alternative accelerator system for PCB latex comprising PNA-5

The primary accelerator chosen to test in the PCB formulations, in place of DPTU and DPG, was the piperazine-1-carbodithioic acid 1,3-diaminopropane complex (PNA-5), identified by



the SafeRubber consortium as a 'safer' alternative accelerator for PCB rubber (*versus* ETU).<sup>8, 18</sup> As explained previously in Chapter 4 (Section 4.1.6), computer-simulated studies conducted by a project partner indicated that this compound was not carcinogenic and subsequent experiments with low molecular weight PCB (oligomers) and the rubber proved it to be an efficient cross-linker. Thus, PNA-5 was also examined in the PCB latex, on its own and in combination with other accelerators.

All of the PNA molecules which materialised from the SafeRubber project (as listed previously in Table 4.4 of Section 4.1.6), comprised two distinct sections to their structures. The sulfur-containing portion acted as the cross-linker, whereas the (di)amine would activate the polymer chain towards cross-linking. In order to facilitate this, the overall complexed structure of the PNA would be disrupted when thermal cross-linking was initiated (*i.e.* on heating the mixture), so that the amine molecule would become separated and subsequently activate the polymer chain, in much the same way as ZnO was found to operate in the newly-proposed mechanism of Berry *et al.* (illustrated previously in Scheme 4.8).<sup>19</sup> In turn, this would enable cross-linking through the sulfur atoms (hence, how ETU was deemed to react).

PNA-5 was synthesised by RBL and a suitable aqueous dispersion had to be formulated before the latex compounding could commence (this is briefly discussed in the subsequent section, 5.3.1). To the best of our knowledge, this was a novel accelerator both for the rubber in its pure form and within the latex sector.

### **5.3.1. Development and stability of the PNA-5 dispersion reagent**

PNA-5 was a novel organic molecule which had been devised by the SafeRubber consortium<sup>8</sup> and subsequently synthesised at RBL. Throughout the cross-linking studies previously described in Chapter 4, this compound was weighed into oligomer mixtures as a neat solid, and was incorporated (milled) into PCB rubber directly during the investigations of Berry.<sup>18</sup> For the latex experiments, however, an aqueous form of this accelerator was required. Hence, a novel dispersion was formulated with PNA-5 and the stability of such was assessed.

This particular dispersion comprised appropriate quantities of PNA-5, DISPERBYK<sup>®</sup> 191 (a surfactant) and water to afford an accelerator concentration of 35 % w/w in solution. The composition (details can be found in Section 2.2.5.1) was based on a dispersion already in use at RBL for another accelerator, PNA-8, which was also employed in these studies and is discussed in Section 5.4. All of the reagents were charged to a ceramic vessel, which contained numerous zirconia balls; mixing was achieved through the use of a vibromill machine. The vessel was affixed into this industrial 'shaker' and subjected to high frequency

vibrations. This ensured that the solid was thoroughly ground down into small particulates, through agitation with the zirconia balls within. Such a procedure is adopted to ultimately ensure an efficient dispersion of solids into an aqueous medium. The vibromill machine does not subject the mixture to a high rate of shear, as it is simply vibrating at very high frequency; prolonged regular shaking (*i.e.* by hand or a fast mechanical stirrer) could jeopardise the stability of the dispersion<sup>20</sup> and would not grind the solid down sufficiently.

On initially compounding the PNA-5 dispersion, the solution was a light green/yellow colour (from the accelerator), homogeneous, with low viscosity. The mixture was divided into two portions (approximately 140 g each) and stored separately, in sealed glass jars, at 40 °C and room temperature (samples 1 and 2, respectively). To determine any change in stability, viscosity measurements were taken periodically over 2 months using a digital Brookfield viscometer; for the 40 °C sample (1), the temperature of the solution was allowed to equilibrate to room temperature before taking measurements. Overall, measuring the viscosities was deemed an appropriate means to assess the stability of the PNA-5 dispersions, whereby any significant fluctuations would infer instability, as this may signify coagulation.<sup>7</sup> Figure 5.2 displays the mean viscosity results obtained over time for the two samples.

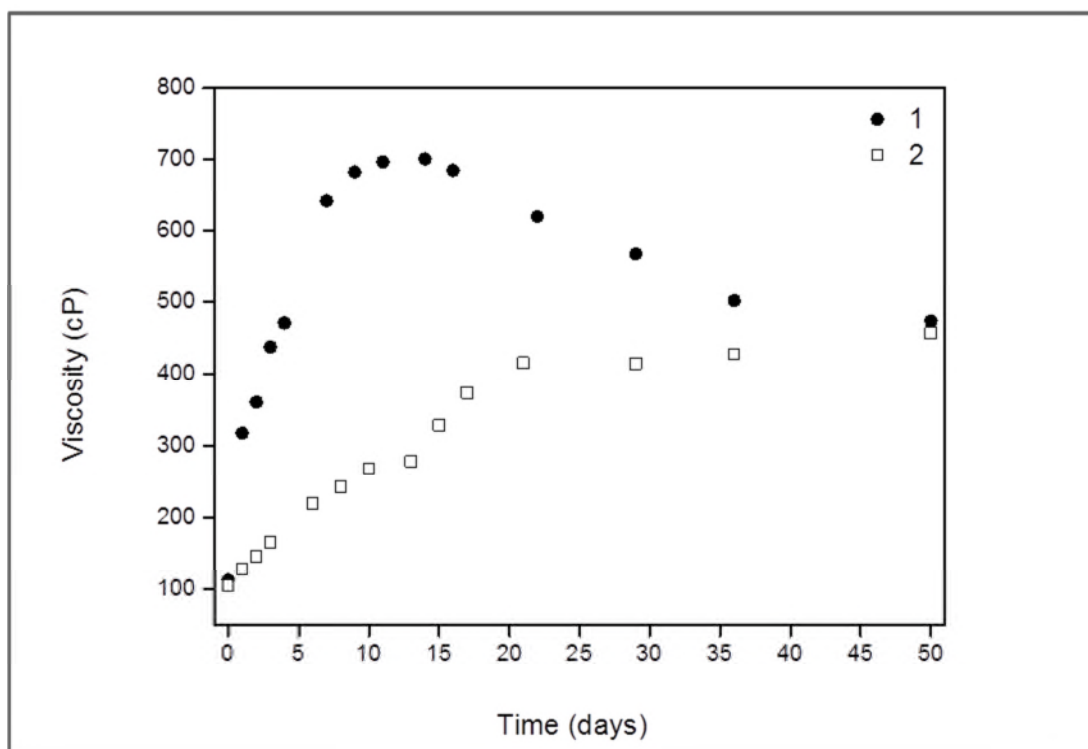


**Figure 5.2. The change in viscosity over time for the PNA-5 dispersion, stored at 40 °C (1, denoted by ●) and at room temperature (2, denoted by □).**

Initially, the viscosities of both samples increased over time, where a more gradual rise occurred in the room temperature sample over 22 days, reaching approximately 400 cP.

Hereafter, a plateau was seen to occur for the remainder of the test, with a slight increase at 50 days to ~460 cP. Conversely, the increase in viscosity for sample **1**, which was stored at the elevated temperature, was more severe and more than quadrupled within just five hours. This sharp rise continued until ~700 cP was achieved at 12 days, which is over 1.5 times the maximum viscosity value obtained for sample **2**. Interestingly, the viscosity for sample **1** then decreased gradually; after 50 days, the final viscosity is comparable to that of the ambient sample (~460 cP).

The change in viscosity of the heated PNA-5 dispersion (sample **1**) was considered to imply degradation, especially given the sizeable initial increase.<sup>7</sup> Although the viscosity also increased in the sample stored under ambient conditions, this rise was not as severe and was more uniform. This, in contrast, reflects relatively superior stability, especially as the viscosity did not reach such a high value (*versus* ~700 cP for sample **1**). Observations of the samples support the viscosity results, whereby the odour of sample **1** was very distinct and sulfurous after one month; the ambient sample (**2**) had only a slight odour by the same point of the trial. The heated sample was unbearably ammoniacal in the headspace by the end of the test, but sample **2** evolved only a slight sulfurous smell. It was possible that PNA-5 was in some way breaking down over time and in turn releasing sulfurous gases (*e.g.* H<sub>2</sub>S) or amines; this process was enhanced at 40 °C (sample **1**). The dispersions themselves did tend to settle out over time, forming two separate phases; after one week, both samples (qualitatively) showed the same degrees of separation, where oily layers appeared on top of the solutions. These layers were apparent throughout the duration of the experiment and became re-dispersed upon brief, gentle agitation, before each viscosity measurement.

Considering these observations, and given the changes in viscosity which reflect diminished stability, a fresh PNA-5 dispersion was compounded each week for use in formulating the appropriate PCB latexes and stored at ambient temperature. This was simply a precaution as sample **2** was not deemed totally unstable; further work at RBL aims to develop the dispersion further to optimise the stability. A higher concentration of the surfactant, for instance, may be necessary to improve the stability of the dispersion and prevent phase separation. After all, the primary role of the surfactant is to provide colloidal stability as a means of preventing coagulation (as detailed in Section 1.3.1.2),<sup>2</sup> which would otherwise alter the viscosity of the medium.

### **5.3.2. PCB latex formulated with PNA-5 alone**

Table 5.5 provides the details of the PCB latex formulation whereby PNA-5 was adopted as the principal accelerator. To note, ZnO was employed throughout these studies to

complement the organic accelerators and act as an activator; an ancillary objective of this work was to find a means to also reduce or eliminate ZnO in the systems, which meant that lesser quantities of this were also compounded into the PCB formulations, where appropriate.

**Table 5.5. Formulation details for the compounding of PCB/PNA-5 latex films (B).**

Reagent		PCB latex	Darvan <sup>®</sup> WAQ	ZnO	Aquanox 2246	Kaolin clay	Darvan <sup>®</sup> SMO	PNA-5
Dispersion level (% w/w)		50	25	50	45	40	30	35
Quantity (phr)	<b>B</b>	100	0.3	5	1.5	10	1	2.5

The films produced from this formulation with PNA-5 (denoted as **B**) were a lighter (cream) colour than the standard DPTU/DPG films and were considerably thinner, so that they were partially translucent. This could be attributed to the fact that only one type of organic accelerator was present in the formulation (PNA-5), whereas films **A** were furnished with DPTU and DPG. Also, the PNA-5 dispersion was less concentrated (35 % w/w), where the DPTU and DPG dispersions were 50 % w/w and 40 % w/w, respectively. Hence, there was an overall lower concentration of accelerator present in the formulation for **B**, which may help rationalise why this film appears thinner. If this was the case, it could be postulated that a higher number of cross-links were furnished during the curing of **A** (due to the elevated concentration of accelerator present, overall), which would in turn produce a greater cross-link density; a superior UTS result (*i.e.* 23.7 MPa *versus* 19.0 MPa for **B**) correlates with this hypothesis, along with a lower elongation at break (861 % *versus* 978 % for **B**), as the material was stronger and more rigid (than **B**). Once the number of cross-links reaches a certain (elevated) level, the elasticity becomes compromised, hence the lower elongation at break for **A**. A representative film for **B** is depicted in Figure 5.3 and the tensile test results are shown in Table 5.6.

Overall, the UTS and modulus results for **B** were all lower than those of **A** and the elongation at break value was considerably higher. The thinness of these new films correlated with a low UTS (19.0 ±2.2 MPa), as it was a soft material and thus may be particularly susceptible to abrasive tearing. Also, the high elongation at break was indicative of such a thin latex which could be greatly extended.

**Table 5.6. Tensile results for the PCB/PNA-5 latex films (B).\***

Accelerator system		UTS (MPa)	Elongation at break (%)	300 % Modulus (MPa)
PNA-5	<b>B</b>	19.0 ±2.2	978 ±17	1.69 ±0.23

\*Mean results were obtained from ten data points in each case. The error given is one standard deviation.

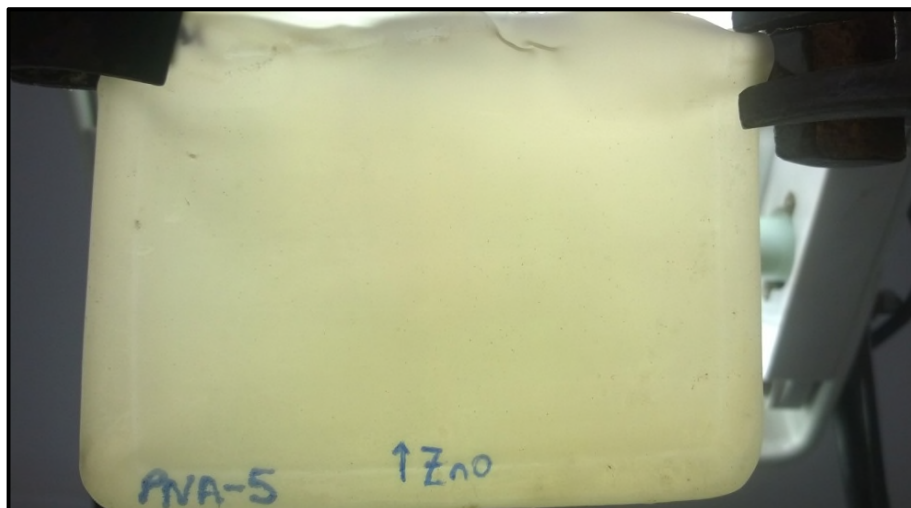


**Figure 5.3. Image of the final PCB/PNA-5 latex film (B).**

### **5.3.3. PCB latex formulated with PNA-5 and 1,4-MFA**

As defined in Section 1.2.1.3, multi-functional additives (MFAs) can: i) activate cross-linking, ii) are efficient (rubber) processing aids and iii) can be used in place of ZnO.<sup>21</sup> Structurally, they generally comprise fatty acid and diamine sections, as shown in Figure 5.4 for 1,4-MFA, which comprises a 1:2 stoichiometric ratio of 1,4-diaminobutane (DAB) and stearic acid; the diamine portion is responsible for activating the polymer chain (in readiness for cross-linking) in the same way that ZnO and the PNAs operate. As highlighted in Section 4.1.6, 1,4-MFA was found capable of cross-linking PCB rubber, independently, and in combination with PNA-5.<sup>18</sup> Thus, it was also relevant to adopt a system incorporating a combination of PNA-5 and 1,4-MFA in the PCB latex studies, as discussed herein.

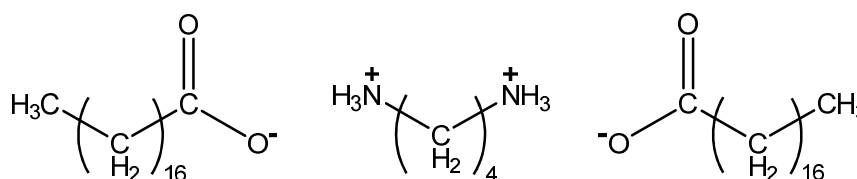


**Figure 5.4. Structure of 1,4-MFA.**

Table 5.7 provides the details of the formulations adopted with PNA-5 and 1,4-MFA. To note, ZnO was also utilised in these systems, at 5 phr and 1 phr (formulations **C** and **D**, respectively), and was not eradicated from the formulation at all. At this point, it was first necessary to assess the behaviour of 1,4-MFA as a dispersion, which was a new concept for PCB latex at RBL. It was intended to eliminate ZnO altogether, eventually, if the results for 1,4-MFA implied that it could act as an equally effective replacement.

**Table 5.7. Formulation details for the compounding of PCB/PNA-5/1,4-MFA latex films (C and D).**

Reagent	PCB latex	Darvan <sup>®</sup> WAQ	ZnO	Aquanox 2246	Kaolin clay	Darvan <sup>®</sup> SMO	PNA-5	1,4-MFA	
Dispersion level (% w/w)	50	25	50	45	40	30	35	25	
Quantity (phr)	<b>C</b>	100	0.3	5	1.5	10	1	2.5	1
	<b>D</b>	100	0.3	1	1.5	10	1	2.5	1

Table 5.8 lists the tensile results for the two types of PCB/PNA-5/1,4-MFA film studied (denoted by **C** and **D**), whereby two contrasting levels of ZnO were adopted in the formulations. When compared against the standard DPTU/DPG films (**A**, Table 5.4), **C** and **D** each afforded lower UTS and modulus results, indicating that they were weaker materials, overall. The elongation at break for film **C**, where the typical 5 phr ZnO was adopted, was comparable to the DPTU/DPG PCB film (873 % *versus* 861 % for film **A**, within experimental error), but that of film **D**, where less ZnO was incorporated, was considerably higher and outside the range of error (916 ±16 %). These elongation results were the main difference between the two PCB/PNA-5/1,4-MFA films, whereby a lower level of ZnO appears to have facilitated an increase in the elasticity of the material, through more efficient cross-linking. UTS and modulus data for **C** and **D** yielded comparable mean values (which overlap within the range of error from one standard deviation); these results indicate that such properties of these films are seemingly independent of ZnO concentration.

**Table 5.8. Tensile results for the PCB/PNA-5/1,4-MFA latex films (C and D).\***

Accelerator system		UTS (MPa)	Elongation at break (%)	300 % Modulus (MPa)
PNA-5/1,4-MFA	<b>C</b>	17.0 ±1.8	873 ±10	1.82 ±0.16
	<b>D</b>	17.4 ±1.9	916 ±16	2.07 ±0.18

\*Mean results were obtained from ten data points in each case. The error given is one standard deviation.

Figure 5.5 shows the two PCB/PNA-5/1,4-MFA films, **C** and **D**, which each display some degree of inhomogeneity (patchiness); the film itself visibly contained solid particulates, suggesting poor dispersion of reagents within the formulation. These patches are thought to contribute to the low UTS results, as they would undoubtedly compromise the strength of the films. As depicted in Figure 5.5, film **C**, produced using a higher level of ZnO, displayed a horizontal strip on the film which would have been situated at the top of the former surface (shown at the bottom of Figure 5.5, **C**). This must have materialised during the dwelling stage of dipping, where some solid (perhaps the ZnO, which was present at a higher concentration) had settled towards the base of the beaker, which would have in turn afforded an uneven distribution throughout the formulation. In the following figure, areas on the films which were particularly patchy are marked out by a dashed red line.

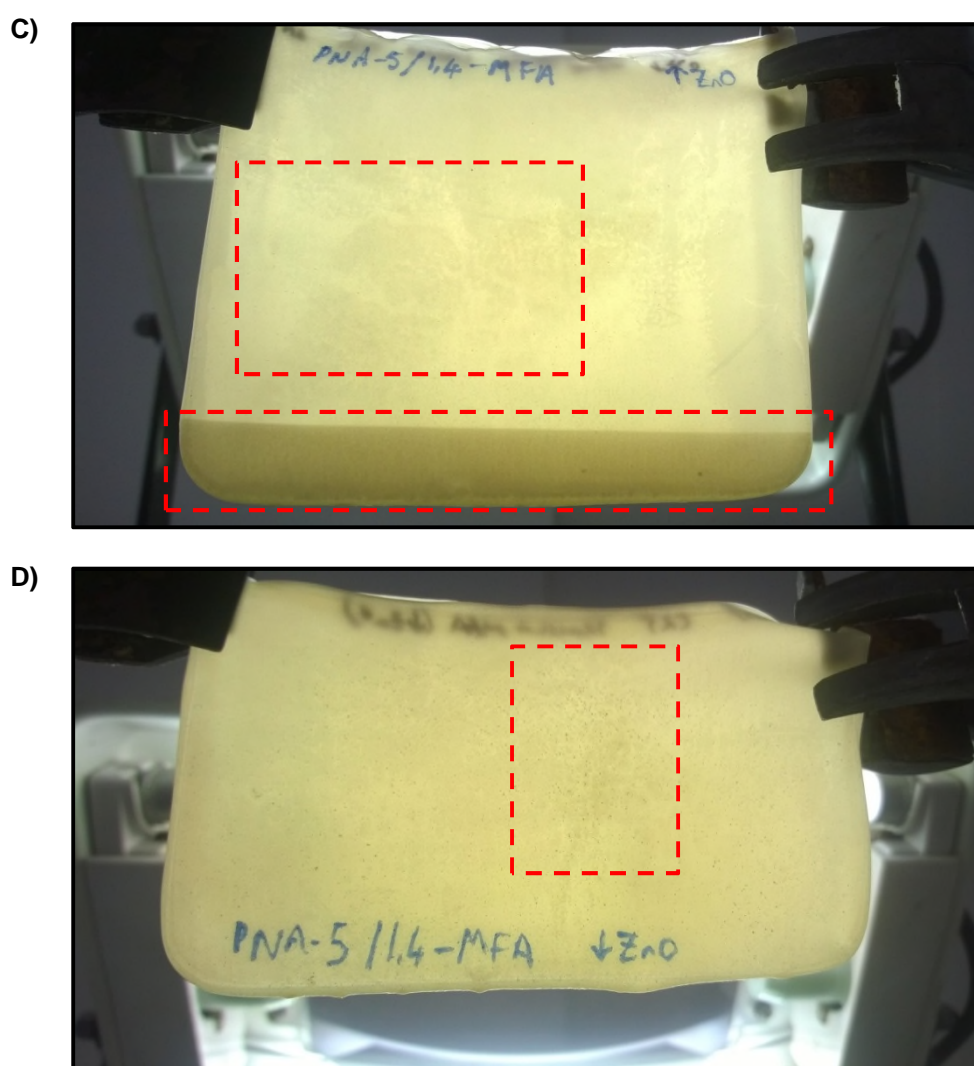


**Figure 5.5. Images of the final PCB/PNA-5/1,4-MFA latex films, whereby the formulations comprised contrasting levels of ZnO (film C: 5 phr ZnO; film D: 1 phr ZnO).**

It is postulated that the combined presence of ZnO and 1,4-MFA in the system may have ultimately been detrimental, as both of these compounds were intended to act as activators (towards cross-linking). The obvious inhomogeneity of film **C**, where a higher level of ZnO was adopted, may have ultimately arisen because of conflicting (or less) activation reactions occurring between ZnO and 1,4-MFA. Low UTS results (~17 MPa) arose for each of these films (**C** and **D**), indicating that less cross-linking had occurred, as the strengths were diminished (certainly compared to films **A** and **B**). In turn, a higher elongation value for **D**, supports this view, as this film incorporated less ZnO, which could have in turn enabled 1,4-MFA to act as the major activator (and thus less conflict would occur, potentially allowing for more efficient cross-linking *via* 1,4-MFA).

#### 5.3.4. PCB latex formulated with PNA-5 and DIXP

Diisopropyl xanthogen polysulfide (DIXP) was chosen as an accelerator primarily due to the findings made by Ohbi *et al.* with bromobutyl rubber (BIIR).<sup>4</sup> In this case, the cross-linking reaction with DIXP was not found to produce any toxic by-products, such as amines, which could potentially leach out from the rubber product and cause harm to the end-user. DIXP was deemed a suitable replacement to the standard dibenzothiazyl disulfide (MBTS)/thiourea accelerator system normally adopted in BIIR, where the final rubber properties were also comparable.<sup>4</sup> At this point in the project, RBL were already experimenting with DIXP within other rubber latex systems and the 40 % (w/w) aqueous dispersion was a well-established reagent within the company. The structure of DIXP is provided in Figure 5.6, whereby the number of sulfur atoms varies between three and five;<sup>22</sup> this accelerator is known to supply sulfur atoms to a cross-linking system, thus enabling the formation of sulfur bridges between polymer chains, which can be seen from the polysulfidic portion of the structure.<sup>4</sup>

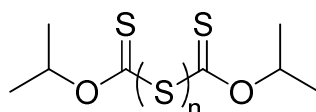


**Figure 5.6. Structure of diisopropyl xanthogen polysulfide (DIXP), where n = 3, 4 or 5.**<sup>22</sup>

DIXP was incorporated into a PCB latex along with PNA-5 and differing levels of ZnO, as detailed in Table 5.9; 5 phr ZnO was used for film **E**, whereas 1 phr ZnO was adopted for film **F** (as in the PNA-5/1,4-MFA study described in Section 5.3.3). DIXP was intended to act as the secondary organic portion of this binary accelerator system, providing additional sulfur cross-links for the final polymer network; PNA-5, also a sulfur-based complex, additionally comprised the 1,3-diaminopropane activator, a type of structure elucidated by the SafeRubber consortium for all of the various PNAs intended for PCB rubber (discussed



previously in Section 4.1.6). RBL advised that DIXP is a particularly active accelerator (as it contributes several sulfur atoms to the reaction) and so the 2.5 phr level of PNA-5 adopted when on its own (Section 5.3.2), or in conjunction with 1,4-MFA (Section 5.3.3), was reduced to 1.5 phr to allow for this. PNA-5 had already facilitated cross-linking independently and, given the apparent high reactivity of DIXP, elevated levels of both of these compounds may have resulted in a very fast rate of cure, or yielded a high cross-link density, or both. This would have subsequently compromised the elasticity of the material, and so intermediary levels of PNA-5 and DIXP were adopted (1.5 phr each).

**Table 5.9. Formulation details for the compounding of PCB/PNA-5/DIXP latex films (E and F).**

Reagent		PCB latex	Darvan <sup>®</sup> WAQ	ZnO	Aquanox 2246	Kaolin clay	Darvan <sup>®</sup> SMO	PNA-5	DIXP
Dispersion level (% w/w)		50	25	50	45	40	30	35	40
Quantity (phr)	E	100	0.3	5	1.5	10	1	1.5	1.5
	F	100	0.3	1	1.5	10	1	1.5	1.5

Table 5.10 shows the tensile results from the physical testing of the resultant PCB/PNA-5/DIXP films. Immediately, the high elongation at break results were noticeable; 931 % ( $\pm 19$  %) was obtained for film **E** (where 5 phr ZnO was adopted) and 914 % resulted for film **F** (which comprised a lower ZnO concentration). Both of these values far exceeded the DPTU/DPG standard PCB film, which itself afforded 861 % ( $\pm 22$  %). The UTS and modulus results for PCB/PNA-5/DIXP were each lower than the standard system. Film **F** yielded the highest UTS value (21.4 MPa *versus* 19.4 MPa) and highest modulus of the two films (1.86 MPa *versus* 1.42 MPa, which lie outside the range of error). Overall, the UTS results were the nearest obtained by this point and were only slightly lower than the value for the standard PCB/DPTU/DPG film (**A** afforded 23.7  $\pm 1.8$  MPa).

**Table 5.10. Tensile results for the PCB/PNA-5/DIXP latex films (E and F).\***

Accelerator system		UTS (MPa)	Elongation at break (%)	300 % Modulus (MPa)
PNA-5/DIXP	E	19.4 $\pm 1.8$	931 $\pm 19$	1.42 $\pm 0.11$
	F	21.4 $\pm 2.1$	914 $\pm 14$	1.86 $\pm 0.15$

\* Mean results were obtained from ten data points in each case. The error given is one standard deviation.

Images of the PCB/PNA-5/DIXP films are shown in Figure 5.7. Qualitatively, these films were comparable to each other in that they had the same smooth texture. However, they were not completely uniform and contained some patches of particulate matter. This is similar to the PNA-5/1,4-MFA PCB films (illustrated previously in Figure 5.5), but to a much lesser extent, so much so that it is not very noticeable in the images and only obvious to the naked eye. As a lower amount of PNA-5 was incorporated into these formulations (*i.e.* in **E** and **F**, 1.5 phr in each *versus* 2.5 phr previously), it may be that this component is contributing to the patches; less PNA-5 being present has reduced the severity of the inhomogeneity. Nevertheless, neither of these films were as thin, smooth or soft as the standard DPTU/DPG or PNA-5 PCB films previously described (in Sections 5.2 and 5.3.2, respectively), which were completely inhomogeneous.

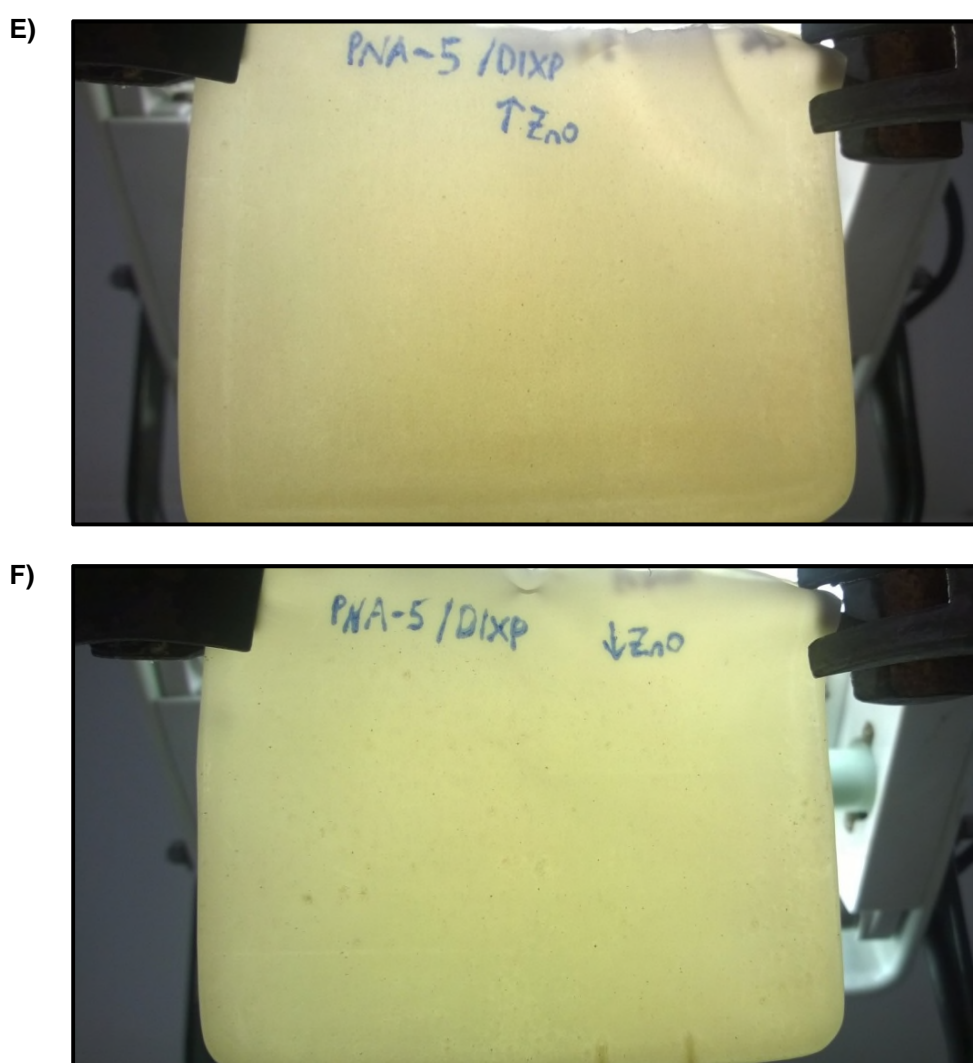


**Figure 5.7. Images of the final PCB/PNA-5/DIXP latex films, whereby the formulations comprised contrasting levels of ZnO (film E: 5 phr ZnO; film F: 1 phr ZnO).**

This was the first instance when PNA-5 was incorporated with a secondary organic accelerator (DIXP); up to this point, PNA-5 had been assessed with ZnO on its own (**B**) and

with 1,4-MFA (**C** and **D**). Overall, this system (for **E** and **F**) was more effective as the resultant films were stronger, with UTS values of approximately 21 MPa. This is far superior to films **C** and **D**, where 1,4-MFA was the principal partner, as these UTS results were approximately only 17 MPa. Therefore, it can be deduced that films **E** and **F** were stronger due to the presence of a secondary accelerator in the cure system (DIXP) which is believed to have created more cross-link chains within the polymer network.

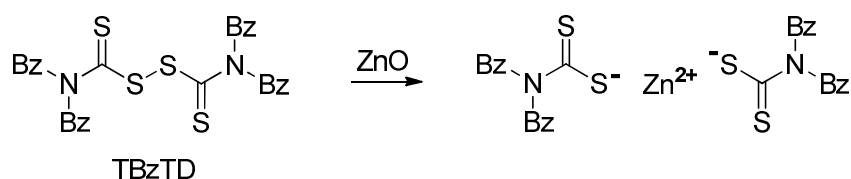
### **5.3.5. PCB latex formulated with PNA-5 and TBzTD**

TBzTD is a thiuram disulfide (structure illustrated previously in Table 5.2); this class of molecule is highlighted by Geier *et al.* as a particularly hazardous latex glove allergen.<sup>6</sup> Thiuram disulfides, especially tetraethyl (TETD) and tetramethyl (TMTD) derivatives, were found to be the most common allergy-causing accelerators used in the production of latex gloves.<sup>6</sup> However, TBzTD is not mentioned in this report, nor in a comprehensive review of rubber glove allergens compiled by Rose *et al.*<sup>5</sup>

TBzTD is a recognised rubber accelerator, as demonstrated in the studies of Debnath and Basu on NR.<sup>23</sup> In this instance, TBzTD was found to be a suitable alternative accelerator to TMTD and was successful in yielding cross-linked rubber with optimum physical properties.<sup>23</sup> That study was similar to this project concerning PCB, as it was driven by the need for a 'safer' accelerator system (but for NR). In this way, the aim was to eliminate the risk of toxic nitrosamines formed during the cross-linking process. This can occur in the case of accelerators which have been derived from secondary amines (*e.g.* dimethyl/diethylamine, morpholine or piperidine).<sup>23</sup> Conversely, TBzTD originates from dibenzylamine, which is a primary amine, from which nitrosamines cannot be produced (as breakdown by-products). This potentially renders TBzTD safe, by way of elimination.<sup>23</sup> Similarly, the absence of TBzTD in the literature specifically listing latex allergens leads to the belief that TBzTD is non-toxic;<sup>5, 6</sup> TBzTD was therefore interesting for these studies, as a seemingly non-toxic rubber accelerator.

Debnath and Basu employed a binary accelerator system utilising sulfenamide- and mercaptobenzothiazole-based compounds as the secondary components.<sup>23</sup> However, these chemicals have also been identified as rubber allergens by Geier *et al.*,<sup>6</sup> and so were not selected for this work. These studies with PCB latex described herein continued to utilise ZnO in the formulations, as this metal oxide has not been established as hazardous when incorporated in the rubber latex itself.<sup>5</sup> The ZnO is present to activate cross-linking, as usual, and is able to complex with TBzTD (through Zn<sup>2+</sup>) in the same way as with TbuT in the rubber/oligomer studies outlined in Chapter 4 (Scheme 5.1 depicts how this is achieved).

This research examined TBzTD predominantly in combination with PNA-5, which completed the binary accelerator system.



**Scheme 5.1. Zn<sup>2+</sup>-complexed TBzTD, where Bz denotes a benzyl group.**

Table 5.11 lists the reagents in the formulation for the two types of PCB film prepared in the presence of PNA-5 and TBzTD. Formulation **G** comprised a higher level of ZnO (5 phr); formulation **H** adopted less ZnO (1 phr), along with an additional 1,4-MFA component (0.5 phr). The hypothesis was to assess the properties of a film incorporating a combined activator system (1,4-MFA and ZnO) with these alternative accelerators (PNA-5 and TBzTD). Within this project it was ultimately desirable to reduce or eliminate the presence of ZnO in the PCB formulations; 1,4-MFA was a potential candidate to facilitate this. Initially, it was postulated that a reduced level of ZnO (*i.e.* 1 phr) should be complimented by the MFA, before completely eradicating the metal oxide. In this instance, as in formulation **H**, 1,4-MFA and ZnO would act as activators, whilst the binary organic accelerator system comprising PNA-5 and TBzTD would essentially facilitate the polymer cross-links. The TBzTD dispersion reagent (50 % w/w) had previously been developed at RBL and was based on a general composition which suited a variety of thiuram derivatives employed within the company.

**Table 5.11. Formulation details for the compounding of PCB/PNA-5/TBzTD latex films (G and H).**

Reagent	PCB latex	Darvan <sup>®</sup> WAQ	ZnO	Aquanox 2246	Kaolin clay	Darvan <sup>®</sup> SMO	PNA-5	TBzTD	1,4-MFA	
Dispersion level (% w/w)	50	25	50	45	40	30	35	50	25	
Quantity (phr)	<b>G</b>	100	0.3	5	1.5	10	1	2.5	0.5	----
	<b>H</b>	100	0.3	1	1.5	10	1	2.0	0.5	0.5

The tensile test results for each PCB film are illustrated in Table 5.12. Film **G** was produced from the PCB/PNA-5/TBzTD formulation, whereas the formulation for film **H** comprised the additional 1,4-MFA component (and reduced ZnO concentration). Overall, the modulus and UTS results of these films are similar to each other (within experimental error), although those of film **G** are marginally higher in each case. The elongation at break for film **H** is

considerably greater than film **G** (928 % *versus* 867 %) and even higher than the PCB/DPTU/DPG film (861 %, **A**). In contrast, the elongation at break for film **G** is comparable to film **A** (and within experimental error). In terms of UTS, each of these films (**G** and **H**) afford reduced values to the standard DPTU/DPG PCB film, but admittedly are not considerably lower (23.7 ±1.8 MPa for **A** *versus* 21.2 ±1.9 MPa for **G** and 20.5 ±1.5 MPa for **H**).

**Table 5.12. Tensile results for the PCB/PNA-5/TBzTD latex films (G and H).\***

Accelerator system		UTS (MPa)	Elongation at break (%)	300 % Modulus (MPa)
PNA-5/TBzTD	<b>G</b>	21.2 ±1.9	867 ±11	2.03 ±0.16
	<b>H</b> (with 1,4-MFA)	20.5 ±1.5	928 ±18	2.00 ±0.21

\*Mean results were obtained from ten data points in each case. The error given is one standard deviation.

The PCB/PNA-5/TBzTD film (**G**) was easier to cut (into dumbbells, for tensile testing) than film **H**, where 1,4-MFA was additional to the formulation. Both films still contained some patches of particulates (which are outlined in red in the figures) and were not perfectly smooth, as would be required eventually for industrial glove applications. Despite this, it was observed that film **H** contained fewer patches and was in fact smoother than film **D** from the previous PCB/PNA-5/1,4-MFA system (described in Section 5.3.3). Thus, it may be that the TBzTD in this case enabled a more uniform dispersion of reagents within the system, in general; if the PNA-5 dispersion or ZnO were the causes of these patches in the films, a reaction between TBzTD and PNA-5 or ZnO may have reduced the excess residual particulates or reagents present in the compounded latex. Indeed, it was previously hypothesised that poor dispersion in the PNA-5/1,4-MFA system (films **C** and **D**) was the result of conflict between the two activators (ZnO and 1,4-MFA), which ultimately negated some degree of cross-linking, as only one organic accelerator was present (PNA-5). However, with the addition of TBzTD here (in film **H**) there was superior homogeneity and enhanced strength (UTS of **H** = 20.5 ±1.5 MPa *versus* 17.4 ±1.9 MPa of **D**) in the film. Thus, the second accelerator (TBzTD), working jointly with PNA-5, may have enabled more cross-linking to take place, after the simultaneous activation of polymer chains by ZnO and 1,4-MFA. It appears that there needs to exist similar respective quantities/concentrations of activator/s and cross-linker/s in order to facilitate efficient cross-linking. For instance, just the one accelerator (PNA-5) with two activators (ZnO and 1,4-MFA) was ineffective (*i.e.* in **C** and **D**); two organic cross-linking agents (PNA-5 and TBzTD) enabled ZnO and 1,4-MFA to operate together, within the same system, (as in **H**).

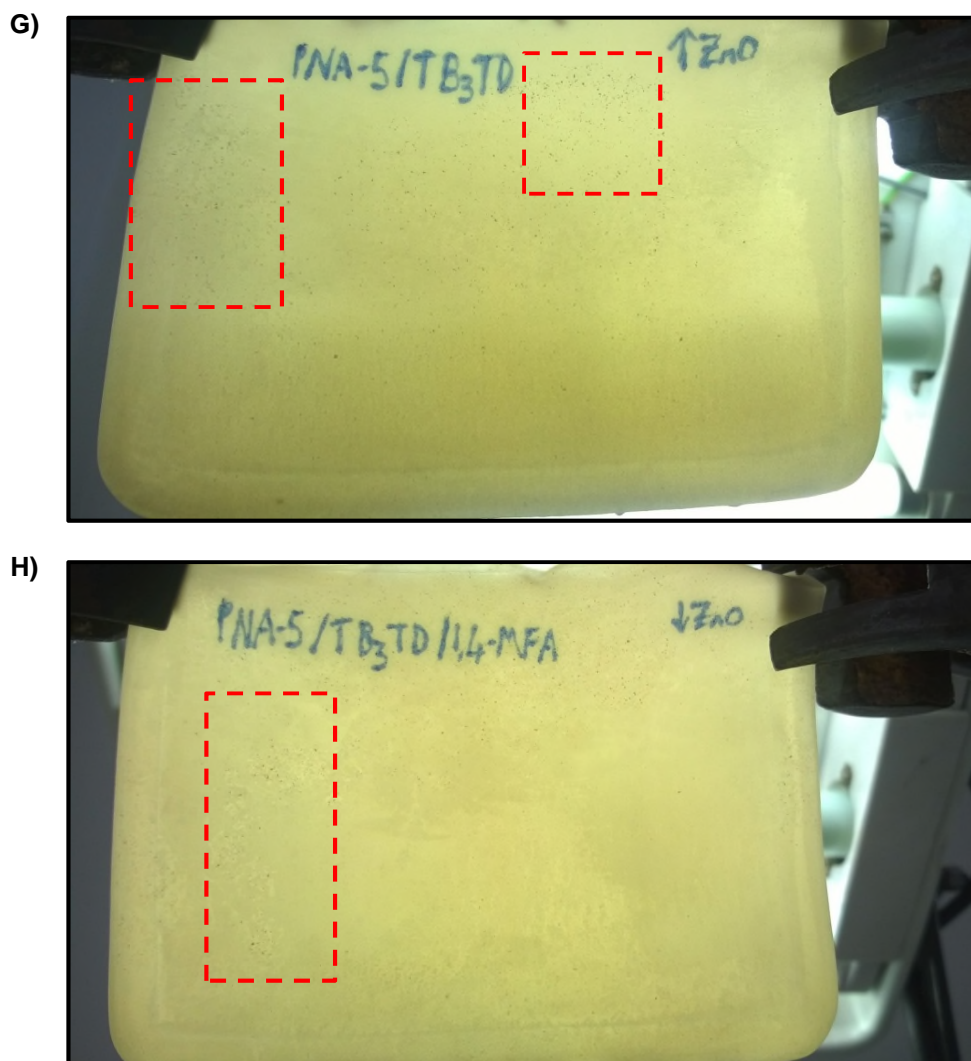


**Figure 5.8. Images of the final PCB/PNA-5/TBzTD latex films, whereby the formulations comprised different levels of ZnO (film G: 5 phr ZnO; film H: 1 phr ZnO) and film H comprised 1,4-MFA (0.5 phr).**

#### **5.4. Alternative accelerator system comprising DIXP and PNA-8**

The final PCB latex comprised DIXP and a novel accelerator, 2,2'-dithio di(ethylammonium)-bis(dibenzylthiocarbamate) (PNA-8). Thus far, all of the latex films incorporating PNA-5 (*i.e.* when used by itself or in unison with 1,4-MFA, DIXP or TBzTD) have yielded low UTS values (compared to the standard DPTU/DPG combination, film **A**) and the materials themselves have been visibly inhomogeneous (patchy). Hence, PNA-5 was eradicated from the PCB formulations at this point. DIXP was retained because it is a known non-toxic accelerator,<sup>4</sup> and was found to cure PCB latex films with PNA-5 and ZnO (as detailed in Section 5.3.4).

PNA-8 (shown in Figure 5.9) is a dithiocarbamate which has been developed by RBL and incorporated into various other cure systems at the company (in both solid rubbers and

aqueous latexes). This accelerator is known by RBL to work synergistically with other classes of accelerator and can enhance the activity of sulfur donors in their function as cross-linkers (by activating polymer chains through the diamine). Crucially, PNA-8 has been researched and tested at the company and deemed safe with regards to cross-linking; this accelerator is non-toxic, in that harmful amine by-products are not produced on heating. Literature supports this, as the research conducted by Geier *et al.* found that only ~3 % of positive allergic reactions resulted from dithiocarbamates in latex gloves (involving almost 2000 human subjects).<sup>6</sup> This is a relatively low proportion considering that up to 15 % of allergies resulted from thiuram-based accelerators, for example. Furthermore, the report states that dithiocarbamates have been employed more frequently in the industrial production of latex gloves in recent years, and so these compounds must release considerably fewer (harmful) residues, thus causing no, or less severe, skin sensitivity.<sup>6</sup> Hence, a combined DIXP/PNA-8 system was considered to be safer overall than the DPTU/DPG standard for the production of PCB latex films.

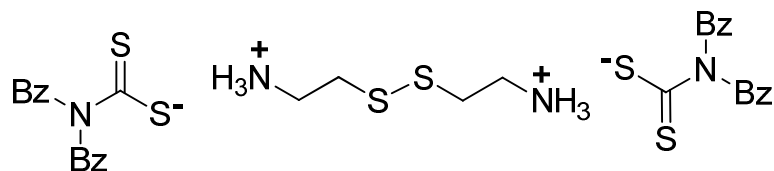


**Figure 5.9. Structure of 2,2'-dithio di(ethylammonium)-bis(dibenzylidithiocarbamate) (PNA-8).**

The PCB/DIXP/PNA-8 formulation is listed in Table 5.13. In this instance, a typical quantity of ZnO was employed (5 phr), as this was the first experiment with this new accelerator system; if initially promising results were generated, the ZnO level could then be a secondary study. Equal quantities of DIXP and PNA-8 were adopted (1.5 phr each); the PNA-8 aqueous dispersion (50 %) had already been optimised at RBL prior to these investigations.

**Table 5.13. Formulation details for the compounding of PCB/DIXP/PNA-8 latex films (I).**

Reagent	PCB latex	Darvan <sup>®</sup> WAQ	ZnO	Aquanox 2246	Kaolin clay	Darvan <sup>®</sup> SMO	DIXP	PNA-8
Dispersion level (% w/w)	50	25	50	45	40	30	35	50
Quantity (phr)	I 100	0.3	5	1.5	10	1	1.5	1.5



The tensile test results for the PCB/DIXP/PNA-8 films (denoted by **I**) are provided subsequently in Table 5.14 and an image of the material is displayed in Figure 5.10. This was the first instance where the obtained UTS result was a close match to the PCB/DPTU/DPG film (**A**); 24.3 ±1.8 MPa was obtained here, which is marginally higher than the 23.7 ±1.8 MPa value for film **A**, but well within the range of experimental error. Crucially, these new films were soft to the touch and absent of any patches or residual solid particulates; they were comparable to the DPTU/DPG PCB films (**A**) in terms of homogeneity (smoothness) but were slightly darker in colouration. These observations correlate with a closely-matching elongation at break result (884 % *versus* 861 % for film **A**, again within error), indicating that the material was equally extendable or elastic. The softness of these films (denoted by **I**) was reflected in the low modulus (1.89 ±0.18 MPa), which is a reduction on the standard DPTU/DPG PCB films (**A**, 2.40 ±0.28 MPa). Overall, the appearances of the films were promising, as were the tensile test results. These PCB/DIXP/PNA-8 films were clearly strong, as shown by a high UTS value, but they retained a reasonable level of elasticity (indicated by the elongation at break result). The combined results certainly suggest that inhomogeneity in the films causes a depreciation in the physical (tensile) properties; the smooth, homogeneous films depicted herein (**I**) boast superior strength *versus* those generated with PNA-5 (films **B** to **H**, inclusive), which all demonstrated some degree of inhomogeneity.

**Table 5.14. Tensile results for the PCB/DIXP/PNA-8 latex films (I).\***

Accelerator system		UTS (MPa)	Elongation at break (%)	300 % Modulus (MPa)
DIXP/PNA-8	<b>I</b>	24.3 ±1.8	884 ±21	1.89 ±0.18

\*Mean results were obtained from ten data points in each case. The error given is one standard deviation.

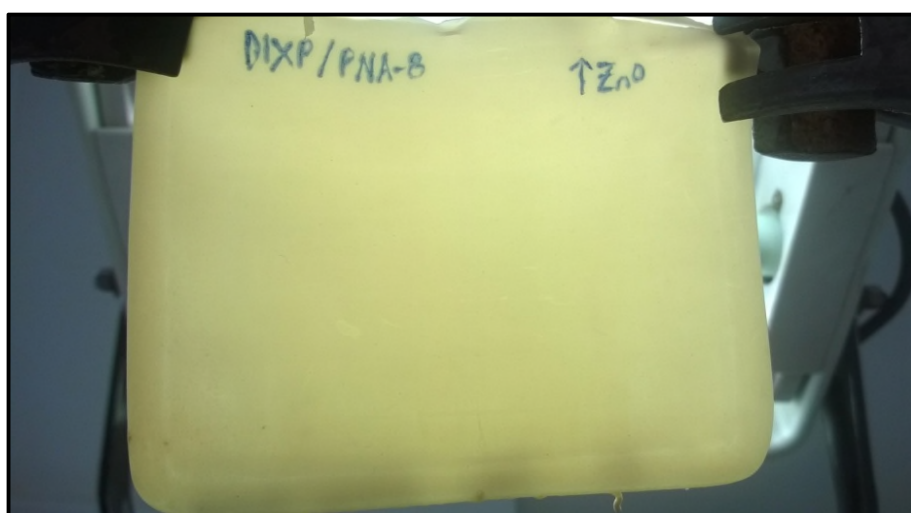


**Figure 5.10. Image of the final PCB/DIXP/PNA-8 latex films (I).**



The DIXP/PNA-8 system combined an organic accelerator component (DIXP) with the bifunctional PNA-8 (which comprises a complex between a diamine and sulfur compound). This is the same way in which the PNA-5/TBzTD system was intended to operate; the performances of films **I** and **G** can therefore be directly compared, relative to the nature of the different accelerators (*i.e.* PNA-5 *versus* PNA-8 and TBzTD *versus* DIXP). Overall, **I** afforded a higher UTS (24.3 MPa *versus* 21.2 MPa of **G**) and a higher elongation at break (884 % *versus* 867 % of **G**), but a lower modulus (1.89 MPa *versus* 2.03 MPa of **G**). It is perceived that the relative enhanced strength, elasticity and softness of **I** can be attributed mainly to the DIXP component. For instance, this accelerator contributed polysulfide cross-links to the polymer system, which would be longer in length than those generated from TBzTD (which were anticipated to be mono- or di-sulfidic as less sulfur atoms were present), for instance. Hence, these longer bridges would offer more flexibility to the polymer and in turn facilitate greater elasticity in the final material; this is reflected by a higher elongation at break result for **I** (*versus* **G**) and may also contribute to the lower modulus (or greater degree of softness). Additionally, the diamine portion of the PNA-8 structure comprises a disulfide bond; it is possible that this was cleaved in the presence of excess  $Zn^{2+}$  and the sulfur atoms would bond to the polymer chain in a similar way to that depicted in the newly-proposed cross-linking mechanism of Berry *et al.* (depicted previously in Scheme 4.8).<sup>19</sup> PNA-8 and PNA-5 are especially distinguishable by the structures of the respective diamine portions, whereby PNA-5 is a propyl chain, composed solely of carbon atoms, but PNA-8 comprises the central sulfur-sulfur bond. Hence, the overall sulfur composition of PNA-8 is greater, *versus* PNA-5, which means that more sulfur atoms would potentially be available to cross-link. Overall, the slightly heightened strength of film **I** may indicate that the binary fashion in which DIXP and PNA-8 functioned was most effective, yielding a greater number of (sulfur) cross-links, but not so much as to compromise the elasticity (elongation) of the latex film.

### 5.5. Comparisons for the development of poly(2-chloro-1,3-butadiene) latex films

The principal drive of these investigations was to identify an alternative accelerator system to DPTU/DPG in PCB latexes, with rubber gloves being the target end-use. Ideally, it would also have been favourable to develop a method which could incorporate less ZnO. Thiourea compounds, as discussed in the cross-linking chapter (4), regarding ETU in particular, are potential carcinogens/mutagens.<sup>11-13, 15</sup> DPTU falls within this category and is therefore of particular concern in terms of the production of PCB latex. Both DPTU and DPG are also reported allergens in the production of PCB gloves.<sup>5</sup>

PCB latex films were initially formulated with the standard organic binary accelerator system comprising DPTU and DPG, in conjunction with ZnO activator. The material from this system

(films denoted by **A**) generated the benchmark tensile results for subsequent films. Numerous other accelerators were thereafter evaluated in place of DPTU and DPG in the PCB latex. These included the complex of piperazine-1-carbodithioic acid and 1,3-diaminopropane (PNA-5), tetrabenzylthiuram disulfide (TBzTD), diisopropyl xanthogen polysulfide (DIXP) and 2,2'-dithio di(ethylammonium)-bis(dibenzylthiocarbamate) (PNA-8). Various combinations of these accelerators were examined, for instance PNA-5 with 1,4-MFA, DIXP and TBzTD, and DIXP with PNA-8. Certain experiments were also conducted with different levels of ZnO. Results concerning the potential safer alternative accelerator system are compared in Section 5.5.1, after first evaluating the effect of reducing ZnO in the PCB formulations.

### **5.5.1. Effect of reducing ZnO in PCB latex formulations**

ZnO is known to aid the cross-linking process and was previously established to activate the PCB polymer chain towards cross-linking (by ETU and other sulfur-containing compounds, as discussed in Chapter 4, Section 4.1.5.2). The way in which this is generally achieved is by the sulfur component of the accelerator forming a complex with the zinc dication and the subsequent displacement of oxygen (as for the ETU mechanism depicted in Scheme 4.8).<sup>19</sup> As advised by RBL, the standard level of ZnO employed in the PCB latex formulation was taken as 5 phr; where possible, a level of 1 phr was also adopted to assess if a reduction in ZnO compromised the physical properties of the latexes (as indicated by the tensile results). The studies involving PNA-5 accelerator, in combination with 1,4-MFA, DIXP and TBzTD separately (detailed in Sections 5.3.3, 5.3.4, and 5.3.5, respectively), contributed to this particular trial. To determine the effect (if any) of reducing ZnO, or by complementing it with 1,4-MFA, each data set are directly compared in turn, *i.e.* the UTS, 300 % modulus and elongation at break results, respectively.

As Figure 5.11 illustrates, reducing the ZnO level in the PCB/PNA-5 formulations with 1,4-MFA, DIXP and TBzTD, respectively, had only a slight effect on the strength of the latex films. The two films from the PCB/PNA-5/1,4-MFA experiments, **C** (5 phr ZnO) and **D** (1 phr ZnO), each gave UTS values of approximately 17 MPa. There is a slight increase in the UTS of the PCB/PNA-5/DIXP films when less ZnO was adopted (21.4 ±2.1 MPa for **F** *versus* 19.4 ±1.8 MPa for **E**). This is in contrast to the PCB/PNA-5/TBzTD films, whereby a lower level of ZnO and additional 1,4-MFA component (film **H**) afforded a lower UTS (20.5 ±1.5 MPa for **H** *versus* 21.2 ±1.9 MPa for **G**). However, these differences are very slight (*i.e.* lie within experimental error) and this suggests that, overall, reducing the ZnO had negligible effect on the resilience of the films. This is a very positive result, implying that

lowering the ZnO content in the formulation would not compromise the physical strength of the PCB films.

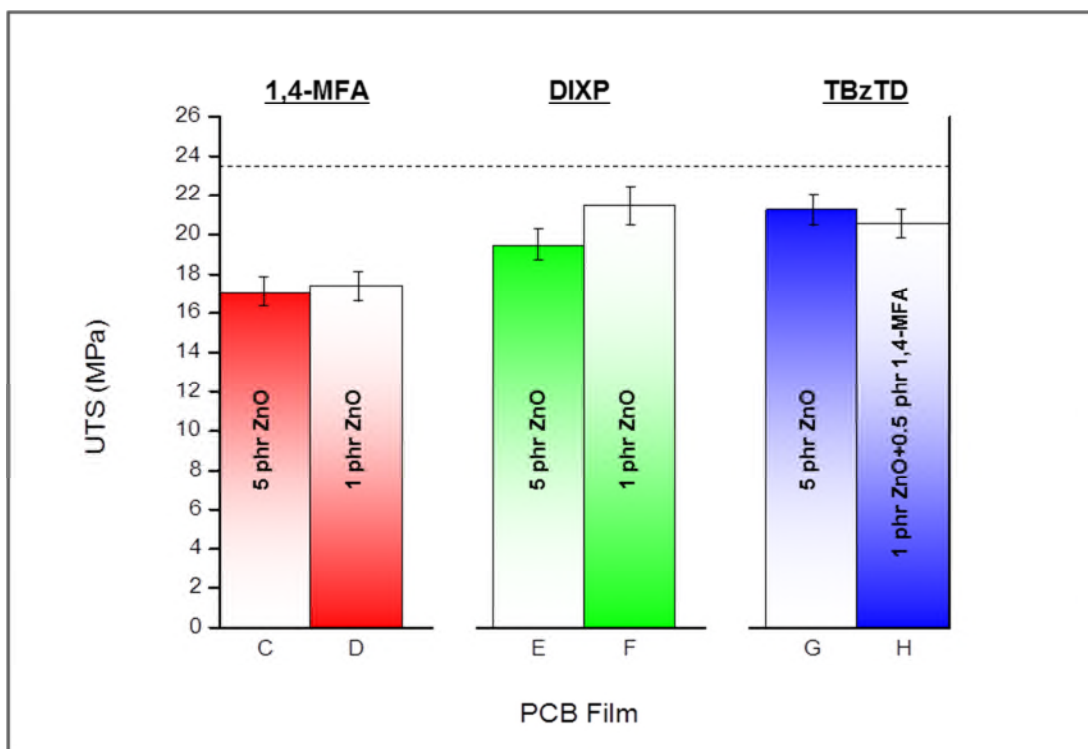


**Figure 5.11. Comparison of UTS for PCB latex films made using PNA-5 combined with 1,4-MFA (red, C and D), DIXP (green, E and F) and TBzTD (blue, G and H), where the latter datum represents a lower level of ZnO in each case (1 phr versus 5 phr). Error bars indicate one standard deviation from ten data points. The dashed line represents the industrial standard UTS value (i.e. film A, 23.7 MPa).**

Comparison of the 300 % modulus results for each formulation (illustrated in Figure 5.12) also implies that reducing ZnO had little effect on the physical properties of the materials. In the PCB/PNA-5/1,4-MFA formulation, a higher level of ZnO yielded a marginally lower modulus ( $1.82 \pm 0.16$  MPa for **C** versus  $2.07 \pm 0.18$  MPa for **D**). This trend was also observed in the PCB/PNA-5/DIXP formulation, where a higher modulus was obtained when less ZnO was used (**F**, 1 phr, gave  $1.86 \pm 0.15$  MPa; **E**, 5 phr, gave  $1.42 \pm 0.11$  MPa). These differences may imply that incorporating more ZnO in the mixtures afforded slightly softer materials. In the PCB/PNA-5/TBzTD formulation, 5 phr ZnO was used to prepare film **G**, whereas 1 phr ZnO was used for film **H**, but with an additional 1,4-MFA component present at 0.5 phr. In this case, the moduli were comparable, at 2.03 MPa and 2.00 MPa, respectively. These relative consistencies collectively indicate that 1,4-MFA could potentially function in the same way as ZnO, which would help towards developing a safer system, in replacing ZnO entirely.

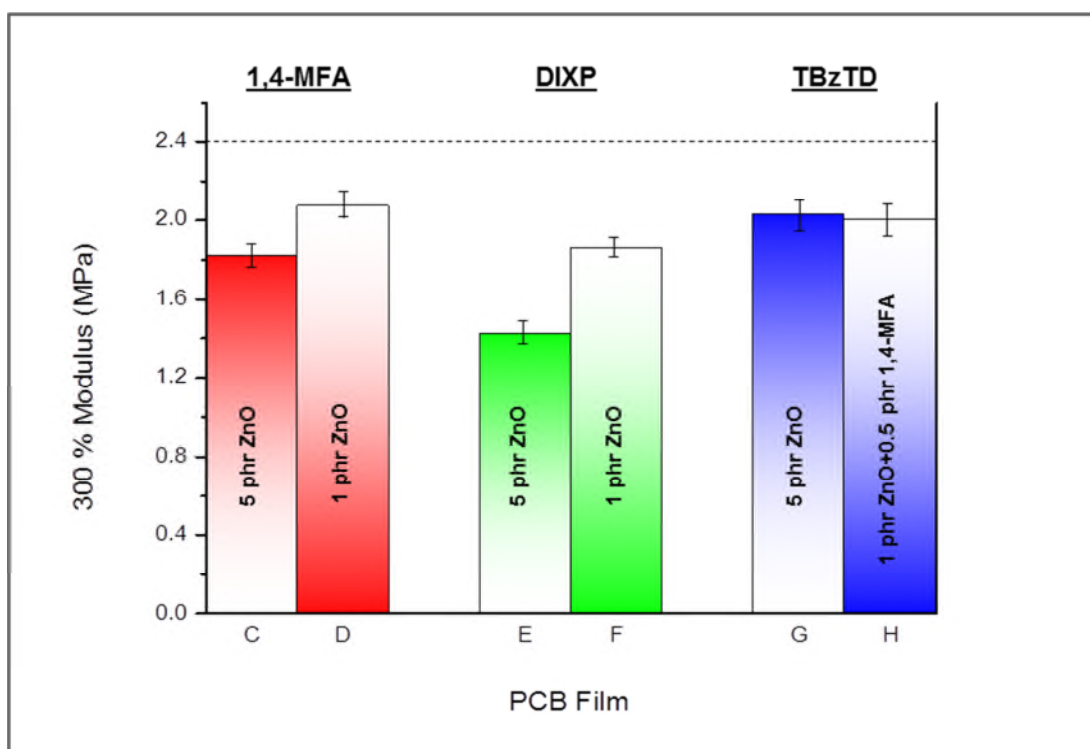


**Figure 5.12. Comparison of 300 % modulus for PCB latex films made using PNA-5 combined with 1,4-MFA (red, C and D), DIXP (green, E and F) and TBzTD (blue, G and H), where the latter datum represents a lower level of ZnO in each case (1 phr versus 5 phr). Error bars indicate one standard deviation from ten data points. The dashed line represents the industrial standard 300 % modulus value (i.e. film A, 2.40 MPa).**

There are more distinct differences amongst the elongation at break data. As Figure 5.13 shows, the seemingly straightforward comparisons between films from the PNA-5/DIXP and PNA-5/1,4-MFA PCB formulations (i.e. films **C** versus **D** and **E** versus **F**, respectively) give contrasting trends. For instance, film **C** (5 phr ZnO) had a lower elongation at break than **D** (1 phr ZnO); film **E** (5 phr ZnO) afforded a higher elongation at break than **F** (1 phr ZnO). Admittedly, the 931 % versus 914 % of the PNA-5/DIXP system is a marginal difference and infers that altering the level of ZnO had little effect on the elongation at break for these films. However, the PCB/PNA-5/1,4-MFA system shows an opposite correlation, where the film containing more ZnO (**C**) gave  $873 \pm 10\%$ , but the elongation at break for film **D** was significantly higher, at  $916 \pm 16\%$ . In Section 5.3.3 it is suggested that the presence of both ZnO and 1,4-MFA in systems **C** and **D** could have ultimately been detrimental. Cross-linking may have actually been hindered due to the presence of both activator molecules, as they are believed to work antagonistically (certainly at the respective concentrations adopted for **C**). A higher elongation for **D** (1 phr ZnO) was obtained with the lower level of the metal oxide, which in turn allowed the 1,4-MFA to function primarily as the activator. Previously, it has been observed that too high a concentration of ZnO in the system contributes too many cross-links, thus rendering diminished physical properties in the materials.

The PCB/PNA-5/TBzTD formulation only adds further complications to the comparison of the elongation at break data; 5 phr ZnO was adopted for film **G** and 1 phr for film **H**, but, crucially, 1,4-MFA was also present in the latter. Here, film **G** afforded  $867 \pm 11$  %, which is much lower than, and outside the range of error for, film **H** ( $928 \pm 18$  %). Unfortunately, TBzTD was not tested with 1,4-MFA alone, which would have potentially settled this disparity amongst the data. As such, it is not possible to draw any significant definitive conclusions, other than to suggest that the effect of a five-fold decrease in ZnO is dependent entirely on the nature of the accelerator system itself. For example, the one instance where a (slightly) higher elongation value resulted when a higher level of ZnO was present was in the PNA-5/DIXP system, where **E** (5 phr ZnO) yielded 931 % (*versus* 914 % for **F**). This was believed to be the effect of the polysulfide cross-link bridges from DIXP; these chains would be long and flexible, thus rendering the material highly elastic. For this system, it may be that the lower elongation of film **F** (although the values may overlap within the experimental error) was the result of fewer points on the polymer chain being activated (by less ZnO) and so a lower quantity of the polysulfide cross-links would exist, thus hindering the elasticity. In support of this, the UTS value obtained for **F** is higher than **E** (21.4 MPa *versus* 19.4 MPa), thus proving that more cross-linking did in fact transpire when more ZnO was adopted (in **E**).

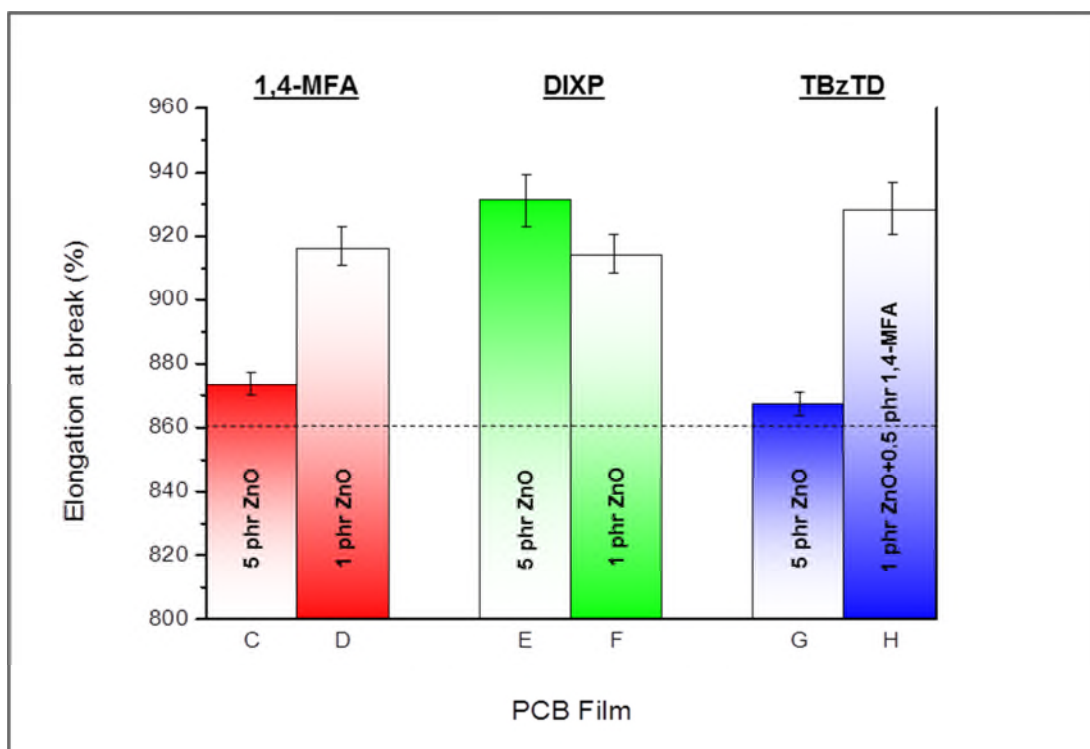


**Figure 5.13. Comparison of elongation at break for PCB latex films made using PNA-5 combined with 1,4-MFA (red, C and D), DIXP (green, E and F) and TBzTD (blue, G and H), where the latter datum represents a lower level of ZnO in each case (1 phr *versus* 5 phr). Error bars indicate one standard deviation from ten data points. The dashed line represents the industrial standard elongation at break value (*i.e.* film A, 861 %).**

Overall, there were few significant results amongst the tensile data which could help to determine the effect of reducing the ZnO concentration in the formulations. The UTS and 300 % modulus in particular seemed to not be greatly affected. Indeed, the little effect that reducing ZnO seemed to have could indicate that 1 phr (a much 'safer' level than 5 phr) could potentially be employed; a lower level should be evaluated in the DPTU/DPG PCB latex as a part of future work, to see what effect this would have on the 'standard' system. It is possible that there is little distinction between the data due to the nature of the accelerators employed. For instance, PNA-5 (and PNA-8, although differing levels of ZnO were not evaluated with this) comprises a diamine activator portion within the structure (as developed by the SafeRubber consortium),<sup>8</sup> which was expected to activate the polymer chain in the same way as ZnO. Hence, there exists more than one activator compound throughout these experiments (as PNA-5 or PNA-8, at least, were always assessed in formulations also comprising ZnO). Originally, these trials were designed with the view that ZnO and the activating diamines would cooperate with one another, but this has ultimately been a disadvantage when attempting to establish the effect that ZnO alone had on the tensile properties of the final materials.

Replacing ZnO with 1,4-MFA at this point seems possible, in that the presence of 1,4-MFA generated reasonable latex films, for instance in the PCB/PNA-5/TBzTD system (with ZnO) as depicted throughout as film **H**. The tensile results for this film (UTS = 20.5 MPa, 300 % modulus = 2.00 MPa, elongation at break = 928 %) were not too dissimilar from those of the DPTU/DPG PCB standard (film **A**, UTS = 23.7 MPa, 300 % modulus = 2.40 MPa, elongation at break = 861 %); further development could aim to enhance the UTS and reduce the elongation at break, in particular. It would be especially advantageous to disregard ZnO completely, as the presence of both of these activators in the PNA-5/1,4-MFA system (films **C** and **D**) generated especially inhomogeneous materials. Film **C**, where more ZnO was included, displayed a horizontal strip on the final, cured film (see Figure 5.5), which was attributed to a distinct lack of cross-linking. In turn, this was justified by conflicting activation reactions possibly occurring between 1,4-MFA and ZnO (at 5 phr). Overall, it was established that the introduction of a secondary organic accelerator, to complement PNA-5, overcame this issue (as in TBzTD, for film **H**).

Additional research should be undertaken with the PCB films comprising PNA-5 accelerator (with DIXP and/or TBzTD, separately) and the formulations replicated with 1,4-MFA, without any ZnO present at all. The tensile results would then indicate whether 1,4-MFA could replace ZnO as the activating species in the production of PCB latex gloves, as has been found possible with PCB rubber.<sup>18</sup>

### 5.5.2. Summary of accelerator systems for PCB latex

The overall aim of this part of the project was to determine a replacement accelerator system for the production of PCB latex gloves. This had to be safer than the DPTU/DPG system currently adopted in industry, which itself is harmful due to the fact that thiourea and guanidine compounds are skin allergens.<sup>6</sup> The accelerators chosen for the investigation included PNA-5, the non-toxic compound from the SafeRubber project,<sup>8</sup> which can cure PCB rubber in place of ETU. Secondly, 1,4-MFA has been found to cross-link PCB by itself and in combination with PNA-5,<sup>18</sup> and was considered here as a potential replacement for ZnO. DIXP and TBzTD were already recognised accelerators at RBL and were deemed safe through relevant testing at the company and according to literature sources.<sup>4-6</sup> PNA-8, a dithiocarbamate derivative, was a novel accelerator in development at RBL at the time; no harmful by-products resulted from various cross-linking (rubber) studies at RBL and this type of compound was deemed low risk in studies by Geier *et al.*<sup>6</sup> Thus, all of the accelerators selected for the trial PCB latex formulations were considerably less harmful than DPTU and DPG.

Table 5.15 combines all of the tensile test results for the PCB latex films investigated; the first set (film **A**) acted as a benchmark, as these transpired from replica industry-standard PCB films made using the DPTU/DPG accelerator system. It was important to aspire to these results, as they reflect the properties required in the final PCB latex rubber material for glove applications; the UTS dictates strength and resilience, elongation at break is a measure of elasticity, and softness is represented by the modulus value.

Noticeably, film **A** (for the standard DPTU/DPG system) afforded the lowest elongation at break (861 %) and highest modulus (2.40 MPa); the only system which exceeded the UTS value (23.7 MPa) was that of film **I** (24.3 MPa), where DIXP and PNA-8 accelerators were adopted in the formulation. This final film (**I**) also generated a similar elongation at break result (884 %), but a lower modulus (1.89 MPa), compared to film **A**.

The appearance and texture of each of the PCB films was crucial and observations were compared against the standard film (**A**). DPTU/DPG afforded rubber latex which was soft to the touch, smooth and cream-coloured. All of the films resulting from formulations with PNA-5 (**B** to **H**, inclusive), were inhomogeneous (patchy), with uneven textures; solid particulates were present, which were thought to have resulted from poorly dispersed reagents (*i.e.* PNA-5), inadequately mixed formulations or less cross-linking taking place (such as for **C** and **D**, where PNA-5 was adopted by itself and the lowest UTS values were obtained). On the whole, these materials would be unacceptable for direct use in glove applications, given their inconsistencies. In stark contrast, film **I**, where DIXP and PNA-8 accelerators were adopted, was soft, with a smooth, even texture, and no patchiness was present.

**Table 5.15. Overall tensile results table for the PCB latex films furnished using various accelerator systems, where mean values are quoted plus/minus the standard deviations.\***

Accelerator system	Film	UTS (MPa)	Elongation at break (%)	300 % Modulus (MPa)
DPTU/DPG	<b>A<sup>†</sup></b>	<b>23.7</b> ( $\pm 1.8$ )	<b>861</b> ( $\pm 22$ )	<b>2.40</b> ( $\pm 0.28$ )
PNA-5	<b>B<sup>†</sup></b>	<b>19.0</b> ( $\pm 2.2$ )	<b>978</b> ( $\pm 17$ )	<b>1.69</b> ( $\pm 0.23$ )
PNA-5/1,4-MFA	<b>C<sup>†</sup></b>	<b>17.0</b> ( $\pm 1.8$ )	<b>873</b> ( $\pm 10$ )	<b>1.82</b> ( $\pm 0.16$ )
	<b>D<sup>‡</sup></b>	<b>17.4</b> ( $\pm 1.9$ )	<b>916</b> ( $\pm 16$ )	<b>2.07</b> ( $\pm 0.18$ )
PNA-5/DIXP	<b>E<sup>†</sup></b>	<b>19.4</b> ( $\pm 1.8$ )	<b>931</b> ( $\pm 19$ )	<b>1.42</b> ( $\pm 0.11$ )
	<b>F<sup>‡</sup></b>	<b>21.4</b> ( $\pm 2.1$ )	<b>914</b> ( $\pm 14$ )	<b>1.86</b> ( $\pm 0.15$ )
PNA-5/TBzTD	<b>G<sup>†</sup></b>	<b>21.2</b> ( $\pm 1.9$ )	<b>867</b> ( $\pm 11$ )	<b>2.03</b> ( $\pm 0.16$ )
	<b>H<sup>‡,¶</sup></b>	<b>20.5</b> ( $\pm 1.5$ )	<b>928</b> ( $\pm 18$ )	<b>2.00</b> ( $\pm 0.21$ )
DIXP/PNA-8	<b>I<sup>†</sup></b>	<b>24.3</b> ( $\pm 1.8$ )	<b>884</b> ( $\pm 21$ )	<b>1.89</b> ( $\pm 0.18$ )

\*Mean results generated from ten data points in each case, whereby one standard deviation is given (as  $\pm x$ , in brackets) and is indicated by error bars in the relevant graphs. <sup>†</sup>5 phr ZnO adopted in formulation. <sup>‡</sup>1 phr ZnO adopted in formulation. <sup>¶</sup>1,4-MFA also included in formulation.

It is clear that the overall most successful formulation amongst those tested was that comprising the DIXP/PNA-8 accelerator system (which included the typical 5 phr ZnO, as denoted by **I** in Table 5.15 and discussed in Section 5.4). Generally, these films afforded the closest-matching tensile results to those of the DPTU/DPG film (**A**), as illustrated in Figure 5.14. This collectively infers that the material was strong (high UTS), flexible (high elongation), elastic and soft (low modulus) which renders film **I** most suitable for latex glove applications, relative to the others produced here. Indeed, the most effective synergistic accelerator system would be expected to yield the maximum tensile results (as in the UTS) which was deduced by Debnath and Basu during their investigations on NR (with other accelerators).<sup>23</sup> DIXP was thought to be especially effective herein due to the polysulfide portion of the structure, which, upon activation, would offer a greater number of sulfur atoms as cross-links. This, in turn, rendered the cross-link bridges longer, which provided enhanced flexibility and thus elasticity and softness to the material. Combining DIXP with PNA-8 may have been especially advantageous because there also resides sulfur atoms in the diamine portion of this complex, which may in turn be released on heating and also contribute to cross-linking. Despite having effected a seemingly satisfactory system (in DIXP/PNA-8), there is more scope for developing the optimum PCB latex, as discussed in the following section.



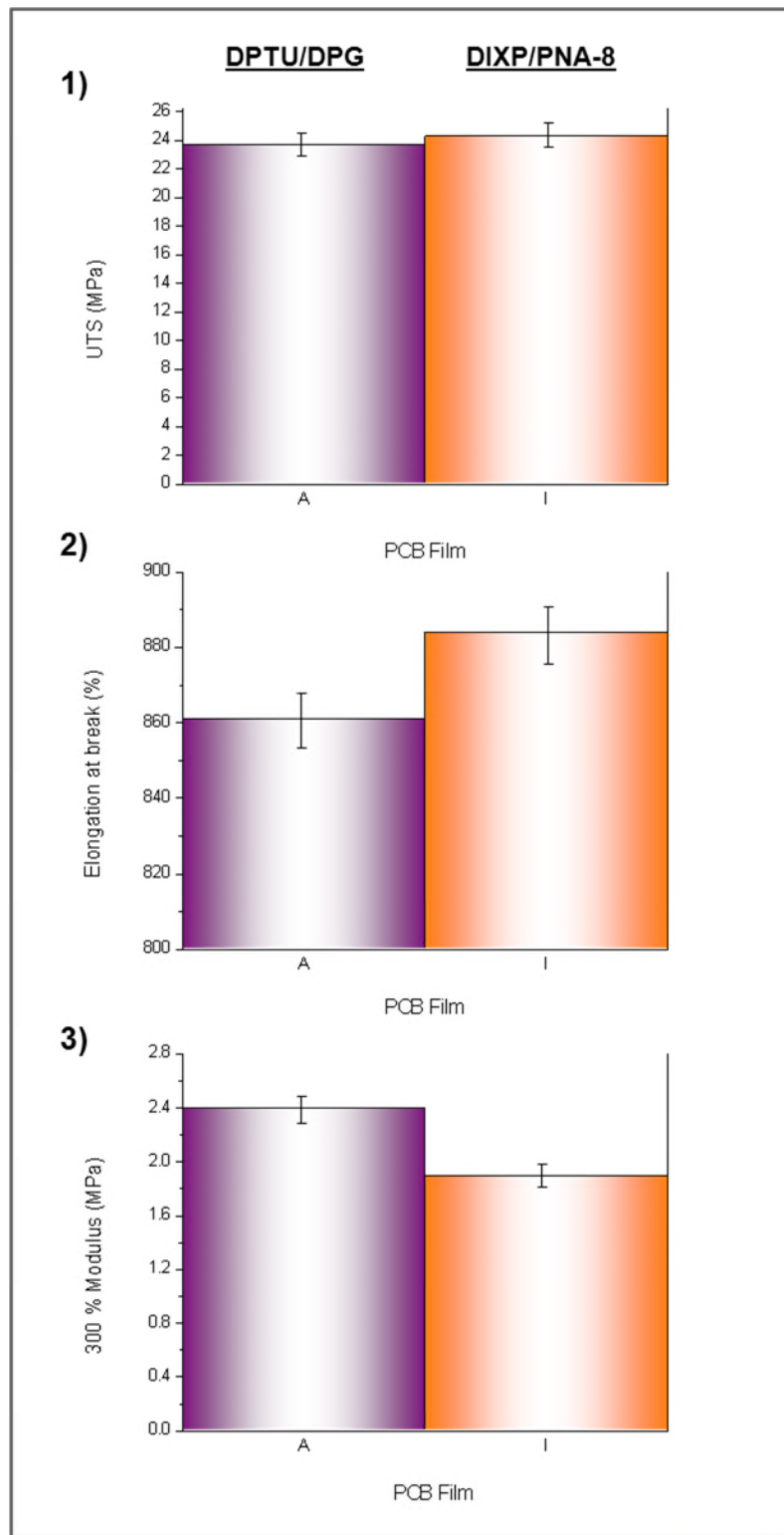


**Figure 5.14. Comparison of tensile test data for PCB latex films made using DPTU/DPG (purple, A) and DIXP/PNA-8 (orange, I). Error bars indicate one standard deviation from ten data points.**

### 5.5.3. Further PCB latex development work

This research was the first step for RBL in developing a safe, optimal PCB rubber latex. A final system cannot be definitively concluded at the time of writing, as there are still many further studies which should be undertaken, as outlined herein.

Although the PCB/DIXP/PNA-8 system afforded films with tensile properties which correlated most closely with the standard DPTU/DPG system (amongst those tested), other formulations also hold some promise. For instance, PNA-5, in combination with DIXP or TBzTD, afforded reasonable tensile results overall; the UTS values were only slightly lower than that of film **A**, where film **G** (from TBzTD/5 phr ZnO) produced relatively similar elongation and modulus results, in particular. The PNA-5/1,4-MFA systems (films **C** and **D**) were the least successful formulations, as they offered the lowest UTS values (both ~17 MPa), which shows that these films were the weakest and, thus, would be more susceptible to tearing. In turn, this proves that PNA-5 requires a secondary (sulfur-based) organic accelerator component, as 1,4-MFA underperformed (compared to DIXP and TBzTD). This was attributed to the fact that 1,4-MFA was acting solely as an additional activator (to ZnO) and was not actually facilitating the cross-links themselves, which would otherwise be provided by an additional sulfur compound. The main concern for the PNA-5 films, overall, was their appearance and texture, as they all contained patches of particulates, which most likely compromised the tensile properties. Inspired by this work, future development by the company will include attempts to optimise the PNA-5 dispersion itself, so that it can become incorporated more homogeneously into the PCB latex formulation and thus yield smoother materials. This could mean working with a more dilute dispersion (*i.e.* lower than 35 % w/w), mixing for longer or altering the ratios of the accelerators within. To also optimise the stability of the PNA-5 dispersion (as discussed in Section 5.3.1), a higher concentration of surfactant may be required; this would certainly need investigating if this reagent were to be adopted worldwide.

Improvement may also be achieved by combining PNA-5 with a different accelerator; for instance, it was observed that film **H** (PNA-5/TBzTD/1,4-MFA) was smoother than film **C** (PNA-5/1,4-MFA). Here, the addition of TBzTD to the PNA-5/1,4-MFA formulation seemed to reduce the inhomogeneity of the films, which was brought about by more cross-linking having taken place, as all of the reagents were more fully incorporated into the reaction. It would be worthwhile assessing if PNA-5 and PNA-8 could operate synergistically and generate even smoother films (which were devoid of patches or particulates, originally caused by PNA-5). However, it is dubious that this combination would be effective, as both molecules comprise similar structures, *i.e.* with a sulfur component and a diamine activator. This work has only seen a PNA molecule and an organic sulfur compound (such as TBzTD or DIXP) work in

unison, where it was perceived that the former would aid in activating the polymer chain, whilst the latter would be primarily responsible for generating the cross-links. Two PNAs, which are structurally so similar, might lack in the sulfur composition (atoms) to form adequate cross-link bridges; PNA-5 and PNA-8 may mostly be concerned with activating the polymer chain. Thus, an overall reduction in the extent of cross-linking may result and yield latex films with poor strength and resilience.

More focus is to be directed on the optimum PCB/DIXP/PNA-8 system. For instance, given that the ancillary aim of this research was to reduce or eliminate ZnO, this film (I) needs replicating with a lower level of ZnO (*i.e.* 1 phr). Hereafter, 1,4-MFA should be incorporated in place of ZnO as a means of determining if this compound is an appropriate alternative activator. Indeed, it would also be a worthwhile experiment to assess the effect of eradicating both the MFA and metal oxide; it may be that PNA-8 is able to sufficiently activate the polymer chain alone, if a high enough concentration is adopted.

Once prospective latex films are identified, the next step is to test for residues through appropriate solvent extractions. This procedure is well-known at RBL, whereby each film would be cut into a specific shape/size and immersed into a suitable solvent; the solution would then be analysed by UV-vis spectroscopy, for instance, after a set time spent agitating. This is important for determining if the accelerator compounds, in particular, are liable to leach out of the rubber material; minimal, or ideally no, residue-leaching is crucial for carrying a system through to large scale industrial production. It is also necessary to assess the thermal stability of the latex films, which is often termed as 'aging' studies (as it is an indication of how the material will behave over time). In this instance, cured films are subjected to a specified temperature for set periods of time, whereby tensile tests are then intermittently undertaken. How the results change over time then dictates the thermal stability of the latex material. Rattanasom *et al.* conducted aging studies on silica-loaded PCB latexes prepared using the standard DPTU/DPG accelerator system and found that the modulus was found to increase over time.<sup>9</sup> Thus, if the modulus was enhanced, and the material rendered less soft, it could be predicted that the strength and elasticity (UTS and elongation, respectively) would be compromised. Aging tests are often conducted at temperatures which far exceed ambient (*e.g.* 100 °C),<sup>9</sup> as much latex application work is undertaken in warm climate countries, such as in the Far East, and so the material should operate well in these conditions.

RBL will be continuing with this work and further developing the PCB latex formulation/s accordingly. This research will also include residues and aging tests, which will be performed on the eventual PCB films which correlate the closest with current PCB latex standards. The preliminary study detailed herein has provided RBL with a platform on which to base further

trials; the accelerators PNA-5, PNA-8 and DIXP will certainly be taken forward, with the overall intention to replace DPTU and DPG.

## 5.6. References

1. H. Ulrich, *Introduction to Industrial Polymers*, Hanser, Munich, 1993.
2. C. D. Anderson and E. S. Daniels, *RAPRA Review Reports*, 2003, **14**, Report 160.
3. S. H. Wakelin and I. R. White, *Clin. Exp. Dermatol.*, 1999, **24**, 245-248.
4. D. S. Ohbi, T. S. Purewal, T. Shah and E. Siores, *J. Appl. Polym. Sci.*, 2007, **106**, 526-533.
5. R. F. Rose, P. Lyons, H. Horne and S. M. Wilkinson, *Contact Dermatitis*, 2009, **61**, 129-137.
6. J. Geier, H. Lessmann, W. Uter and A. Schnuch, *Contact Dermatitis*, 2003, **48**, 39-44.
7. D. C. Blackley, *High Polymer Latices - Their Science and Technology. Volume 2: Testing and Applications*, Maclaren & Sons Ltd., London, 1966.
8. SafeRubber, <http://www.saferubber.eu/>, Accessed 11/03/2014.
9. N. Rattanasom, P. Kueseng and C. Deeprasertkul, *J. Appl. Polym. Sci.*, 2012, **124**, 2657-2668.
10. A. A. J. Feast, in *Polymer Latices and their Applications*, ed. K. O. Calvert, Applied Science Publishers, London, 1982, pp. 21-46.
11. R. S. Chhabra, S. Eustis, J. K. Haseman, P. J. Kurtz and B. D. Carlton, *Fundam. Appl. Toxicol.*, 1992, **18**, 405-417.
12. D. M. Smith, *Br. J. Ind. Med.*, 1984, **41**, 362-366.
13. D. M. Smith, *Occup. Med.*, 1976, **26**, 92-94.
14. T. Iwase, M. Yamamoto, M. Shirai, F. Akahori, T. Masaoka, T. Takizawa, K. Arishima and Y. Eguchi, *J. Vet. Med. Sci.*, 1997, **59**, 59-61.
15. J. Ashby, *Mutagenesis*, 1986, **1**, 3-16.
16. C. M. Blow and C. Hepburn, eds., *Rubber Technology and Manufacture*, Butterworths, London, 1982.
17. J.-M. Charrier, *Polymeric Materials and Processing: Plastics, Elastomers and Composites*, Hanser, New York, 1990.
18. K. I. Berry, *The Quest for a Safer Accelerator for Polychloroprene Rubber*, PhD Thesis, Aston University, Birmingham, 2013.
19. K. I. Berry, M. Liu, K. Chakraborty, N. Pullan, A. West, C. Sammon and P. D. Topham, *Rubber Chem. Technol.*, 2014, Accepted.
20. K. O. Calvert, in *Polymer Latices and their Applications*, ed. K. O. Calvert, Applied Science Publishers, London, 1982, pp. 1-10.
21. G. Heideman, J. W. M. Noordermeer and R. N. Datta, *Rubber Chem. Technol.*, 2006, **79**, 561-588.
22. V. Zenzen, T. M. Ali, M. Kuproth, H. Zankl, C. Janzowski and G. Eisenbrand, *Mutat. Res., Genet. Toxicol. Environ. Mutagen.*, 2003, **535**, 161-170.
23. S. C. Debnath and D. K. Basu, *J. Appl. Polym. Sci.*, 1996, **60**, 845-855.

## **CHAPTER 6**

# **CONCLUSIONS AND FUTURE WORK**

## 6. Conclusions and future work

This chapter provides a synopsis of the research undertaken during this project and discusses the further work which could benefit each respective area. An outline of the project as a whole is firstly provided.

### 6.1. Outline of the project

This PhD project contributed to the SafeRubber enterprise, whereby a Europe-wide consortium aimed to replace ethylene thiourea (ETU) as the industrial accelerator for cross-linking poly(2-chloro-1,3-butadiene) (PCB) rubber (commonly known as neoprene). Concerns over the toxicity of this reagent have arisen, which has put its use, and thus the production of neoprene, in jeopardy. Hence, the manner in which ETU cross-links PCB required elucidating, as this was not known before the project commenced. Once this had been established, alternative, non-toxic cross-linking reagents were evaluated to test the proficiency of the reaction systems, *versus* the performance of ETU. The intention was that the optimum candidate would yield comparable, if not improved, properties in the PCB rubber and would become a commercialised reagent.

In order to assess the cross-linking mechanism, various reactions were undertaken on PCB rubber by K. Berry (at Robinson Brothers Ltd.), but solution-state chemical analyses were difficult due to the high molecular weight of the material. As such, PCB was rendered completely insoluble once cross-linked; physical (tensile) testing was the primary analytical method available, as well as FTIR. In contrast, low molecular weight PCB (*i.e.* oligomers) was hypothesised to be more straightforward, i) to handle and process, and ii) to analyse by spectroscopic methods. The polymer in this form was not expected to fully cross-link (like the rubber), but would become branched, and so the material would remain soluble. Thus, it was the principal objective of this project to furnish oligomeric PCB in a controlled manner. Subsequently, the polymer generated this way would be employed in reactions with various additives to add substance to the mechanistic research being performed by K. Berry with the rubber.

The second industrial portion of this work concerned PCB in the latex form. Aqueous-based polymers are adopted in a variety of applications, including coatings, adhesives and in the production of rubber gloves. It is here where PCB latex is especially relevant; on the whole, PCB latex gloves are safer than natural rubber (NR) equivalents and so are widely applied throughout the professions. However, in a similar way to the ETU/PCB rubber issue, the standard chemicals employed to cross-link PCB latex, namely diphenyl guanidine (DPG) and diphenyl thiourea (DPTU), are known skin allergens. Hence, alternative, safer reagents are

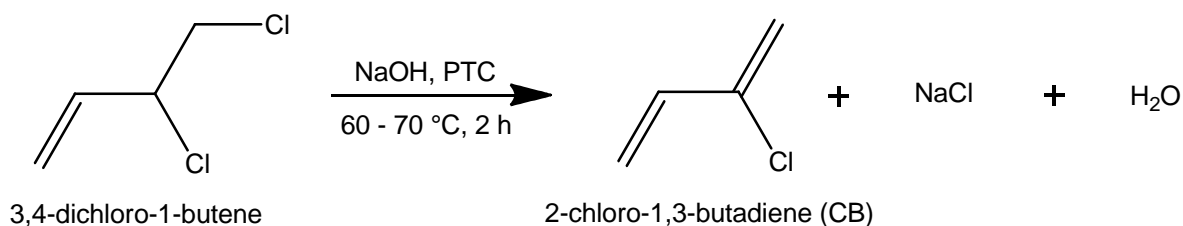
required to facilitate the production of PCB latex (through cross-linking). Chapter 5 of this thesis described the efforts taken to develop such a system.

## 6.2. Conclusions

Herein summarises the findings from the experimental work undertaken during this project.

### 6.2.1. Synthesis of 2-chloro-1,3-butadiene

CB was synthesised by the dehydrochlorination of 3,4-dichloro-1-butene, as depicted by Scheme 6.1. The starting material was readily available and inexpensive and the reaction was facilitated by base (NaOH). An optimum NaOH concentration of 25 % (w/v) gave rise to 88 % yield; lower concentrations led to a severe depreciation in the product yield, which verified the literature.<sup>1</sup> A phase-transfer catalyst (PTC) was employed to enable reasonable reaction times and temperatures, which was vital in preventing self-polymerisation of CB, as it formed.



**Scheme 6.1. The synthesis of 2-chloro-1,3-butadiene (CB) by the dehydrochlorination of 3,4-dichloro-1-butene, where PTC denotes a phase-transfer catalyst.**

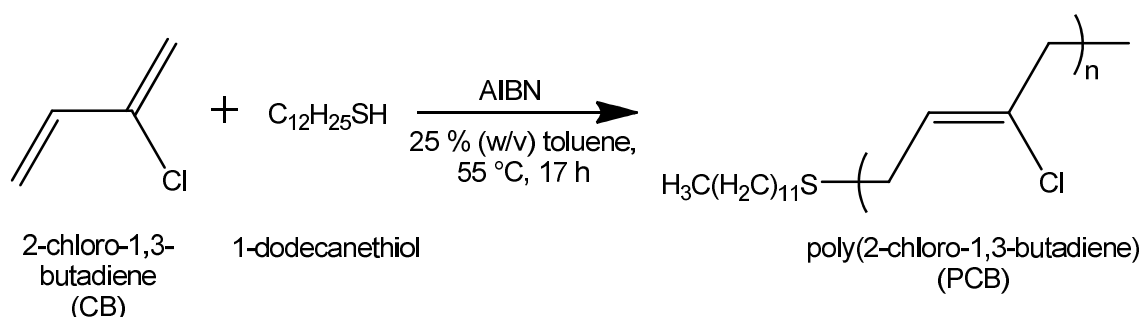
Water was generated as a by-product and distilled over with CB as an azeotrope. Drying (over MgSO<sub>4</sub>) readily removed such moisture and further purification by vacuum distillation yielded pure CB (as assessed by <sup>1</sup>H NMR). Storage under ambient conditions revealed CB to be highly unstable, as self-polymerisation was observed (through <sup>1</sup>H NMR) within just two hours. A suitable storage procedure was successfully deduced, whereby 0.1 % (w/w) phenothiazine was incorporated into the (dried) material and acted as a stabiliser. This rendered CB reliably stable at room temperature for two weeks. However, as a further precaution, (stabilised) CB was stored in cold conditions, before being distilled prior to polymerisation.

### 6.2.2. Synthesis of poly(2-chloro-1,3-butadiene)

In the first instance, PCB oligomers were synthesised *via* an ‘uncontrolled’ route, using a simple thiol chain transfer agent (CTA). Thereafter, a controlled-radical method was sought, which would offer more precision over the system.

#### 6.2.2.1. Uncontrolled polymerisation of 2-chloro-1,3-butadiene

The thiol CTA (1-dodecanethiol) functioned as a mediator, in capping the polymer chains. In this way, the polymerisation of PCB was regulated to a certain degree, but was not fully controlled. Scheme 6.2 depicts the reaction, which was a procedure modified from the literature.<sup>2</sup>



**Scheme 6.2. The uncontrolled polymerisation of 2-chloro-1,3-butadiene (CB) using 1-dodecanethiol CTA (the main 1,4-*trans* polymer isomer configuration is shown).**

Pure CB was a crucial precursor for producing suitable PCB. As described in Section 3.2.1, the use of crude monomer (*i.e.* that which did not undergo distillation) yielded high molecular weight impurities, which were observed by GPC analysis, as minor peaks were afforded at lower retention times (compared to the main PCB peak).

In assessing various different concentrations of 1-dodecanethiol in the reaction, it was found that this system could only yield PCB with molecular weights ranging between 2000 and 3000 g/mol. That is, despite also occasionally extending the duration of the reaction. The molecular weight distributions (dispersity,  $M_w/M_n$ ,  $\bar{D}$ ) were broad, typically around 2. Thus, it was established that this polymerisation system, incorporating 1-dodecanethiol CTA, was limited to furnishing polymer only within a distinct range of molecular weights; true control was not evident, as the  $\bar{D}$  values were substantial (*i.e.*  $\gg 1.2$ , which is the generally accepted limit for controlled systems, such as RAFT).



### 6.2.2.2. RAFT polymerisation of 2-chloro-1,3-butadiene

The main thrust of this project was to determine a synthetic method for PCB which could predetermine the molecular weight and yield monodisperse polymer. RAFT polymerisation was selected over alternative controlled-radical techniques, such as nitroxide-mediated and atom transfer radical polymerisation (denoted as NMP and ATRP, respectively), as metal catalysts are not necessary (as in ATRP) and the reaction conditions are generally milder (NMP can require very high temperatures). As such, no reports existed in the literature describing such a system for CB (RAFT or otherwise), which provided additional motivation for this research.

The CTAs trialled throughout these studies are illustrated in Figure 6.1, comprising S-1-dodecyl-S'-( $\alpha,\alpha'$ -dimethyl- $\alpha''$ -acetic acid)trithiocarbonate (DDMAT), S-(thiobenzoyl)thioglycolic acid (TBTA), 2-cyano-2-propylbenzodithioate (CPD) and cyanomethyl methyl(phenyl)carbamodithioate (CMPCD). These compounds have been successful in mediating the RAFT polymerisations of other monomers, in particular 2-methyl-1,3-butadiene,<sup>3</sup> styrene (St),<sup>4</sup> methyl methacrylate (MMA)<sup>5, 6</sup> and vinyl chloride (VC),<sup>7</sup> respectively. For each CTA, the CB polymerisation reactions were performed in solution conditions, with xylene and THF separately (each at 1:1 w/w with respect to monomer), with AIBN at 60 °C, and targeted ~4000 g/mol. The kinetics of each system were assessed, where GPC afforded  $M_n$  and  $\mathcal{D}$  results and <sup>1</sup>H NMR was employed to monitor monomer conversion.

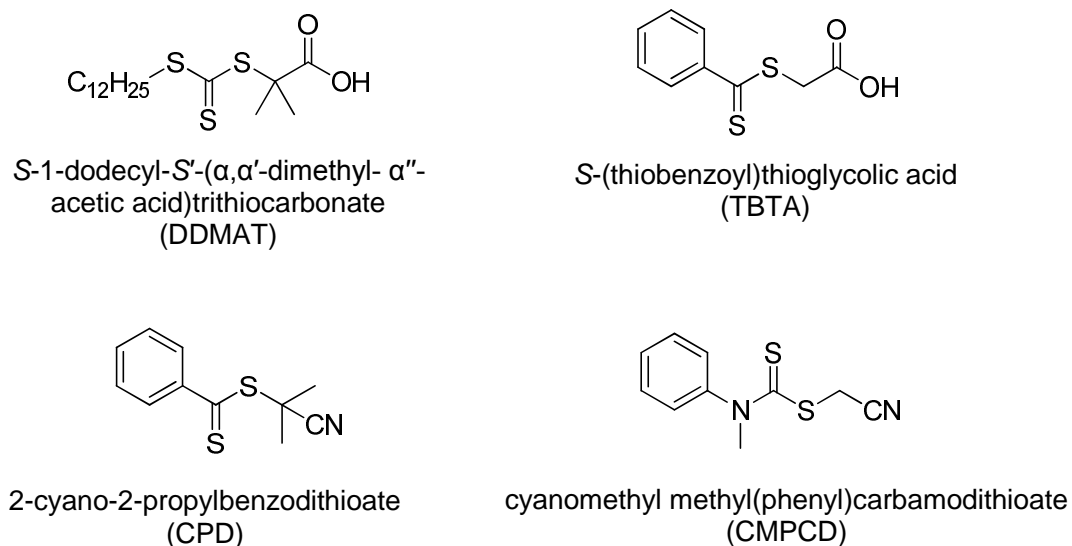


**Figure 6.1. Structures of the CTAs trialled in the RAFT polymerisation of CB.**

Overall, the least successful CTA was CMPCD, whereby both systems (in xylene and THF) furnished very high molecular weights early on in the reactions (up to 130,000 g/mol within 20 % conversion). Low molecular weight species subsequently formed as time progressed,

resulting in broad, bimodal distributions. Both of the TBTA systems also exceeded the target molecular weight ( $M_n^{\text{th}}$ , 4000 g/mol) and afforded  $\mathcal{D}$  values of 1.5 – 2.0. DDMAT and CPD offered the most promise as they each achieved the  $M_n^{\text{th}}$  (in both solvents for DDMAT and in THF for CPD). Overall, the distinguishing factor between the two CTAs was that CPD afforded lower  $\mathcal{D}$  values, overall, which were  $\leq 1.3$  throughout the polymerisation; the dispersities in the DDMAT systems were all  $>1.3$ . CPD in THF conditions were found to be optimum for CB; the low  $\mathcal{D}$  values and linear evolution of molecular weight with conversion (which reached 80 % at the point of  $M_n^{\text{th}}$ ) confirmed that the system was controlled. Figure 6.2 summarises the kinetics results for the CPD/THF system.

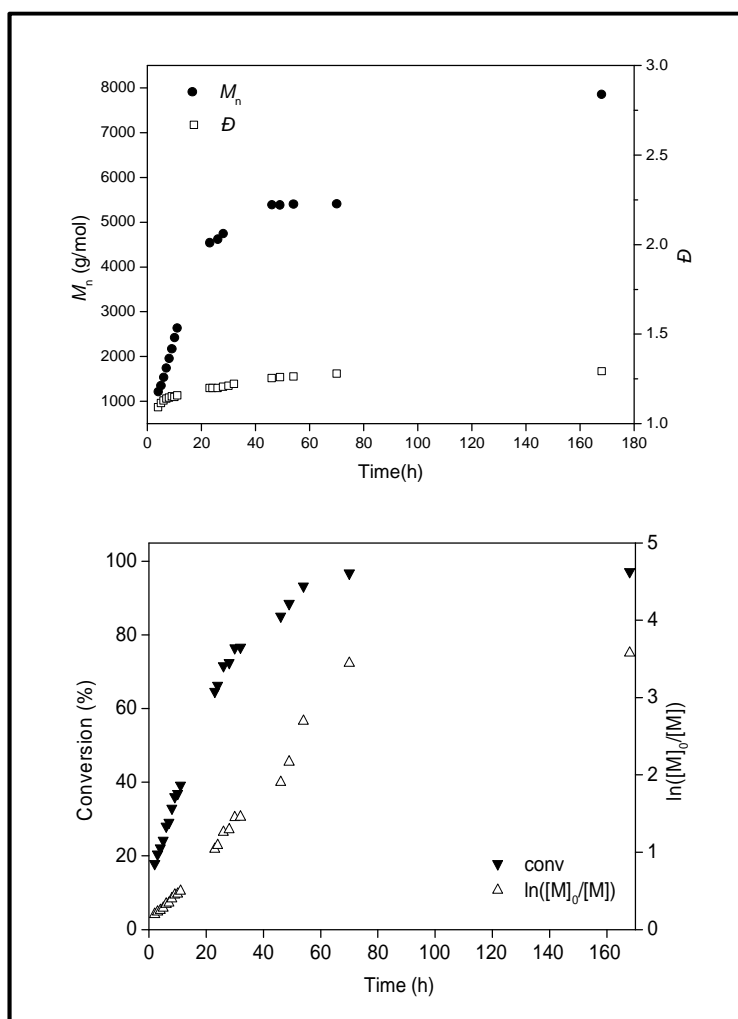


**Figure 6.2. Kinetic plots for the optimum RAFT polymerisation of CB under the following conditions:  $[AIBN]_0/[CPD]_0/[CB]_0 = 0.2/1/45$  at 60 °C in THF (50 % w/w).**

DDMAT and CPD, the most effective CTAs, were also tested with CB in bulk conditions. In contrast to in solution, DDMAT was superior to CPD in this case, as the  $M_n^{\text{th}}$  was attained and the dispersity decreased from 1.4 – 1.25. The CPD system exceeded the  $M_n^{\text{th}}$  and higher  $\mathcal{D}$  values resulted, overall, indicating that this was less efficient. The DDMAT/bulk system may have been more effective because DDMAT was more soluble in the monomer

(compared to CPD). Thus, the CPD/THF system remained the optimum system, of all of the conditions tested, as the dispersity remained low throughout the entire polymerisation ( $\bar{D} \leq 1.3$ ). This system was further evaluated by isolating a sample of macroCTA and performing a self-blocking experiment. Chain end fidelity was proven as the subsequent reaction with a second portion of CB saw an increase in the molecular weight and the final (extended) polymer retained a low  $\bar{D}$ . Furthermore, higher molecular weights were targeted by altering the monomer:CTA ratio; up to ~50,000 g/mol, low dispersity PCB was synthesised by this method.<sup>8</sup>

The success of CPD was attributed to the nature of the R group,  $C(Me)_2CN$ , which yields a superior, stable tertiary radical and is an effective leaving group.<sup>9</sup> Incorporating this CTA into a RAFT reaction (depending on the monomer application) is understood to enable faster rates of fragmentation, which in turn facilitates enhanced control over polymerisation.

The most noticeable effect of solution conditions (compared to bulk) was that reactions proceeded considerably slower. This is not unusual and can be attributed to the diminished monomer concentration. Xylene and THF were compared, which are vastly different solvents in terms of polarity and chemical structure. In general, slower polymerisations occurred in THF, which in turn seemed to offer more control. For instance, THF was even found to improve the CMPCD system, as xylene yielded bimodal GPC peaks, whereas those from THF were unimodal (albeit broad/tailing). This was a similar phenomenon to that of DDMAT, where more uniform GPC peaks arose in THF. For the optimum CTA (CPD) the  $M_n^{th}$  was attained at high conversion in THF, but less control was evident in xylene as this value (4000 g/mol) was exceeded. Overall, it was concluded that CB could have a greater affinity for THF, which may justify why superior control was shown in these conditions. Also, it is possible that the reagents, namely CPD and AIBN, were more soluble in THF (than in xylene).

A further conclusion was drawn from this work, in classifying CB as a more-activated monomer (MAM). This derives from the apparent applicability (and inapplicability) of certain CTAs in the RAFT polymerisations of this monomer. For instance, CMPCD was clearly unsuccessful for CB, but was trialled initially because of the reported success of this with VC (*i.e.* a chlorinated vinyl molecule), which is defined as a less-activated monomer (LAM).<sup>7</sup> LAMs and MAMs are classified according to the reactivity of the associated growing polymer propagating radical; poly(MAM)s have effective homolytic leaving groups, whereas poly(LAM)s are poor. Furthermore, MAMs comprise carbon-carbon double bonds which are conjugated to an aromatic ring, carbonyl or cyano group; this bond in a LAM is situated adjacent to a hetero-aromatic ring, a nitrogen lone pair or a saturated carbon or oxygen.<sup>10</sup> Hence, the conjugation that exists between the two double bonds in the CB structure would

suggest that this is a MAM, by definition. The relatively successful control offered by DDMAT in these experiments adds weight to this argument, as trithiocarbonates are known to be effective CTAs for MAMs.<sup>11</sup> Also, CPD, the CTA of the final optimum CB system, was effective for MMA, which is also a MAM. Collectively, the results certainly imply that CB is a MAM, with respect to such classification within the realm of RAFT chemistry.

### **6.2.3. Industrial applications of poly(2-chloro-1,3-butadiene)**

The introduction to this chapter (Section 6.1) described how it was important to perform cross-linking experiments on low molecular weight PCB, so as to ultimately define the mechanism by which ETU reacts. It was intended for PCB furnished *via* RAFT polymerisation to be employed in these investigations, but this was not feasible as this work had to complement that in RBL and, thus, be undertaken promptly. As a result, the ~3000 g/mol PCB generated from the uncontrolled method was adopted.

A separate, yet related, study concerned the development of a safer accelerator system for PCB latex. As with ETU in the rubber, RBL were looking to replace DPG and DPTU as the components in a standard industrial PCB latex accelerator system. Thus, PCB latex films were furnished using various non-hazardous compounds. Comparison of the tensile test results of the development films, with those from a DPG/DPTU system, ultimately revealed serious contenders (in replacing DPG and DPTU), as the physical properties of certain materials were analogous.

#### 6.2.3.1. Cross-linking poly(2-chloro-1,3-butadiene)

Low molecular weight (oligomeric) PCB was employed in reactions with ETU and ZnO, separately and in unison, which aimed to imitate the cross-linking system employed in industry with the rubber material. PCB was subsequently reacted with model compounds (in the absence and presence of ZnO), including piperazine (PIP), 1,4-diaminobutane (DAB), dibutyl thiourea (DBTU) and 1,8-octanedithiol (ODT), and an alternative accelerator, tetrabutylthiuram disulfide (TbuT). The intention of this approach was to deduce which functionality of ETU was involved in the cross-linking, *i.e.* through the sulfur, nitrogen or carbon atoms. Reactions were undertaken at the appropriate temperature (160 °C) and were monitored by periodic FTIR spectroscopic analyses (NMR and GPC techniques unfortunately yielded no beneficial data which added to the results).

Allylic rearrangement of the 1,2-PCB isomer was verified as the primary stage of the cross-linking mechanism. This was found by observing the associated FTIR peak, at ~925 cm<sup>-1</sup>,

which diminished over time; the presence of ZnO accelerated this process considerably. This trend was observed in the experiments with ETU, model compounds and TbuT.

Various existing cross-linking theories were disproved, such as the possibility of ether linkage<sup>12</sup> and those of Vukov<sup>13</sup> and Desai,<sup>14</sup> who each implied that ZnCl<sub>2</sub> was a distinct by-product of the reaction with ZnO. However, it was eventually postulated that ZnCl<sub>2</sub> was indeed generated, after all, when ETU and ZnO were employed in a combined system. In the oligomeric PCB reaction with both of these reagents, a white solid precipitated from the solution; this was found to be the (unidentified) product of a reaction between ZnCl<sub>2</sub> and ETU. Thus, this further implied that ZnCl<sub>2</sub> was generated *in situ* during the reaction and was subsequently involved in another reaction. Additionally, EU was furnished as a by-product in the rubber cross-linking investigations of Berry,<sup>15</sup> although this was not replicated in the oligomer studies. Overall, this helped to substantiate the theory of Pariser.<sup>16</sup>

During these studies, the oligomeric form of PCB was particularly advantageous, not least of all because the material was more practical, but also as this made the detection of by-products possible. For instance, hydrochloride gas (HCl) was evolved in the PCB/ETU reaction, which in turn helped to support the bis-alkylation theory of Kovacic (as this emits HCl after forming cross-links *via* the nitrogen atoms).<sup>17</sup> Cross-linking with alternative compounds, such as the diamines (PIP, DAB and DBTU), in contrast, produced alkaline vapours, which was ultimately linked to the formation of HCl salts. These findings were reinforced by the relevant FTIR spectra, as new peaks were formed in the 1600 – 1500 cm<sup>-1</sup> region. This work was crucial as the testing for evolved gases, for instance, was not possible during the rubber investigations of Berry,<sup>15</sup> where the reactions took place under high pressure in an enclosed rheometer machine.

ZnO was integral to the mechanism and ultimately enabled cross-linking to occur through the sulfur atoms of certain molecules. ODT could not facilitate the cross-linking of PCB by itself (in oligomers or rubber) but was successful when ZnO was present. Changes in the FTIR spectra of the TbuT reactions revealed that the N-C=S functionality was disrupted more readily with ZnO and a new peak at 1560 cm<sup>-1</sup> indicated the formation of C-S bonds. Hence, the conclusion was made that ZnO was enabling cross-linking through sulfur; it is perceived that this is facilitated by the Zn<sup>2+</sup> dication.

Overall, this work indicated that more than one mechanism occurs when PCB is cross-linked with ETU and ZnO. The bis-alkylation theory of Kovacic<sup>17</sup> was validated by the clear formation of HCl (in conditions comprising ETU). Subsequently, the Pariser mechanism<sup>16</sup> seems likely as ZnCl<sub>2</sub> and EU by-products have been detected (although EU was only found in the rubber experiments) and C-S bonds form. However, it is clear that ETU cannot react directly with the polymer chain through the sulfur atom as results were negative when dithiols

were employed independently. Thus, the novel theory of activation by ZnO was realised. As illustrated previously in Chapter 4 (Scheme 4.8), the newly-proposed mechanism of cross-linking PCB<sup>18</sup> is initiated by rearrangement of the 1,2-isomer (as usual). ZnO subsequently removes the chlorine atom; displacement of oxygen (from ZnO) then takes place by the sulfur (of ETU), so that ZnCl<sub>2</sub> and EU are yielded. Overall, the result is cross-link bridges through carbon-sulfur bonds. The latter stages of this mechanism compare to Pariser, but, crucially, ZnO has been found to react ahead of ETU.

#### 6.2.3.1.1. A safer accelerator system for cross-linking PCB rubber

Elucidating the nature of the ETU/ZnO cross-linking reaction made it possible for the SafeRubber project to progress towards an alternative accelerator system. The prerequisite of this was for the compound to be safer (*i.e.* non-toxic) and perform in the same way. Thus, the SafeRubber consortium collectively realised proposed new accelerators (PNAs), the structures of which each combined a (di)amine with a sulfur component. The theory was that the amine portion would activate the polymer chain (as ZnO was found to achieve) and the sulfur atoms would be provided from the sulfur-containing component. Computer-simulated studies by a project partner revealed that these molecules were non-hazardous. All of the PNAs (which are listed in Table 4.4 of Chapter 4) were trialed at RBL with PCB rubber; the piperazine-1-carbodithioic acid 1,3-diaminopropane complex (PNA-5) was deemed most effective as the final material yielded physical (tensile and rheological) properties which were similar to PCB furnished *via* the ETU/ZnO system. PNA-5 was subsequently tested in the PCB oligomer and sufficient evidence was produced that the compound had successfully reacted in the same fashion as ETU/ZnO. The structure of PNA-5 is illustrated in Figure 6.3.

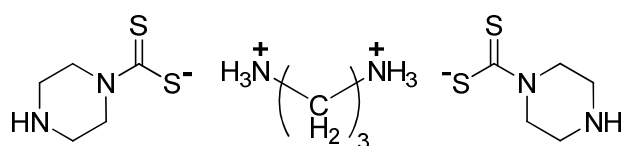


**Figure 6.3. Structure of piperazine-1-carbodithioic acid 1,3-diaminopropane complex (PNA-5).**

Overall, the objectives of the SafeRubber enterprise have been successfully met. PNA-5 is a promising novel accelerator for PCB and more comprehensive testing with the rubber will substantiate the effectiveness of replacing ETU. Additionally, the design of a multi-functional additive (namely 1,4-MFA) has led to the potential for replacing ZnO in certain applications. The commercialisation of PNA-5 by RBL is in progress at the time of writing and it is expected that the cost of this new compound will be similar to that of ETU. ETU is currently acquired by RBL at the price of £7/kg; even if PNA-5 was eventually offered at a slightly

higher rate, the benefits of this new cross-linker molecule being non-toxic, with a similar performance, would still render this a viable replacement within industry.

#### 6.2.3.2. Poly(2-chloro-1,3-butadiene) latex development

In a similar way to the PCB cross-linking studies which centred on ETU, the second industrial portion of this project concerned the development of PCB rubber in the latex form (as detailed in Chapter 5). In this case, the hazardous nature of the diphenyl thiourea (DPTU) and diphenyl guanidine (DPG) accelerators adopted in industry was the concern and alternative reagents were sought.

Variations of accelerator systems comprising the complex of piperazine-1-carbodithioic acid and 1,3-diaminopropane (PNA-5), tetrabenzylthiuram disulfide (TBzTD), diisopropyl xanthogen polysulfide (DIXP) and 2,2'-dithio di(ethylammonium)-bis(dibenzylthiocarbamate) (PNA-8) were employed to produce PCB latex films; tensile test results were compared against those of a standard DPTU/DPG film (depicted as **A** throughout), which acted as a benchmark. Different levels of ZnO activator (namely, 5 phr *versus* 1 phr) were also evaluated, as was the performance of a multi-functional additive (1,4-MFA). A secondary aim was to develop a method which would reduce the level of ZnO in the system, or eradicate it completely. The findings from these trials are summarised in the following sub-sections.

##### 6.2.3.2.1. The effect of ZnO in PCB latex films

ZnO is known to act as an activator in terms of cross-linking and was found to initiate the process for ETU (in PCB rubber and oligomers) in the novel mechanism proposed by Berry *et al.*<sup>18</sup> ZnO was considered to operate in the same way in the latex systems, by enabling the sulfur-containing accelerator components to react with polymer chains. Certain formulations, namely those involving PNA-5 in combination with 1,4-MFA (films **C** and **D**), DIXP (films **E** and **F**) and TBzTD (films **G** and **H**), compared higher and lower concentrations of ZnO. To note, 1,4-MFA was an additional component within **H**, which included 1 phr ZnO. Overall, reducing the quantity of ZnO in the formulation had negligible effect on the strength (UTS) of the PCB films, which was a positive result regarding the capacity for adopting a lower concentration. However, it was postulated that a higher level could enhance the softness of the materials, as **E** (5 phr ZnO, 1.42 ±0.11 MPa) yielded a lower modulus than **F** (1 phr ZnO, 1.86 ±0.15 MPa). The modulus results also indicated that 1,4-MFA could potentially function in the same way as ZnO, as the value for **H** (incorporating 1 phr ZnO and

0.5 phr 1,4-MFA) was comparable to **G** (5 phr ZnO), at approximately 2 MPa. Elongation at break data also revealed few trends and the only possible conclusions were associated with the nature of the accelerator (as discussed subsequently in Section 6.2.3.2.2). Overall, it was established that a five-fold decrease in the concentration of ZnO was viable for a PCB latex formulation, certainly for the conditions adopted herein.

In assessing 1,4-MFA as a potential alternative to ZnO, it was found that the presence of both of these activators in a system was detrimental if only one organic accelerator was present. For instance, films **C** and **D**, produced through PNA-5/1,4-MFA and contrasting levels of ZnO (5 phr in **C**, 1 phr in **D**), afforded very low UTS results, around 17 MPa. Such low strengths were attributed to the antagonistic nature of the dual activator system; ZnO and 1,4-MFA were believed to be competing in order to activate the polymer chains and, as such, less cross-linking resulted. In **D**, with less ZnO, the UTS and elongation were higher (differences in the latter data were more distinct, *i.e.* 916 % *versus* 873 % for **C**), which indicated that more cross-links were formed from this system. This was justified by 1,4-MFA being able to act as the major activator and so more cross-linking occurred. Further evidence for this came from qualitative assessments of the films, as the inhomogeneity of film **C** seemed to arise from excess ZnO being present (as less was incorporated into cross-linking reactions).

#### 6.2.3.2.2. *New accelerators for the production of PCB latex films*

The success of PNA-5 in cross-linking PCB rubber and oligomers (highlighted in Section 4.1.6) justified trialling this substance in the latex systems. In summary, this accelerator performed poorly when adopted by itself (as in film **B**) and when combined with 1,4-MFA (with ZnO). PCB films produced this way yielded low UTS values, compared to the standard DPTU/DPG system (**A**), which was attributed to fewer cross-links being materialised. Film **B** was an especially thin material, which resulted from a drastically reduced concentration of accelerator in the formulation; a high elongation at break reflected that fewer cross-links were present, which would otherwise render the film more rigid.

On combining PNA-5 with a secondary sulfur-containing organic accelerator molecule the systems were vastly improved. For instance, the UTS was increased when DIXP and TBzTD were united (separately) with PNA-5 and the inhomogeneity of these films was not as severe. It was clear that more cross-linking was taking place when two organic accelerators were being employed and that they functioned in a synergistic manner. In support of this, film **H**, from the PNA-5/TBzTD system with ZnO and 1,4-MFA, was an improvement on **D**, where PNA-5 was used alone with 1,4-MFA (where both adopted 1 phr ZnO). The physical



properties and appearance of **H** were superior to **D** because the dual accelerator system (PNA-5 and TBzTD) operated more effectively alongside the two activators (ZnO and 1,4-MFA). Thus, activation was occurring simultaneously and cross-linking was being facilitated more efficiently.

Film **I**, which incorporated PNA-8 and DIXP accelerators and 5 phr ZnO, was particularly significant to these studies as optimum tensile results were generated, which correlated closely with those from **A** (the standard system). By eradicating PNA-5 from the formulation, the final material became smooth and free from inhomogeneous patches, which, as a result, rendered the film strong (UTS =  $24.3 \pm 1.8$  MPa). This film was elastic and soft due to the presence of highly flexible sulfur-based cross-links; the polysulfide portion of DIXP was deemed to provide more sulfur atoms (than other molecules), which made the cross-link bridges longer than in any of the other systems. At this point, the PNA-8/DIXP system seems to be a contender for replacing the industrial (hazardous) DPTU/DPG standard.

### **6.3. Future work**

The following sections describe the experimental work which should succeed this project, considering the progress which has been made to-date (previously summarised).

#### **6.3.1. Further development of the 2-chloro-1,3-butadiene synthetic protocol**

Overall, the dehydrochlorination reaction adopted to synthesise CB was highly capricious, in that variable yields were observed throughout, irrespective of the reaction conditions. As highlighted in Section 3.1.3, on the occasions when two comparable syntheses were undertaken, the final product yields would never compare. Overall, yields varied within approximately 20 – 90 %. It is possible that the rate of stirring (of the reaction mixture) was a factor, as a slower speed may have caused inadequate mixing of reagents and ultimately resulted in lower yields. It is unlikely, though, that this can be held solely accountable for such dramatic differences.

Higher concentrations of the base should be assessed to firstly establish if higher yields can be obtained this way (*i.e.* >88 %, which was acquired with 25 % w/w NaOH). This may also contribute to resolving the variable yields issue, as this particular variable may not actually be optimum at this 25 % (w/w) level and, once rectified, the entire process could be made more reliable.

### **6.3.2. Future studies for the RAFT polymerisation of 2-chloro-1,3-butadiene**

Successful RAFT polymerisation conditions for CB have been deduced which can predefine low dispersity PCB up to 50,000 g/mol. However, it was not necessary for this work to target higher than this; a part of future work should be to probe this system further so as to attain higher molecular weights (*i.e.* >50,000 g/mol). The synthesis of relatively large polymers in a controlled manner is potentially useful for industrial applications and this RAFT reaction would be a relatively straightforward set-up for adopting on a large scale (*i.e.* few, simple reagents and moderate temperature).

It is possible that an alternative initiator (to AIBN), and/or concentration of such, may also be suitable for the RAFT polymerisation of CB. The low boiling point of this monomer (62 °C) does, however, limit the options. It would be especially advantageous to successfully design a low-temperature reaction system, which would in turn be even more viable for industry. This system should perform as successfully, if not more so, than the AIBN/60 °C system, with CPD in THF. Lauroyl peroxide is a possible candidate, as this initiator can be used at temperatures as low as 40 °C.

It would be ideal to also evaluate a wider range of solvents, and concentrations thereof, in the RAFT system. THF was found to offer more control over the polymerisation of CB than xylene, and bulk systems were more rapid but compromised the values of  $\bar{M}_w$ . Thus, one approach could involve simply altering the concentration of THF in the system, *i.e.* assess solutions comprising up to 50 % (or 1:1 w/w), so that a compromise between optimal dispersities and reaction times could be realised. Likewise, an altogether different solvent could be as or more effective. A variety of solvents should be tested, over a range of polarities, densities, chemical reactivities, *etc.*, so that a more comprehensive catalogue of results was realised. Only then could more definitive conclusions be made regarding the effect of solvent in RAFT polymerisation, at least with CB.

### **6.3.3. Optimisation of oligomer cross-linking experiments**

Employing low molecular weight (oligomeric) material contributed significantly to the cross-linking studies surrounding PCB, on the whole. For instance, it was possible to observe certain by-products of the reactions, which in turn enabled the ETU/ZnO mechanism to be deduced. Hence, complete optimisation of the oligomer experiments should be considered for future trials of this nature, so that future research can be conducted more efficiently.

Ethylene urea (EU) was not detected during the oligomer ETU/ZnO reaction but the equivalent trial with rubber (by K. Berry)<sup>15</sup> did prevail. It is not clear why the latter experiment

was more successful at this; incorporating the reagents through milling could have been a more proficient mixing process. Sonicating the oligomer mixtures may not, therefore, have been sufficient; a more rigorous mixing procedure should be sought, so that the reagents are mixed more thoroughly to be fully involved in the reaction (with PCB). Furthermore, the FTIR results should be supplemented by other analytical data. For instance, a specialised, high resolution  $^1\text{H}$  NMR spectroscopic method, or HPLC/LC-MS techniques, may offer more insight into the cross-linking mechanism and contribute more knowledge to these systems.

#### **6.3.4. Further development of poly(2-chloro-1,3-butadiene) latex**

Further research is to take place at RBL for the production of PCB latex films in the absence of ZnO, entirely. The full capabilities of 1,4-MFA will be assessed (as a replacement to ZnO) by adopting this compound alone in certain systems, including the standard DPTU/DPG formulation. Further work in this area should also include evaluating PNA-8/DIXP (the most promising system of those tested) with less ZnO (*i.e.* 1 phr) and with 1,4-MFA (without ZnO); results from such trials would indicate whether reducing or replacing ZnO was possible for this particular formulation.

Each PCB latex film which was synthesised with PNA-5 was rendered inhomogeneous, containing various extents of patches of particulates. Thus, should work continue with this accelerator, the dispersion itself would have to be developed further. It may be necessary to reduce the concentration of the dispersion (*i.e.* <35 % w/w), so that the solids content is reduced, or to increase the quantity of surfactant present. More surfactant would be anticipated to improve the (thermal) stability of the reagent, as an elevated temperature (40 °C) drastically compromised the stability during this research, as shown by distinct increases in viscosity over time (as discussed in Chapter 5).

Additional experiments on the rubber films are also necessary, such as in performing solvent extractions to determine any accelerator residues, and undertaking aging studies to understand the thermal stability of the materials. Such trials should proceed on films which possess the most favourable tensile properties or those most closely matching the industry standard material. Ideally, no (or minimal) residues would be liberated from the new PCB latex (which would otherwise cause harm to the glove-wearer) and the physical (tensile) properties would not be compromised over time.

## 6.4. References

1. *EP Pat.*, 0001905, 1978.
2. *US Pat.*, 5523355, 1996.
3. D. S. Germack and K. L. Wooley, *J. Polym. Sci., Part A: Polym. Chem.*, 2007, **45**, 4100-4108.
4. S. C. Farmer and T. E. Patten, *J. Polym. Sci., Part A: Polym. Chem.*, 2002, **40**, 555-563.
5. Y. K. Chong, J. Krstina, T. P. T. Le, G. Moad, A. Postma, E. Rizzardo and S. H. Thang, *Macromolecules*, 2003, **36**, 2256-2272.
6. M. Benaglia, E. Rizzardo, A. Alberti and M. Guerra, *Macromolecules*, 2005, **38**, 3129-3140.
7. C. M. R. Abreu, P. V. Mendonça, A. C. Serra, J. F. J. Coelho, A. V. Popov, G. Gryn'ova, M. L. Coote and T. Guliashvili, *Macromolecules*, 2012, **45**, 2200-2208.
8. N. Pullan, M. Liu and P. D. Topham, *Polym. Chem.*, 2013, **4**, 2272-2277.
9. J. B. McLeary, F. M. Calitz, J. M. McKenzie, M. P. Tonge, R. D. Sanderson and B. Klumperman, *Macromolecules*, 2004, **37**, 2383-2394.
10. D. J. Keddie, G. Moad, E. Rizzardo and S. H. Thang, *Macromolecules*, 2012, **45**, 5321-5342.
11. G. Moad, E. Rizzardo and S. H. Thang, *Acc. Chem. Res.*, 2008, **41**, 1133-1142.
12. A. S. Aprem, K. Joseph and S. Thomas, *Rubber Chem. Technol.*, 2005, **78**, 458-488.
13. R. Vukov, *Rubber Chem. Technol.*, 1984, **57**, 284-290.
14. H. Desai, K. G. Hendrikse and C. D. Woolard, *J. Appl. Polym. Sci.*, 2007, **105**, 865-876.
15. K. I. Berry, The Quest for a Safer Accelerator for Polychloroprene Rubber, PhD Thesis, Aston University, Birmingham, 2013.
16. R. Pariser, *Kunststoffe*, 1960, **50**, 623-627.
17. P. Kovacic, *Ind. Eng. Chem. Res.*, 1955, **47**, 1090-1094.
18. K. I. Berry, M. Liu, K. Chakraborty, N. Pullan, A. West, C. Sammon and P. D. Topham, *Rubber Chem. Technol.*, 2014, Accepted.